UNIVERSITY OF CALIFORNIA
RIVERSIDE

Derivatives of Dodecahalo-*Closo*-Dodecaborate Di-Anion

A Dissertation submitted in partial satisfaction
of the requirements for the degree of

Doctor of Philosophy

in

Chemistry

by

Amy C. Avelar

December 2009

Dissertation Committee:
Dr. Christopher A. Reed, Chairperson
Dr. Guy Bertrand
Dr. Pingyun Feng

This Dissertation of Amy C. Avelar is approved:

_____

_____

_____
Committee Chairperson

University of California, Riverside

ACKNOWLEDGEMENTS

I would like to acknowledge Reed group members, past and present. I am grateful to Kee- Chan Kim, Mark Juhasz, Stephen Hoffman, Yun Zhang, Paul Richardson, James Wright, Gabe Mueck, Matt Nava, as well as crystallographers Fook Tham and Bruno Donnadieu. A very special thank you is in order for Evgenii Stoyanov and Irina Stoyanov; both of whom taught me so much! Their insights to synthesis and infrared spectroscopy were invaluable. I am especially grateful to Dr. Christopher Reed, who let me explore synthetic chemistry and guided me wisely throughout the process. I would also like to acknowledge the National Science Foundation for the graduate fellowship.

I would also like to acknowledge my colleagues at SBVC, Sheri Lillard, Susan Bangasser, John Stanskas, Michael Torrez, and Denise Bailey who have constantly encouraged me. I am very thankful and dedicate this dissertation to my husband Alvaro, and my children, AJ, Alex, and Andrew. Alvaro- you rock! Thank you for all of your support and for the coffee late at night…

ABSTRACT OF THE DISSERTATION

Derivatives of the Dodecahalo-*Closo*-Dodecaborate Di-Anion

by

Amy C. Avelar

Doctor of Philosophy, Graduate Program in Chemistry
University of California, Riverside, December 2009
Dr. Christopher A. Reed, Chairperson

The di-anion, dodecahalo-*closo*-dodecaborate, $B_{12}X_{12}^{2-}$, where the X = Cl or Br, has been determined to be a useful weakly coordinating anion, WCA. Despite the di-negative charge, several elusive and reactive cationic species were stabilized with $B_{12}X_{12}^{2-}$ as the counterion. Of particular interest was the synthesis of the di-protic acid, $H_2(B_{12}X_{12})$,[1] $H_2(B_{12}X_{12})$ is the *di*-protic analogue to the recently developed strongest isolable *mono*-protic Brønsted acid, $H(CHB_{11}Cl_{11})$.[2] The basicity of the di-anion, $B_{12}Cl_{12}^{2-}$, was shown to be surprisingly similar to basicity of the carborane anion, $CHB_{11}Cl_{11}^{1-}$, based on the νN-H anion basicity scale.[3]

The methodology used to synthesize the carborane acids was modified in order to successfully synthesize the di-protic acids, $H_2(B_{12}X_{12})$. Several of the precursors to the acids are new compounds, and the precursors display remarkably similar properties as the analogous carborane compounds. The di-protic acids themselves are superacids due to

their ability to protonate arenes, such as benzene and toluene.[1] Also investigated was the stabilization of elusive di-cations with $B_{12}X_{12}^{2-}$ counterions, and preliminary data are discussed in Chapter 6, including future work.

References

1. "Superacidity of Boron Acids $H_2(B_{12}X_{12})$ (X= Cl, Br)" Avelar, A.; Tham, F.S.; Reed, C.A. *Angew. Chem.* **2009**, *121*, 3543-3545. (*Angew Chem., Int. Ed.* **2009**, *48*, 3491-3493.)

2. "The Strongest Isolable Acid," Juhasz, M.; Hoffmann, S.; Stoyanov, E.; Kim, K.-C.; Reed, C.A. *Angew. Chem. Int. Ed.* **2004**, *43*, 5352-5255.

3. "An Infrared νNH Scale for weakly basic anions. Implications for Single-Molecule Acidity and Superacidity," Stoyanov, E.S.; Kim, K.-C.; Reed, C.A. *J. Am. Chem. Soc.* **2006,** *128*, 8500-8508.

Table of Contents

List of Figures

List of Tables

List of Reaction Schemes

CHAPTER 1

Introduction

1.1 Introduction

Weakly coordinating, weakly basic anions such as carboranes ($CHB_{11}R_5X_6^-$ where R = Me, H, or halide and X = Cl, Br, or I) allow for the isolation and study of otherwise elusive and highly reactive cations because the anions counter, not destroy or are destroyed by, the targeted cation.[1] The ideal weakly coordinating anion, WCA, is chemically robust, has delocalized charge over a large, weakly or non-nucleophilic volume, and is inexpensive.[2] The carborane anion fits the first two criterion exceptionally well, but it is rather expensive in comparison to other WCAs in current use. Some examples of WCAs besides carboranes include anions such as triflate, $CF_3SO_3^-$, the tetraphenylborate-based anion, $[B(Ar^F)_4]^-$ (where Ar=3,5-$(CF_3)_2C_6H_3$), and the fluorometallate anion, $Sb_2F_{11}^-$. Despite the expense of carborane anions, they have been used to successfully characterize targets when other WCAs have failed.[1]

Non-carborane based WCAs exhibit a number of weaknesses. One drawback of some WCAs includes the reaction, or lack of stabilization, with the target species. WCAs that are based on poly- (or per-) fluorinated alkoxy or aryloxy metallates have been known to coordinate via the oxygen atom.[3] Some WCAs have been shown to decompose, sometimes violently, rather than stabilize the target.[2] The decomposition of $M(OC_6F_5)_6^-$ (M = Ta or Nb) of $[Ph_3C][M(OC_6F_5)_6]$ is observed as the phenoxide is transferred to Zr/Ti metallocene dimethyls.[4] Other WCAs may also form by-products or mixtures

which then react with the sought species. For example, strong oxidizing agents are available in solutions of fluorometallates (e.g., SbF_5 from $Sb_2F_{11}^-$) which may in turn oxidize the target.[2]

The above-mentioned problems are largely circumvented through the use of carborane anions, and were it not for their high cost, carboranes would be in widespread usage in modern chemistry.[1] The thesis of this present work is that the much less expensive isostructural di-anion, dodecahydro-*closo*-dodecaborate, $B_{12}H_{12}^{2-}$, and its halogenated derivatives (Figure 1.1) may be similarly useful WCAs. The cost for 1 gram of $[(CH_3CH_2)_3NH]_2[B_{12}H_{12}]$ is approximately $20 (as of Fall 2009) based on the reagents priced from Fisher Scientific[5a] for its synthesis using procedures described by Knapp.[6] The synthesis takes 2–3 days. In comparison, decaborane, $B_{10}H_{14}$, the *starting* material for the carborane anion, ranges in cost from $20 to $35 per gram depending on vendor and availability.[5b] The synthesis of $CHB_{11}H_{11}^{1-}$ requires many more reagents and about 2–3 weeks to synthesize. The di-anion therefore is much more cost effective and, as will be discussed in this thesis, exhibits similar WCA properties as the analogous carborane monoanion.

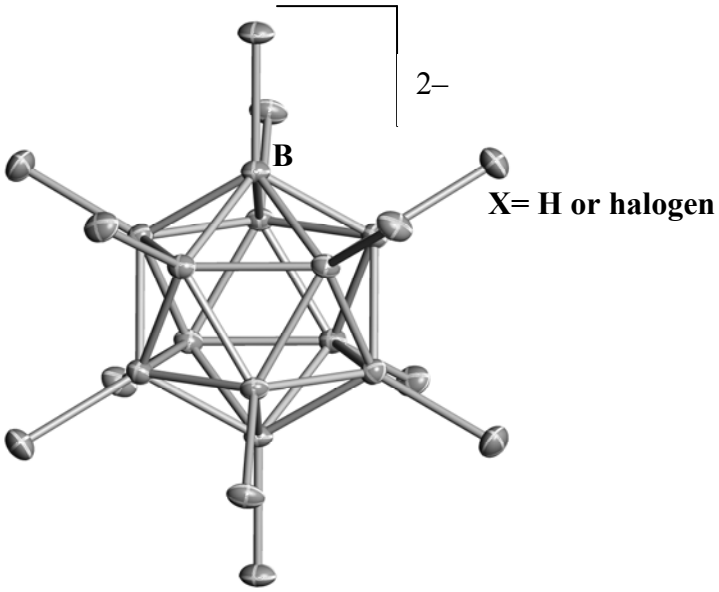

Figure 1.1 $B_{12}X_{12}^{2-}$ where X = H or halogen

1.2 $B_{12}X_{12}^{2-}$ (X = H or halogen)

Before its actual discovery, $B_{12}H_{12}$ was predicted to be stable only as the di-anion, $B_{12}H_{12}^{2-}$, via early molecular orbital calculations by Longuet-Higgins and Roberts.[7] The di-anion itself was isolated soon afterwards.[8] Studies since have shown that the di-anion exhibits thermal and chemical stability even greater than that of the carborane anion. For example, $Cs_2[B_{12}H_{12}]$ has been shown to be stable up to 810 °C while differential scanning calorimetry (DSC) studies indicate that the cesium salt of the monoanion, $Cs[CHB_{11}H_{11}]$, is stable to approximately 420 °C.[9,10]

There are various reports of salts, double salts, and complexes isolated with the $B_{12}H_{12}^{2-}$ anion.[11] These compounds illustrate the weakly coordinating ability of the di-anion. A key application includes their use in Boron Neutron Capture Therapy (BNCT)

with a salt such as $Na_2[B_{12}H_{11}SH]$.[12] Many other derivatives include the substitution of hydrogen of the $B_{12}H_{12}^{2-}$ di-anion by alkyl, amine, phenyl, carbonyl, hydroxyl, or thiol groups. These $B_{12}H_{12}^{2-}$ derivatives are discussed in detail by Sivaev and co-workers.[11] The syntheses of di-anion derivatives are similar to the syntheses of many carborane derivatives, and most carborane derivatives known thus far are nicely outlined in a review by Michl, et al.[13]

The high versatility displayed by both the carborane anion and dodecahydro-*closo*-dodecaborate di-anion is due mainly to their chemical and thermal stability. Their stabilities and solubilities may be adjusted by modifying the cages. Substitution of hydrogen for a halogen or a methyl group is common for both species.[1,11] Generally, reactions occur on the perimeter of the parent anion $CB_{11}H_{12}^{1-}$ and $B_{12}H_{12}^{2-}$ rather than destruction of the cage because of σ–aromaticity within the CB_{11} and B_{12} icosahedral cores. The substitution reactions noted with these icosahedral cages are analogous to those of benzene, where, due to π–aromaticity, reactions occur on the perimeter of the ring rather than cause ring destruction or loss of aromaticity.[1]

Current Reed group research interests involve the extensive use of the halogenated/methylated carborane derivatives, $CHB_{11}R_5X_6^{1-}$ (where R = Me, H or halide and X = Cl, Br, or I). The substitution of the hydrogen atoms on the parent anion by electronegative substituents aids in the delocalization and burying of the –1 charge. In addition, hydride abstraction via oxidation is prevented when the anion is partially halogenated.[14] A key derivative is the carbocation salt, trityl (triphenylmethyl) carborane.[1] The trityl carborane salts are precursors to silylium ion-like species ($R_3Si^{\delta+}$

where R = alkyl or aryl). The silylium compounds, in turn, are precursors to the strongest isolable Brønsted acids, methylating reagents, and other species well characterized with the use of carboranes.[15] There is also the potential for the use of carborane-based catalysts in the synthesis of inorganic polymers.[16] Thus, based on work done with the halogenated carboranes, the present work employed the halogenated derivatives, $B_{12}X_{12}^{2-}$ (where X = Cl or Br) to test whether reagents useful in mono-anionic carborane chemistry could be obtained with the di-anionic boranes.

The per-halogenated derivatives, $B_{12}X_{12}^{2-}$ (where X = Cl, Br, I), as well as mixed halogen species (e.g. $B_{12}Br_8F_4^{2-}$), were extensively studied in the 1960s.[17] Interest in these di-anions fell shortly thereafter, perhaps due to the –2 charge and the assumption that the higher negative charge results in a more basic, more coordinating anion. Though the syntheses of the halogenated derivatives have been in the literature for more than 40 years, there has been a minimal focus on using them as WCAs. In a recent literature search, only a handful of articles investigate the use of the per-halogenated di-anions, and mostly as Group 1 salts or Ag^+ salts.[18] More recently, $B_{12}Cl_{12}^{2-}$ salts containing imidazolium cations were shown to be ionic liquids.[19]

The following chapters show that despite the di-negative charge, the di-anions, $B_{12}X_{12}^{2-}$ (X = halogen), are indeed viable WCA candidates. These syntheses were accomplished by running comparable reactions to those of the isostructural carboranes. The di-anions themselves were synthesized and halogenated initially using literature preparations, although improvements in the procedures were required and are

documented in Chapter 2.[20] While this work was in progress Knapp et al. reported similar studies on di-anion chlorination.[6]

1.3 Reagents and Reactive Cations

1.3.1 Trityl Salts

Since their isolation and characterization, trityl carborane salts have been extremely useful reagents for the preparation of target cations normally not attainable through conventional metathesis reactions.[21] Trityl salts themselves are synthesized via the metathesis reaction of trityl bromide and silver carborane. The resultant carbocation salt is a powerful hydride abstractor and can abstract hydride from silanes.[22] The key to the isolation of these species is the carborane anion. As an ideal WCA, the monoanion does not detrimentally interfere with the reaction or the product once it forms.[22]

The analogous reaction starting with the silver salts of $B_{12}X_{12}^{2-}$ will herein be shown to occur and to result in new useful trityl reagents. The isolation of the trityl salts proved to be much more labor–intensive than that of the trityl carborane salts. But, once isolated, the trityl salt was used to successfully isolate the silylium compound and is discussed in Chapter 3.

1.3.2 Silylium Ion-like Compounds

Through the use of carboranes, the long sought, truly ionic species, R_3Si^+, was isolated when the bulky R group, mesityl, was used.[22] Silicon, though in the same group as carbon, does not form the silylium cation when exposed to conditions that readily generate carbocations, therefore its isolation was a remarkable find.[22] As the precursor

silane to R_3Si^+, allyltrimesitylsilane, is not readily available and its preparation is quite tedious, the reported synthesis was a milestone achievement, but not an one ideal for practical laboratory syntheses.[23] Therefore, to be used as a silylium carborane reagent, alkyl R groups such as ethyl are employed instead. The resulting "ion-like" silylium compounds have found wide applications in recent years.[1,15] They are now reagents used to isolate to even more elusive cation or cation-like targets.

Silylium carborane compounds are commonly obtained by the hydride abstraction from R_3SiH by trityl carborane. The analogous reactions using the trityl salts of di-anions $B_{12}X_{12}^{2-}$ will also be discussed in Chapter 3.

1.3.3 Brønsted Superacids

The carborane acids, $H(CHB_{11}X_{11})$, have been shown to be the strongest, isolable Brønsted acids.[24] Although previous studies have shown that strong, aqueous acids form when using $B_{12}X_{12}^{2-}$ di-anions as conjugate bases, the anhydrous acids themselves were not obtained, as the hydrate was always isolated.[17] Therefore, the anhydrous Brønsted acids, $H_2(B_{12}X_{12})$, were a prime target of the present research using the same reaction conditions as those used to obtain the carborane acids. A further goal was to determine if the di-protic acids, $H_2(B_{12}X_{12})$, were of similar or of greater acid strength compared to the carborane acids. Chapter 4 includes the synthesis and the finding that the di-protic acids are indeed of comparable strength to the mono-protic acids.

1.3.4 Arenium Ions

Until carboranes were used as counter-ions, protonated arenes had only been studied at low temperatures via ^1H and ^{13}C NMR.[25,26] Arenium ions have now been

isolated and structurally characterized at ambient temperatures.[26] The question of whether or not the di-protic acids, $H_2(B_{12}X_{12})$, are able to protonate arenes is explored to give insight into their acid strengths. Since the di-protic acids are herein shown to protonate benzene in Chapter 5, their acid strengths are comparable to the analogous mono-protic carborane acids. A paper reporting the studies of sections 1.3.1–1.3.4 has recently been published.[27]

1.3.5 Stabilizing 2+ Cations

The halogenated di-anions may serve as particularly useful counterions to labile, reactive di-cations because of the more favorable lattice energies of 1:1 versus 2:1 electrolytes recently reported and calculated.[28] The halogenated di-anions have been shown to be useful WCAs for the isolation and structural characterization of $[Li_2(SO_2)_8][B_{12}Cl_{12}]$ at the expense of $[Li(SO_2)_4]_2[B_{12}Cl_{12}]$, which minimize electrostatic repulsions.[28] The higher lattice energies calculated for 1:1 versus 2:1 electrolytes may be key to the stabilization of reactive di-cations with the use of di-anions as counter ions. To further test this hypothesis, several di-cationic species were targeted.

Di-carbocations were the initial targets in this regard, but analysis of material obtained after synthesis proved to be elusive itself. The material was found to be insoluble in the very limited solvent choices. Preliminary data therefore, is inconclusive of di-carbocations stabilized with the use of $B_{12}X_{12}^{2-}$ and is discussed in Chapter 6.

Another test target examined was hexamethylhydrazinium, $(CH_3)_6N_2^{2+}$, a unique compound that has been shown to overcome "Coulomb explosion" or the decomposition of a compound due to adjacent covalently bonded atoms containing formal positive

charges.[29] The di-cation has yet to be structurally characterized crystallographically. Once again, after material was isolated, it was found to be insoluble in the limited choices of solvents and characterization was therefore inconclusive. Surprisingly, crystals that were obtained were 2:1 electrolytes when the conditions were modified to produce 2:1 salts. This result may indirectly support that the 1:1 electrolytes do have much higher lattice energies than the 2:1 electrolytes as the 1:1 salts, if indeed the salts would not dissolve as did the 2:1 salts.

In route to the $(CH_3)_6N_2^{2+}$ salts, preliminary evidence suggests the formation of the di-methyl compound, $(CH_3)_2(B_{12}X_{12})$. This compound may be analogous in use to the carborane based methylating agent.[30] The carborane based methylating agents have been found to be stronger than methyl triflates.[30] All of these compounds are discussed in Chapter 6 as well as possible future projects involving the use of $B_{12}X_{12}^{2-}$ ion.

1.4 Conclusions

The di-anion $B_{12}X_{12}^{2-}$ displays similar chemical properties as the monoanion $CHB_{11}H_{11}^{1-}$ despite the di-negative charge. In Chapter 2, the synthesis of $B_{12}H_{12}^{2-}$ and its perhalogenation is discussed. The syntheses of trityl and silylium compounds are shown in Chapter 3, while the anhydrous Brønsted acids as described in Chapter 4. The acids are as strong as the carborane acids, and can protonate arenes as discussed in Chapter 5. Chapter 6 investigates di-cationic targets and the methylating ability of $(CH_3)_2(B_{12}X_{12})$ as future work.

1.5 References

1. "Carboranes: A New Class of Weakly Coordinating Anions for Strong Electrophiles, Oxidants, and Superacids," Reed, C.A. *Acc. Chem. Res.* **1998**, *31*, 133-139.

2. "Weakly Coordinating Anions," Krossing, I.; Raabe, I. *Angew. Chem. Int. Ed.* **2004**, *43*, 2066-2090.

3. "Weakly Coordinating Al-, Nb-, Ta-, Y-, and La-Based Perfluoroaryloxymetalate Anions as Cocatalyst Components for Single-Site Olefin Polymerization," Metz, M.V.; Sun, Y.; Stern, C.L.; Marks, T.J. *Organometallics* **2002**, *21*, 3691- 3702.

4. "Al-, Nb-, and Ta-Based Perfluoroaryloxide Anions as Cocatalyst for Metallocene-Mediated Ziegler- Natta Olefin Polymerization," Sun, Y.; Mertz, M.V.; Stern, C.L.; Marks, T.J. *Organometallics* **2000**, *19*, 1625- 1627.

5. a) Reagent pricing based on data obtained from Fisher Scientific: www.fishersci.com. b) Decaborane is available from Alfa Aeser: 25g for $872.15.

6. "Synthesis and Characterization of Synthetically Useful Salts of the Weakly-Coordinating Dianion $[B_{12}Cl_{12}]^{2-}$," Geis, V.; Guttsche, K.; Knapp, C.; Schere, H.; Uzun, R. *Dalton Transactions* **2009**, *15*, 2687-2694.

7. "The Electronic Structure of an Icosahedron of Boron Atoms," Longuet-Higgins, H.C.; Roberts, M. deV. *Proc. R. Soc. Lond. A* **1955**, *230*, 110-119.

8. "The Isolation of the Icosahedral $B_{12}H_{12}^{2-}$ Ion," Pitochelli, A.R.; Hawthorne, F.M. *J. Am. Chem. Soc.* **1960**, *82* (12), 3228-3229.

9. "Chemistry of Boranes. VIII. Salts and Acids of $B_{10}H_{10}^{2-}$ and $B_{12}H_{12}^{2-}$," Muetterties, E.L.; Balthis, J.H.; Chia, Y.T.; Knoth, W.H.; Miller, H.C. *Inorg. Chem.* **1964**, *3*, 444-451.

10. "Thermal, Structural and Possible Ionic-Conductor Behaviour of $CsB_{10}CH_{13}$ and $CsB_{11}CH_{12}$," Romerosa, A.M. *Thermochim. Acta* **1993**, *217*, 123.

11. "Chemistry of *closo*-Dodecaborate Anion $[B_{12}H_{12}]^{2-}$: A Review," Sivaev, I.B.; Bregadze, V.I.; Sjoberg, S. *Collect. Czech. Chem. Commun.* **2002**, *67*, 679-727.

12. "Boron Neutron-Capture Therapy for Cancer Realities and Prospects," Barth, R.F.; Sloway, A.H.; Fairchild, R.G.; Bruggder, R.M. *Cancer* **1992**, *70*, 2995-3007.

13. "Chemistry of the Carbo-*closo*-dodecaborate(-) Anion, $CB_{11}H_{12}^{-}$," Körbe, S.; Schreiber, P.J.; Michl, J. *Chem. Rev.* **2006**, *106*, 5208- 5249.

14. “New Weakly Coordinating Anions. 2. Derivatization of the Carborane Anion $CB_{11}H_{12}^-$,” Jelinek, T.; Baldwin, P.; Scheidt, W.R.; Reed, C.A. *Inorg. Chem.* **1993**, *32*, 1982- 1990.

15. “Carborane Acids. New “Strong Yet Gentle” Acids for Organic and Inorganic Chemistry,” Reed, C.A. *Chem. Commun.* **2005**, 1669-1677.

16. “Ambient Temperature Ring-Opening Polymerisation (ROP) of Cyclic Chlorophosphazene Trimer $[N_3P_3Cl_6]$ Catalyzed by Silylium Ions,” Xhang, Y.; Huynh, K.; Manners, I.; Reed, C.A. *Chem. Commun*. **2008**, 494-496.

17. “Chemistry of Boranes. IX. Halogenation of $B_{10}H_{10}^{2-}$ and $B_{12}H_{12}^{2-}$,” Knoth, W.H.; Miller, H.C.; Sauer, J.C.; Balthis, J.H.; Chia, Y.T.; Muetterties, E.L. *Inorg. Chem.* **1964**, *3*, 159-167.

18. “The Crystal structures of the Dicesium Dodecahalogeno-*closo*-Dodecaborates $Cs_2[B_{12}X_{12}]$ (X= Cl, Br, I) and their Hydrates,” Tiritiris, I.; Schleid, T. *Z. Anorg. Allg. Chem.* **2004**, *630*, 1555-1563. “The Crystal Structure of Solvent-Free Silver Dodecachloro-closo-dodecaborate $Ag_2[B_{12}Cl_{12}]$ from Aqueous Solution,” Tiritiris, I.; Schleid, T. *Z. Anorg. Allg. Chem*. **2003**, *629*, 581-583. “Single Crystals of the Dodecaiodo-closo-dodecaborate $Cs_2[B_{12}I_{12}]\cdot 2CH_3CN$ ($\equiv\{Cs(NCCH_3)\}_2[B_{12}I_{12}]$) from Acetonitrile,” Tiritiris, I.; Schleid, T. *Z. Anorg. Allg. Chem*. **2001**, *627*, 2568-2570.

19. “Ionic Liquids Containing Boron Cluster Anions,” Nieuwenhuyzen, M.; Seddon, K.R.; Teixidor, F.; Puga, A.V.; Vinas, C. *Inorg. Chem.* **2009**, *48*, 889-901.

20. Miller, H.C.; Muetterties, E.L. *Inorg. Synth.* **1967**, *10*, 88-91. “Chemistry of Boranes. IX. Halogenation of $B_{10}H_{10}^{2-}$ and $B_{12}H_{12}^{2-}$,” Knoth, W.H.; Miller, H.C.; Sauer, J.C.; Balthis, J.H.; Chia, Y.T.; Muetterties, E.L. *Inorg. Chem.* **1964**, *3*, 159-167.

21. “New Weakly Coordinating Anions 3: Useful Silver and Trityl Salt Reagents of Carborane Anions,” Xie, Z.; Jel□nek, T.; Bau, R.; Reed, C.A. *J. Am. Chem. Soc*. **1994**, *116*, 1907- 1913.

22. “Crystallographic Evidence for a Free Silylium Ion,” Kim, K.-C.; Reed, C.A.; Elliot, D.W.; Mueller, L.J.; Tham, F.; Lin, L.; Lambert, J.B. *Science* **2002**, *297*, 825-827.

23. “Torsional Distortions in Trimesitylsilanes and Trimesitylgermanes,” Lambert, J.B.; Stern, C.L.; Zhao, Y.; Tse, W.C.; Shawl, C.E.; Lentz, K.T.; Kania, L. *Journal of Organometallic Chemistry* **1998**, *568*, 21-31.

24. “The Strongest Isolable Acid,” Juhasz, M.; Hoffmann, S.; Stoyanov, E.; Kim, K.-C.;

Reed, C.A. *Angew. Chem. Int. Ed.* **2004**, *43*, 5352-5255.

25. "*The Action of the Catalyst Couple Aluminum Chloride-Hydrogen on Toluene at Low Temperatures; the Nature of Friedel-Crafts Complexes*," Brown, H.C.; Pearsall, H.W. *J. Am. Chem Soc.* **1952**, *74*, 191-195. "*Certain Trialkyalted Benzenes and Their Compounds with Aluminum Chloride and with Aluminum Bromide*," Norris, J.F.; Ingraham, J.N. *J. Am. Chem. Soc.* **1940**, *62*, 1298-1301. "*Isolation of the Stable Boron Trifluoride-Hydrogen Fluoride Complexes of the Methylbenzenes; the Onion salt (or σ-Complex) Structure of the Friedel-Crafts Complexes*," Olah, G.A.; Kuhn, S.; Pavlath, A. *Nature* **1956**, 693- 694. "*Proton Magnetic Resonance of Aromatic Carbonium Ions I. Structure of the Conjugate Acid*," MacLean, C.; Van der Waals, J.H.; Mackor, E.L. *Mol. Phys*. **1958**, *1*, 247- 256. "*The 1,1,2,3,4,5,6-heptamethylbenzenonium Ion*," von E. Doering, W.; Saunders, M.; Boyton, H.G.; Earhart, H.W.; Wadley, E.F.; Edwards, W.R.; Laber, G. *Tetrahedron* **1958**, *4*, 178-185. "*Nuclear Magnetic Resonance Studies of the Protonation of Weak Bases in Fluorosulphuric Acid III. Methylbenzenes and Anisole*," Birchall, T.; Gillespie, R.J. *Can. J. Chem.* **1964**, *42*, 502- 513. "*Stable Carbocations. CXXIV. Benzenium Ion and Monoalkylbenzenium Ions*," Olah, G.A.; Schlosberg, R.H.; Porter, R.D.; Mo, Y.K.; Kelly, D.P.; Mateescu, G.D. *J. Am. Chem. Soc.* **1972**, *94*, 2034-2043. "*Arenium Ions-Structure and Reactivity*," Koptyug, V.A. Rees, C.; Ed; Springer-Verlag: Heidelberg, Germany, **1984**, 1-227.

26. "Isolating Benzenium Ion Salts," Reed, C.A.; Kim, K.-C.; Stoyanov, E.S.; Stasko, D.; Tham, F.S.; Mueller, L.J.; Boyd, P.D.W. *J. Am. Chem. Soc.* **2003**, *125*, 1796-1804.

.

27. "Superacidity of Boron Acids $H_2(B_{12}X_{12})$ (X= Cl, Br)" Avelar, A.; Tham, F.S.; Reed, C.A. *Angew. Chem.* **2009**, *121*, 3543-3545. (*Angew Chem., Int. Ed.* **2009**, *48*, 3491-3493.)

28. "How to overcome Coulomb explosions in labile dications by using the $[B_{12}Cl_{12}]^{2-}$ dianion," Knapp, C.; Schulz, C. *Chem. Comm.* **2009** DOI: 10.1039/b908970e

29. "Can the hexamethylhydrazinium dication $[Me_3N\text{-}NMe_3]^{2+}$ be prepared?" Zhang, Y.; Reed, C.A. *Dalton Trans.* **2008**, 4392-4394.

30. "Optimizing the Least Nucleophilic Anion. A New, Strong Methyl$^+$ Reagent," Stasko, D.; Reed, C.A. *J. Am. Chem. Soc*. **2002**, *124*, 1148-1149. "Alkylating Agents Stronger than Alkyl Triflates," Kato, T.; Stoyanov, E.; Geier, J.; Grützmacher, H.; Reed, C.A. *J. Am. Chem. Soc.* **2004**, *126*, 12451-12457.

CHAPTER 2

Synthesis of Dodecahydro-*closo*-dodecaborate ($B_{12}H_{12}^{2-}$) Anion and its Halogenation

2.1 Introduction

There are a number of reported methods for the synthesis of the $B_{12}H_{12}^{2-}$ di-anion.[1] For example, $B_{12}H_{12}^{2-}$ may be prepared through the pyrolysis of boron hydrides, such as the pyrolysis of $Na[B_3H_8]$.[2] Other boron cages, such as $B_9H_9^{2-}$, are also reported to form as byroducts from the pyrolysis of boron hydrides.[1] Another synthetic route for the preparation of $B_{12}H_{12}^{2-}$ is the reaction of a borane, such as pentaborane, with a trialkylamine borane. For practical laboratory use, decaborane, though toxic and costly, is the most convenient borane from which to synthesize the di-anion.[1] The product can be produced on a large scale (~70 g $[Et_3NH]_2[B_{12}H_{12}]$) with minimal formation of side products.[3] The reaction between decaborane and triethylamine borane (Reaction Scheme 2.1) results in 92% yield of the product.[3] Recently, Knapp and co-workers reported a large–scale synthesis from cheaper starting materials, $Na[BH_4]$ and I_2 in diglyme, and report a 51% yield.[4]

$$B_{10}H_{14} + 2\ Et_3N{\cdot}BH_3 \xrightarrow[190\ ^oC]{\text{kerosene}} [Et_3NH]_2[B_{12}H_{12}] + 3\ H_2$$

Reaction Scheme 2.1- Synthesis of $B_{12}H_{12}^{2-}$ from decaborane

The $B_{12}H_{12}^{2-}$ cage was halogenated in order to avoid any potential B-H cleavage by a future derivative, the trityl cation. The per-halogenation (Cl or Br) of $B_{12}H_{12}^{2-}$ was first reported in 1964.[5] The perbrominated derivative, $B_{12}Br_{12}^{2-}$, was obtained by reaction

of $B_{12}H_{12}^{2-}$ with elemental bromine at ambient pressures, although the reaction time was not specified.[5] The original synthesis of $B_{12}Cl_{12}^{2-}$ required high pressures of Cl_2.[5] In 1982, Brody reported the synthesis of $B_{12}Cl_{12}^{2-}$ at ambient pressures and used infrared (IR) spectroscopy to determine complete chlorination after 8.5 hours.[6] In the present work, these procedures were found to result in incomplete chlorination of $B_{12}H_{12}^{2-}$ based on the ^{11}B nuclear magnetic resonance (NMR) spectrum. It is important to note that the majority of the published syntheses described above are at least 40 years old. As NMR was in its infancy, characterization of the product and purity was established mainly by IR spectroscopy. One of the purposes of this chapter is to discuss syntheses of $B_{12}H_{12}^{2-}$, and to document improvements made to the procedure, including purifications. The purification steps are extremely important, as impurities not removed from these precursor di-anions were found to hinder subsequent chemistry.

2.2 Experimental

All reagents were used as received, except for kerosene, which was dried following literature methods.[7] NMR spectra were obtained on a Bruker Avance 300 MHz spectrometer. FTIR spectra were obtained on a Perkin Elmer Spectrum 100 Series spectrometer in a nitrogen filled glovebox.

The bis-triethylammonium salt of dodecahydro-*closo*-decaborate, $[Et_3NH]_2[B_{12}H_{12}]$, was prepared following literature procedures.[3] The brominated derivative, $B_{12}Br_{12}^{2-}$, was also prepared following literature procedures.[5] If $Na_2[B_{12}H_{12}]$

was the salt used as the reactant, then the product was converted to $Cs_2[B_{12}Br_{12}]$ through the addition of CsCl to the solution.

$Na_2[B_{12}H_{12}]$ 7.7 g (193 mmol) of NaOH were added to a solution of 32.06 g (92.6 mmol) of $[Et_3NH]_2[B_{12}H_{12}]$ dissolved in 1000 mL hot water. The solution was heated at a low boil until the volume decreased to 250 mL. The solution was evaporated to dryness using a rotary evaporator. The hygroscopic white solid immediately became visibly hydrated. The product was checked for purity via ^1H and ^{11}B NMR. If necessary, the product was purified further by several hot filtrations until revealed as pure in the ^1H and ^{11}B NMR spectra. ^1H NMR: (300 MHz, δ, D_2O) broad band ~1.2 (Figure 2.2). ^{11}B NMR: (300 MHz, unreferenced), doublet, $^1J_{BH}$= 126 Hz (Figure 2.1).

$Cs_2[B_{12}H_{12}]$ 7.6 g of $CsOH{\cdot}xH_20$ was dissolved in 100 mL of water and added to a solution of 6.82 g (19.7 mmol) $[Et_sNH]_2[B_{12}H_{12}]$ dissolved in 500 mL of hot water. The solution was heated at a low boil until the volume decreased to 200 mL. The solution was evaporated to dryness using a rotary evaporator. The resultant white solid was purified further by several hot filtrations until pure in the ^1H and ^{11}B NMR spectra. ^1H NMR: (300 MHz, δ, D_2O) broad band ~1.2. ^{11}B NMR: (300 MHz, unreferenced), doublet, J_{BH}= 127 Hz.

$Ag_2[B_{12}Br_{12}]$ 1.81 g (1.33 mmol) $Cs_2[B_{12}Br_{12}]$ was dissolved in ~150 mL hot water and allowed to cool. If the pH of the cooled solution was determined to be acidic with universal pH indicator paper, then the solution was made neutral by incrementally adding individual sodium hydroxide pellets, while stirring, and checking the pH after each one dissolved. The solution of $Cs_2[B_{12}Br_{12}]$ was then heated to a boil and cooled.

$Cs_2[B_{12}Br_{12}]$ crystals were collected and dissolved in 100 mL of hot water. Two equivalents of $AgNO_3$ (dissolved in 5 mL water) were added. A white precipitate of $Ag_2[B_{12}Br_{12}]$ immediately formed (90% yield, 1.57 g, 1.20 mmol). $Ag_2[B_{12}Br_{12}]$ was dried under vacuum at 100 °C for at least 4 hours and was determined to be anhydrous by infrared spectroscopy. IR (KBr): 987m, 983s (Figure 2.9).

$M_2[B_{12}Cl_{12}]$ (M = Na or Cs) Into a three-neck round bottom flask approximately 10 g of $M_2[B_{12}H_{12}]$ were added. 150 mL of water were added and the solution was acidified with approximately 1 mL of concentrated hydrochloric acid. The flask was fitted with a water-jacketed condenser, a hose adapter, and a rubber septum. The solution was heated to 90 °C (M = Na) or 135 °C (M = Cs) and chlorine gas was bubbled through the solution. The excess chlorine gas and HCl (g) generated were destroyed by bubbling the effluent gases through a $NaOH/Na_2SO_3$ trap. Aliquots of the mother liquor were periodically removed to determine complete halogenation (by ^{11}B NMR) and the time required ranged over several days. If the sodium salt was used as the reactant, the product was converted to the cesium salt by metathesis with approximately 2 equivalents of cesium chloride and the solution was cooled to room temperature. The sodium salts were found to be extremely hygroscopic, making them very difficult to transfer and weigh. Therefore, $Na_2[B_{12}X_{12}]$ salts were converted to the less hygroscopic cesium salts. $Na_2[B_{12}H_{12}]$ could also be converted to the cesium salt prior to halogenation.

The white precipitate was collected and dissolved in ~300 mL of hot water. If the pH of the cooled solution was determined to be acidic with universal pH indicator paper, then the solution was made neutral by incrementally adding individual sodium hydroxide

pellets while stirring and checking the pH after each one dissolved. The solution of $Cs_2[B_{12}Cl_{12}]$ was then heated to a boil and cooled. $Cs_2[B_{12}Cl_{12}]$ crystals were collected (typical yields ~70%) and the purity was assessed. ^{11}B NMR: (300MHz, unreferenced), singlet (Figure 2.5).

$Ag_2[B_{12}Cl_{12}]$ 2.17 g $Cs_2[B_{12}Cl_{12}]$ (2.64 mmol) were dissolved in 40 mL of water and a solution (1 mL) of aqueous silver nitrate (1.38 g, 8.12 mmol) was added. Any initial precipitate was due to impurities and was removed by filtration. The filtrate volume was reduced by boiling the volume of water down to approximately 30 mL and cooled to room temperature, and then chilled in an ice bath (0 °C). The crystalline white precipitate was collected (68% yield) and dried under vacuum at 100 °C for at least 4 hours. IR (KBr): 1039s, 534m (Figure 2.10).

2.3 Results and Discussion

Although there are several published methods to obtain the $B_{12}H_{12}^{2-}$ cage, the procedure using decaborane described in 1967 was used because it reported a high percentage yield and low formation of other $B_nH_n^{2-}$ cages.[1,3] This method does, however, require the use of decaborane, which is both very costly and toxic. A recent report demonstrates the synthesis of the starting material, $[NEt_3H]_2[B_{12}H_{12}]$, from $NaBH_4$ and I_2, leading to a large scale synthesis with relatively inexpensive starting materials, although with a 51% yield.[4] Either way, the $B_{12}H_{12}^{2-}$ cage has been previously characterized by NMR, IR, and elemental analysis.[3] Recently, however, elemental analysis of compounds containing dodecaborate anions have come into question as they have been shown to be

unreliable.[8] In a report by Gabel, et. al, the elemental analysis of samples of the same compound resulted in inconsistent data.[8] Despite inconsistencies in the elemental analysis, NMR and IR were found to be reliable.

The starting material, triethylammonium salt, $[NEt_3H]_2[B_{12}H_{12}]$, has low solubility in aqueous solutions and produces unwanted side products when the cage is halogenated. Therefore, the salt was converted to a Group 1 salt (Reaction Scheme 2.2). Muetterties described the ^{11}B NMR spectrum of the $B_{12}H_{12}^{2-}$ di-anion as a doublet and the ^{1}H NMR peak as a broad plateau with the ends slightly higher.[9] Figures 2.1 and 2.2 are consistent with this description. Figure 2.1 shows the ^{11}B NMR spectrum of purified $Na_2[B_{12}H_{12}]$. Because all the boron atoms are equivalent, only one signal is expected in the ^{11}B NMR spectrum. However, the peak appears as a doublet due to coupling with hydrogen from the cage. The hydrogen atoms on the cage appear as a broad multiplet in the ^{1}H NMR at 1–2 ppm (Figure 2.2).

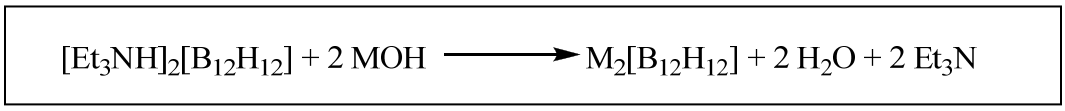

Reaction Scheme 2.2 Synthesis of $M_2[B_{12}H_{12}]$ M = Na or Cs

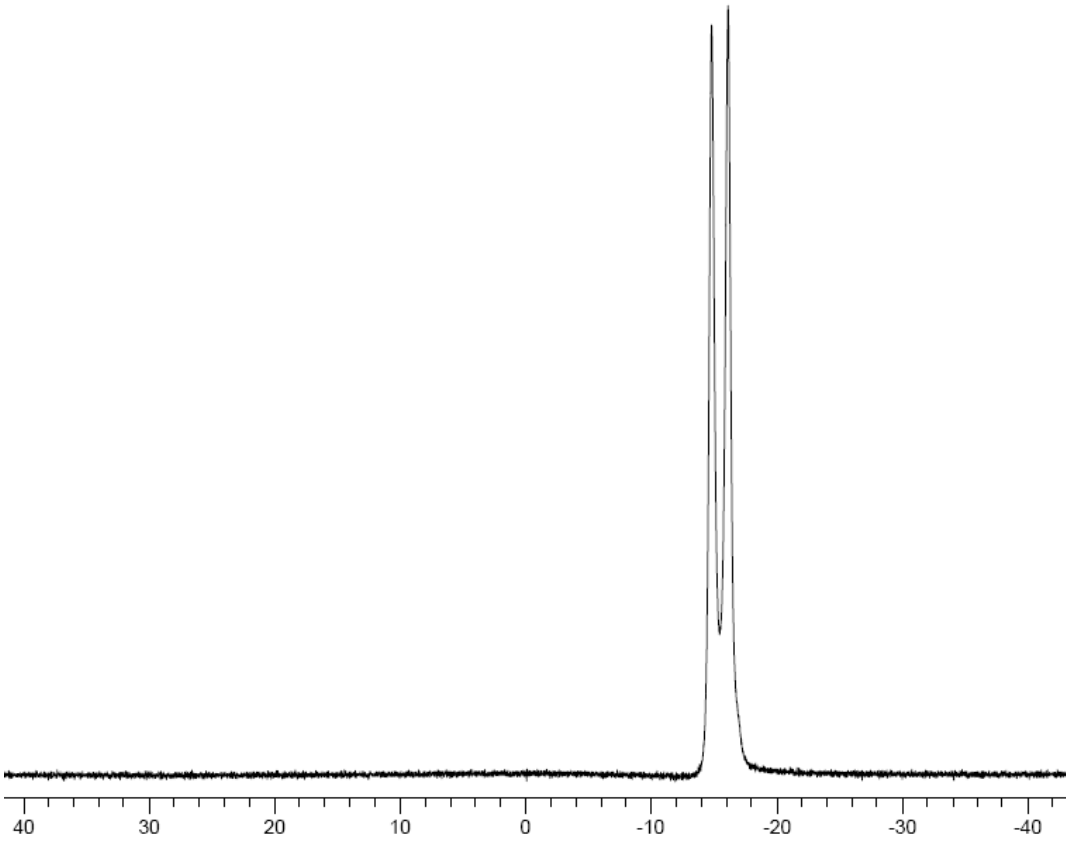

Figure 2.1 ^{11}B NMR spectrum of $Na_2[B_{12}H_{12}]$

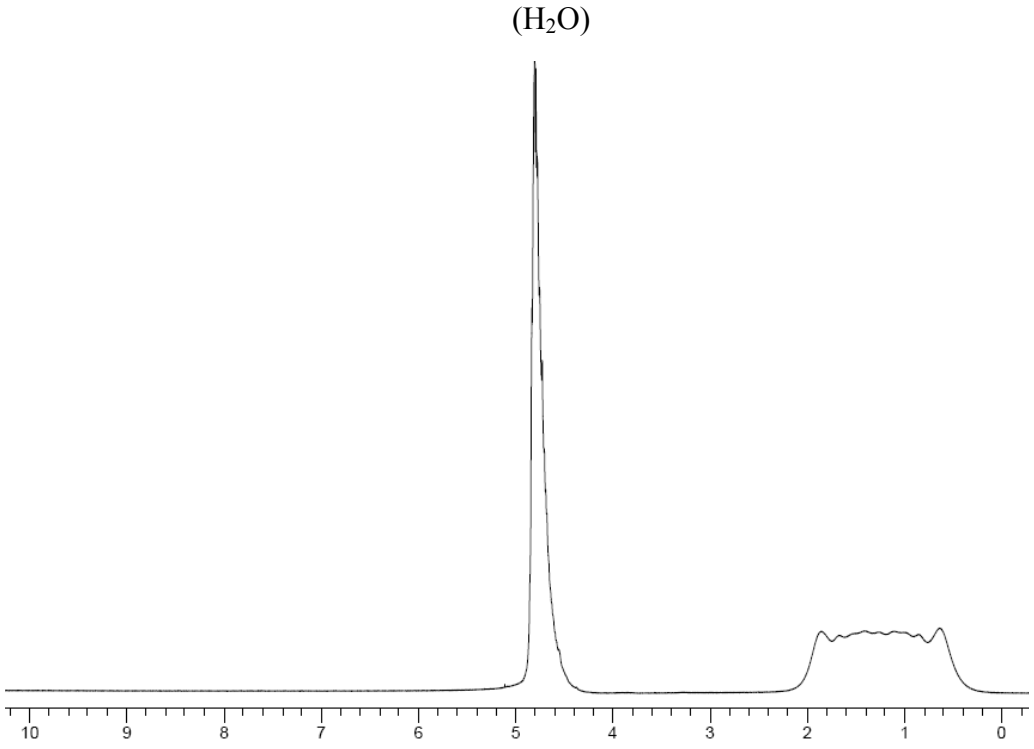

Figure 2.2 ^{1}H NMR spectrum of $Na_2[B_{12}H_{12}]$ in D_2O

When the spectra of the crude reaction product were analyzed, an impurity was observed and is noted in Figures 2.3 and 2.4 with arrows. The peaks are most likely due to the formation of the triethylammonioborane monoanion, $Et_3NB_{12}H_{11}^-$, similar to $R_3NB_{12}H_{11}^-$ (R = H or methyl) anions reported in 1964.[10] These monoanions were synthesized using hydroxylamine-O-sulfonic acid, NH_2OSO_3H, and then alkylated with dimethylsulfate.[10] $Et_3NB_{12}H_{11}^-$ itself was reported as a side product during the formation of the $B_{12}H_{12}^{2-}$ cage from the reaction between decaborane and triethylamine borane, but its characterization was not given.[11] The 12 borons of the cage in $Et_3NB_{12}H_{11}^-$ are no longer symmetrical, and the ^{11}B NMR spectrum would be expected to have four peaks, in the ratios of 1:5:5:1. The peaks would all be doublets, except for one peak which would

be a singlet due to the B-N bond. In the ^{11}B NMR spectra of the crude product, the impurity could not clearly be assigned to be the monoanion, $Et_3NB_{12}H_{11}^-$, but bands may have overlapped. The bands due to the impurity in ^1H NMR spectrum of the crude product were more indicative because the triplet quartet pattern common for ethyl groups was present as shown with arrows in Figure 2.4. Therefore, the impurity was treated as if it was indeed $Et_3NB_{12}H_{11}^-$, and the compound purified as such. In the present work, the mono-anionic salt formed with Na^+ was found to have lower solubility in water than $Na_2[B_{12}H_{12}]$, which has high solubility in water, and was removed with a few hot filtrations and verified via ^1H and ^{11}B NMR.

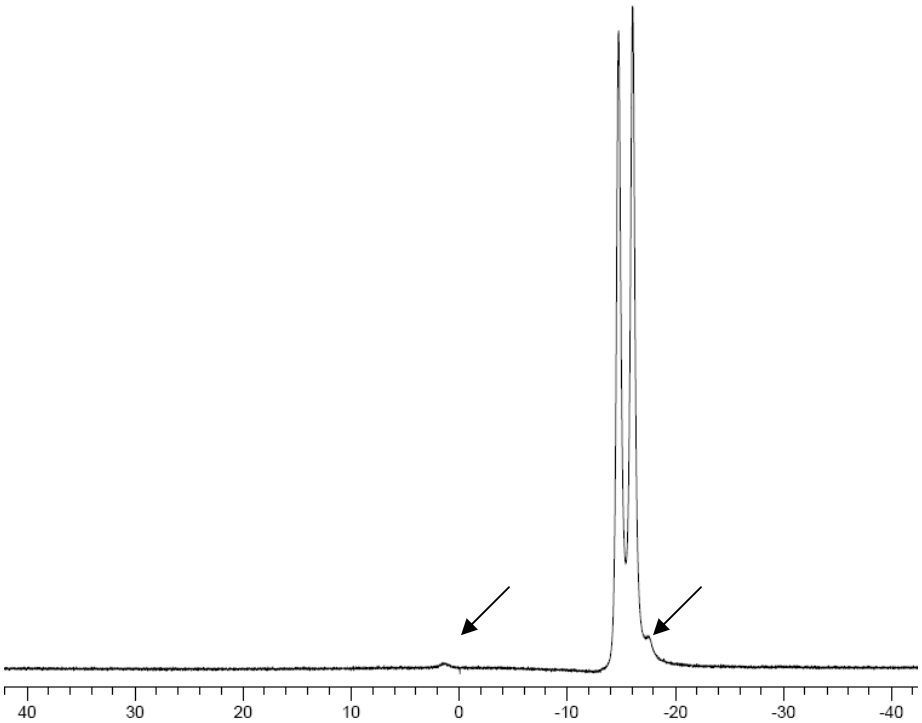

Figure 2.3 ^{11}B NMR spectrum of crude $Na_2[B_{12}H_{12}]$ (unreferenced) (arrows mark impurities)

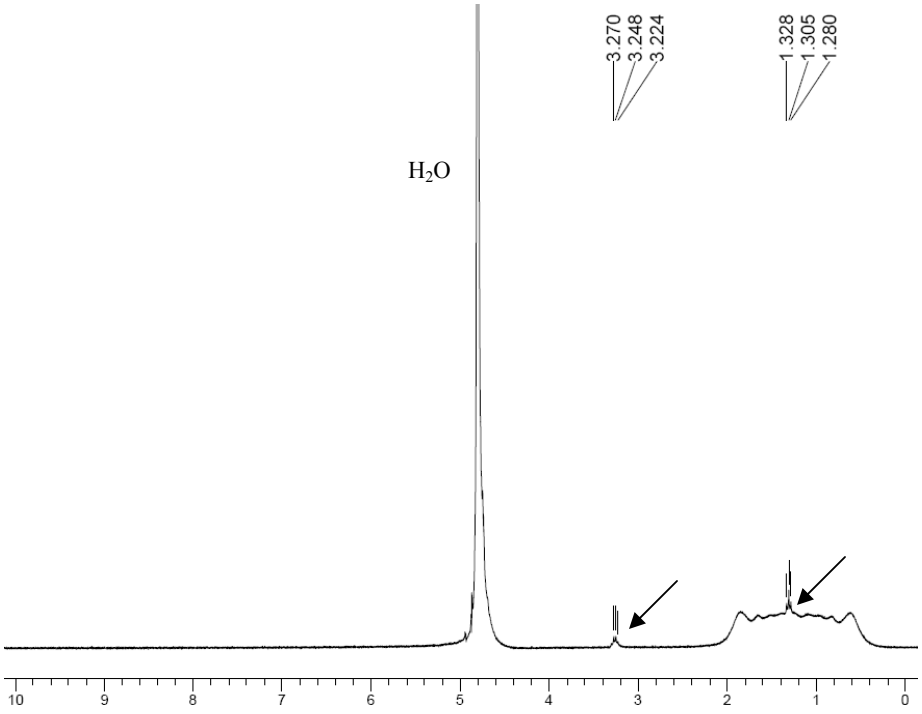

Figure 2.4 ^{1}H NMR spectrum of crude $Na_2[B_{12}H_{12}]$ in D_2O (arrows mark impurities)

The per-halogenation of the cage (Reaction Scheme 2.3) was originally followed by others using IR spectroscopy.[5,12-14] The B-H stretching band, specifically a strong band at about 2480 cm^{-1}, was noted to diminish and the rise of a new strong band, at about 990 cm^{-1} for bromination and 1030 cm^{-1} for chlorination, was used as the guide for per-halogenation.[5] The per-halogenation of the cage was considered complete when the B-H stretching band in the IR spectrum disappeared, and for per-chlorination, the reaction was reported to take 8.5 hours.[5,6] The absence of the B-H stretching band, however, was found not to be indicative of complete halogenation in the present work. In the ^{11}B NMR spectrum, small doublets are still observed after the literature-reported reaction time was allowed to elapse. The doublets collapse to singlets in ^{1}H decoupled ^{11}B NMR spectrum indicating the presence of B-H bonds and incomplete chlorination.

$$M_2[B_{12}H_{12}] + Cl_2\ (g) \xrightarrow{HCl\ (aq)} M_2[B_{12}Cl_{12}] + HCl$$

$$M_2[B_{12}H_{12}] + Br_2\ (l) \xrightarrow{50\%\ aq\ methanol} M_2[B_{12}Br_{12}] + HBr$$

Reaction Scheme 2.3 Halogenation of $B_{12}H_{12}^{2-}$

Based on the ^{11}B NMR spectrum, several days were required for completion of the per-chlorination reaction instead of the reported 8.5 hrs.[6] In the ^{11}B NMR spectrum, the doublet collapses to a singlet, as shown in Figures 2.5 and 2.6 for $B_{12}Cl_{12}^{2-}$ and $B_{12}Br_{12}^{2-}$, respectively, due to all the boron atoms being identical and no longer having adjacent NMR-active nuclei. This effect was also recently noted by Knapp.[4] In the ^{1}H NMR spectrum, the broad signal due to the hydrogens bonded to borons of the cage is gone, as can be noted in Figure 2.7 and 2.8 for $B_{12}Cl_{12}^{2-}$ and $B_{12}Br_{12}^{2-}$, respectively.

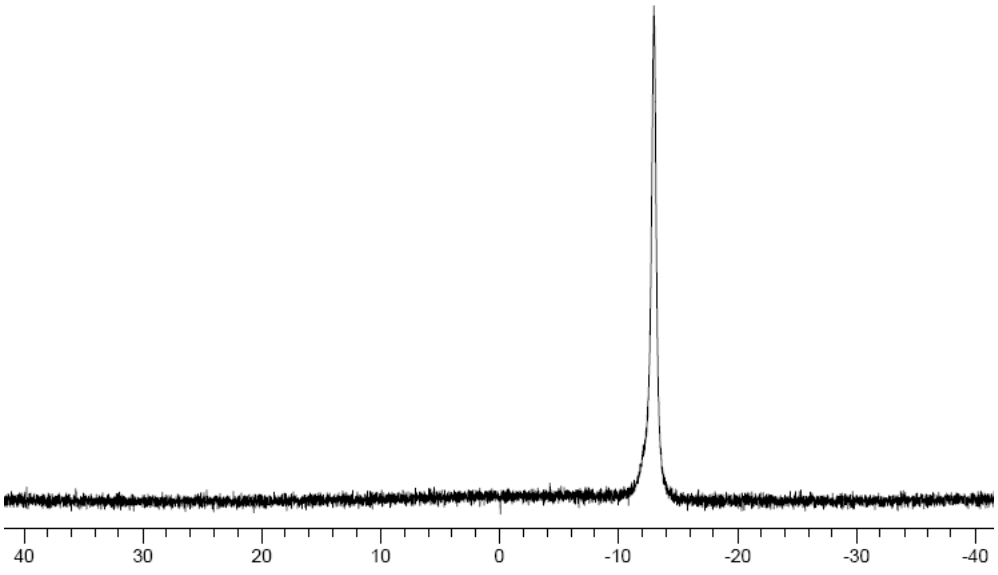

Figure 2.5 ^{11}B NMR spectrum of $Cs_2[B_{12}Cl_{12}]$ in reaction solution (unreferenced)

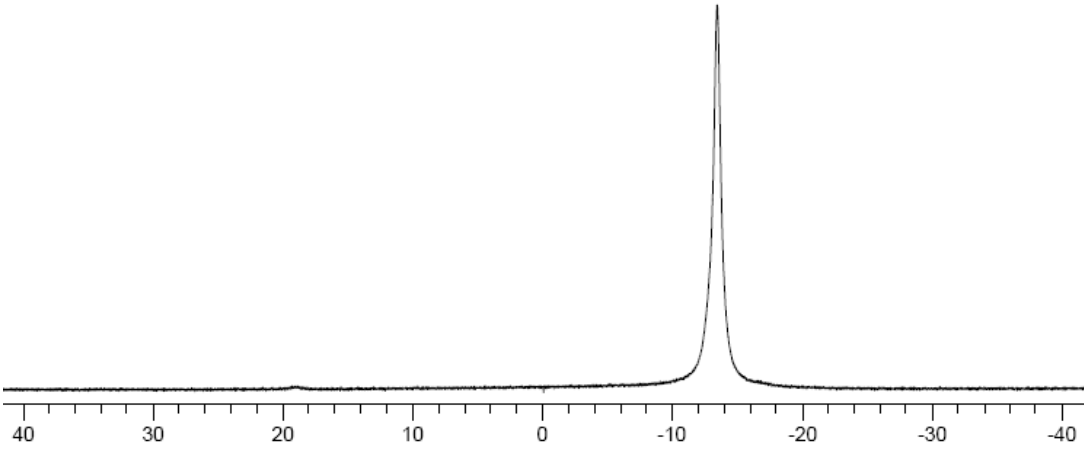

Figure 2.6 ^{11}B NMR spectrum of $Na_2[B_{12}Br_{12}]$ in reaction solution (unreferenced)

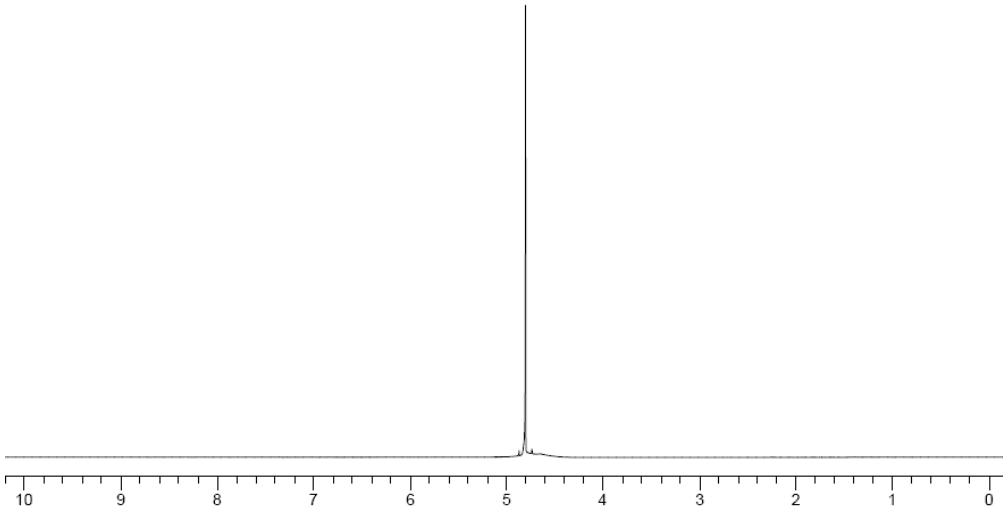

Figure 2.7 ^{1}H NMR spectrum of $Cs_2[B_{12}Cl_{12}]$ in D_2O

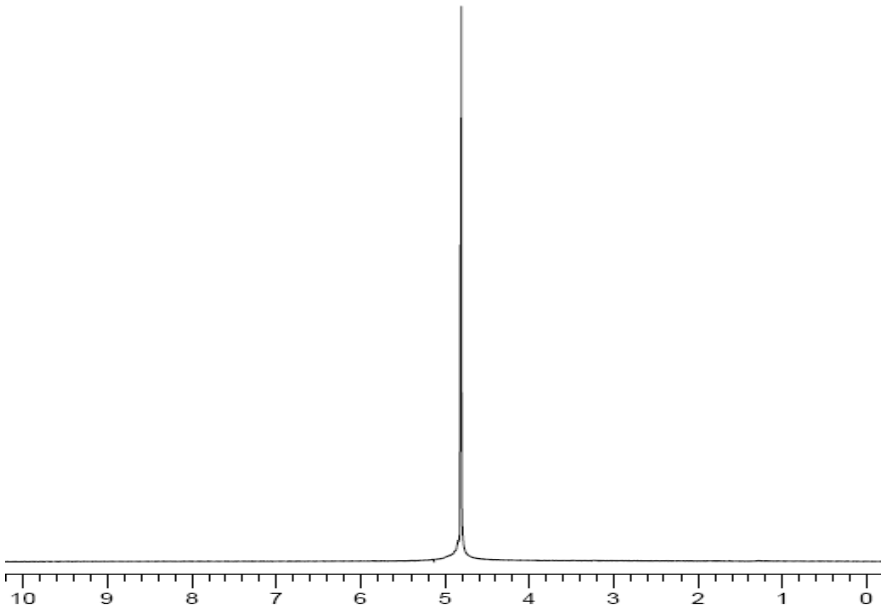

Figure 2.8 ^{1}H NMR spectrum of $Na_2[B_{12}Br_{12}]$ in D_2O

The metathesis to $Ag_2[B_{12}Br_{12}]$ was followed by heating the solid under vacuum in order to remove trace amounts of water. $Ag_2[B_{12}Br_{12}]$ was determined to be anhydrous by IR spectroscopy. The IR spectrum of the anhydrous product (Figure 2.9) shows the characteristic strong B-Br and B-B stretching bands at 997 and 983 cm^{-1}, respectively, and the minimal signal of νOH at ~3650 cm^{-1}.

$Ag_2[B_{12}Cl_{12}]$ was found to be very soluble in water and hygroscopic. The salt was made anhydrous by heating under vacuum, and was determined to be anhydrous by IR spectroscopy (Figure 2.10). The IR spectrum of $Ag_2[B_{12}Cl_{12}]$ has characteristic strong bands at 1039 cm^{-1} (due to B-Cl and B-B stretching) and at 534 cm^{-1}. The spectra for both samples were obtained in the solid state as KBr pellets.

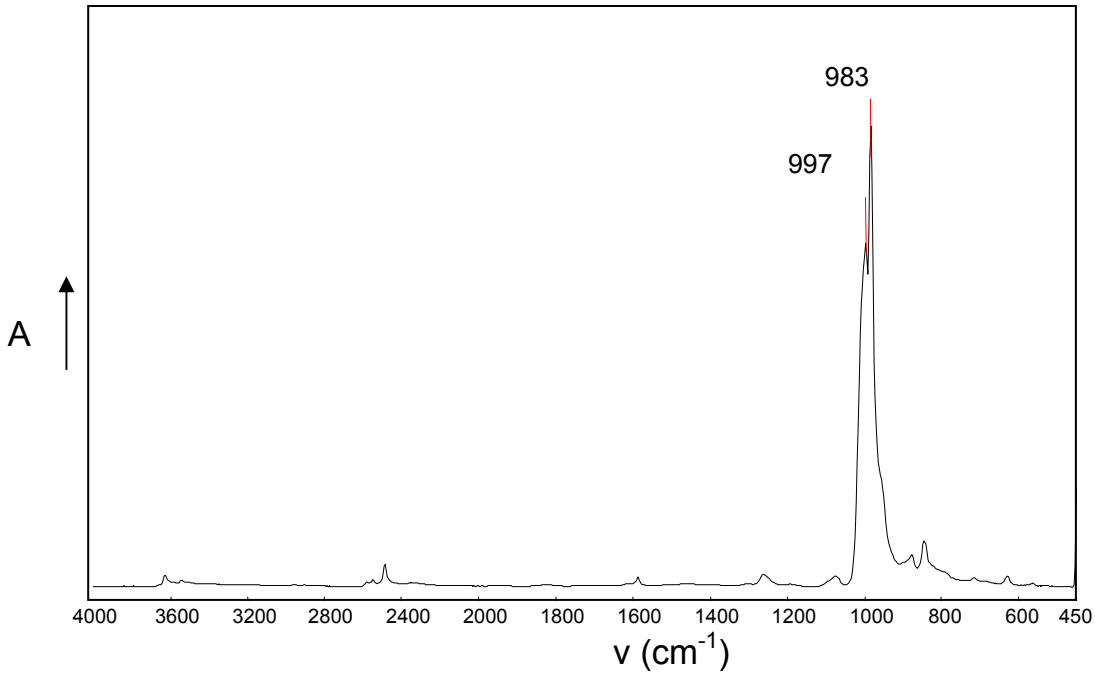

Figure 2.9 FT-IR spectrum of $Ag_2[B_{12}Br_{12}]$

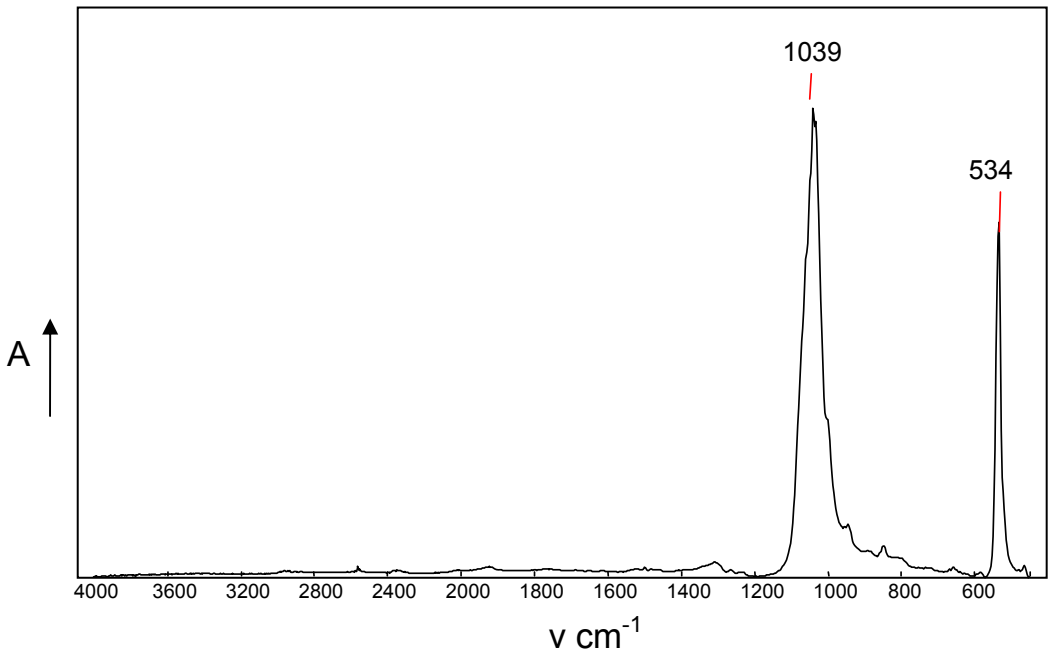

Figure 2.10 FT-IR spectrum of $Ag_2[B_{12}Cl_{12}]$

2.4 Conclusions

The $B_{12}H_{12}^{2-}$ anion was synthesized and halogenated following modified literature procedures, specifically in the purification of the products and in the ensuing per-halogenation. For example, the metathesis to cesium salts allowed for better isolation of the products from the mother liquor. Drying the silver salts by heating under vacuum was determined to be an important step to remove water. These purification steps were found to be critical because the presence of unremoved impurities or solvents interferes with their subsequent chemistry as described in later chapters.

The silver salts of the $B_{12}X_{12}^{2-}$ ions displayed characteristics similar to their carborane analogues. $Ag_2[B_{12}Br_{12}]$ was found to be insoluble in water as is $Ag[CHB_{11}H_5Br_6]$. $Ag_2[B_{12}Cl_{12}]$ was found to be very soluble in water, as is $Ag[CHB_{11}Cl_{11}]$. The identification of these products and the establishment of their purity has been recently reported.[4] Since both silver salts can be made anhydrous by simply heating under vacuum for several hours, they are suitable for the isolation of reactive cations such as trityl, and in uses where even trace amounts of water are deleterious.

2.5 References

1. "Chemistry of *closo*-Dodecaborate Anion $[B_{12}H_{12}]^{2-}$: A Review," Sivaev, I.B.; Bregadze, V.I.; Sjoberg, S. *Collect. Czech. Chem. Commun.* **2002**, *67*, 679-727.

2. "A Convenient Preparation of $B_{12}H_{12}^{2-}$ Salts," Ellis, I.A.; Schaeffer, R.; Gaines D.F. *J. Am. Chem. Soc.* **1963**, *85*, 3885.

3. Miller, H.C.; Muetterties, E.L. *Inorg. Synth.* **1967**, *10*, 88-91.

4. "Synthesis and Characterization of Synthetically Useful Salts of the Weakly-Coordinating Dianion $[B_{12}Cl_{12}]^{2-}$," Geis, V.; Guttsche, K.; Knapp, C.; Schere, H.; Uzun, R. *Dalton Transactions* **2009**, *15*, 2687-2694.

5. "Chemistry of Boranes. IX. Halogenation of $B_{10}H_{10}^{2-}$ and $B_{12}H_{12}^{2-}$," Knoth, W.H.; Miller, H.C.; Sauer, J.C.; Balthis, J.H.; Chia, Y.T.; Muetterties, E.L. *Inorg. Chem.* **1964**, *3*, 159-167.

6. "Lithium Closoborane Electrolytes III. Preparation and Characterization," Johnson, J.W.; Brody, J.F. *J. Electrochem. Soc.,* **1982***, 129*, 2213-2219.

7. Perrin, D.D.; Armarego, W.L.F.; Perrin, D.R. *Purification of Laboratory Chemicals*; 2nd ed, Pergamon Press Ltd.: Sydney, **1980**.

8. "Trialkylammoniododecaborates: Anions for Ionic Liquids with Potassium, Lithium, and Protons as Cations," Justus, E.; Rischka, K.; Wishart, J.F.; Werner, K.; Gabel, D. *Chem. Eur. J.* **2008**, *14*, 1918- 1923.

9. "Chemistry of Boranes. VIII. Salts and Acids of $B_{10}H_{10}^{2-}$ and $B_{12}H_{12}^{2-}$," Muetterties, E.L.; Balthis, J.H.; Chia, Y.T.; Knoth, W.H.; Miller, H.C. *Inorg. Chem.* **1964**, *3*, 444-451.

10. "Chemistry of Boranes. XIV. Amination of $B_{10}H_{10}^{2-}$ and $B_{12}H_{12}^{2-}$ with Hydroxylamine-O-Sulfonic Acid," Hertler, W.R.; Raasch, M.S. *J. Am. Chem. Soc.* **1964**, *86*, 3661-3668.

11. "A Novel Synthesis of the $B_{12}H_{12}^{2-}$ Anion," Greenwood, N.N.; Morris, J.H. *Proceedings of the Chemical Society of London*. **1963**, 338.

12. "Chemistry of Boranes III. The Infrared and Raman Spectra of $B_{12}H_{12}^{2-}$ and Related Anions," Muetterties, E.L.; Merrifield, R.E.; Miller, H.C.; Knoth Jr., W.H.; Downing, J.R. *J. Am. Chem. Soc.* **1962**, *84*, 2506-2508.

13. "Vibrations in Icosahedral Boron Molecules and in Elemental Boron Solids," Weber,

W.; Thorpe, M.F. *J. Phys. Chem. Solids* **1975**, *36*, 967- 974.

14. "Vibrational Spectra of Icosahedral Closoborate Anions $B_{12}X_{12}^{2-}$ (X=H, D, Cl, Br, I)," Leites, L.A.; Bukalov, S.S.; Kurbakova, A.P.; Kaganski, M.M.; Gaft, Y.U.; Kuznetsov, N.T.; Zakharova, I.A. *Spectrochim. Acta* **1982**, *38 A*, 1047-1056.

CHAPTER 3

Synthesis of Trityl Salts and Silylium Derivatives of $B_{12}X_{12}^{2-}$

3.1 Introduction

The carbocation, triphenylmethyl (trityl), is one of chemistry's classical carbocations. It was first observed in 1901 and since then has been extensively studied.[1] Trityl salts containing weakly coordinating counterions, such as the tetraphenylborates and carboranes, $CB_{11}Y_5X_6^-$, (where Y = CH_3, X, or H and X = Cl, Br, or I) have recently been characterized.[2] Trityl carborane salts have had immediate use in several important metathesis reactions.[3] The di-anion, $B_{12}X_{12}^{2-}$ (where X = F, Cl, or Br), also has the potential to serve as the counter-ion to the trityl cation. In 2003, Strauss and co-workers reported the crystal structure of the trityl salt with the $B_{12}F_{12}^{2-}$ di-anion. The authors alluded to the preliminary synthesis of a more reactive trialkyl silylium compound but further work has yet to be reported.[4] Since the preparation of $B_{12}F_{12}^{2-}$ requires specialized equipment and training, the trityl salts with the di-anions $B_{12}Br_{12}^{2-}$ and $B_{12}Cl_{12}^{2-}$ were the targets in this chapter as the precursors to the silylium derivatives.

One key application for the trityl carborane has been as a hydride abstractor from tri-alkyl and -aryl silanes.[5] The crystallization of the extremely electrophilic product, silylium ($R_3Si^{\delta+}$) carborane, answered an important question regarding how analogous the cationic nature of silicon was when compared to carbon.[6] Total ionic character of the silicon center was achieved when the substituents on silicon were bulky mesityl groups.[6] Depending on the R group, silylium carborane compounds are best classified as "ion-

like". As well, silylium compounds have been of interest due to the ability of the silicon center to coordinate with very weak nucleophiles such as *ortho*-dichlorobenzene (ODCB), SO_2, and even to trialkylsilanes.[7]

Silylium carboranes are the precursors to some of the strongest isolable Brønsted acids known, with the strongest being $H(CHB_{11}Cl_{11})$.[3] If the trityl and silylium compounds using the di-anions are isolated, then there is the possibility that the *di*-protic Brønsted acid may also be isolated. Since the preliminary report of the formation of silylium compounds with $B_{12}F_{12}^{2-}$, both the $B_{12}Cl_{12}^{2-}$ and $B_{12}Br_{12}^{2-}$ ions are considered as potential counterions to the trialkyl silylium moiety. This chapter will discuss the synthesis and structural characterization of new silylium compounds using these anions.

3.2 Experimental

Air–sensitive materials were handled in helium filled Vacuum Atmospheres gloveboxes (O_2, H_2O < 2 ppm) or on a vacuum manifold using standard Schlenk techniques. Acetonitrile, benzene, hexanes, ODCB, and toluene were dried following literature methods and stored under molecular sieves.[8] Bromotriphenylmethane, purchased from Acros Organics, was used as received. NMR spectra were obtained on a Bruker Avance 300 MHz spectrometer. FTIR spectra were obtained on a Perkin Elmer Spectrum 100 Series spectrometer in a nitrogen filled glovebox.

$[Ph_3C]_2[B_{12}Br_{12}]$·2toluene, 1. $Ag_2[B_{12}Br_{12}]$ (1.65 g, 1.27 mmol) was dissolved in acetonitrile (175 mL). Bromotriphenylmethane (0.82 g, 2.55 mmol) was added and the solution slowly changed from colorless to dark red. The dark red slurry was left stirring at

room temperature overnight. The off-white precipitate (AgBr) was removed by filtration, the filtrate volume was decreased to approximately 20 mL, and the red-orange solid was collected. This solid was washed with 3x1 mL portions of hexane, and then dried under vacuum in a Schlenk tube at 95 °C for at least 4 hours. A crystal suitable for X-ray diffraction was obtained by layering a saturated solution of **1** in toluene with hexane. Full details for the X-ray crystal structure are listed in Appendix A. (1.29 g, 65%) ^{1}H NMR: (300 MHz, δ, CD_3CN), 7.72 (dd, 12H), 7.88 (t, 12H), 8.28 (t, 6H). ^{11}B NMR: (300 MHz, unreferenced), singlet. IR (KBr): 3058w, 1580s, 1481s, 1449s, 1355s, 1294s, 1184m, 995s, 981s, 840m, 804w, 765s, 699s, 622w, 608w.

$[Ph_3C]_2[B_{12}Cl_{12}]$·2ODCB, 2. $Ag_2[B_{12}Cl_{12}]$ (2.27 g, 2.95 mmol) was dissolved in acetonitrile (50 mL). Bromotriphenylmethane (2.18 g, 6.75 mmol) was dissolved in toluene (15 mL) and added to the $Ag_2[B_{12}Cl_{12}]$ solution. Precipitation of both AgBr and $[Ph_3C]_2[B_{12}Cl_{12}]$ was observed, so 100 mL of acetonitrile was added and the mixture was left to stir at room temperature for at least 5 hours. The orange slurry was filtered off and the precipitate washed several times with acetonitrile until the remaining precipitate (AgBr) was off-white. The filtrate volume was decreased to approximately 20 mL, and the orange precipitate was collected, washed with 3x1 mL hexane, and placed into a Schlenk tube for drying under vacuum at 95 °C for at least 4 hours. A crystal suitable for X-ray diffraction was obtained by layering a saturated solution of **2** in ODCB with hexane. Full details for the X-ray crystal structure are presented in Appendix B. (1.7053 g, 56%) ^{1}H NMR: (300 MHz, δ, CD_3CN), 2.33 (s, toluene), 7.23 (m, toluene), 7.71 (d), 7.89 (t, 24H), 8.28 (t, 6H). ^{11}B NMR: (300 MHz, unreferenced), singlet. IR (KBr):

3061w, 1579s, 1476m, 1452m, 1358s, 1297m, 1188m, 1033m, 994m, 848m, 760m, 708m, 698m, 623w, 532m.

$(Et_3Si)_2(B_{12}Br_{12})$·ODCB, 3. Approximately 1 mL of ODCB was added to **1** (150 mg, 0.16 mmol) and stirred. A few drops of $(C_2H_5)_3SiH$ were added and the solution turned from orange to colorless. The solution was left stirring over several days during which a white precipitate formed. The solid was collected via filtration. A crystal suitable for X-ray diffraction was obtained by layering a saturated solution of **3** in ODCB with hexane. Full details for the X-ray crystal structure are shown in Appendix C. (0.30 g, 73%) ^{1}H NMR: (300 MHz, δ, ODCB-d_4), 0.92(t, 18H), 1.36 (q, 12H). ^{11}B NMR: (300 MHz, unreferenced), singlet. IR (KBr): 2965m, 2941m, 2911w, 2880m, 2335w, 2310w, 1667w, 1575w, 1455m, 1436m, 1385m, 1234m, 1128w, 1008s, 985s, 973s, 842w, 747s, 736s, 676s, 581m.

$[Et_3Si\text{-}H\text{-}SiEt_3]_2[B_{12}Br_2]$, 4. This compound was synthesized in a similar manner as **3** except that a greater excess of triethylsilane was used. IR (KBr): 2962m, 2936w, 2906w, 2877m, 1872 broad, 1594w, 1452m, 1398m, 1380m, 1226m, 979s, 895, 841w, 780m, 739m, 675s, 580m, 564m, 477m, 442m, 431m.

$(Et_3Si)_2[B_{12}Cl_2]$, 5. Approximately 1 mL of ODCB was added to **2** (358.7 mg, 0.3443 mmol) and stirred, forming an orange slurry. About 3.5 equivalents of triethylsilane (150 mg, 1.2 mmol) were added. The solution slowly changed from orange to colorless over a day and a white precipitate was formed, which was filtered off and washed with 2x1 mL of dry hexane. A crystal suitable for X-ray diffraction was obtained by layering a saturated solution of **4** in ODCB with hexane. Full details for the X-ray crystal structure

are in Appendix D. (262.7 mg, 96%) ^{1}H NMR: (300 MHz, δ, ODCB-d_4), 0.91 (t, 18H), 1.31 (q, 12H). ^{11}B NMR (Fig. S11): (300 MHz, unreferenced), singlet. IR (KBr): 2966m, 2941w, 2922w, 2913w, 2883m, 1464m, 1454m, 1405m, 1384m, 1325m, 1228m, 1064s, 1044s, 989s, 903w, 758s, 750s, 688s, 605w, 574w, 540s, 513s.

$[Et_3Si\text{-}H\text{-}SiEt_3]_2[B_{12}Cl_2]$, 6. This compound was synthesized in a similar manner as **5** except that a greater excess of triethylsilane was used. IR: 2969m, 2941m, 2913w, 2882m, 2309w, 2200w, 1879 broad, 1455m, 1404m, 1385w, 1229m, 1033s, 884w, 839w, 751m, 678m, 537s.

3.3 Results and Discussion

The metathesis reaction between bromotriphenylmethane and silver carborane is driven by the precipitation of silver bromide and results in the formation of $[Ph_3C][CHB_{11}X_{11}]$. Initially, the same procedure used in the preparation of $[Ph_3C][CHB_{11}X_{11}]$ was used to prepare $[Ph_3C]_2[B_{12}X_{12}]$. The halide abstraction occurred as determined by the change in color of the colorless slurry to an orange-red slurry and is shown in Reaction Scheme 3.1. Not anticipated, however, was the very low solubility of $[Ph_3C]_2[B_{12}X_{12}]$ in the toluene/acetonitrile ratio initially used.

Initial attempts to isolate the trityl salts following the procedure used for the analogous trityl carboranes were unsuccessful. The volume of toluene was increased in an attempt to improve the solubility of $[Ph_3C]_2[B_{12}X_{12}]$, but this increase did not aid the solubility of the product. The volume of acetonitrile used was then increased significantly. In the analogous carborane synthesis, a few drops of acetonitrile are used in

order to improve solubility of the product, but too much added acetonitrile may result in the formation of oils. In order to dissolve $[Ph_3C]_2[B_{12}X_{12}]$, however, volumes in excess of 200 mL of dry acetonitrile were used and minimal amounts of toluene were used to dissolve the reactant, trityl bromide, in a separate flask before adding to the reaction flask. When the solutions were mixed, oil formation was not observed. The solid silver bromide was removed by filtration and almost 100% recovered by weight. The filtrate volume was reduced significantly under vacuum and a precipitate formed which was yellow-orange to dark orange, depending on the anion.

$$Ag_2\,[B_{12}X_{12}] + 2(C_6H_5)_3CBr \xrightarrow{CH_3CN} [(C_6H_5)_3C]_2\,[B_{12}X_{12}] + 2\,AgBr$$

Reaction Scheme 3.1 Synthesis of $[(C_6H_5)_3C]_2[B_{12}X_{12}]$

Although the problem of $[Ph_3C]_2[B_{12}X_{12}]$ insolubility was solved, the crude solid product was found to contain occluded acetonitrile. If the acetonitrile was not removed, the formation of byproducts in the subsequent steps was observed. Therefore, solid $[Ph_3C]_2[B_{12}X_{12}]$ was heated to 95–100 °C under vacuum for several hours to remove any residual solvents. ^{1}H NMR and ^{11}B NMR spectra were obtained for both $[Ph_3C]_2[B_{12}Br_{12}]$ and $[Ph_3C]_2[B_{12}Cl_{12}]$ before and after the heating of the solids, because the ^{1}H NMR spectrum changes after the solvent is removed. The ^{1}H NMR spectrum (Figure 3.1) of the solvated $[Ph_3C]_2[B_{12}Br_{12}]$ before heating has a broadened arene resonance (~7.0–7.5 ppm). This broad resonance was also reported by Hoffmann with the salt

$[Ph_3C][CHB_{11}Cl_{11}]$, due to that salt also being solvated.[9] After heating under vacuum, the ^1H NMR spectrum changed to a pattern similar but not identical to that of the analogous carborane salts. The ^1H NMR spectrum of $[Ph_3C][CHB_{11}Cl_{11}]$, after heating under vacuum, contained in the arene region the following peak pattern: triplet, triplet, and doublet.[9] The ^1H NMR spectrum of the dried $[Ph_3C]_2[B_{12}Br_{12}]$ contained the pattern: triplet, triplet, and a doublet of doublets (Figure 3.2). The ^{11}B NMR spectrum remained unchanged before and after heating, containing a single peak (Figure 3.3) because the cage itself was unchanged from $B_{12}X_{12}^{2-}$. The IR spectrum for $[Ph_3C]_2[B_{12}Br_{12}]$ is shown in Figure 3.4 and contains similar bands as reported by Xie for $[Ph_3C][CHB_{11}H_5Br_6]$.[2]

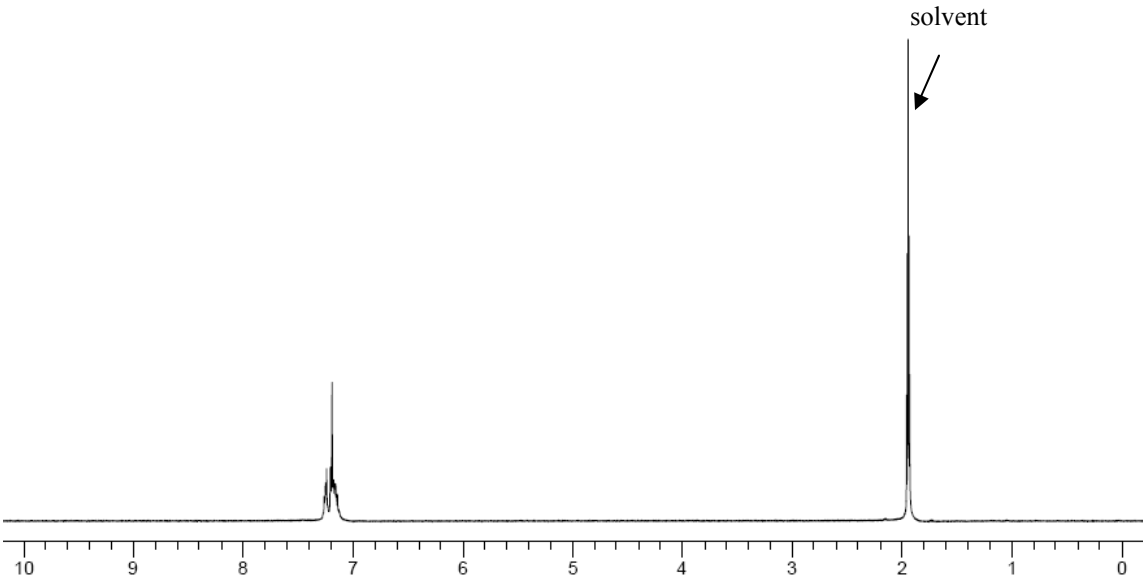

Figure 3.1 ^1H NMR (CD_3CN) spectrum of $[Ph_3C]_2[B_{12}Br_{12}]$ before heating the solid

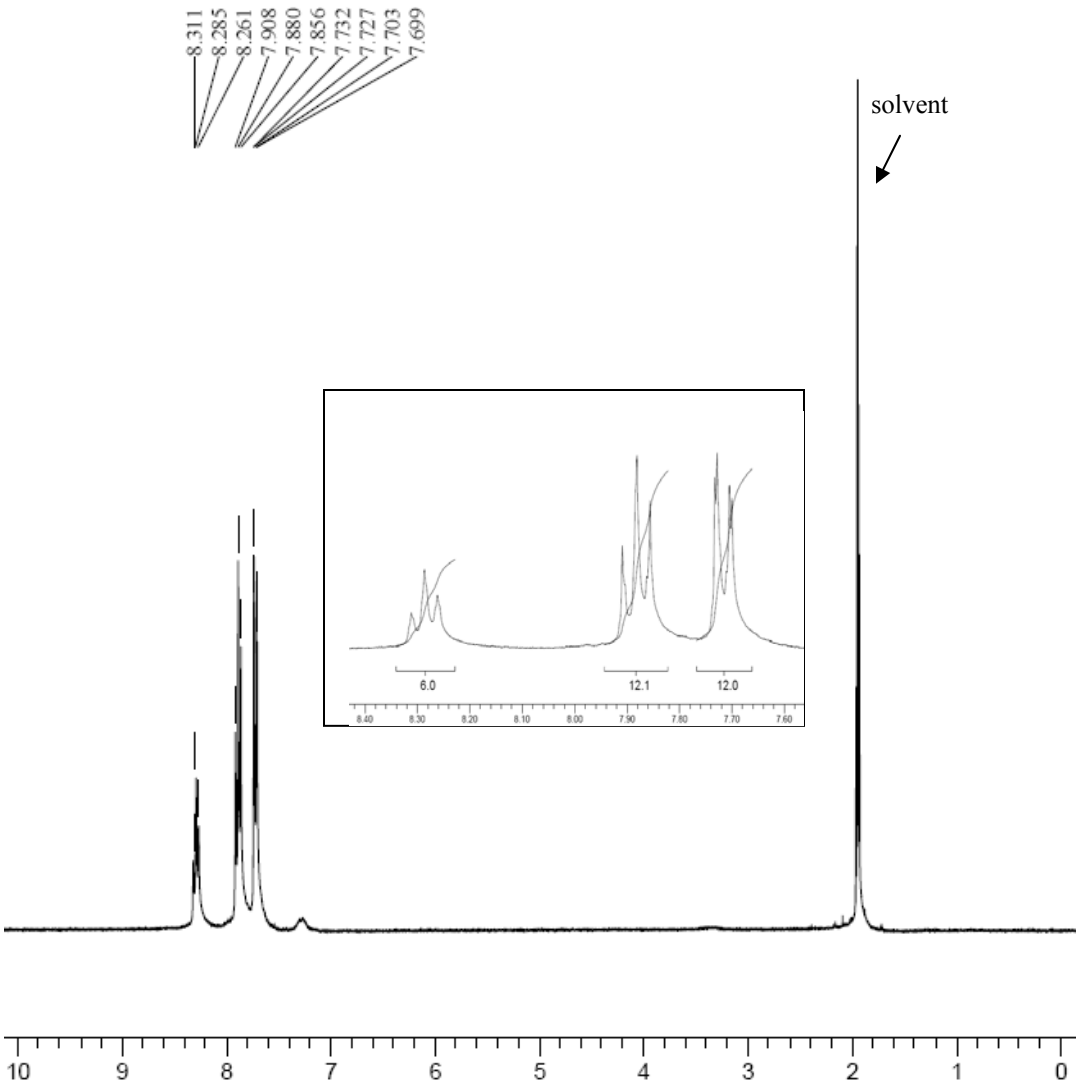

Figure 3.2 ^{1}H NMR (CD_3CN) spectrum of $[Ph_3C]_2[B_{12}Br_{12}]$ after heating the solid

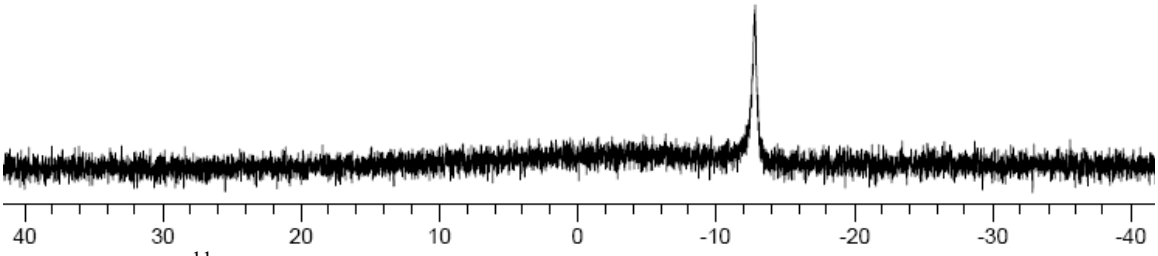

Figure 3.3 ^{11}B NMR (CD_3CN) spectrum of $[Ph_3C]_2[B_{12}Br_{12}]$ after heating the solid (unreferenced)

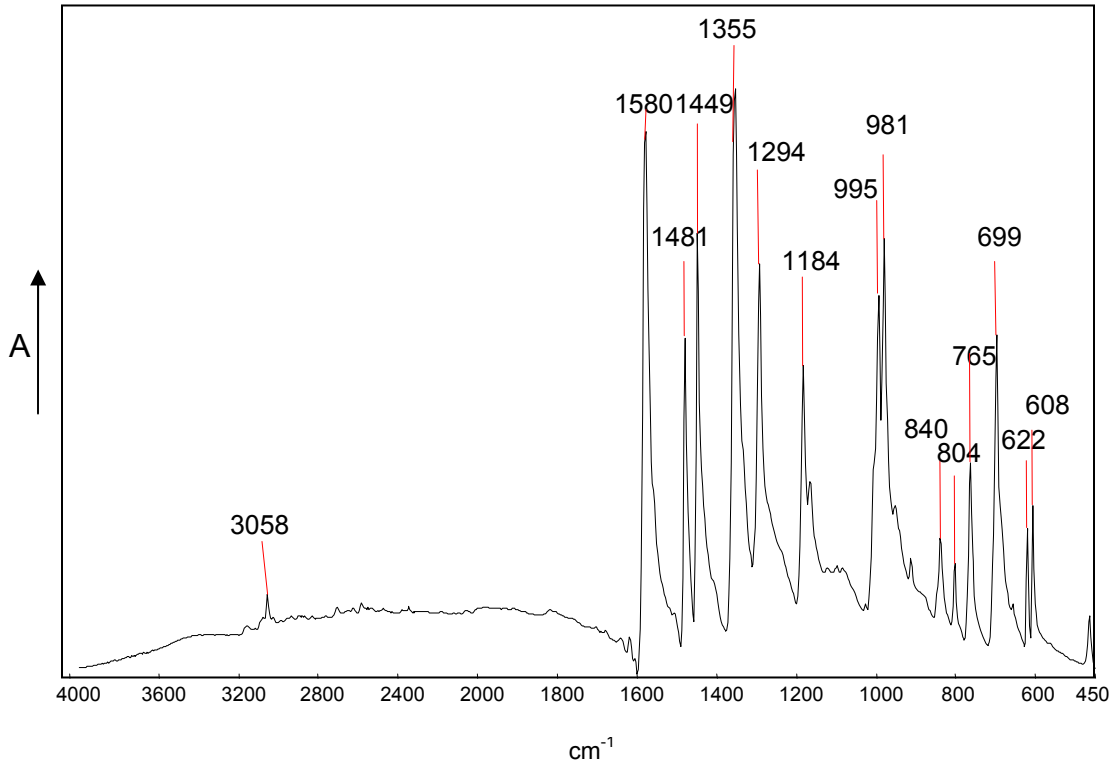

Figure 3.4 FT-IR spectrum of $[Ph_3C]_2[B_{12}Br_{12}]$ after heating the solid

The ^{1}H NMR spectrum of $[Ph_3C]_2[B_{12}Cl_{12}]$ (Figure 3.5) had a broad peak downfield (7–8 ppm) when the crude product was analyzed. After the product was heated under vacuum, the expected arene peak pattern was observed (Figure 3.6), although it is evident that even after heating the sample, toluene was still present. Toluene was

minimized though by washing the crude product with hexanes and then drying. The ^{11}B NMR spectrum remained unchanged before and after heating, and the ^{11}B NMR spectrum after heating is shown in Figure 3.7. The IR spectrum of $[Ph_3C]_2[B_{12}Cl_{12}]$ (Figure 3.8) is also consistent with a trityl salt based on comparison to the trityl carborane IR spectrum reported by Reed, et al.[2] The spectrum in figure 3.8 is similar to the FT-IR spectrum of $[Ph_3C]_2[B_{12}Br_{12}]$ further supporting the formation of the trityl salts.

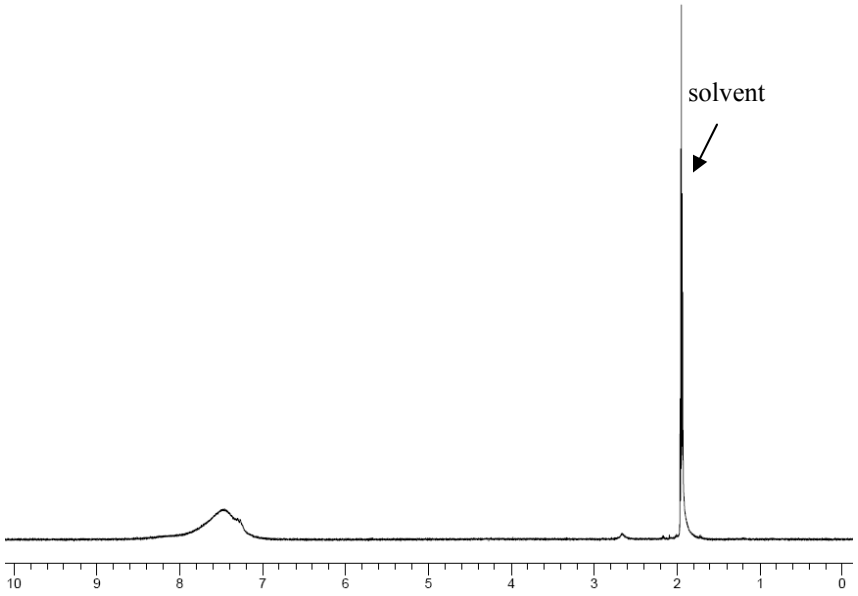

Figure 3.5 ^1H NMR (CD_3CN) spectrum of $[Ph_3C]_2[B_{12}Cl_{12}]$ before heating the solid

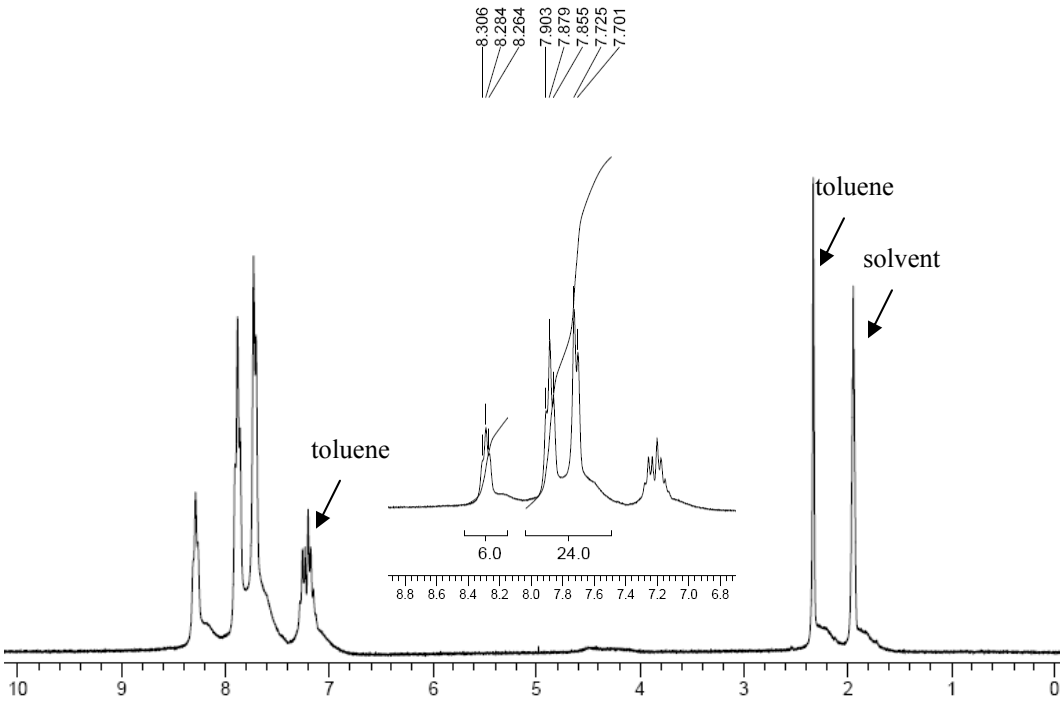

Figure 3.6 ^{1}H NMR (CD_3CN) spectrum of $[Ph_3C]_2[B_{12}Cl_{12}]$ after heating the solid

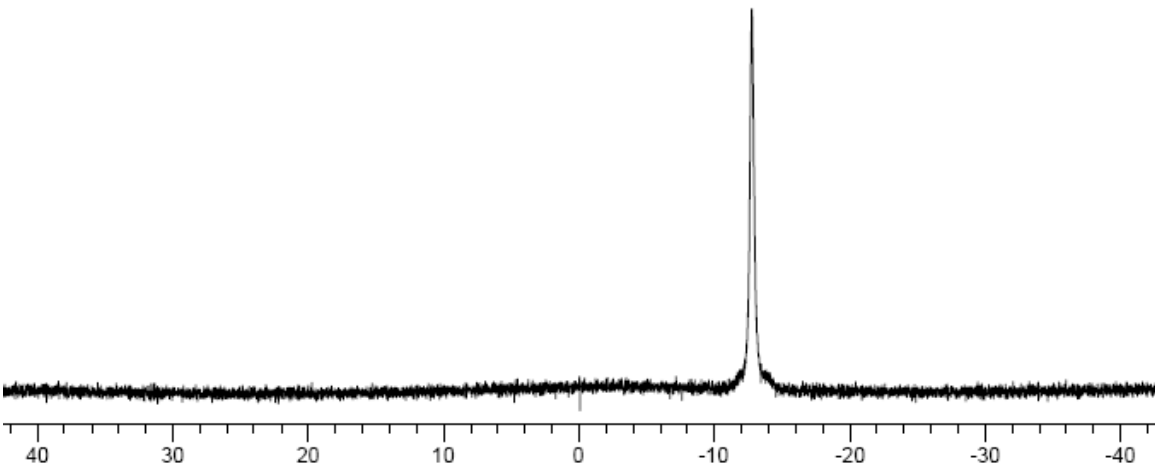

Figure 3.7 ^{11}B NMR (CD_3CN) spectrum of $[Ph_3C]_2[B_{12}Cl_{12}]$ after heating the solid

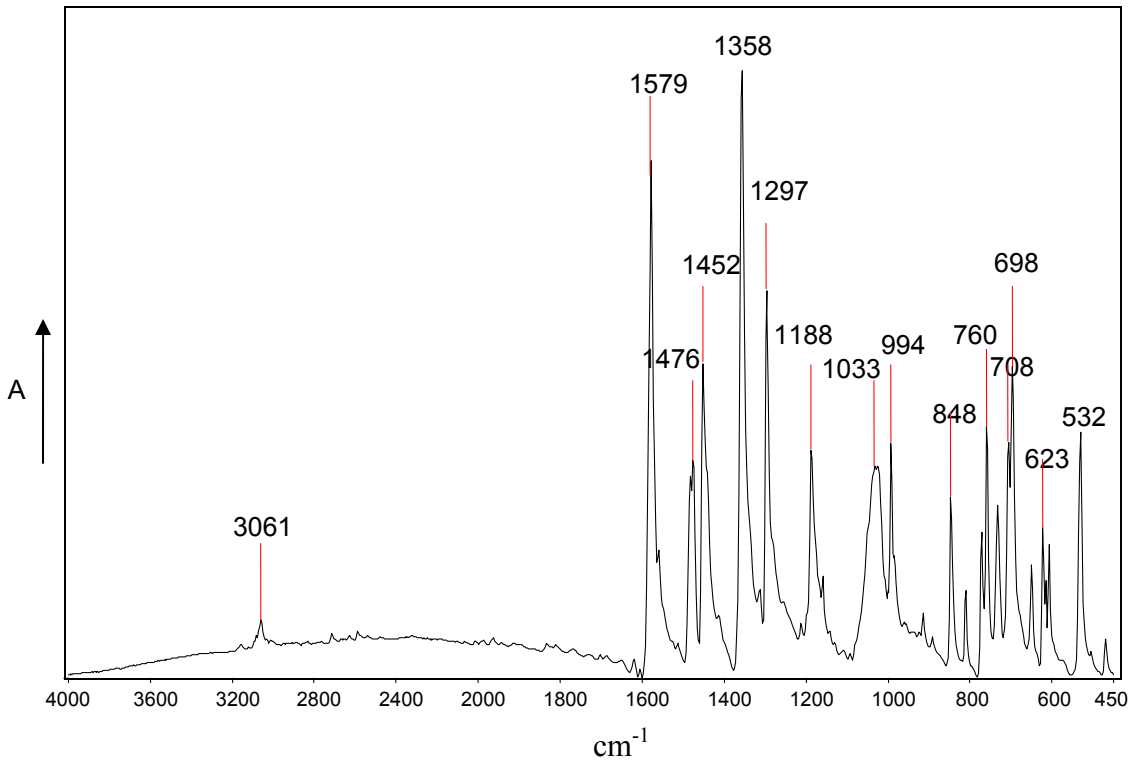

Figure 3.8 FT-IR spectrum of $[Ph_3C]_2[B_{12}Cl_{12}]$ after heating

The structures of both $[Ph_3C]_2[B_{12}Br_{12}]\cdot 2$toluene (Figure 3.9) and $[Ph_3C]_2[B_{12}Cl_{12}]\cdot 2$ODCB (Figure 3.10) have been determined by X-ray diffraction. Structure and refinement data are shown in Table 3.1 for $[Ph_3C]_2[B_{12}Br_{12}]\cdot 2$toluene and in Table 3.2 for $[Ph_3C]_2[B_{12}Cl_{12}]\cdot 2$ODCB. It is interesting to note that the structure of a similar trityl salt, $[(C_6H_5)_3C]_2[B_{12}F_{12}]$ had been previously determined, as the per-fluorinated B_{12} cage is also expected to be a WCA.[2] The dimensions of the trityl cation are similar to the reported values.[2]

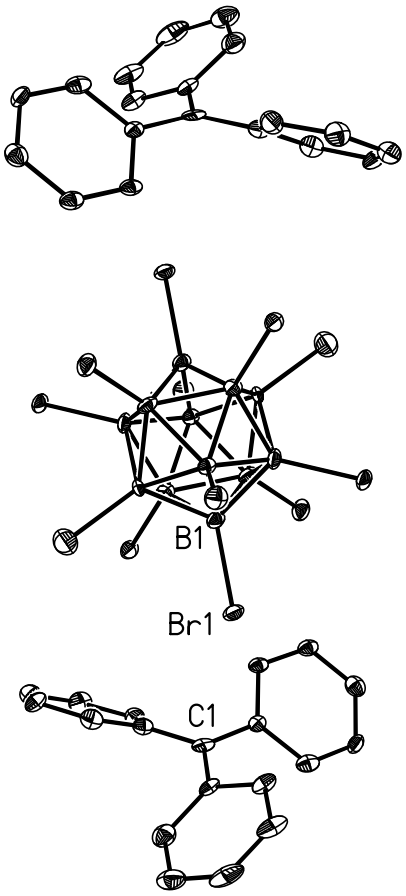

Figure 3.9 Thermal ellipsoid plot of $[Ph_3C]_2[B_{12}Br_{12}]\cdot 2$toluene (50% probability ellipsoids except for hydrogen atoms, which are not shown. Solvent omitted for clarity.)

Table 3.1 Crystal structure and refinement data for $[Ph_3C]_2[B_{12}Br_{12}]\cdot 2$toluene

Identification code	cr215_0m	
Empirical formula	C26 H23 B6 Br6	
Formula weight	879.76	
Temperature	100(2) K	
Wavelength	0.71073 Å	
Crystal system	Monoclinic	
Space group	P2(1)/n	
Unit cell dimensions	a = 9.9081(4) Å	α = 90°.
	b = 15.7107(7) Å	β = 90.6020(10)°.
	c = 18.9335(9) Å	γ = 90°.
Volume	2947.1(2) $Å^3$	
Z	4	
Density (calculated)	1.983 Mg/m^3	
Absorption coefficient	8.192 mm^{-1}	
F(000)	1676	
Crystal size	0.07 x 0.06 x 0.01 mm^3	
Theta range for data collection	1.68 to 26.37°.	
Index ranges	-12<=h<=12, -19<=k<=19, -23<=l<=23	
Reflections collected	34988	
Independent reflections	6031 [R(int) = 0.0972]	
Completeness to theta = 26.37°	100.0 %	
Absorption correction	None	
Max. and min. transmission	0.9226 and 0.6180	
Refinement method	Full-matrix least-squares on F^2	
Data / restraints / parameters	6031 / 0 / 344	
Goodness-of-fit on F^2	1.026	
Final R indices [I>2sigma(I)]	R1 = 0.0463, wR2 = 0.0985	
R indices (all data)	R1 = 0.0824, wR2 = 0.1123	
Largest diff. peak and hole	1.067 and -1.913 $e.Å^{-3}$	

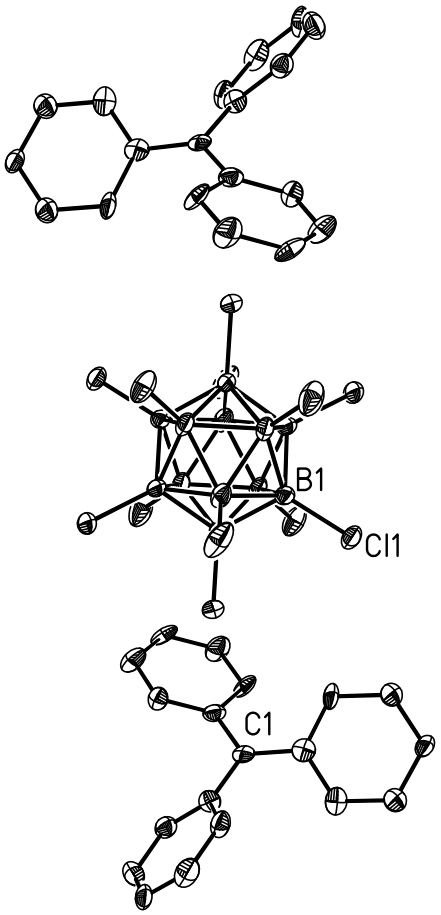

Figure 3.10 Thermal ellipsoid plot of $[Ph_3C]_2[B_{12}Cl_{12}]\cdot 2ODCB$ (50% probability ellipsoids except for hydrogen atoms, which are not shown. Solvent omitted for clarity.)

Table 3.2 Crystal structure and refinement data for $[Ph_3C]_2[B_{12}Cl_{12}]\cdot 2ODCB$

Identification code	cr303_0m	
Empirical formula	C25 H19 B6 Cl8	
Formula weight	667.86	
Temperature	100(2) K	
Wavelength	0.71073 Å	
Crystal system	Monoclinic	
Space group	C2/c (#15)	
Unit cell dimensions	a = 30.6533(12) Å	α = 90°.
	b = 10.2904(4) Å	β = 111.5814(7)°.
	c = 19.7470(8) Å	γ = 90°.
Volume	5792.2(4) $Å^3$	
Z	8	
Density (calculated)	1.532 Mg/m^3	
Absorption coefficient	0.796 mm^{-1}	
F(000)	2680	
Crystal size	0.34 x 0.05 x 0.02 mm^3	
Theta range for data collection	2.10 to 24.71°.	
Index ranges	-36<=h<=36, -12<=k<=12, -23<=l<=23	
Reflections collected	44242	
Independent reflections	4931 [R(int) = 0.0991]	
Completeness to theta = 24.71°	100.0 %	
Absorption correction	Semi-empirical from equivalents	
Max. and min. transmission	0.9843 and 0.7730	
Refinement method	Full-matrix least-squares on F^2	
Data / restraints / parameters	4931 / 1014 / 599	
Goodness-of-fit on F^2	1.058	
Final R indices [I>2sigma(I)]	R1 = 0.0418, wR2 = 0.0806	
R indices (all data)	R1 = 0.0866, wR2 = 0.0987	
Largest diff. peak and hole	0.878 and -0.489 $e.Å^{-3}$	

Hydride abstraction from triethylsilane by trityl cation formed cation-like triethylsilylium carboranes, Et_3Si(carborane), when trityl carborane salts were used. The analogous reaction with $[Ph_3C]_2[B_{12}X_{12}]$ is shown in Reaction Scheme 3.2. Both $(Et_3Si)_2(B_{12}Br_{12})$ and $(Et_3Si)_2(B_{12}Cl_{12})$ were isolated and characterized. $(Et_3Si)_2(B_{12}Br_{12})$ was sufficiently soluble in ODCB-d_4 to obtain both ^1H and ^{11}B NMR spectra (Figures 3.11 and 3.12). The triplet-quartet pattern characteristic of ethyl protons was observed in the ^1H NMR spectrum. $(Et_3Si)_2(B_{12}Cl_{12})$ was much more soluble in ODCB-d_4 than was $(Et_3Si)_2(B_{12}Br_{12})$. The corresponding ^1H and ^{11}B NMR spectra for $(Et_3Si)_2(B_{12}Cl_{12})$ are shown in Figures 3.13 and 3.14. In the ^1H NMR spectrum of each compound, there appears to be a slight aromatic impurity, which may be the solvent from the synthesis and are the circled peaks in the ^1H NMR spectra.

$$[(C_6H_5)_3C]_2[B_{12}X_{12}] + 2\ Et_3SiH \xrightarrow{\text{ODCB}} (Et_3Si)_2(B_{12}X_{12}) + 2\ (C_6H_5)_3CH$$

Reaction Scheme 3.2 Synthesis of $(Et_3Si)_2(B_{12}X_{12})$

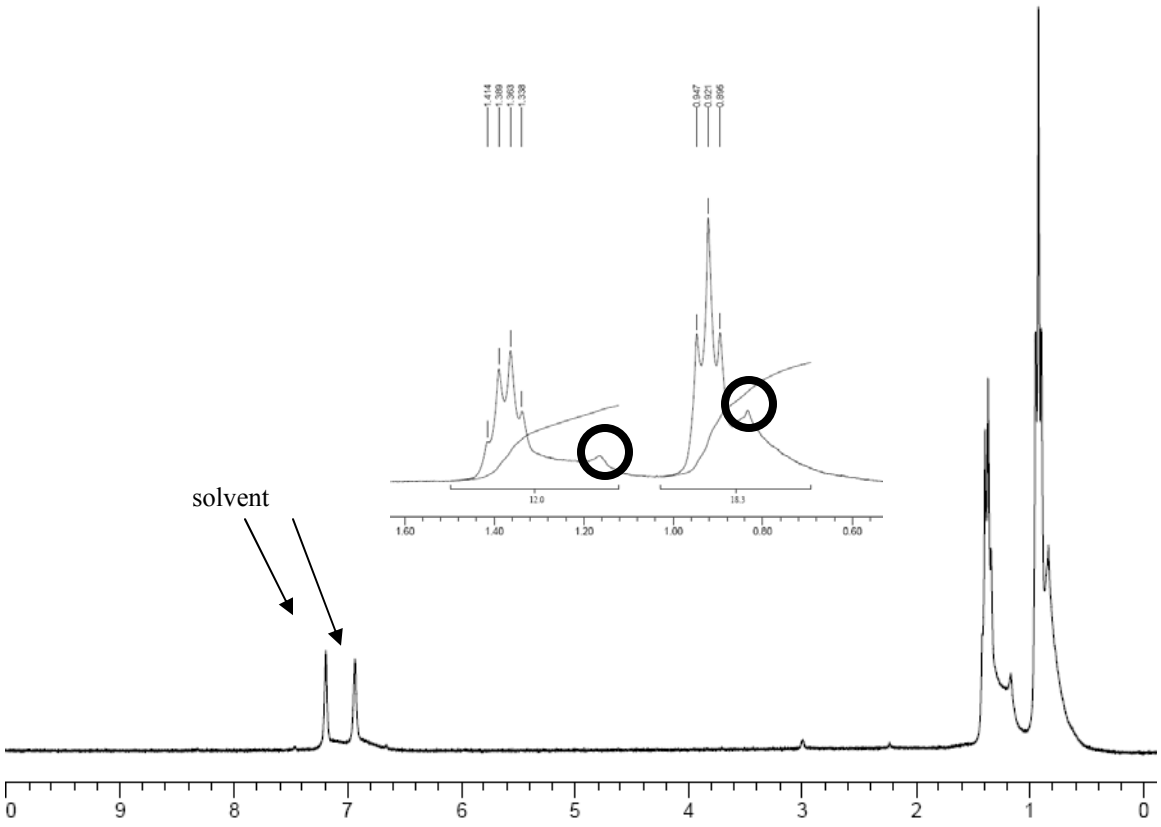

Figure 3.11 ^{1}H NMR spectrum of $(Et_3Si)_2(B_{12}Br_{12})$ in ODCB-d_4

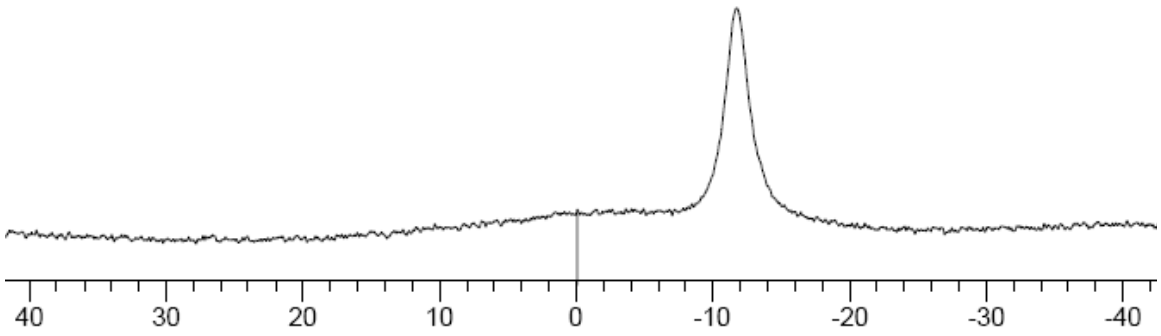

Figure 3.12 ^{11}B NMR spectrum of $(Et_3Si)_2(B_{12}Br_{12})$ (unreferenced)

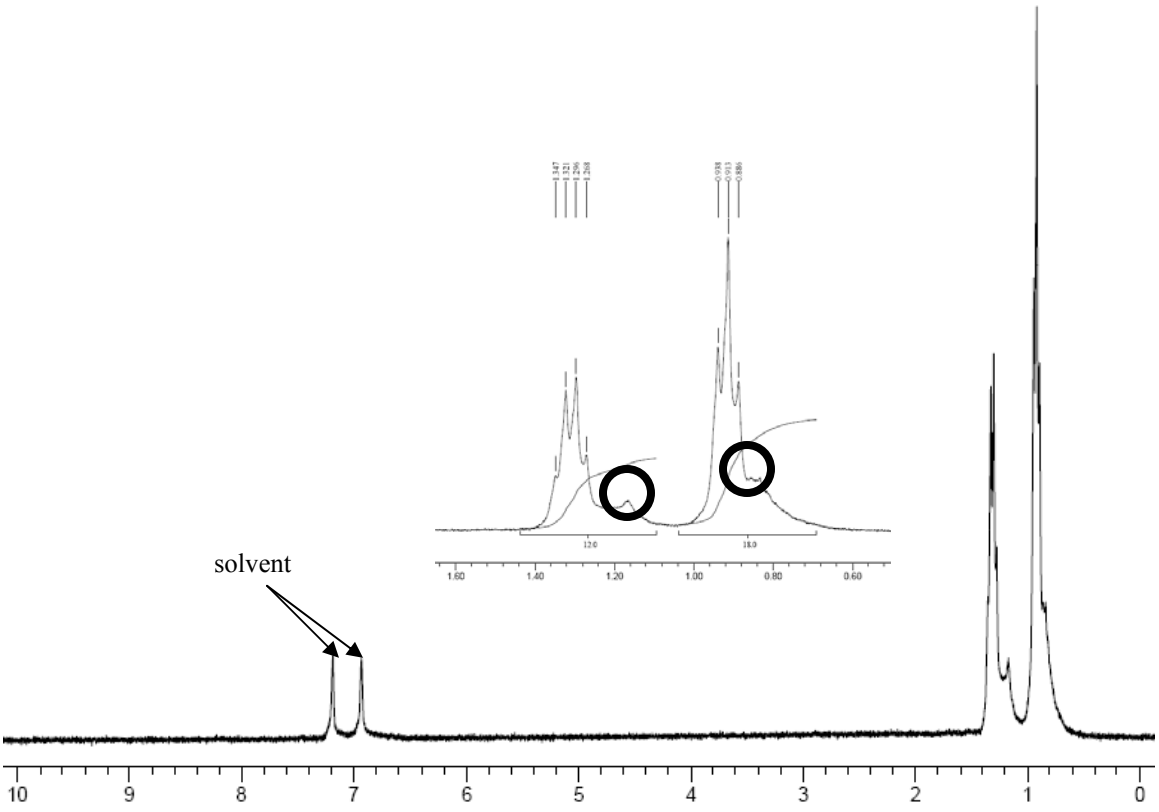

Figure 3.13 ^{1}H NMR spectrum of $(Et_3Si)_2(B_{12}Cl_{12})$ in ODCB-d_4

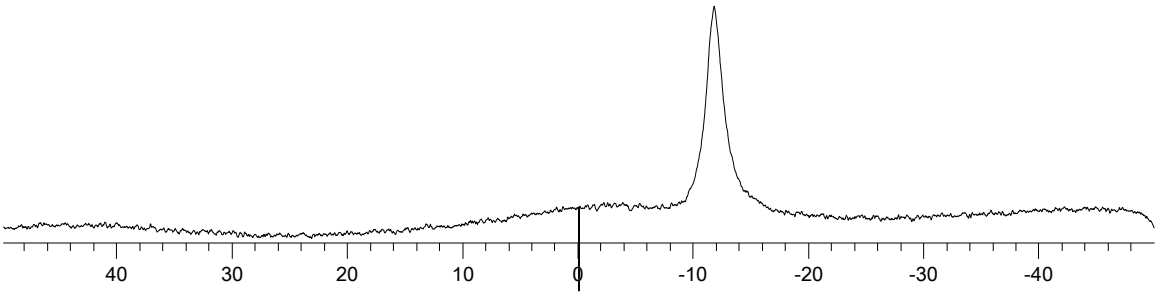

Figure 3.14 ^{11}B NMR spectrum of $(Et_3Si)_2(B_{12}Cl_{12})$ (unreferenced)

The ^{1}H NMR spectra of $(Et_3Si)_2(B_{12}Br_{12})$ and $(Et_3Si)_2(B_{12}Cl_{12})$ were very similar. The peaks due to the ethyl groups were split in the expected triplet-quartet pattern, although the quartet, assigned to the methylene hydrogens based on integrated intensity, was further downfield than the triplet. The pattern switch is characteristic of ethyl groups attached to the silicon center. As well, in the ^{1}H NMR spectra for both compounds, there are broad signals adjacent to the triplet and the quartet, which may be due to hexanes.

Due to the presence of the solvent bands in the IR spectrum, it was evident from the IR spectroscopic data of both $(Et_3Si)_2(B_{12}Br_{12})$ and $(Et_3Si)_2(B_{12}Cl_{12})$ that it was necessary to use ODCB as the solvent for the synthesis. Benzene and toluene were more difficult to remove from the solid and were subsequently protonated in the acid preparation. For example, the IR spectrum (Figure 3.15) of $(Et_3Si)_2(B_{12}Br_{12})$, when synthesized in toluene, results in residual toluene still present and the peaks due to toluene are circled in the spectrum. The ^{1}H NMR spectrum also shows the presence of the arene. Similar results were obtained when benzene was used as a solvent.

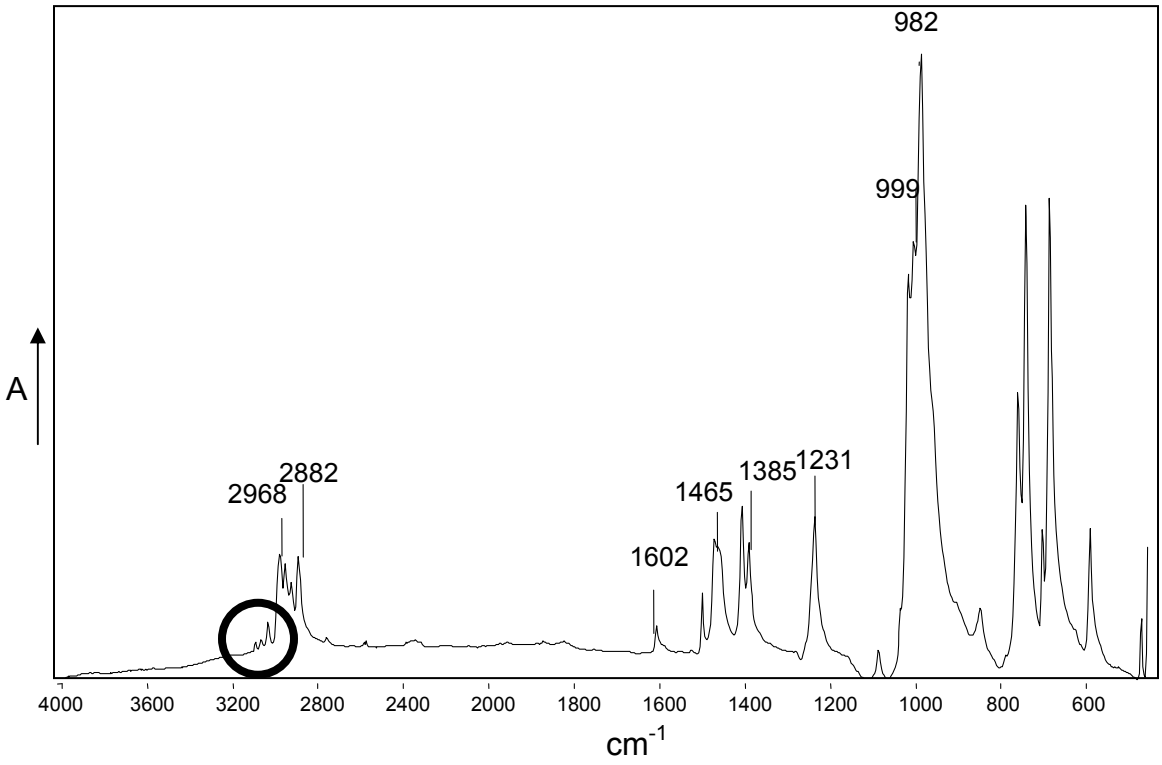

Figure 3.15 FT-IR spectrum of $(Et_3Si)_2(B_{12}Br_{12})$ synthesized in toluene

When excess amounts of triethylsilane were used with the trityl salts, the IR spectrum of the product indicated the presence of hydride bridging between two triethylsilylium groups, i.e., formation of the $[Et_3Si–H–SiEt_3]^+$ cation. Such bridging has occurred with the use of $CHB_{11}Cl_{11}^-$ as a counterion.[7] The asymmetric Si–H–Si stretching frequency occurs as a broad and intense peak at about 1900 cm^{-1} in $[Et_3Si–H–SiEt_3][CHB_{11}Cl_{11}]$.[7] A similar broad peak at 1872 cm^{-1} is attributed to the Si–H–Si bridge in the $B_{12}Br_{12}^{2-}$ salt (Figure 3.16) and at 1879 cm^{-1} for the $B_{12}Cl_{12}^{2-}$ salt (Figure 3.17). The observation of the hydride–bridging silylium cations when either di-anion is used brings forth the realization that despite the di-negative charge, both di-anions are as weakly coordinating as their mono-anion counterparts.

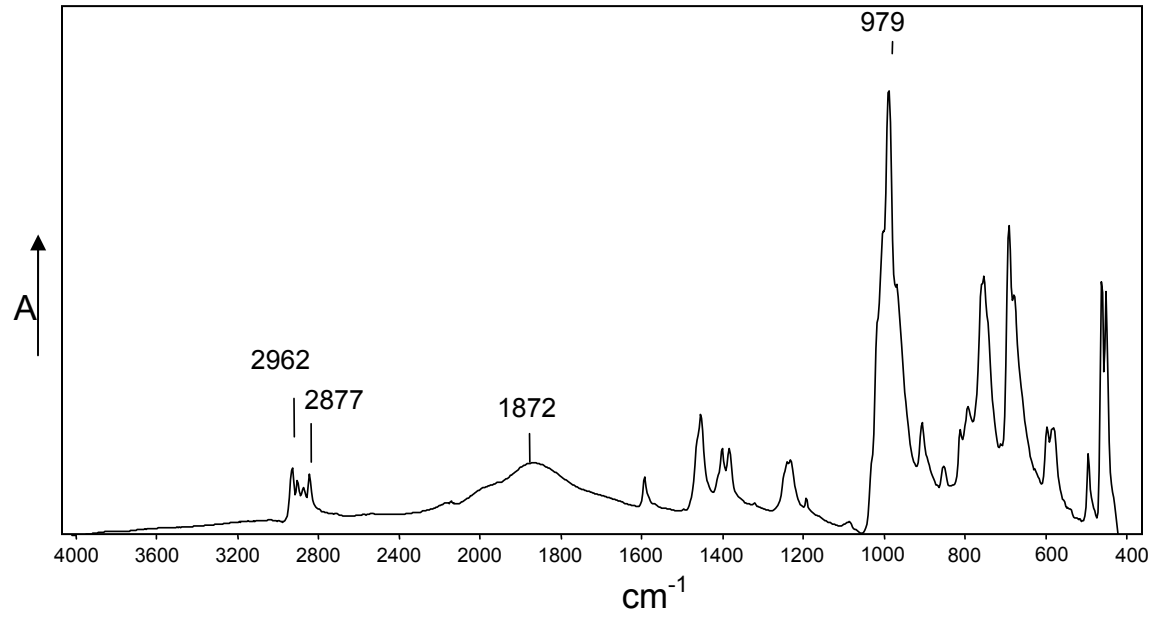

Figure 3.16 FT–IR spectrum of $[Et_3Si–H–SiEt_3]^+$ with $B_{12}Br_{12}^{2-}$

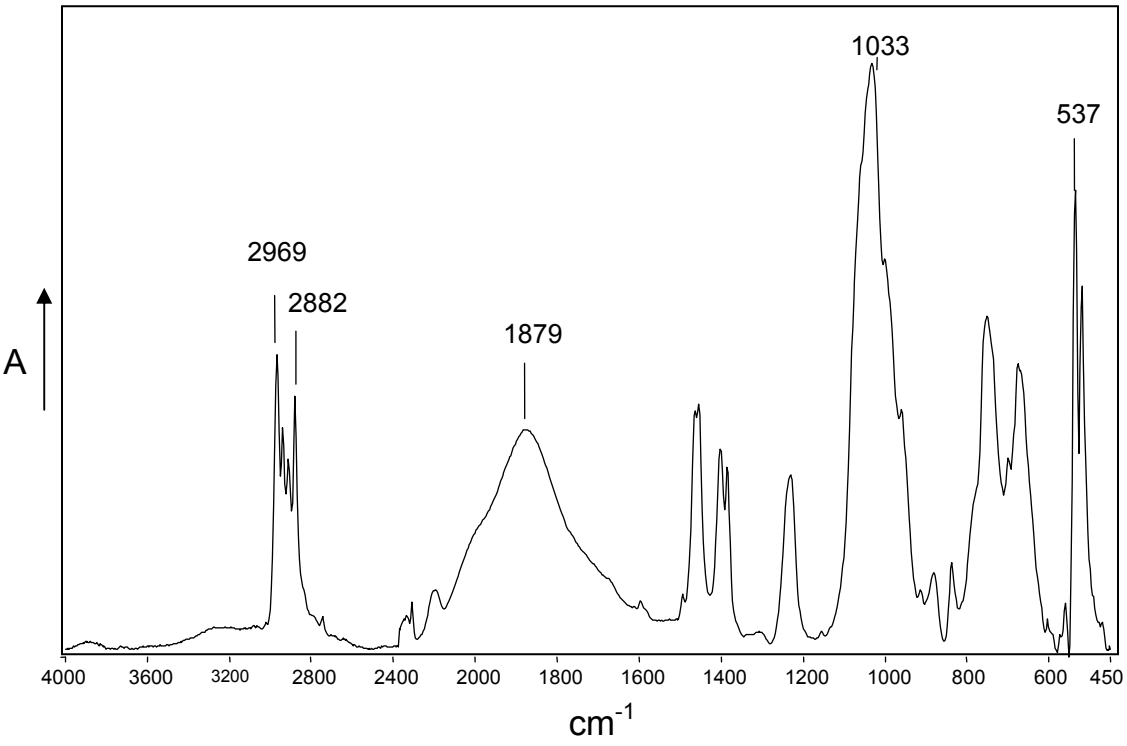

Figure 3.17 FT–IR spectrum of $[Et_3Si–H–SiEt_3]^+$ with $B_{12}Cl_{12}^{2-}$

When approximately two equivalents of triethylsilane are used instead of an excess, the broad band attributed to asymmetric Si–H–Si stretching is absent in the IR spectrum of the products (Figure 3.18 for $(Et_3Si)_2(B_{12}Br_{12})$ and Figure 3.19 for $(Et_3Si)_2(B_{12}Cl_{12})$). In both spectra the peaks in the region between 600 – 800 cm^{-1} sharpen relative to those when excess silane was used. The presence of acetonitrile may be determined if bands at about 2400 cm^{-1} are present. The amount of acetonitrile can vary from almost completely absent, as in Figure 3.19, to a small amount as in Figure 3.18. The amount of acetonitrile is dependent on the time the trityl precursors were heated under vacuum. Without the desolvation of the trityl salts, the intensity of the bands at 2400 cm^{-1} were found to be as intense as the alkyl stretching bands between 2800 and 2900 cm^{-1}, indicating considerable occlusion of acetonitrile in the crystal lattice.

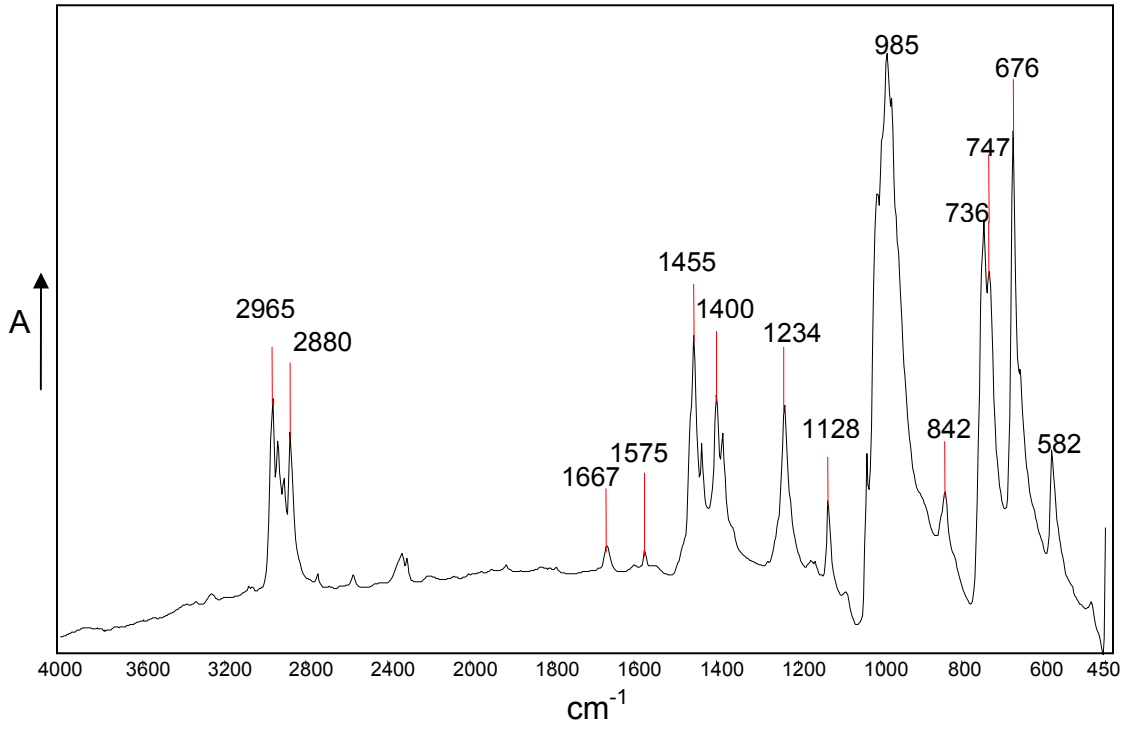

Figure 3.18 FT-IR spectrum of $(Et_3Si)_2(B_{12}Br_{12})$

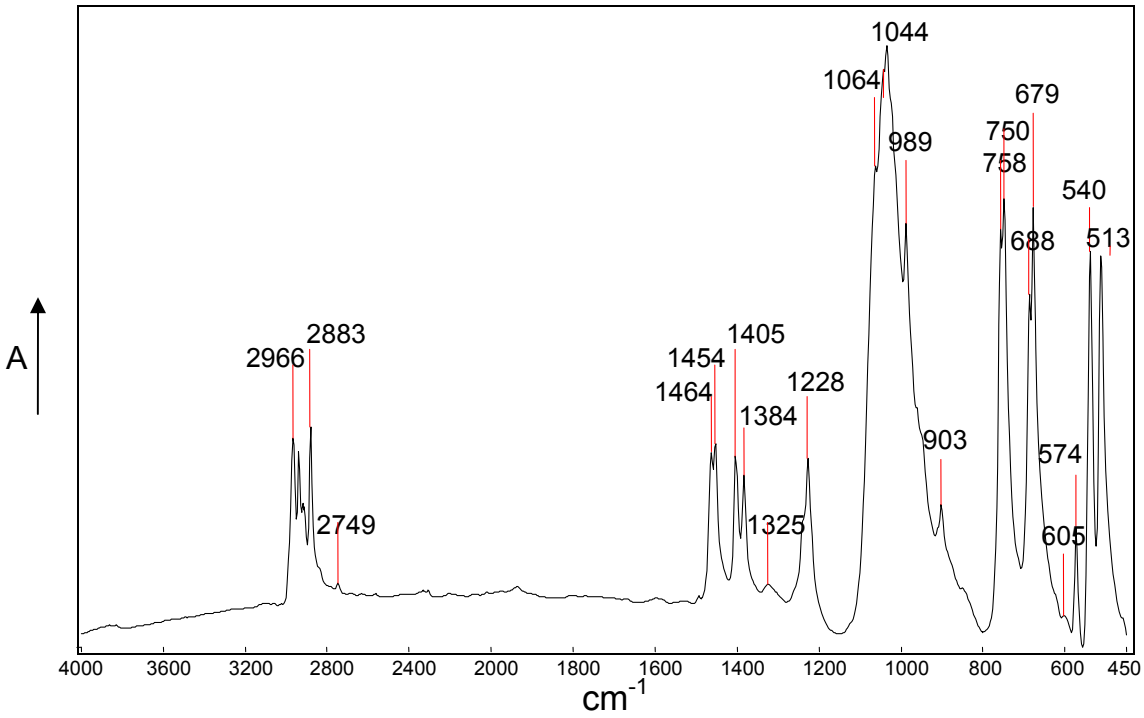

Figure 3.19 FT-IR spectrum of $(Et_3Si)_2(B_{12}Cl_{12})$

Both $(Et_3Si)_2(B_{12}Cl_{12})$ and $(Et_3Si)_2(B_{12}Br_{12})$ have been characterized via X-Ray diffraction, and the structures are shown in Figures 3.20 and 3.21 respectively. The compounds are "ion-like", since covalent character is still evident from the crystallographic data. A truly three coordinate ionic species would have a bond angle of 120° and would be planar.

As shown in Table 3.3, the C-Si-C bond angles of $(Et_3Si)_2(B_{12}Cl_{12})$ average 116.05° which is comparable to the average of the C-Si-C bond angles (116.5°) of $(Et_3Si)(CHB_{11}Cl_{11})$. The Si-Cl bond length is 2.311 Å, and this is also comparable to $(Et_3Si)(CHB_{11}Cl_{11})$ with a Si-Cl bond length of 2.334 Å. The coordinated Cl has a B-Cl bond length of 1.845 Å, which is elongated slightly, since the average B-Cl bond length for uncoordinated Cl is 1.780 Å. Similarly, in $(Et_3Si)(CHB_{11}Cl_{11})$, the coordinated Cl has

a B-Cl bond length of 1.841 Å while the average B-Cl bond length for uncoordinated Cl is 1.769 Å. These data suggest that the coordination to the di-anion by the triethylsilylium moiety is weak and similar to that with the mono-anion.

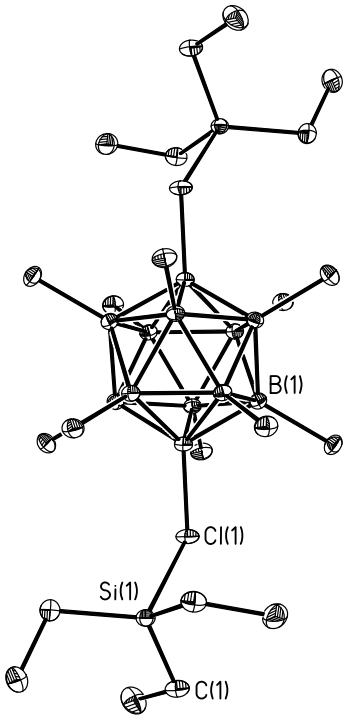

Figure 3.20 Thermal ellipsoid plot of $(Et_3Si)_2(B_{12}Cl_{12})$ (50% probability ellipsoids except for hydrogen atoms, which are not shown.)

Table 3.3 Selected Bond Angles (°)

	$(Et_3Si)_2(B_{12}Cl_{12})$	$(Et_3Si)(CHB_{11}Cl_{11})$[7]
C-Si-C	117.74(5)	118.16(4)
C-Si-C	116.88(5)	116.85(4)
C-Si-C	113.52(5)	114.50(4)
Σ	348.14(5)	349.51(4)
Mean	116.05(5)	116.5°

Table 3.4 Crystal data and structure refinement data for $(Et_3Si)_2(B_{12}Cl_{12})$

Identification code	cr306_0m	
Empirical formula	C12 H30 B12 Cl12 Si2	
Formula weight	785.66	
Temperature	100(2) K	
Wavelength	0.71073 Å	
Crystal system	Monoclinic (#14)	
Space group	P2(1)/n	
Unit cell dimensions	a = 9.1338(7) Å	α = 90°.
	b = 19.3255(14) Å	β = 93.0356(10)°.
	c = 9.5172(7) Å	γ = 90°.
Volume	1677.6(2) $Å^3$	
Z	2	
Density (calculated)	1.555 Mg/m^3	
Absorption coefficient	1.072 mm^{-1}	
F(000)	788	
Crystal size	0.41 x 0.25 x 0.09 mm^3	
Theta range for data collection	2.11 to 30.51°.	
Index ranges	-12<=h<=13, -27<=k<=27, -13<=l<=13	
Reflections collected	39414	
Independent reflections	5118 [R(int) = 0.0239]	
Completeness to theta = 30.51°	99.9 %	
Absorption correction	Semi-empirical from equivalents	
Max. and min. transmission	0.9087 and 0.6676	
Refinement method	Full-matrix least-squares on F^2	
Data / restraints / parameters	5118 / 0 / 175	
Goodness-of-fit on F^2	1.052	
Final R indices [I>2sigma(I)]	R1 = 0.0181, wR2 = 0.0495	
R indices (all data)	R1 = 0.0202, wR2 = 0.0508	
Largest diff. peak and hole	0.481 and -0.283 $e.Å^{-3}$	

The basicity of the $B_{12}Br_{12}^{2-}$ di-anion is expected to be greater than the basicity of the $B_{12}Cl_{12}^{2-}$ di-anion because of the decrease in halogen electronegativity. The crystallographic data for the silylium compounds support this expectation. The two silylium groups in crystral structure of $(Et_3Si)_2(B_{12}Br_{12})\cdot C_6H_4Cl_2$ were found to not be identical. The average bond angles for each of the different C-Si-C with $B_{12}Br_{12}^{2-}$ di-anion are 115.48 and 115.40° (Table 3.6). These averages are about 0.5° less than the average when the anion was $B_{12}Cl_{12}^{2-}$ (116.05°).

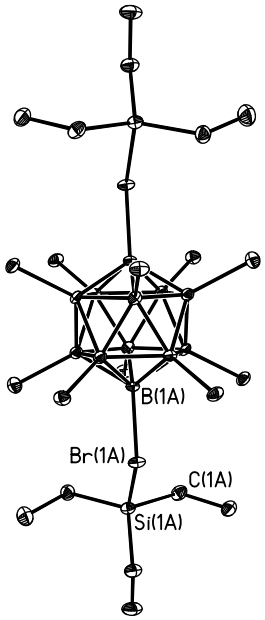

Figure 3.21 Thermal ellipsoid plot of $(Et_3Si)_2(B_{12}Br_{12})\cdot C_6H_4Cl_2$ (50% probability ellipsoids except for hydrogen atoms, which are not shown.)

Table 3.5 Crystal structure and refinement data for $(Et_3Si)_2(B_{12}Br_{12})\cdot C_6H_4Cl_2$

Empirical formula	$C_{18}H_{33}B_{12}Br_{12}Cl_2Si_2$	
Formula weight	1465.16	
Temperature	100(2) K	
Wavelength	0.71073 Å	
Crystal system	Monoclinic	
Space group	P2(1)/c	
Unit cell dimensions	a = 18.3119(4) Å	α = 90°
	b = 11.9561(2) Å	β = 110.9080(10)°
	c = 21.0939(4) Å	γ = 90°
Volume	4314.18(14) $Å^3$	
Z	4	
Density (calculated)	2.256 Mg/m^3	
Absorption coefficient	11.338 mm^{-1}	
F(000)	2732	
Crystal size	0.36 x 0.19 x 0.15 mm^3	
Theta range for data collection	1.98 to 26.37°	
Index ranges	-22<=h<=22, -14<=k<=14, -26<=l<=26	
Reflections collected	41588	
Independent reflections	8810 [R(int) = 0.0234]	
Completeness to theta = 26.37°	100.0 %	
Absorption correction	Sadabs	
Max. and min. transmission	0.2811 and 0.1057	
Refinement method	Full-matrix least-squares on F^2	
Data / restraints / parameters	8810 / 0 / 422	
Goodness-of-fit on F^2	1.042	
Final R indices [I>2sigma(I)]	R1 = 0.0217, wR2 = 0.0547	
R indices (all data)	R1 = 0.0262, wR2 = 0.0563	
Extinction coefficient	0.000016(19)	
Largest diff. peak and hole	1.088 and -1.040 $e.Å^{-3}$	

Table 3.6 Selected Bond Angles *Et_3Si groups are not equivalent in structure **Crystallizes into two independent molecules in the unit cell.

	Et_3Si	Et_3Si^*	$[Et_3Si][CB_{11}H_5Br_6]$	$[Et_3Si][CB_{11}H_5Br_6]$**
C-Si-C	117.80(15)	116.33(15)	111.2(10)	113.4(10)
C-Si-C	113.53(15)	115.18(15)	114.6(9)	117.4(8)
C-Si-C	115.11(15)	114.70(15)	119.2(10)	118.2(9)
Σ	346.44(15)	346.21(15)	345.0(10)	349.0(9)
Mean	115.48(15)	115.40(15)	115.0(10)	116.3(9)

In both structures, there are notable differences between the three ethyl groups with respect to their Si-C bond lengths and the Si-C-C angles. Similar differences were also noted with the Et_3Si ($CHB_{11}H_5Br_6$) and *i*-$Pr_3Si(CHB_{11}H_5Br_6)$.[10] The data are suggestive of stabilization of the ion-like Si center via either C-C or C-H bond hyperconjugation. If the stability is due to C-C hyperconjugation, then it is expected that the ethyl group with the shortest Si-C bond would also have the smallest <Si-C-C. If instead, the stability is due to C-H hyperconjugation, then the ethyl group with the shortest Si-C bond would have the greatest <Si-C-C.[10] As shown in Table 3.7, when the counterions are $B_{12}Cl_{12}^{2-}$ or $B_{12}Br_{12}^{2-}$, the shortest Si-C bond distance corresponds to the largest C-C-Si angle and is indicative of C-H hyperconjugation stability of the silicon center.

Table 3.7 Key Bond Distances and Angles of Et_3Si compounds with $B_{12}X_{12}^{2-}$ Anions
*Et_3Si groups are not equivalent in structure

Anion	Si-C bond	Si-C bond length (Å)	<C-C-Si (degree)
$B_{12}Cl_{12}^{2-}$	Si(1)-C(3)	1.8402(10)	115.40(7)
	Si(1)-C(5)	1.8421(10)	108.45(7)
	Si(1)-C(1)	1.8516(10)	114.11(7)
$B_{12}Br_{12}^{2-*}$	Si(1A)-C(1A)	1.844(3)	116.2(2)
	Si(1A)-C(5A)	1.845(3)	114.2(2)
	Si(1A)-C(3A)	1.853(3)	108.8(2)
	Si(1B)-C(5B)	1.846(3)	116.8(2)
	Si(1B)-C(1B)	1.848(3)	116.4(2)
	Si(1B)-C(3B)	1.855(3)	109.3(2)

In comparison, Table 3.8 shows that when the counter-ion to $Et_3Si^{\delta+}$ is $CHB_{11}Cl_{11}^-$, then it may be possible for stability via C-C hyperconjugation, whereas when the counter-ion is $CHB_{11}H_5Br_6^-$ the stability may be due to C-H hyperconjugation. It is evident that the pattern indicates the occurrence of hyperconjugation, rather than just sole packing phenomena.

Table 3.8 Key Bond Distances and Angles of Et_3Si compounds with $CHB_{11}X_{11}^-$ (X = halogen or H) Anions
* Crystallizes into two independent molecules in the unit cell.

Anion	Si-C bond	Si-C bond length (Å)	<C-C-Si (degree)
$CHB_{11}Cl_{11}^-$ ref. 7	Si(1)-C(2)	1.8398(9)	109.46(6)
	Si(1)-C(6)	1.8444(9)	115.35(6)
	Si(1)-C(4)	1.8508(9)	116.75(7)
$CHB_{11}H_5Br_6^{-*}$ ref. 10	Si-C(2)	1.85(3)	114.5(14)
	Si-C(4)	1.84(2)	116.6(13)
	Si-C(6)	1.80(2)	122.6(14)
	Si-C(2a)	1.82(2)	114.6(13)
	Si-C(4a)	1.85(2)	120.7(20)
	Si-C(6a)	1.86(2)	109.2(11)

3.4 Conclusions

Trityl and silylium derivatives of $B_{12}Cl_{12}^{2-}$ and $B_{12}Br_{12}^{2-}$, precursors to $H_2(B_{12}X_{12})$ superacids, have been synthesized and characterized by various techniques. These compounds display similar structural characteristics to the corresponding carborane compounds, but there are significant differences in terms of both solubility and affinity for lattice solvents. First, there is noticeably lower solubility of $B_{12}X_{12}^{2-}$ relative to carborane compounds. This decrease in solubility may be due to the higher lattice energies. It is also more difficult to remove trace solvents from the $B_{12}X_{12}^{2-}$ solid products, which compromises subsequent reactions. Despite these complications, it has been possible to isolate and characterize silylium compounds that should have useful applications in halide abstraction chemistry.

3.5 References

1. "100 Years of Carbocations and Their Significance in Chemistry," Olah, G.A. *J. Org. Chem.* **2001**, *66*, 5943-5957.

2. "New Weakly Coordinating Anions 3: Useful Silver and Trityl Salt Reagents of Carborane Anions," Xie, Z.; Jelínek, T.; Bau, R.; Reed, C.A. *J. Am. Chem. Soc.* **1994**, *116*, 1907-1913.

3. "Carboranes: A New Class of Weakly Coordinating Anions for Strong Electrophiles, Oxidants, and Superacids," Reed, C.A. *Acc. Chem. Res.* **1998**, *31*, 133-139.

4. "Synthesis and Stability of Reactive Salts of Dodecafluoro-closo-dodecaborate(2-)" Ivanov, S.V.; Miller, S.M.; Anderson, O.P.; Solntsev, K.A.; Strauss, S.H. *J. Am. Chem. Soc.* **2003**, *125*, 4694-4695.

5. "Closely Approaching the Silylium Ion (R_3Si^+)," Reed, C.A.; Xie, Z.; Bau, R.; Benesi, A. *Science*, **1993**, *263*, 402-404.

6. "Crystallographic Evidence for a Free Silylium Ion," Kim, K.-C.; Reed, C.A.; Elliot, D.W.; Mueller, L.J.; Tham, F.; Lin, L.; Lambert, J.B. *Science* **2002**, *297*, 825-827.

7. "Novel Weak Coordination to Silylium Ions: Formation of Nearly linear Si-H-Si Bonds," Hoffmann, S.P.; Kato, T.; Tham, F.S.; Reed, C.A. *Chem. Commun.* **2006**, 767-769.

8. Perrin, D.D.; Armarego, W.L.F.; Perrin, D.R. *Purification of Laboratory Chemicals*; 2nd ed, Pergamon Press Ltd.: Sydney, **1980**.

9. *The Strongest Isolable Acid* (Thesis) Hoffmann, S. University of California, Riverside, **2005**.

10. "The Silylium Ion (R_3Si^+) Problem: Effect of Alkyl Substituents R," Xie, Z.; Bau, R.; Benesi, A.; Reed, C.A. *Organometallics*, **1995**, *14*, 393im3-3941.

CHAPTER 4

Synthesis of $H_2(B_{12}X_{12})$ (X = Cl, Br)

4.1 Introduction

Thus far, the strongest isolable Brønsted acids are the carborane acids, $H(CHB_{11}X_{11})$ (X = Cl, Br). These acids have opened the field to the protonation and stabilization of many species previously unattainable, most at ambient temperatures.[1] The success of the carborane acids leads to the question of whether the analogous diprotic acids, $H_2(B_{12}X_{12})$ (X = Cl, Br) can be synthesized and if so, will their acidity be comparable to carborane superacids. Hydrated acids, $[H(H_2O)_n]_2[B_{12}X_{12}]$, synthesized though the use of acidic ion exchange resin, have been previously reported, but the anhydrous di-protic acids could not be prepared at that time by simple dehydration.[2] Since the superacid $H(CHB_{11}X_{11})$ is synthesized by the metathesis reaction of gaseous HCl with $R_3Si(CHB_{11}X_{11})$ under dry conditions,[1] the same methodology should be applicable for obtaining $H_2(B_{12}X_{12})$. Given that carborane acids are superacids, i.e., stronger than 100% sulfuric acid,[1] it is likely that $H_2(B_{12}X_{12})$ will also be superacidic.

The strength of a strong acid is usually measured with the Hammett acidity function, H_0.[3] The function can be viewed as an extension to the pH scale, with the formula: $H_0 = pK_{BH+} - \log [BH^+]/[B]$. The onset of superacidity is defined as $H_0 \leq -12$ (100% H_2SO_4). In order to calculate acidity based on the Hammett acidity function, the acid must be a liquid. The carborane acids are solids, suggesting that the analogous $H_2(B_{12}X_{12})$ compounds will also be solids. Therefore, their acidities cannot easily be

placed on the Hammett scale. Since carborane acids are able to protonate benzene, but triflic acid ($H_0 = -15$) cannot, the carborane acid acidities have been approximated to at least $H_0 = -17$.[4] As this value was only an estimation, it was clear that another method for determining acidity was needed.

Another method for determining acid strength was developed by Farcasiu and adapted for determining the acidity of carborane superacids. In this technique, acid strength is related to the extent of protonation of mesityl oxide and has been used to measure H(carborane) acidity.[5] In their work, ^{13}C NMR of α,β-unsaturated ketones was shown to be related to the acidity of the acid in which the ketone was dissolved. Protonation results in the formation of positive charge on C^{β}, while C^{α} remains virtually unchanged when compared to the structure before protonation (Reaction Scheme 4.1). Therefore, the chemical shift difference ($\delta C^{\beta} - \delta C^{\alpha}$) or $\Delta\delta$ ^{13}C NMR, is the measure of the extent of protonation, which is related to acid strength. The larger the $\Delta\delta$ ^{13}C NMR value is, the stronger the acid. With carborane acids, it is evident from the data that acidity leveling occurs; therefore, there is no discrimination between carborane acid strengths.[5] Though carborane acid strengths are not differentiated from each other by this scale, the data do show that carborane acids are much stronger than conventional oxyacids. Worth noting is that the acids themselves need to be soluble in liquid SO_2 in order to use this method for determining the acidity. Since the acids, $H_2(B_{12}X_{12})$ where X = Cl or Br, were found in this present work to have low solubility in SO_2, the Farcasiu method is not useful.

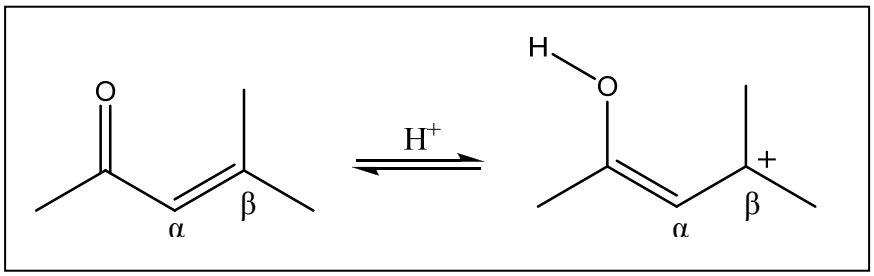

Reaction Scheme 4.1 Protonation of Mesityl Oxide

As the acidity scales mentioned above cannot be used to directly determine the acidity of $H_2(B_{12}X_{12})$, probing into the basicity of the di-anion instead may elucidate the conjugate acid strength. Anion basicity measurements have served in the past as indicators of conjugate acid strength. A basicity scale developed recently employs H-bonded contact ion pairs of the general type R_3N^+—$H^{\cdots}A^-$ (where R = n-octyl for solubility purposes, A = anion).[5,6] The lower the basicity of A^-, the weaker the $H^{\cdots}A$ interaction, and the stronger the N–H bond. Furthermore, the νN-H is greater than 2800 cm^{-1} when A^- is a weak base, which is far removed from the $\nu(H^{\cdots}A^-)$ at less than 400 cm^{-1}. The higher in frequency νN–H is, then the weaker the $H^{\cdots}A^-$ interaction, which is indicative of a weaker base. This method allowed for the differentiation of basicity between various carborane anions and thus the strengths of the conjugate acids, in which previous methods had led to the leveling of the acidity. This scale can be useful in determining the basicity of $B_{12}X_{12}^{2-}$ anions and therefore conjugate acid strength.

SO_2 has been the solvent of choice for obtaining the ^1H NMR spectrum of H(carborane) because SO_2 is a weakly basic solvent. But, the carborane acid is suspected

of fully protonating SO_2. Thus, the acidity is attributed to $H(SO_2)_2^+$, that is, that in solution state, full protonation of the solvent occurs (thus leveling acidity).[1] The chemical shift due to the acidic proton of $H(SO_2)_2^+$ is uniquely downfield at approximately 20 ppm. If the ^1H NMR spectrum of the acid, $H_2(B_2X_{12})$, taken in SO_2, contains the unique peak at 20 ppm, that would indicate that the acid strength of $H_2(B_2X_{12})$ is comparable to the carborane superacids, but would not indicate which acid was stronger.

The anhydrous carborane acids have also been used to elucidate the infrared bands associated with simple proton hydrates such as H_3O^+, $H_5O_2^+$, $H_7O_3^+$, and so forth.[7] Since it was found that certain frequency regions were associated with ν-OH, regardless of the environment, the absence of those ν-OH frequencies would provide further evidence of the anhydrous acid, $H_2(B_{12}X_{12})$. The slow hydration of the anhydrous acid would also be of interest as the expected ν-OH frequencies should then be detected.

4.2 Experimental

Air sensitive materials were handled in helium filled Vacuum Atmospheres gloveboxes (O_2, H_2O < 2 ppm) or on a vacuum manifold using standard Schlenk techniques. Tri-*n*-octylammonium chloride was synthesized following literature procedures by Irena Stoyanov.[8] Liquid SO_2 was dried/stored over P_2O_5 and transferred via vacuum at dry ice/acetone temperature. NMR spectra were obtained on a Bruker Avance 300 MHz or a Varian Inova 500 MHz spectrometer using Wilmad J-Young NMR tubes. FT-IR and Attenuated Total Reflectance (ATR) spectra were obtained on a Perkin Elmer Spectrum 100 Series spectrometer in a nitrogen filled glovebox.

[(n-$CH_3(CH_2)_6CH_2)_3NH]_2[B_{12}Br_{12}]$ $Cs_2[B_{12}Br_{12}]$ (0.1486 g, 0.1097 mmol) was dissolved in 2 mL of water. Tri-*n*-octylammonium chloride (0.0890 g, 0.228 mmol) was dissolved in 2 mL of CCl_4. The solutions were mixed and shaken. The precipitate that formed in the organic layer was collected on a glass frit and dried under vacuum.

[(n-$CH_3(CH_2)_6CH_2)_3NH]_2[B_{12}Cl_{12}]$ $Cs_2[B_{12}Cl_{12}]$ (0.1386 g, 0.1688 mmol) was dissolved in 2 mL of water. Tri-*n*-octylammonium chloride (0.1317 g, 0.3376 mmol) was dissolved in 2 mL of CCl_4. The solutions were mixed and shaken. The precipitate that formed in the organic layer was collected on a glass frit and dried under vacuum.

$H_2(B_{12}X_{12})$ $(Et_3Si)_2(B_{12}X_{12})$ was placed in a thick-walled Schlenk tube with a wide bore Teflon stopcock and dried under vacuum for 1 hour. Dry HCl gas was condensed onto $(Et_3Si)_2(B_{12}X_{12})$ at –192 °C and the mixture stirred at –5 °C for 1.5 hours. The excess HCl gas and Et_3SiCl by-product were removed under vacuum to give an off-white solid. ^{11}B NMR of $H_2(B_{12}Cl_{12})$ in SO_2 (300 MHz, unreferenced): singlet. ^1H NMR of $H_2(B_{12}Cl_{12})$ in SO_2: 19.3 ppm (singlet). (NMR of $H_2(B_{12}Br_{12})$ was not obtained due to low solubility in SO_2.)

4.3 Results and Discussion

The potential acidity of $H_2(B_{12}X_{12})$ may be gauged by quantifying how weakly basic $B_{12}X_{12}^{2-}$ is compared to other known anions. As noted earlier, the νN-H scale allows for such a measurement. The νN-H frequencies of various $octyl_3NH^+A^-$ salts have been previously determined.[6] Several frequencies for salts with isostructural anions as well as the only di-anion, $(HSO_4)_2^{2-}$, are shown in Table 4.1.[6] The data were obtained

from ion pairs in the solution state with CCl_4 as the solvent. The lower ΔνN-H is attributed to the weaker the base, or, the greater νN-H, the weaker the base. When comparing different carborane anions, it was determined that when A^- was $CHB_{11}Cl_{11}^-$, νN-H was the greatest at 3163 cm^{-1}, making the anion the least basic of the carboranes. Δν is therefore defined as the difference, in wavenumbers, of the N-H stretching frequency of νN-H when A^- is $CHB_{11}Cl_{11}^-$ and the νN-H when A^- is a different anion.

Table 4.1 νN-H, in cm^{-1}, for $Octyl_3NH^+$ salts in CCl_4 (reference 6)

Anion	νN-H in CCl_4	ΔνN-H
$CHB_{11}Cl_{11}^-$	3163	0
$CHB_{11}H_5Cl_6^-$	3148	15
$CHB_{11}Me_5Cl_6^-$	3143	20
$CHB_{11}Br_{11}^-$	3140	23
$CHB_{11}H_5Br_6^-$	3125	38
$CHB_{11}Me_5Br_6^-$	3120	43
$(HSO_4)_2^{2-}$	3021, 2660	138

When $[Octyl_3NH][CHB_{11}Cl_{11}]$ was dissolved in CCl_4, the resultant νN-H was observed at 3163 cm^{-1}. In comparison, when $B_{12}Cl_{12}^{2-}$ was the counterion to the $Octyl_3NH^+$ cation, the νN-H frequency was at 3165 cm^{-1} in CCl_4 (Figure 4.1 (a)). This close similarity was surprising since it was indicative of a *di*-anion basicity similar to the isostructural *mono*-anion.

A similar comparison could not be made with the trioctylammonium salt of $B_{12}Br_2^{2-}$ anion to $CHB_{11}Br_{11}^-$ anion due to poor solubility of the $B_{12}Br_{12}^{2-}$ salt in CCl_4. However, salts of both $B_{12}Cl_{12}^{2-}$ and $B_{12}Br_{12}^{2-}$ were soluble in 1,2-dichloroethane (DCE). As shown in Figure 4.1, νN-H for the $B_{12}Cl_{12}^{2-}$ salt was observed at 3146 cm^{-1} (b), and

the νN-H for $B_{12}Br_{12}^{2-}$ was 3121 cm^{-1} (c). Since the solid state νN-H for the $B_{12}Cl_{12}^{2-}$ salt observed at 3167 cm^{-1} (Figure 4.2 (a)) is comparable to the stretching frequency found at 3165 cm^{-1} in CCl_4, the solid phase stretching frequency may be used to determine anion basicity. The difference in νN-H between in the solid phase and in solution (DCE solvent) for the $B_{12}Cl_{12}^{2-}$ salt is 21 cm^{-1}. For the $B_{12}Br_{12}^{2-}$ salt, the solid phase frequency was observed at 3140 cm^{-1} (Figure 4.2 (b)), resulting in a difference between solid and solution (DCE solvent) phase of 19 cm^{-1}. Therefore, it can be predicted that with the anion as the $B_{12}Br_{12}^{2-}$, the νN-H would be at approximately 3140 cm^{-1} in CCl_4, which is the same frequency reported for the isostructural *mono*-anion salt of $CHB_{11}Br_{11}^{1-}$.

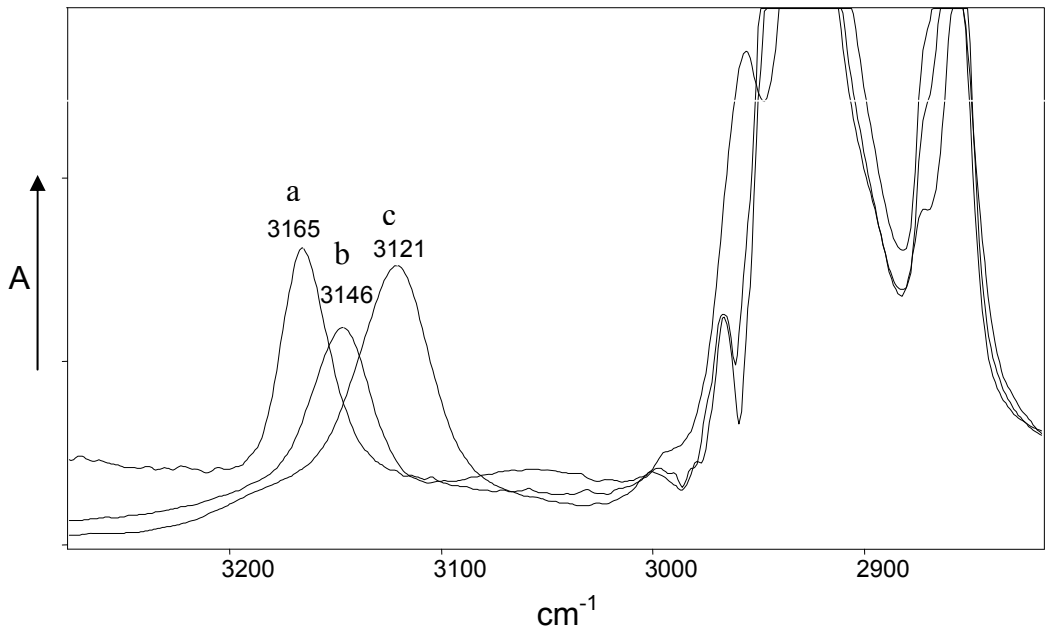

Figure 4.1 Infrared spectra of the νNH (>3000 cm^{-1}) for trioctylammonium salts with (a) $B_{12}Cl_{12}^{2-}$ in CCl_4, (b) $B_{12}Cl_{12}^{2-}$ in CH_2Cl_2, and (c) $B_{12}Br_{12}^{2-}$ in CH_2Cl_2

The νN-H was expected to be lower when A^- was the di-anion versus the mono-anion because the di-anion was expected to be the stronger base due to the higher negative charge. It was initially surprising to find that the νN-H when the di-anion was used was very similar with the νN-H found using the analogous mono-anion, as shown in Table 4.2. Those results indicate that the di-anion basicity is similar to the mono-anion basicity rather than a stronger basicity. The low basicity of the di-anion may be due to the high symmetry, sigma delocalization of the di-negative charge, and the charge being buried under a layer of halide substituents. The di-anion therefore is as weakly basic as the carborane. Thus, the conjugate acids of $B_{12}X_{12}^{2-}$ are predicted to have similar strengths to the carborane acids.

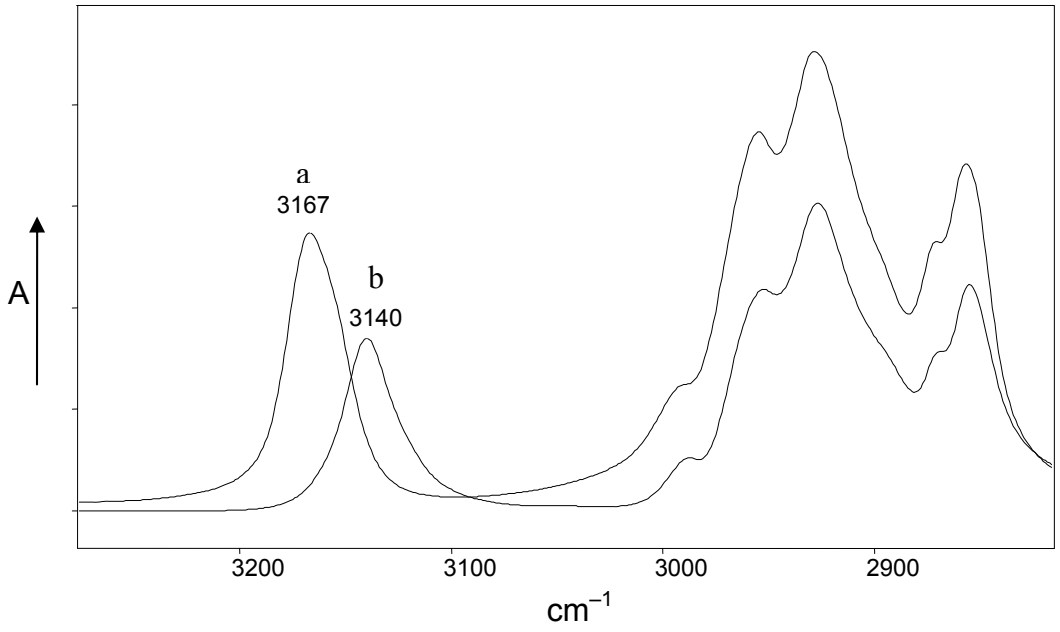

Figure 4.2 Infrared spectra of the νN–H (>3000 cm^{-1}) for trioctylammonium salts in the solid state with (a) $B_{12}Cl_{12}^{2-}$ and (b) $B_{12}Br_{12}^{2-}$

Table 4.2 νN–H, in cm^{1-}, with different anions

Anion	νN–H in CCl_4	νN–H solid	νN–H in $C_2H_4Cl_2$
$CHB_{11}Cl_{11}^{-}$ (ref 5)	3163	3180	--
$B_{12}Cl_{12}^{2-}$	3165	3167	3146
$CHB_{11}Br_{11}^{-}$ (ref 5)	3140	3150	--
$B_{12}Br_{12}^{2-}$	insol	3140	3121

Initial attempts to synthesize the anhydrous diprotic acid were unsuccessful, as the Brønsted acid, $H_2(B_{12}X_{12})$, was not the only product from the reaction of $(Et_3Si)_2(B_{12}X_{12})$ with HCl gas. One problem was the retention of small amounts of acetonitrile from the trityl salt synthesis that was then retained in the silylium compound. The acetonitrile was protonated as was evident in the infrared and NMR spectra of the material obtained from the initial acid preparation attempts. The removal of most of the acetonitrile was accomplished by heating the trityl salts under vacuum.

Another problem was the choice of solvent for the silylium synthesis. When either benzene or toluene was used as the solvent to prepare $(Et_3Si)_2(B_{12}X_{12})$, the solid evidently also contained small amounts of the solvent. Both arenes were protonated during the subsequent acid preparation as observed in the infrared spectra, and an example is shown in Figure 4.3. Therefore, initial data for the acid itself correspond to mixed (or possible double) salt formation. The material may be a mixture containing $H_2(B_{12}X_{12})$, $H(H(arene))(B_{12}X_{12})$ and possibly $H((Et_3Si)B_{12}X_{12})$. Even when the silylium starting material was under vacuum before the acid synthesis, as is done with the analogous silylium carboranes, trace amounts of solvent (toluene or benzene) were not removed. Slight heating, insufficient to destroy the silylium compound, did not remove trace amounts of solvent from the solid.

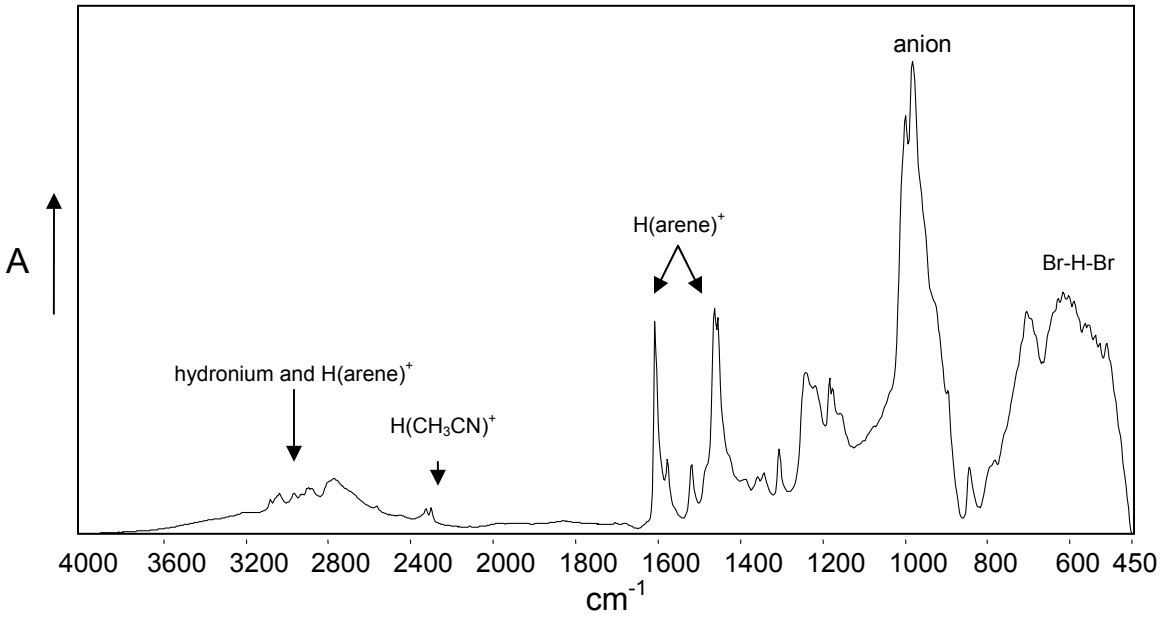

Figure 4.3 FT-IR spectrum of $H_x(B_{12}Br_{12})$ mixture

When *ortho*-dichlorobenzene was used as the solvent for the silylium preparation, followed by washing with small amounts of dry hexanes (minimal amounts are used to suppress contamination by water), the acid was produced much more cleanly (though not completely solvent-free). The observation that weakly basic and neutral solvents coordinated to the silylium compounds further supports the conclusion of the $B_{12}X_{12}^{2-}$ anions are very weakly basic.

Both acids, $H_2(B_{12}Br_{12})$ and $H_2(B_{12}Cl_{12})$, were mainly characterized by infrared spectroscopy, due to the low solubility of the acids in liquid SO_2. These infrared spectra were then compared to the spectra of the carborane acids. Broad, low-energy absorptions arising from symmetric hydrogen bonding via X-H-X bridges were observed in the IR

spectrum of the mono-anion acid, $H(CHB_{11}Cl_{11})$ (Figure 4.4). $H(CHB_{11}Cl_{11})$ was distinctively characterized by bands associated with the anti-symmetric stretching and doubly degenerate bending of the Cl-H-Cl moiety. As shown in Figure 4.4, a broad band appears at 1100 cm^{-1}, assigned to the anti-symmetric stretch and another at approximately 615 cm^{-1}, assigned to the bending.[1] Similar broad bands were noted in the IR spectra of the di-protic acids. As shown in Figure 4.5, for $H_2(B_{12}Cl_{12})$, the bands appeared at 1200 cm^{-1} and approximately 620 cm^{-1}. Figure 4.5 shows the original spectrum containing small amounts of protonated acetonitrile and hydronium while Figure 4.6 has both the impurities subtracted and a Gaussian fit for the band appearing at 1200 cm^{-1}. The corresponding absorption bands for $H_2(B_{12}Br_{12})$ were at 1080 cm^{-1} and approximately 570 cm^{-1} (Figure 4.7).

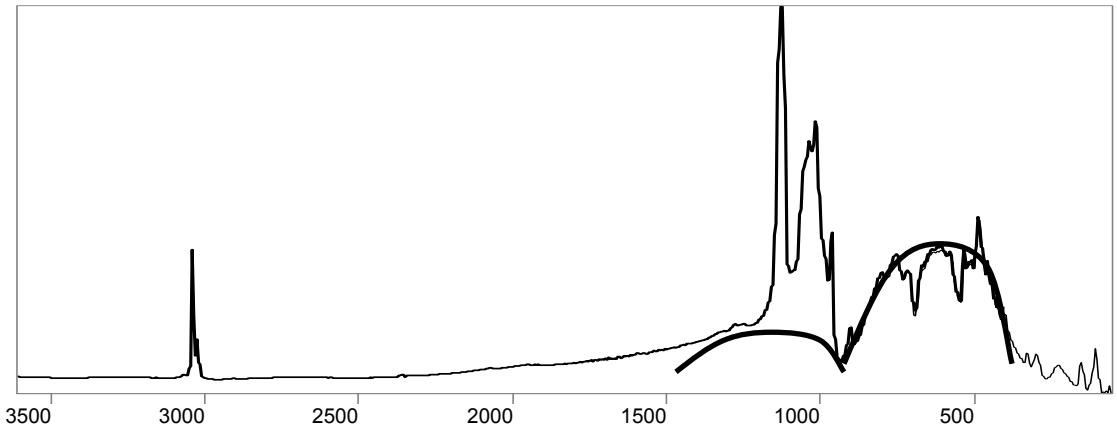

Figure 4.4 FT-IR spectrum of $H(CHB_{11}Cl_{11})$

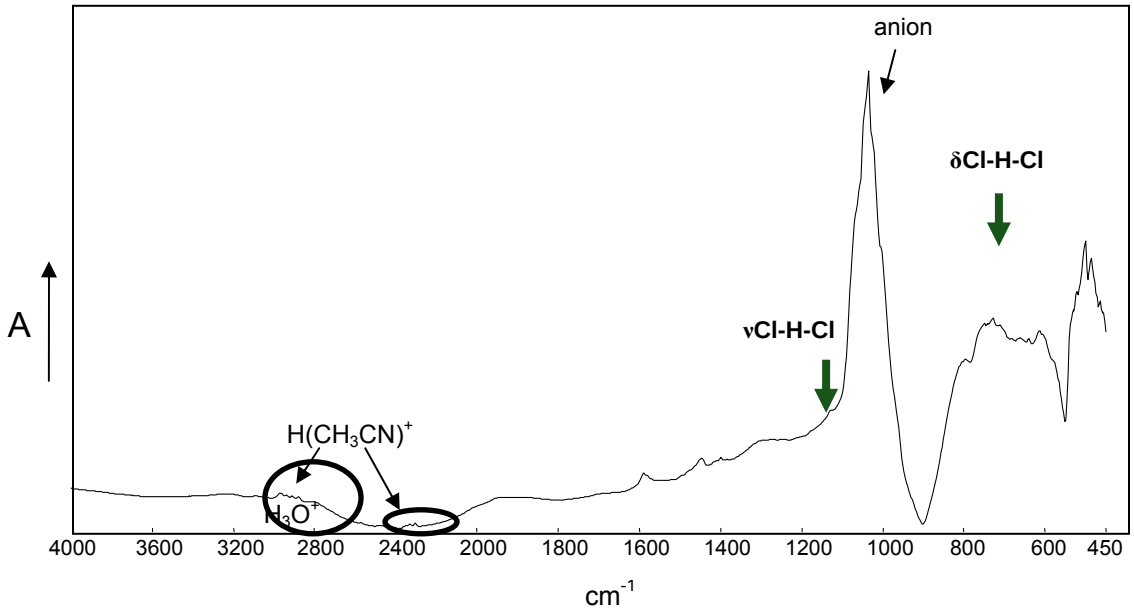

Figure 4.5 FT-IR spectrum of $H_2(B_{12}Cl_{12})$

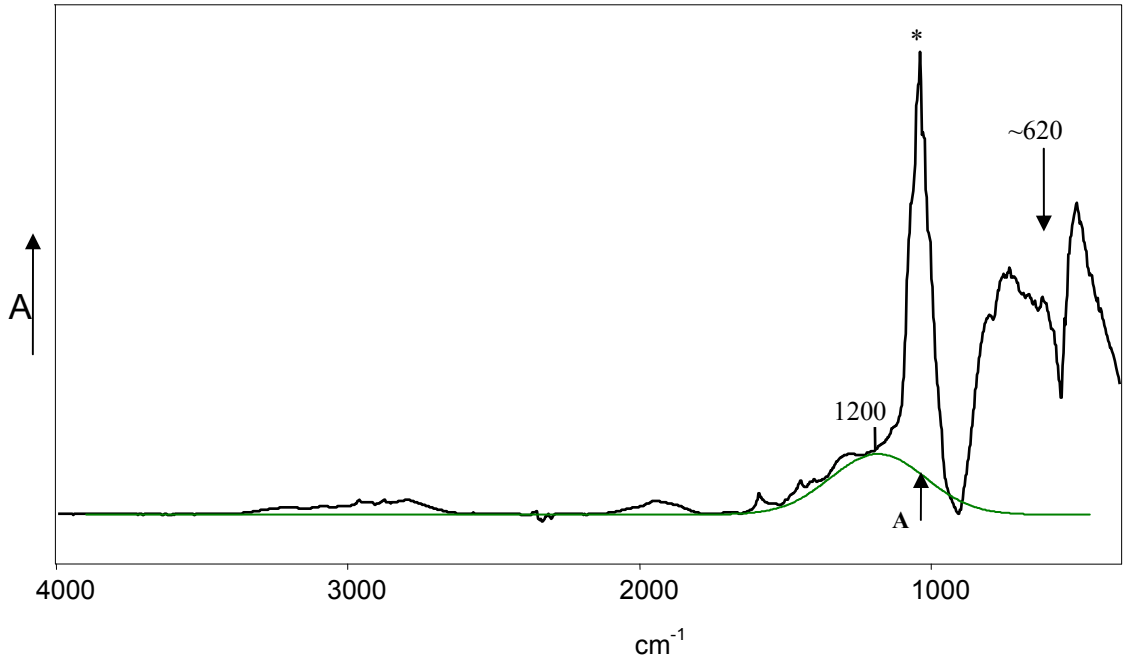

Figure 4.6 FT-IR spectrum of $H_2(B_{12}Cl_{12})$ after computer subtraction of impurities (arising from protonated CH_3CN and H_2O) showing a Gaussian fit (Band A) to one of the bands associated with the bridging proton. The lower frequency band at ~620 cm^{-1} could not be fit because of Evans holes. *Denotes anion band.

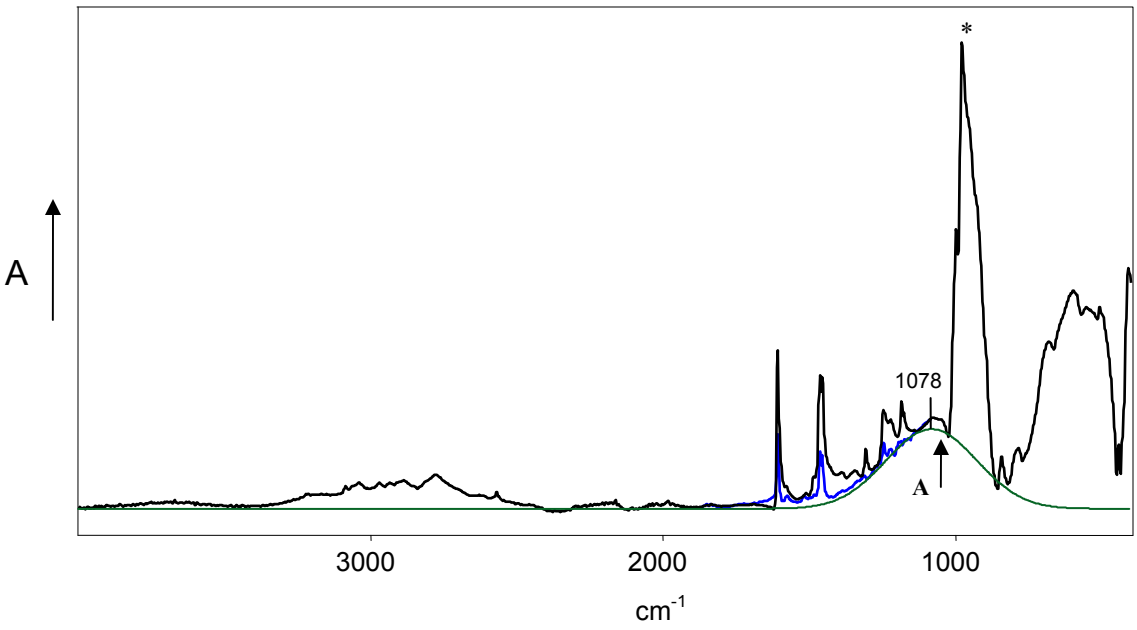

Figure 4.7 ATR spectrum of $H_2(B_{12}Br_{12})$ showing a Gaussian fit (Band A) to one of the bands associated with the bridging proton. The lower frequency band at ~650 cm^{-1} could not be fit because of Evans holes. *Denotes anion band.

The characterization of the di-protic acids via NMR spectroscopy proved to be more difficult. As has been previously shown with $H(CHB_{11}Cl_{11})$, the least basic solvent that will dissolve the acid is liquid SO_2.[1] The acid is insoluble in less basic solvents. Despite the fact that $H(CHB_{11}Cl_{11})$ is sufficiently soluble in SO_2 for ^{1}H and ^{11}B NMR spectroscopy, both di-protic acids were found to have poor solubility in SO_2. Nevertheless, the solubility of $H_2(B_{12}Cl_{12})$ was sufficient to obtain ^{1}H and ^{11}B NMR spectra. The ^{11}B NMR spectrum of $H_2(B_{12}Cl_{12})$ contained a single broad peak (Figure 4.8). The broadness of the peak may be due to material that did not dissolve in the solution. The solution was not filtered as further manipulation was noted to lead to contamination, specifically hydration.

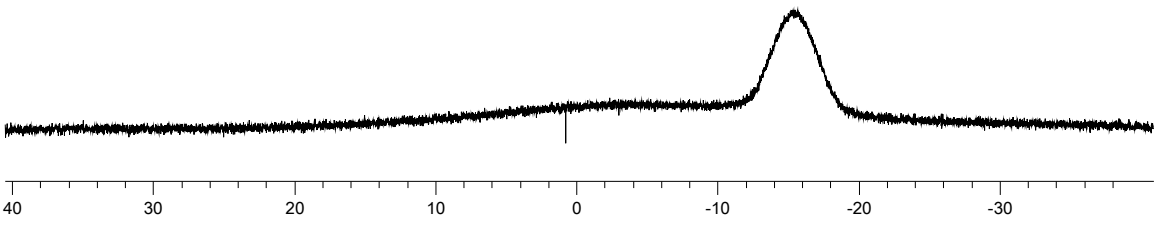

Figure 4.8 ^{11}B NMR spectrum of $H_2(B_{12}Cl_{12})$ in SO_2

The ^{1}H NMR spectrum of $H_2(B_{12}Cl_{12})$ had several peaks (Figure 4.9) The peaks that are upfield were attributed to impurities in the SO_2 (Figure 4.10). The singlet at 19.27 ppm is attributed to the proton that protonates SO_2 and forms the dimer, $(SO_2)_2H^+$. The peak at 11.20 ppm is attributed to the hydrogens of the hydronium ion, H_3O^+.

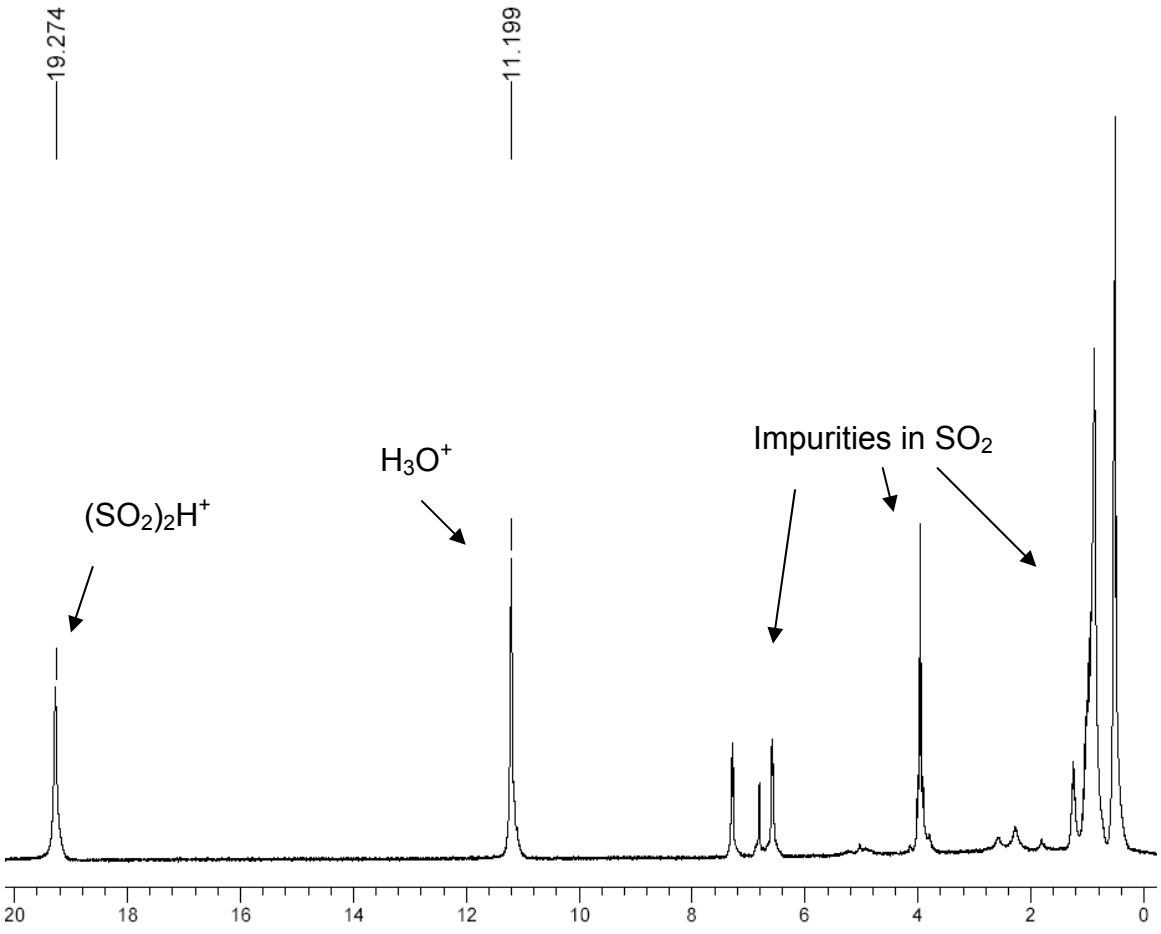

Figure 4.9 ^{1}H NMR spectrum of $H_2(B_{12}Cl_{12})$ in SO_2

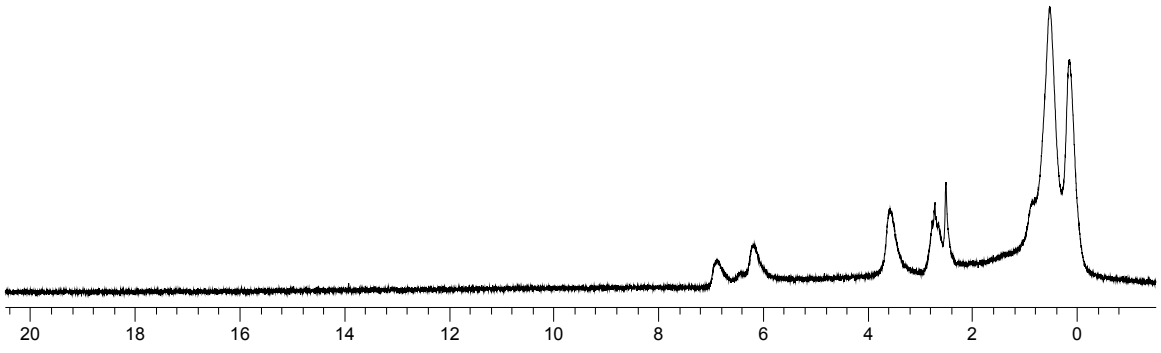

Figure 4.10 ^{1}H NMR spectrum of SO_2

The solubility of $H_2(B_{12}Br_{12})$ in SO_2 was so poor that there was no noticeable ^{11}B signal. It is of interest to note that although no boron signal was obtained in the ^{11}B NMR spectrum of $H_2(B_{12}Br_{12})$, when the SO_2 was removed, the infrared spectrum of the solid did contain characteristic bands due to the cage, specifically the strong band at 983 cm^{-1} (Figure 4.11). The broad band at ~650 cm^{-1} due to Br-H-Br, was absent, though, there were new bands at 1211, 1155, and 1079 cm^{-1}. These broad bands are possibly due to the solvated bridged proton between two SO_2 molecules, as a similar spectrum was observed by Hoffman.[9] This hypothesis is preliminary, and further work is needed to assign those bands positively.

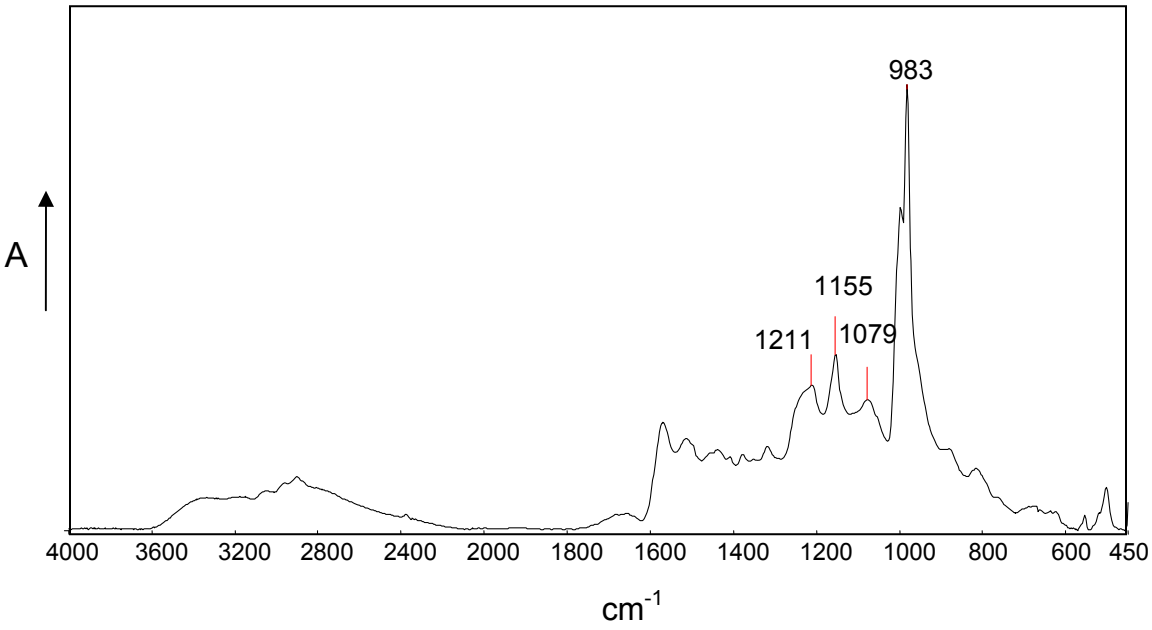

Figure 4.11 FT-IR spectrum of $H(SO_2)_2^+$ with $B_{12}Br_{12}^{2-}$

The hydrated acid, $H(H_2O)_n(B_{12}Br_{12})$, was found to dissolve in SO_2 much better than did $H_2(B_{12}Br_{12})$. Both ^{11}B (Figure 4.12) and ^{1}H NMR (Figure 4.13) spectra were obtained. The ^{11}B spectrum consisted of an expected singlet. The ^{1}H NMR spectrum had a singlet assignable to hydronium ion at 10.03 ppm, and upfield signals may be due to impurities such as grease.

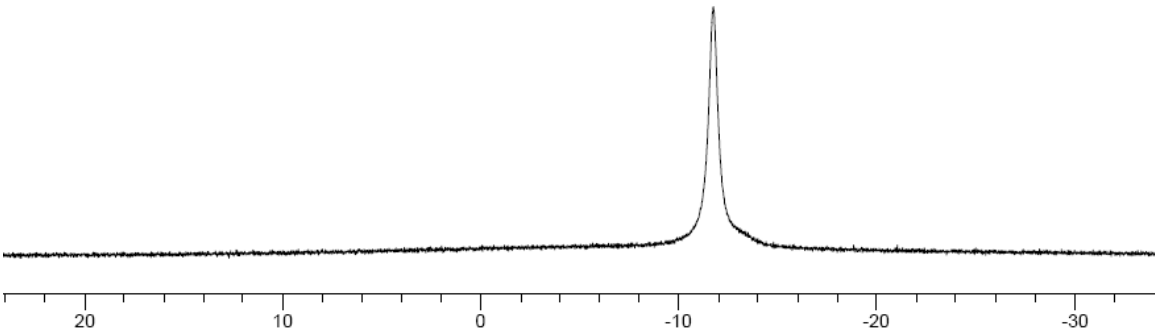

Figure 4.12 ^{11}B NMR spectrum of $H(H_2O)_n(B_{12}Br_{12})$ in SO_2

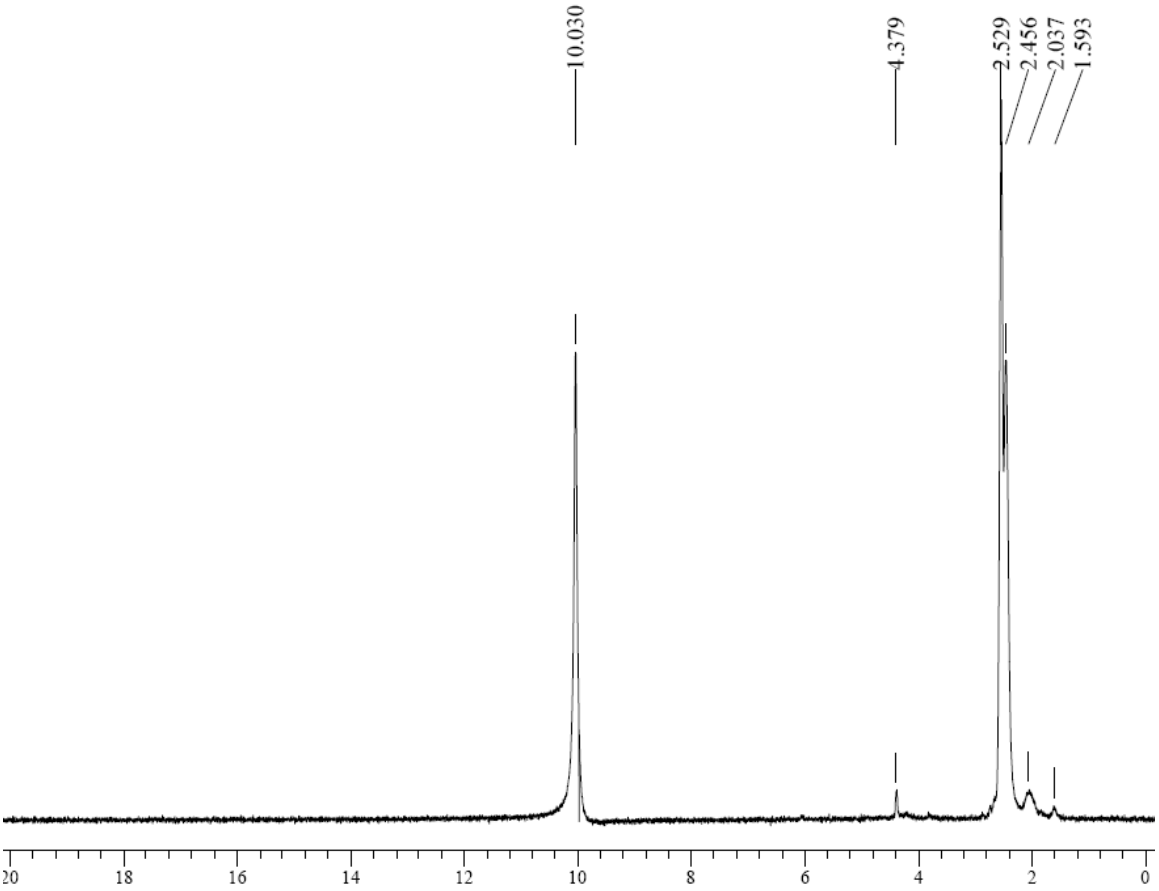

Figure 4.13 ^{1}H NMR spectrum of $H(H_2O)_n(B_{12}Br_{12})$ in SO_2

The di-protic acids have the ability to abstract water even from the gloveboxes with O_2, H_2O < 2 ppm. Exposure of $H_2(B_{12}Cl_{12})$ in a KBr pellet to the box atmosphere allowed for the slow hydration of the acid and was monitored via IR spectroscopy, as is noted in Figure 4.14.

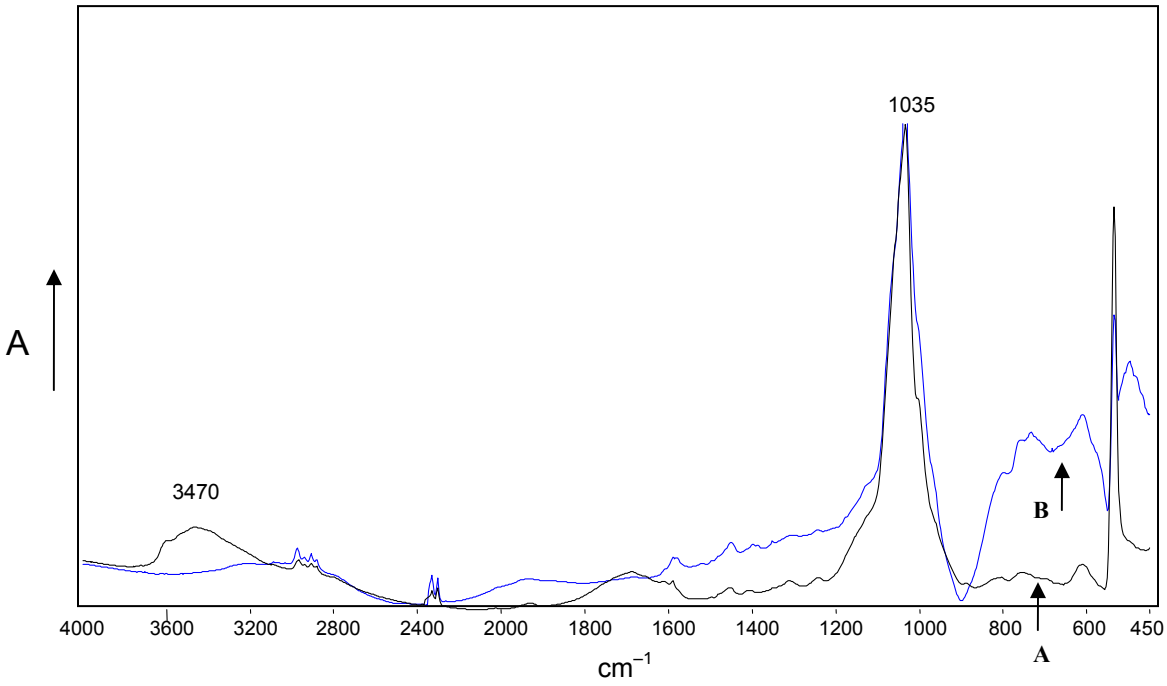

Figure 4.14 FT-IR spectrum of air-exposed $H_2(B_{12}Cl_{12})$ showing formation of $H_5O_2^+$ and $H_7O_3^+$ salts (Band A). Band B is the spectrum is that of the anhydrous acid. Note the disappearance of the broad bands at ca. 1200 and 700 cm^{-1} arising from bridging protons.

Various attempts were made to purify the di-protic acids via sublimation, but were unsuccessful. Despite the use of high vacuum and temperatures exceeding 200 °C, neither $H_2(B_{12}Cl_{12})$ nor $H_2(B_{12}Br_{12})$ sublimed. The analogous mono-protic carborane acid, $H(CHB_{11}Cl_{11})$, may be sublimed under high vacuum at 150 °C.[9] The higher degree of H-bonding of the di-protic acids compared to the mono-protic acid may be the reason for the unsuccessful sublimation.

4.4 Conclusions

The anhydrous di-protic superacids, $H_2(B_{12}X_{12})$, have been prepared and analyzed with infrared and NMR spectroscopy. They have similar properties to carborane acids. Both acids contain the anhydrous bridged proton as determined by IR spectroscopy and both protonate SO_2 and benzene. They do differ in their solubility properties however, and this may be due to 3D H-bonding giving rise to higher lattice energies. Anion basicity data for $B_{12}X_{12}^{2-}$ using the νN-H scale indicates similar anion basicities as carborane analogues. The di-protic acids themselves are very reactive as they abstract water quite readily from dried glassware and the glovebox atmosphere. These observations lead to the conclusion that the acidities of the di-protic acids are comparable to the mono-protic acids. The protonation of arenes is further investigated in the next chapter.

4.5 References

1. "The Strongest Isolable Acid," Juhasz, M.; Hoffmann, S.; Stoyanov, E.; Kim, K.-C.; Reed, C.A. *Angew. Chem. Int. Ed.* **2004**, *43*, 5352-5255.

2. "Chemistry of Boranes. IX. Halogenation of $B_{10}H_{10}^{2-}$ and $B_{12}H_{12}^{2-}$," Knoth, W.H.; Miller, H.C.; Sauer, J.C.; Balthis, J.H.; Chia, Y.T.; Muetterties, E.L. *Inorg. Chem.* **1964**, *3*, 159- 167.

3. *Superacids*; John Wiley & Sons: New York, 1985; and references therein

4. "Carboranes: A New Class of Weakly Coordinating Anions for Strong Electrophiles, Oxidants, and Superacids," Reed, C.A. *Acc. Chem. Res.* **1998**, *31*, 133-139.

5. "Acidity Functions from 13C NMR," Fărcaiu, D.; Ghenciu, A. *J. Am. Chem. Soc.* **1993**, *122*, 10901-10908.

6. "An Infrared νNH Scale for weakly basic anions. Implications for Single-Molecule Acidity and Superacidity," Stoyanov, E.S.; Kim, K.-C.; Reed, C.A. *J. Am. Chem. Soc.* **2006,** *128*, 8500-8508.

7. "IR Spectrum of the $H_5O_2^+$ Cation in the Context of Proton Disolvates L-H^+-L," Stoyanov, E.S.; Reed, C.A. *J. Phys. Chem. A*. **2006**, *110*, 12292- 13002.

8. Stoyanov, E.S.; Popandopulo Yu, I.; Bagreev, V.V. *Coord. Chem. (Translation of Koord. Khim.)* **1980**, *6*, 1809- 1814.

9. *The Strongest Isolable Acid,* (Thesis) Hoffmann, S.P. University of California, Riverside, **2005**.

CHAPTER 5

Isolation of Arenium Ions With $B_{12}X_{12}^{2-}$ Counterions (X = Cl, Br)

5.1 Introduction

The synthesis of the di-protic acids, $H_2(B_{12}X_{12})$, led to the investigation of whether their acidities were greater than or comparable to carborane acids, $H(CHB_{11}X_{11})$, and other superacids. The ability to protonate arenes serves as a method to determine whether $H_2(B_{12}X_{12})$ is indeed a superacid, and bracket the acid strength. Consider the acid strength necessary to protonate several arenes. The hydronium ion, H_3O^+, in benzene, can protonate 1,3,5-trimethylbenzene (mesitylene), which is also the most basic arene investigated. The protonation of toluene, an arene that is less basic than mesitylene, requires an acid strength of at least 100% sulfuric acid.[1] Although the onset of superacidity is defined to be 100% sulfuric acid, this mineral acid is not able to protonate benzene. Other stronger mineral acids, such as triflic acid, cannot protonate benzene either, but, the carborane acids can.[1] Therefore, the protonation of benzene by $H_2(B_{12}X_{12})$ would provide evidence that the acidities of $H_2(B_{12}X_{12})$ are at least comparable to the acidities of carborane acids.[1] By studying the protonation of various arenes, approximation of the relative acid strengths of the solid $H_2(B_{12}X_{12})$ may be made. Figure 5.1 is a scale depicting the relative acidities necessary to protonate the arenes investigated. Note how the Hammett scale, H_0, is can be seen as an extension of the pH scale.

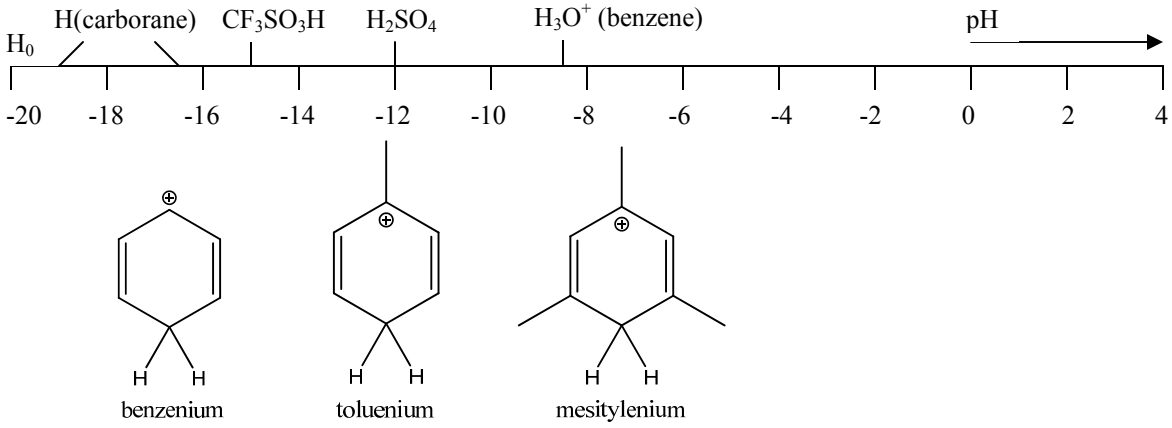

Figure 5.1 H_0 Scale of Protic Acids and Their Ability to Protonate Arenes (adapted from reference 1)

Arenium ions are the intermediates of electrophilic aromatic substitution reactions, and were previously thought to be transients species, as they were initially observed only in superacidic media at low temperatures.[2,3] These intermediates were characterized mainly by ^1H and ^{13}C NMR spectroscopy, because crystals suitable for x-ray diffraction were not grown due to difficulties that arose with the media used and the low temperatures required.[3] With the use of carboranes as counterions however, arenium ions were isolated as crystalline salts.[4] The isolation of arenium ion salts was done at ambient temperatures and was a remarkable advance in understanding these once elusive intermediates. Now, arenium ions may have a potential role as useful reagents, since they are much easier to handle as solid salts compared to viscous low temperature media.

It was expected that the acids, $H_2(B_{12}X_{12})$, would protonate various arenes because the basicity data shown in Chapter 4 indicated that the acid strengths of $H_2(B_{12}X_{12})$ should be similar to that of carborane acids. There are several questions to

consider. First, are both protons of the di-protic acids sufficiently acidic to protonate arenes? Second, will arenium salts of $B_{12}X_{12}^{2-}$ be soluble? It is important to note that the carborane arenium salts are insoluble in the arene from which they are derived.[4] In addition, solvent choices for NMR studies become limited, as one risks reaction with the solvent. Will solubility also be an issue and hinder the analysis of the areniums stabilized with $B_{12}X_{12}^{2-}$? Based on these considerations, the isolation and characterization of arenium ions stabilized with the $B_{12}X_{12}^{2-}$ are reported herein.

5.2 Experimental

Air sensitive materials were handled in helium filled Vacuum Atmospheres gloveboxes (O_2, H_2O < 2 ppm) or on a vacuum manifold using standard Schlenk techniques. Benzene, mesitylene, and toluene were dried following literature methods and stored under molecular sieves.[5] Liquid SO_2 was dried/stored over P_2O_5 and transferred via vacuum at dry ice/acetone temperature. NMR spectra were obtained on a Bruker Avance 300 MHz or Inova 500 MHz spectrometer. FT-IR spectra were obtained on a Perkin Elmer Spectrum 100 Series spectrometer in a nitrogen- filled glovebox.

$[C_6H_7]_2[B_{12}X_{12}]$ Enough benzene to cover the solid was added to approximately 100 mg of $H_2(B_{12}X_{12})$. The slurry was left stirring for at least one hour resulting in a light yellow solid that was filtered off.

X = Cl, IR (KBr): 3092w, 3070w, 3035w, 2910w, 2804w, 2712b, 2451w, 2309w, 1600m, 1479m, 1446m, 1403w, 1200w, 1179m, 1032s, 953w, 902w, 813w, 689m, 638m, 580w, 535s.

X = Br, IR (KBr): 3084w, 3061w, 3029w, 2664b, 1597m, 1516w, 1477w, 1441s, 1400w, 1326w, 1255w, 1208m, 1177m, 1159m, 997s, 980s, 903m, 811w, 773w, 686m, 637m, 579w, 440m.

$[C_7H_9]_2[B_{12}X_{12}]$ Enough toluene to cover the solid was added to approximately 100 mg of $H_2(B_{12}X_{12})$. The slurry was left stirring for at least one hour resulting in a white powder that was collected by filtration.

X = Cl, IR (KBr): 3090w, 3069w, 3036w, 2974w, 2883w, 2833b, 2742b, 2310w, 1612m, 1459m, 1355w, 1310m, 1248m, 1222w, 1187m, 1143w, 1032s, 964w, 899m, 847w, 769w, 742w, 711w, 696w, 587w, 535s, 514m, 499w.

X = Br, IR (KBr): 3083w, 3060w, 3033w, 2819b, 2711b, 1609s, 1531w, 1486w, 1457s, 1385m, 1352m, 1308m, 1243m, 1218m, 1185m, 1142w, 1001s, 984s, 899m, 844m, 767w, 738w, 709m, 586w, 515m, 497w.

$[(CH_3)_3C_6H_4]_2[B_{12}X_{12}]$ Enough mesitylene to cover the solid was added to approximately 100 mg of $H_2(B_{12}X_{12})$ and stirred. The slurry was filtered and the white powder collected.

X = Cl, ATR: 3240w, 2911b, 2779b, 1620s, 1474b, 1383m, 1254m, 1154w, 1027s, 872w, 840w, 689w, 532m, 495w.

X = Br: ^{1}H NMR (300 MHz, -20°C, δ, CD_2Cl_2): 0.84, 1.22 (m, hexane), 2.22 (s, 36H- CH_3, free mesitylene), 2.75, 2.86 (s, 9H- CH_3, mesitylenium), 4.63 (s, 2H, mesitylenium), 6.76 (s, 12H, free mesitylene), 7.31, 7.34 (s, 2H), 7.53 (s, 2H, mesitylenium). IR (KBr): 3240w, 2906b, 2832b, 2732b, 1620s, 1475b, 1381m, 1283m, 1251m, 1153w, 1000s, 983s, 870w, 839m, 688w, 567w, 495w.

5.3 Results and Discussion

Arenium ions were found to be stable with $B_{12}X_{12}^{2-}$ counter-ions at ambient temperatures as long as inert conditions were maintained. The salts are solids like the carborane analogues, and were mainly characterized with solid state FT-IR spectroscopy in a KBr pellet. This method was possible because the compounds were found to be unreactive with KBr within the time frame of analysis. The resultant spectra showed unambiguously the formation of various arenium ions, when their spectra were compared to those obtained previously for arenium salts with carborane anions.

There are several key vibrational modes for the benzenium, $C_6H_7^+$, ion. The gas phase frequencies of the benzenium ion show that the average νCH_2 for the most acidic, sp^3 carbon, is at 2803 cm^{-1}. As shown in Table 5.1, the average νCH_2 for the benzenium ion with either carborane or $B_{12}X_{12}^{2-}$ is lower (2733 cm^{-1} when the anion is $B_{12}Cl_{12}^{2-}$ and 2664 cm^{-1} when the anion is $B_{12}Br_{12}^{2-}$). This peak can be attributed to H-bonding to the halide atoms of the anions, as was observed with carborane counterions. Figure 5.2 contains IR spectra of the benzenium ion salt between 3200 and 2600 cm^{-1}. Another diagnostic band is that due to $\nu(CH)_{aromatic}$ and $\nu(CC) + \delta(CCH)$ near 1600 cm^{-1}. The data are tabulated in Table 5.1 and compared to the carborane analogues.

Table 5.1 Frequencies of Benzenium versus Counterion (a: ref. 6; b: ref. 4)

Counterion	$\nu(CH_2)$ (average)	$\nu(CH)_{aromatic}$	$\nu(CC) + \delta(CCH)$
none (cald.)[a]	2810, 2795 (2803)	3110, 3080	
$CB_{11}H_6Cl_6^-$ [b]	2770, 2720 (2745)	3100, 3072, 3040, 3028	1601
$B_{12}Cl_{12}^{2-}$	2753, 2713 (2733)	3092, 3070, 3035	1600
$CB_{11}H_6Br_6^-$ [b]	2757, 2714 (2736)	3095, 3073, 3066, 3023	1600
$B_{12}Br_{12}^{2-}$	2664	3084, 3060, 3028, 3015	1597

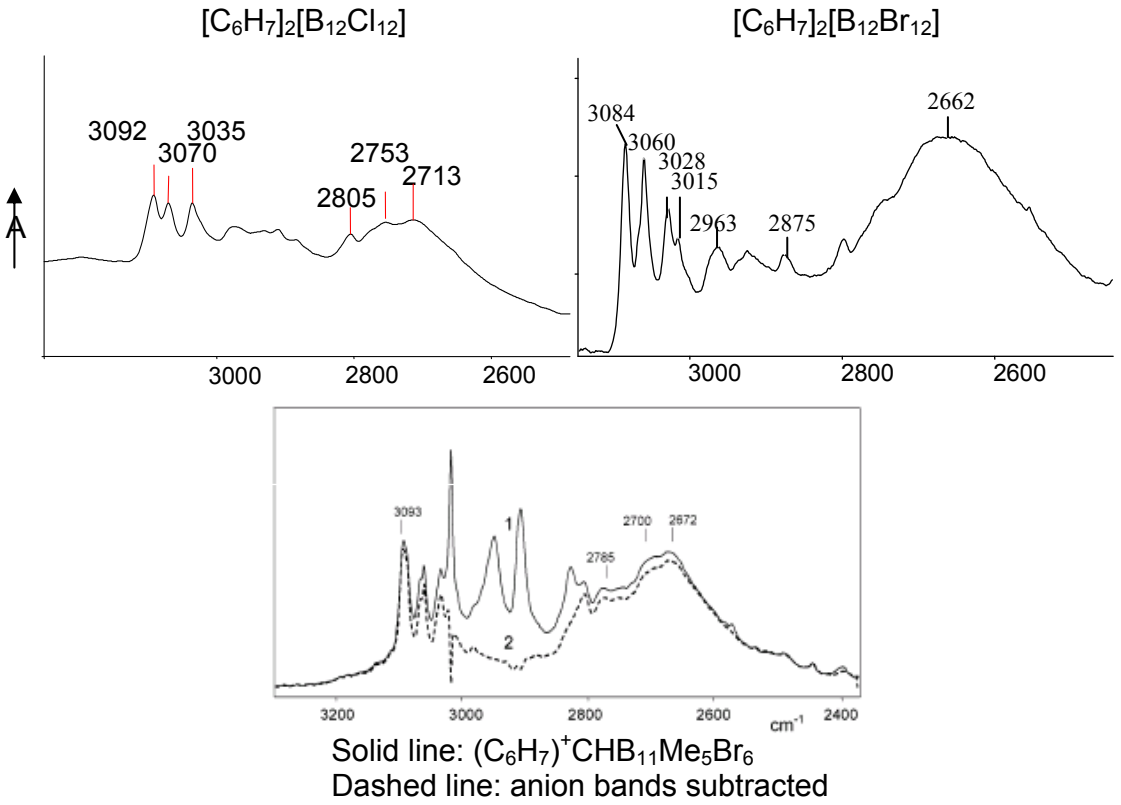

Figure 5.2 Portions of the FT-IR spectrum of benzenium with $B_{12}X_{12}^{2-}$ counterions

The infrared spectrum of all the arenium ion salts synthesized provides evidence for the 2:1 salts. Apparently, both protons of the acids, $H_2(B_{12}X_{12})$, are acidic enough to protonate the arenes. As can be seen in the IR spectra of the benzenium salts, $[C_6H_7]_2[B_{12}Cl_{12}]$ (Figure 5.3) and $[C_6H_7]_2[B_{12}Br_{12}]$ (Figure 5.4), the broad bands due to the anti-symmetric stretching and bending of the symmetric H-bonding, X-H-X, in the starting acid are absent.

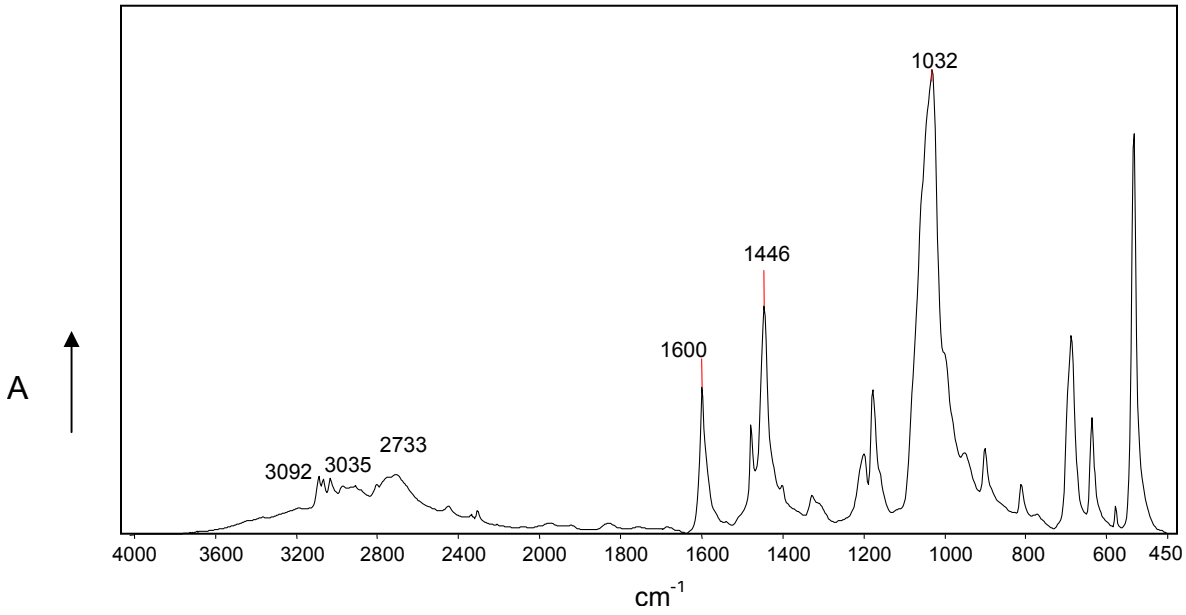

Figure 5.3 IR spectrum of $[C_6H_7]_2[B_{12}Cl_{12}]$

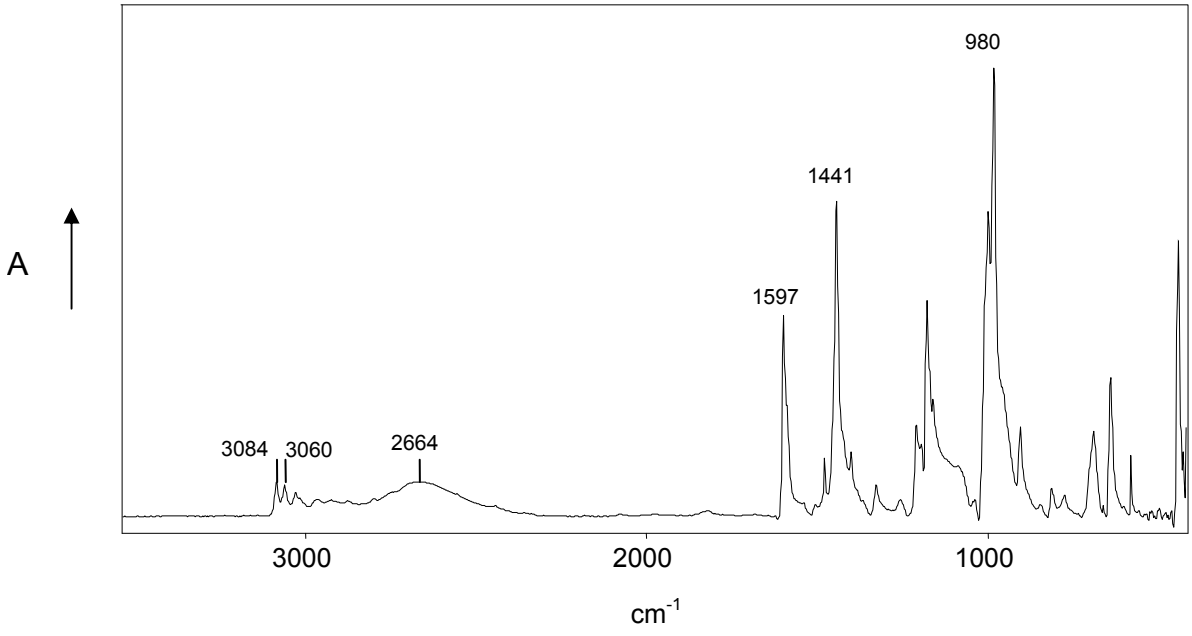

Figure 5.4 FT-IR spectrum of $[C_6H_7]_2[B_{12}Br_{12}]$

The benzenium ion salts were found to be insoluble in benzene like the analogous carborane benzenium salts. The ^{1}H NMR spectrum of benzenium with the $B_{12}Cl_{12}^{2-}$ counter-ion was obtained in SO_2.[7] It is important to note that under strong acidic conditions, benzene and toluene react with SO_2.[8,9] Therefore, the purpose of this analysis was to find indirect evidence for the precursor benzenium salt.[8,9]

A sample of $[C_6H_7]_2[B_{12}Cl_{12}]$ was dissolved in SO_2 and resulted in the formation of benzenesulfinic acid, as had been previously noted to form when benzene was in the superacidic medium HF-SbF_5-SO_2.[7,8,9] The downfield region of the ^{1}H NMR spectrum at –50 °C is shown in Figure 5.5 and the chemical shifts are in good agreement with literature.[8] The integrated areas of the peaks agreed less well. The peak at 9.66 ppm should integrate to 4 hydrogen atoms (2 for each benzenesulfinic acid) but instead integrates to less than 3 hydrogen atoms.[8] There is also evidence of "free" benzene in the ^{1}H NMR spectrum at 7.46 ppm and hydronium at 10.37 ppm. Therefore, the material obtained may best be described as a mixture of the arenium, unprotonated arene, and hydronium, rather than a pure sample of an arenium ion salt.

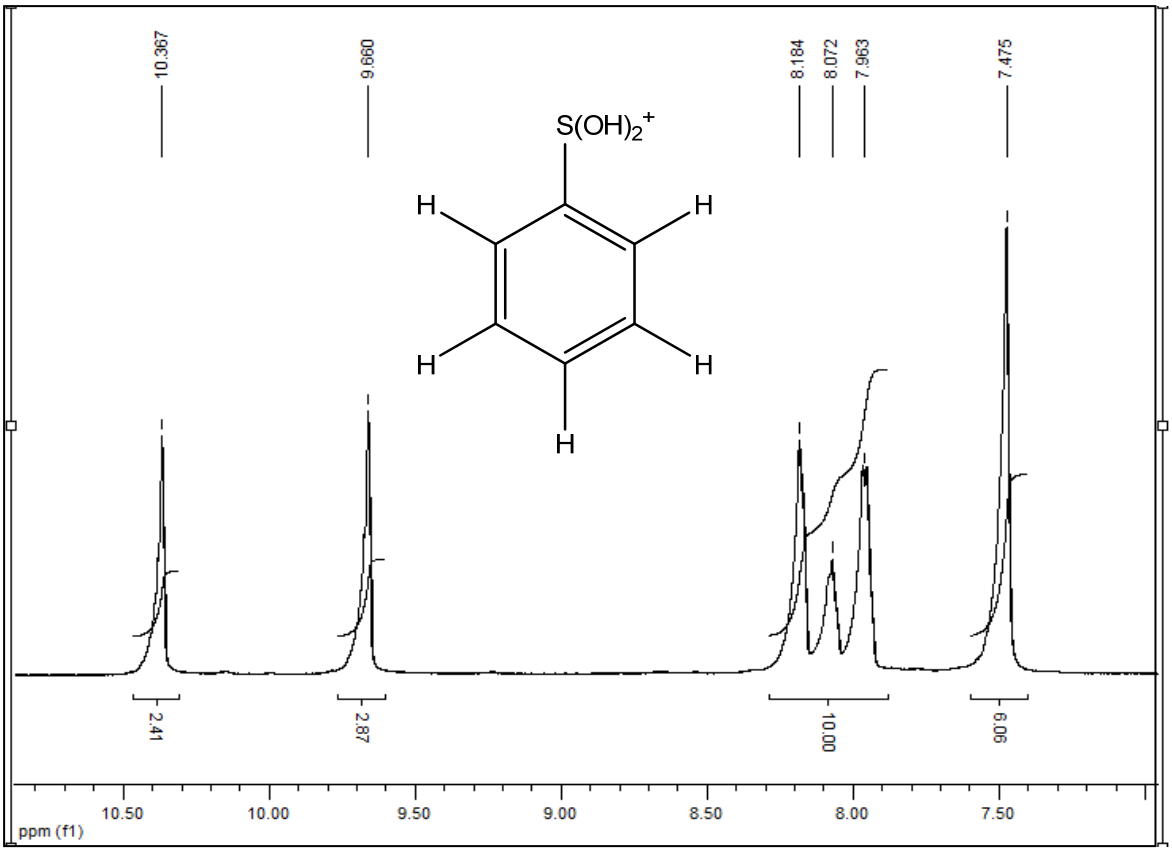

Figure 5.5 ^{1}H NMR spectrum of benzenium dissolved in SO_2 with $B_{12}Cl_{12}^{2-}$ at –50 °C

The toluenium ion, $C_7H_9^+$, was also isolated with the use of $B_{12}X_{12}^{2-}$ counterions. The IR spectra of toluenium with both counter-ions $B_{12}Cl_{12}^{2-}$ (Figure 5.6) and $B_{12}Br_{12}^{2-}$ (Figure 5.7) were diagnostic for both species as $[C_7H_9]_2[B_{12}X_{12}]$ salts. As with the benzenium ion, the toluenium ion also has diagnostic IR bands.

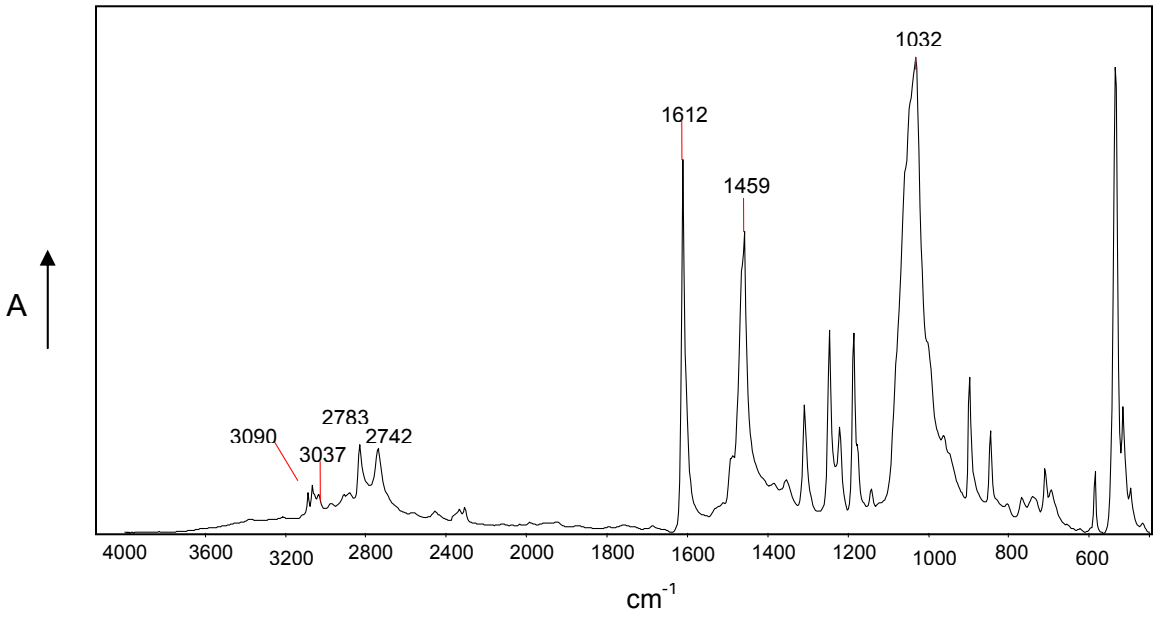

Figure 5.6 FT-IR spectrum of toluenium ion salt, $[C_7H_9]_2[B_{12}Cl_{12}]$

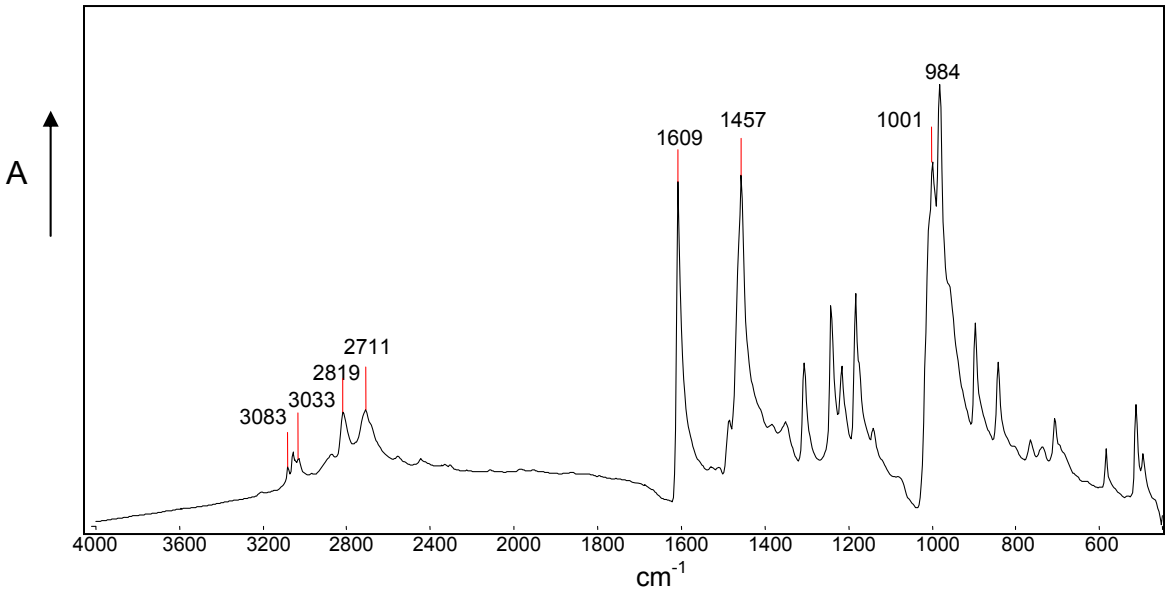

Figure 5.7 FT-IR spectrum of toluenium ion salt, $[C_7H_9]_2[B_{12}Br_{12}]$

1,3,5-trimethylbenzene (mesitylene) was the most basic of the three arenes protonated. Mesitylenium was characterized by both infrared and NMR spectroscopy. The IR spectrum is shown in Figure 5.8 for $[C_9H_{13}]_2[B_{12}Cl_{12}]$ and has the bands that coincide well with the known mesitylenium frequencies. The ^1H NMR spectrum for $[C_9H_{13}]_2[B_{12}Br_{12}]$ was obtained in CD_2Cl_2 at –20 °C (Figure 5.9) and 25 °C (Figure 5.10). Both were in accordance with protonated mesitylene. There was also evidence of free mesitylene.

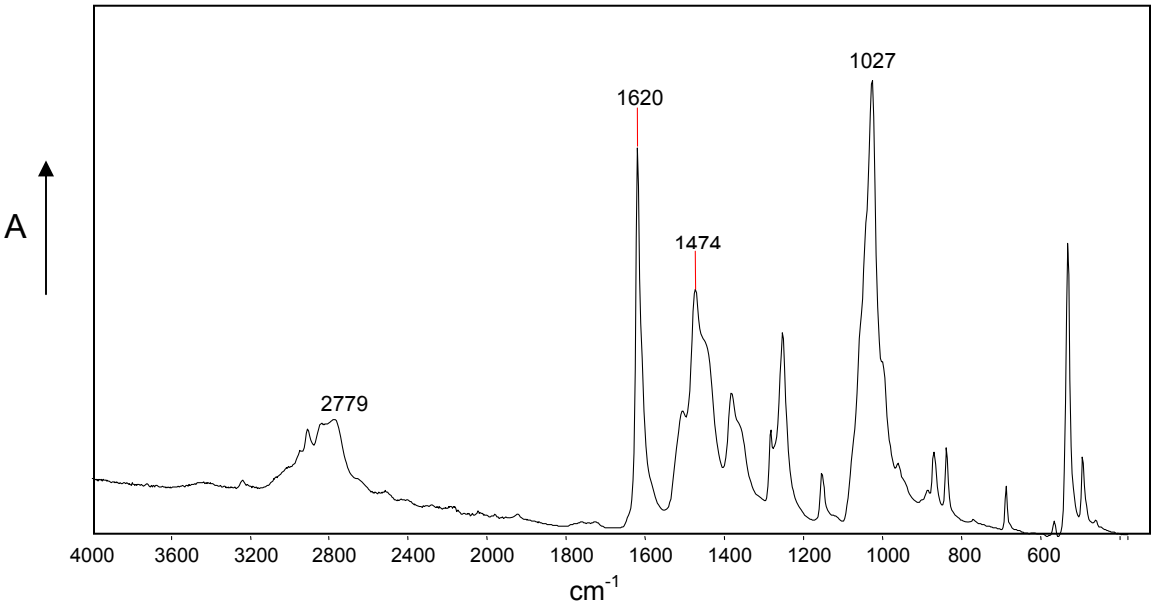

Figure 5.8 FT-IR spectrum of mesitylenium ion salt, $[C_9H_{13}]_2[B_{12}Cl_{12}]$

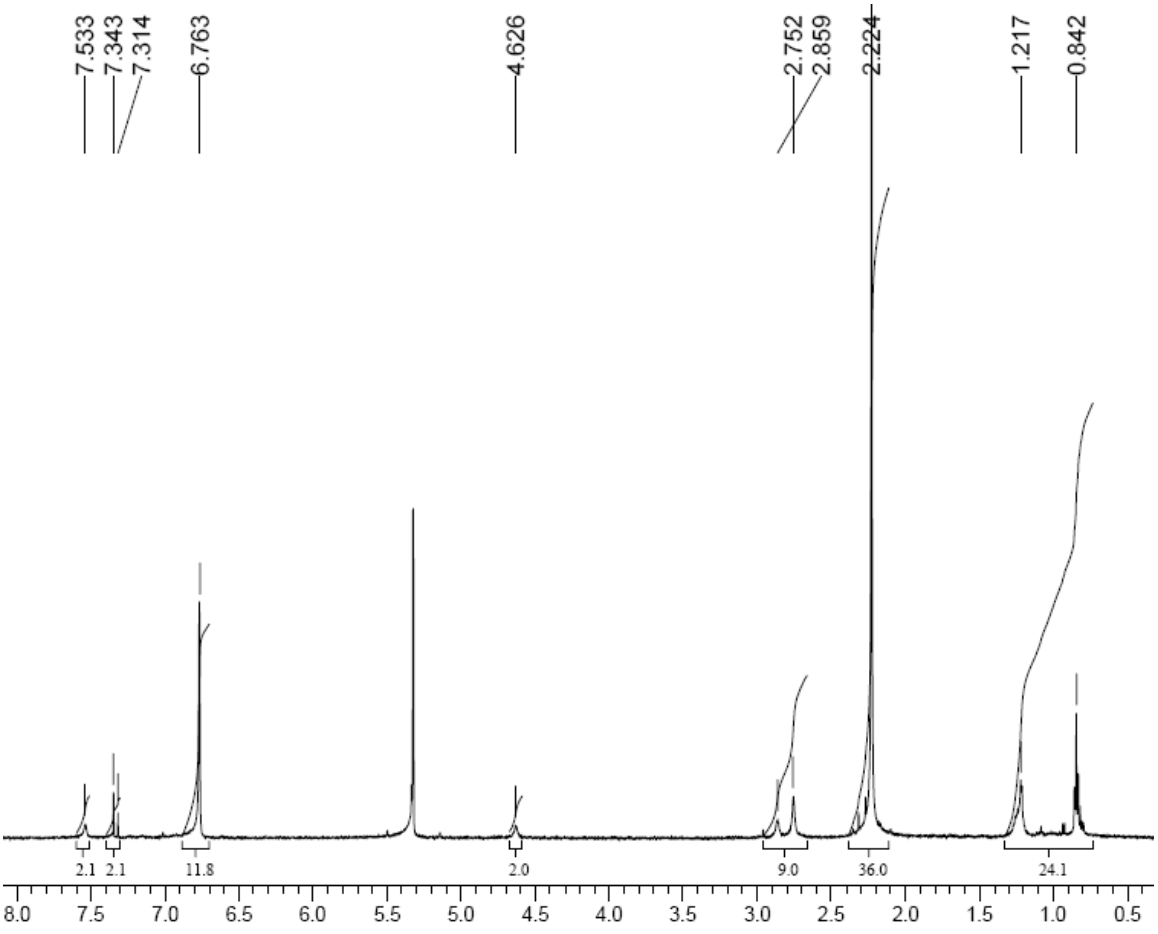

Figure 5.9 ^{1}H NMR spectrum of mesitylenium with $B_{12}Br_{12}^{2-}$ in CD_2Cl_2 at –20 °C

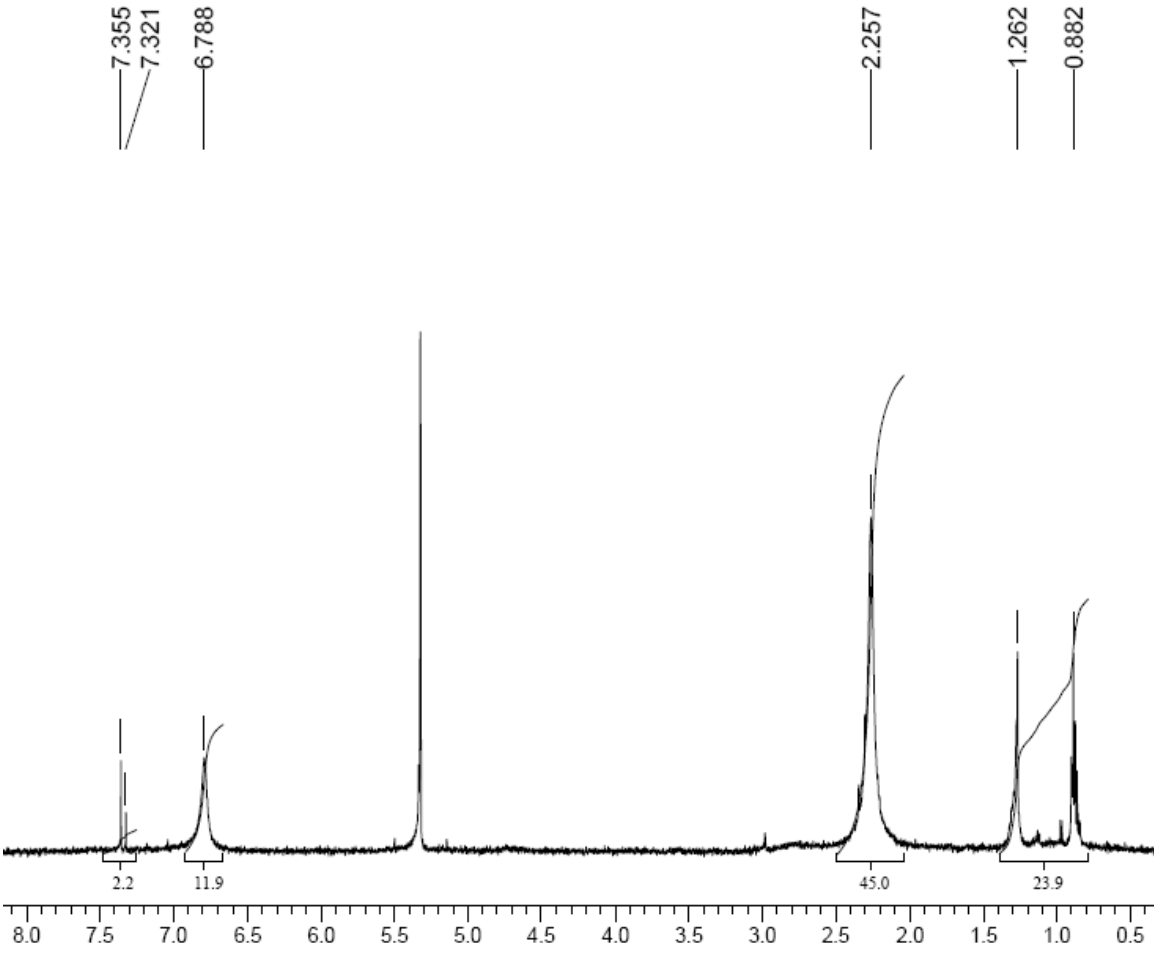

Figure 5.10 ^{1}H NMR spectrum of mesitylenium with $B_{12}Br_{12}^{2-}$ in CD_2Cl_2 at 25 °C

Though many attempts were made by varying solvents as well as temperature conditions, no crystals suitable for x-ray diffraction studies of any of the arenium ion salts were obtained (except inadvertently when attempting to synthesize di-cation salts). This outcome may have been due the unfavorable solvent-arenium interactions; that is, the ionic compound the arenium forms is insoluble in the nonpolar solvent. Despite the

arenium ion salts being solids, they were also found to contain unprotonated solvent molecules, as was noticed in the ^{1}H NMR spectrum of mesitylenium.

Another factor to consider is the time required for crystal growth. Though care was taken to seal the samples that were left to crystallize, inadvertent use of an electron-donor solvent, however small, may produce enough vapors to affect the crystal. For example, a sample of toluenium in a mixture of benzene and hexane produced crystals containing protonated tetrahydrofuran, a solvent not used in any of the syntheses. The structure is shown in Figure 5.11 and its corresponding data in Table 5.2.

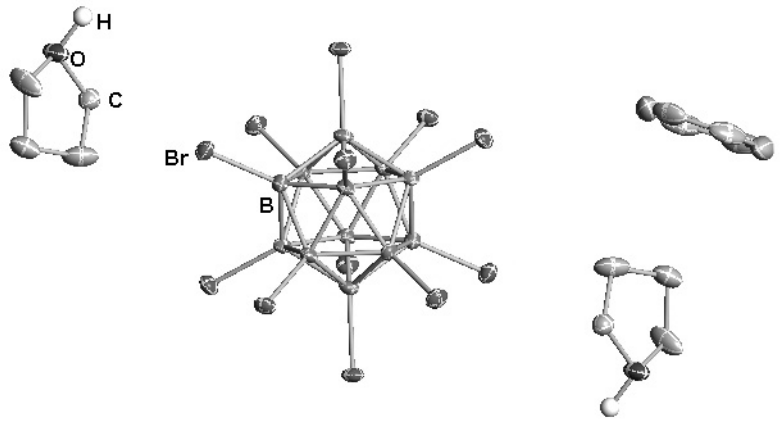

Figure 5.11 Thermal ellipsoid plot of $[HC_4H_8O]_2[B_{12}Br_{12}]\cdot C_6H_6$ (50% probability)

Table 5.2 Crystal structure and refinement data for $[HC_4H_8O]_2[B_{12}Br_{12}]\cdot C_6H_6$

Identification code	cr317_0m-4	
Empirical formula	C14 H24 B12 Br12 O2	
Formula weight	1312.97	
Temperature	100(2) K	
Wavelength	0.71073 Å	
Crystal system	Monoclinic	
Space group	I2/a	
Unit cell dimensions	a = 17.0638(9) Å	α = 90°.
	b = 12.0666(7) Å	β = 110.2597(8)°.
	c = 18.5359(10) Å	γ = 90°.
Volume	3580.5(3) $Å^3$	
Z	4	
Density (calculated)	2.436 Mg/m^3	
Absorption coefficient	13.442 mm^{-1}	
F(000)	2416	
Crystal size	0.10 x 0.09 x 0.08 mm^3	
Theta range for data collection	2.05 to 30.03°.	
Index ranges	-24<=h<=22, 0<=k<=16, 0<=l<=26	
Reflections collected	12357	
Independent reflections	5244 [R(int) = 0.0431]	
Completeness to theta = 30.03°	100.0 %	
Absorption correction	Semi-empirical from equivalents	
Max. and min. transmission	0.4127 and 0.3467	
Refinement method	Full-matrix least-squares on F^2	
Data / restraints / parameters	5244 / 69 / 194	
Goodness-of-fit on F^2	1.061	
Final R indices [I>2sigma(I)]	R1 = 0.0318, wR2 = 0.0696	
R indices (all data)	R1 = 0.0467, wR2 = 0.0735	
Largest diff. peak and hole	1.099 and -0.719 $e.Å^{-3}$	

Besides the above-mentioned areniums, another interesting target was the di-cationic species shown in Figure 5.12. This species was studied in superacidic media by Olah using NMR techniques, and the di-positive charge is believed to be delocalized throughout the ring.[9] It was hypothesized in this work that the di-cationic target may be stabilized by the di-anion, $B_{12}X_{12}^{2-}$ and therefore allow for the structural characterization via X-ray diffraction studies to confirm the di-positive charge distribution.

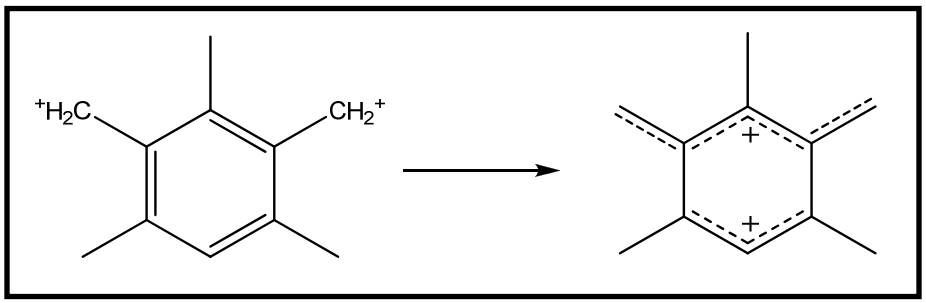

Figure 5.12 Di-cationic Target

Several attempts to isolate the target following Reaction Scheme 5.1 did not yield the di-cationic species. X-Ray diffraction of a crystal obtained contained two different mono-cationic areniums in the lattice. Both cation structures are shown in Figure 5.13. Note how both chlorines are absent in each of the mono-cationic species. Rearrangement also appears to have occurred due to the mixture of cationic products. Future work in obtaining the di-cationic shown in Figure 5.12 could involve the use of low temperatures for the synthesis and solvents such as methylene chloride.

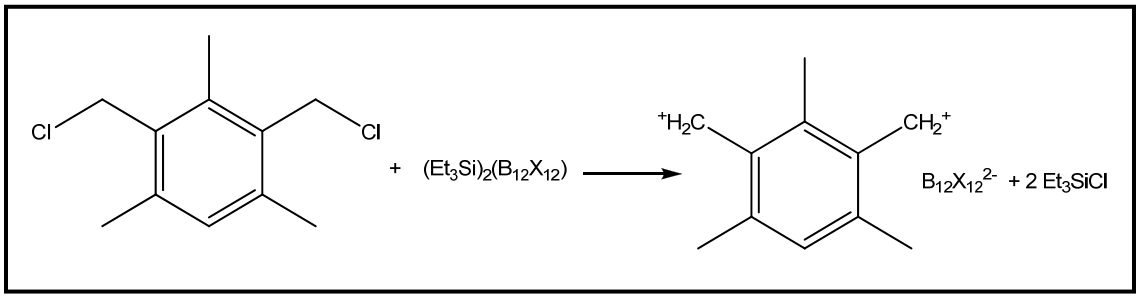

Reaction Scheme 5.1 Proposed Synthesis of Di-cationic Target

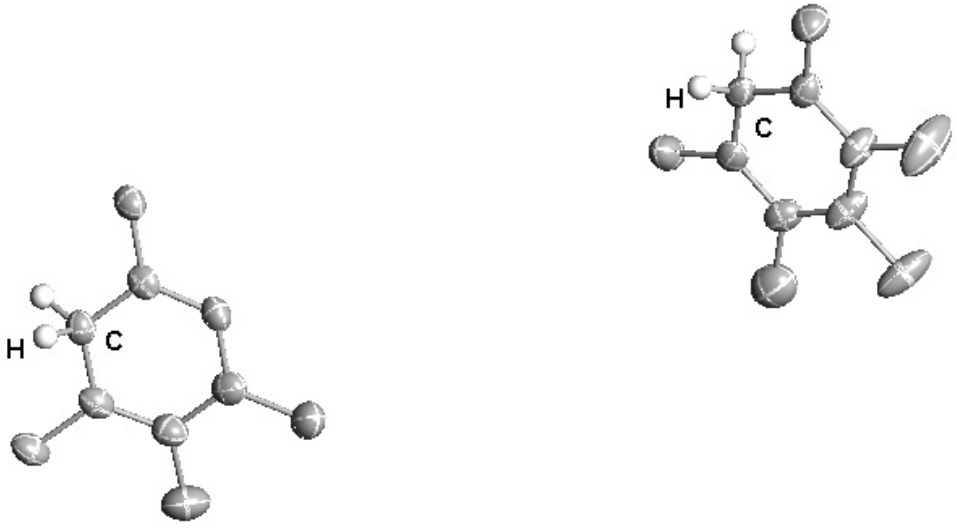

Figure 5.13 Thermal ellipsoid plot of the tetramethylbenzenium and pentamethylbenzenium (50% probability ellipsoids, except for the di-anion which was omitted for clarity)

Table 5.3 Crystal structure and refinement data for cr308_0m.

Identification code	cr308_0m	
Empirical formula	C27 H47 Ag0.01 B18 Cl18 Si	
Formula weight	1232.96	
Temperature	100(2) K	
Wavelength	0.71073 Å	
Crystal system	Trigonal	
Space group	P-3	
Unit cell dimensions	a = 31.6284(8) Å	a = 90°.
	b = 31.6284(8) Å	b = 90°.
	c = 9.1064(2) Å	γ = 120°.
Volume	7889.2(3) $Å^3$	
Z	6	
Density (calculated)	1.557 Mg/m^3	
Absorption coefficient	0.988 mm^{-1}	
F(000)	3715	
Crystal size	0.16 x 0.13 x 0.09 mm^3	
Theta range for data collection	1.29 to 28.28°.	
Index ranges	-42<=h<=42, -42<=k<=42, -12<=l<=12	
Reflections collected	165029	
Independent reflections	13039 [R(int) = 0.0668]	
Completeness to theta = 28.28°	99.9 %	
Absorption correction	Semi-empirical from equivalents	
Max. and min. transmission	0.9189 and 0.8571	
Refinement method	Full-matrix least-squares on F^2	
Data / restraints / parameters	13039 / 0 / 603	
Goodness-of-fit on F^2	1.063	
Final R indices [I>2sigma(I)]	R1 = 0.0452, wR2 = 0.1102	
R indices (all data)	R1 = 0.0706, wR2 = 0.1254	
Largest diff. peak and hole	1.128 and -0.573 $e.Å^{-3}$	

5.4 Conclusions

The di-negative charge of $B_{12}X_{12}^{2-}$ may have led one to predict a more basic anion and therefore a less acidic conjugate acid. However, both protons were found to be sufficiently acidic to protonate arenes. Since benzene was protonated, the anhydrous acids, $H_2(B_{12}X_{12})$ are of comparable strength to the carborane acids, specifically $H(CHB_{11}Cl_{11})$. Since $H(CHB_{11}Cl_{11})$ is currently the strongest isolable Bronsted acid because it can protonate benzene, the same conclusion can be made about the di-protic acid, $H_2(B_{12}Cl_{12})$. Though the acids strengths are similar, future investigations may include differentiating between the two acid strengths.

5.5 References

1. "Carborane Acids. New "Strong Yet Gentle" Acids for Organic and Inorganic Chemistry," Reed, C.A. *Chem Commun*. **2005**, 1669-1677.

2. "*The Action of the Catalyst Couple Aluminum Chloride-Hydrogen on Toluene at Low Temperatures; the Nature of Friedel-Crafts Complexes*," Brown, H.C.; Pearsall, H.W. *J. Am. Chem Soc.* **1952**, *74*, 191-195. "*Certain Trialkyalted Benzenes and Their Compounds with Aluminum Chloride and with Aluminum Bromide*," Norris, J.F.; Ingraham, J.N. *J. Am. Chem. Soc.* **1940**, *62*, 1298-1301. "*Isolation of the Stable Boron Trifluoride-Hydrogen Fluoride Complexes of the Methylbenzenes; the Onion salt (or σ-Complex) Structure of the Friedel-Crafts Complexes*," Olah, G.A.; Kuhn, S.; Pavlath, A. *Nature* **1956**, 693- 694. "*Proton Magnetic Resonance of Aromatic Carbonium Ions I. Structure of the Conjugate Acid*," MacLean, C.; Van der Waals, J.H.; Mackor, E.L. *Mol. Phys*. **1958**, *1*, 247- 256. "*The 1,1,2,3,4,5,6-heptamethylbenzenonium Ion*," von E. Doering, W.; Saunders, M.; Boyton, H.G.; Earhart, H.W.; Wadley, E.F.; Edwards, W.R.; Laber, G. *Tetrahedron* **1958**, *4*, 178- 185. "*Nuclear Magnetic Resonance Studies of the Protonation of Weak Bases in Fluorosulphuric Acid III. Methylbenzenes and Anisole*," Birchall, T.; Gillespie, R.J. *Can. J. Chem.* **1964**, *42*, 502- 513. "*Stable Carbocations. CXXIV. Benzenium Ion and Monoalkylbenzenium Ions*," Olah, G.A.; Schlosberg, R.H.; Porter, R.D.; Mo, Y.K.; Kelly, D.P.; Mateescu, G.D. *J. Am. Chem. Soc.* **1972**, *94*, 2034-2043.

3. "*Arenium Ions- Structure and Reactivity*," Koptyug, V.A. Rees, C.; Ed; Springer-Verlag: Heidelberg, Germany, **1984**, 1-227.

4. "*Isolating Benzenium Ion Salts*," Reed, C.A.; Kim, K.-C.; Stoyanov, E.; Stasko, D.; Tham, F.S.; Mueller, L.J.; Boyd, P.D.W. *J. Am. Chem. Soc*. **2003**, *125*, 1796- 1804.

5. Perrin, D.D.; Armarego, W.L.F.; Perrin, D.R. *Purification of Laboratory Chemicals*; 2nd ed, Pergamon Press Ltd.: Sydney, **1980**.

6. "*Protonated Benzene: IR Spectrum and Structure of $C_6H_7^+$*," Solcá, N.; Dopfer O. *Angew. Chem. Int. Ed*. **2002**, *41*, 3628-3631.

7. "*Stable Carbonium Ions. IX. Methylbenzenonium Hexafluoroantimonates*," Olah, G.A. *J. Am. Chem. Soc*. **1965**, *87*, 1103-1108.

8. "*The Behavior of the 3-Phenyl-2-butanols in SO_2-FSO_3H-SBF_5*," Brookhart, M.; Anet, F.A.L.; Winstein, S. *J. Am. Chem. Soc.* **1966**, *88*, 5657- 5659.

9. "*Protonation of Simple Aromatics in Superacids. A Reexamination*," Farcasiu, D. *Acc. Chem. Res*. **1982**, *15*, 46-51.

CHAPTER 6

Di-cationic Targets, Methyl Derivatives, and Future Work with $B_{12}X_{12}^{2-}$ (X = Cl, Br)

6.1 Introduction

The $B_{12}X_{12}^{2-}$ di-anions are hypothesized to stabilize highly electrophilic di-cations that may otherwise not be stabilized by mono-anions.[1] The underlying principle to this hypothesis is that, as determined through volume-based approach calculations, 1:1 salts have much greater lattice energies contributing to the salt's stability than the lattice energies of comparable 2:1 salts.[1,2] Knapp and Schulz recently reported an experimental proof of this principle with the synthesis and structural characterization of the 1:1 salt, $[Li_2(SO_2)_8][B_{12}Cl_{12}]$, which formed instead of the 2:1 salt, $[Li(SO_2)_4]_2[B_{12}Cl_{12}]$.[1] Though electrostatic repulsions would be minimized in the 2:1 salt, the lattice energy of the 1:1 compensates for the electrostatic repulsion that could have resulted in a "Coulombic explosion" or the di-cation's decomposition due to positive charges close in proximity.[1] The 1:1 salt itself is the first example of a di-nuclear SO_2 complex, and such species have never been observed with weakly coordinating *mono*-anions.[1]

It is of interest in this chapter to provide further proof to the above-mentioned principle targeting a di-cation with the positive charges on *adjacent* atoms, such as elusive hexamethylhydrazinium ion, $(CH_3)_3N^+–N^+(CH_3)_3$, $Me_6N_2^{2+}$, with $B_{12}X_{12}^{2-}$ as the counter-ion. In $[Li(SO_2)_4]_2[B_{12}Cl_{12}]$, the positive charges are not on adjacent atoms, but rather, the two Li^+ ions are separated by SO_2 molecules that aid in lowering the potential for a "Coulombic explosion". In Me_6N^{2+}, there is no such cushion, and its isolation would

truly support the principle of greater lattice energy stabilization of 1:1 salts versus 2:1 salts, despite electrostatic repulsions within the di-cation.

Thus far, the elusive di-cation hexamethylhydrazinium has yet to be characterized by X-ray crystallography, but there is strong spectroscopic evidence for its formation using the carborane mono-anion as the counter-ion in a 1:2 salt.[3] If, instead, $B_{12}X_{12}^{2-}$ is the counter-ion, the 1:1 the salts may have more favorable lattice energies, and form crystals suitable for X-ray diffraction studies. $Me_6N_2^{2+}$ is predicted to be isolable despite the adjacent positive charges. Thermodynamic calculations have shown that the analogous, di-protonated hydrazine, $H_6N_2^{2+}$, is unstable because the adjacent di-positive charges would result in the homolytic bond dissocation of N-N.[4] But, the activation energy required for fission is high enough for $H_6N_2^{2+}$ to be stable at room temperature.[4] If the activation energy of $Me_6N_2^{2+}$ is assumed to be similar to that of the di-protonated analogue, $H_6N_2^{2+}$, then $Me_6N_2^{2+}$ may be isolated with the use of a WCA.[3,4]

Various attempts were made in this present work to obtain crystals suitable for X-ray diffraction studies of the 1:1 salt, $[Me_6N][B_{12}X_{12}]$ (X = Cl or Br). The amorphous solid materials obtained in the syntheses described herein were found to be insoluble in the very limited choice of solvents for crystallization. A hypothesis for the low solubility of the product is that the material is indeed the 1:1 salt therefore and therefore the lattice energies are significantly large enough that they do not allow for the solvation of the salt that is necessary for crystallizing. In the work described in previous chapters, the crystals that were analyzed have always been 2:1 salts. Herein this chapter, the crystals obtained were mostly 2:1 salts, and this may serve as indirect evidence that 2:1 salts have lower

lattice energies when compared to similar 1:1 salts. As future work, other di-cationic species with adjacent positive charges could also be investigated, such as those discussed in a review by Alabugin, et al.[5]

Despite the fact that $[Me_6N][B_{12}X_{12}]$ was not positively characterized, other potentially useful compounds were preliminarily identified en route. For example, preliminary data suggest that the dimethyl derivative, $(CH_3)_2(B_{12}Cl_{12})$, forms. This compound may have analogous properties to that of the methylating reagent, "Mighty Methyl", $CH_3(CHB_{11}X_{11})$.[6] When alkylating agents, such as methyl triflate, are not reactive enough to alkylate, alkyl carboranes have been able to do so.[7] The question arose as to whether $(CH_3)_2(B_{12}X_{12})$ would also be an alkylating or di-alkylating reagent as are the analogous carborane methylating reagents. This possibility was tested via the attempts to di-methylate tetramethylhydrazine. As the product could not be positively identified due to the very poor solubility, a definite conclusion cannot be made. Research into the alkylating ability of $(CH_3)_2(B_{12}X_{12})$ and other similar compounds would be future work.

Herein is described the preliminary data for the synthesis of $(CH_3)_2(B_{12}X_{12})$ and discussion of the methodologies used in the attempts to dimethylate tetramethylhydrazine.

6.2 Experimental

Air sensitive materials were handled in helium filled Vacuum Atmospheres gloveboxes (O_2, H_2O < 2 ppm) or on a vacuum manifold using standard Schlenk techniques. *Ortho*-dichlorobenzene and n-hexane were dried following literature methods

and stored under molecular sieves. Liquid SO_2 was dried/stored over P_2O_5 and transferred via vacuum at dry ice/acetone temperature. NMR spectra were obtained on a Bruker Avance 300 MHz or Inova 500 MHz spectrometer. FT-IR spectra were obtained on a Perkin Elmer Spectrum 100 Series spectrometer in a nitrogen-filled glovebox.

$(CH_3)_2(B_{12}X_{12})\cdot xCF_3SO_3CH_3$. Enough methyl triflate, MeOTf, was added to barely cover ~200 mg $(Et_3Si)_2(B_{12}X_{12})$ that was chilled in a bath of copper shots cooled with liquid nitrogen. The slurry was stirred for at least 5 minutes and the off-white to light yellow solid collected.

X = Br: ^{1}H NMR: (500 MHz, externally referenced with acetone-d_6, –60 °C) 4.10 (s), 4.18 (s), 4.34 (s). ^{13}C NMR: (500 MHz, externally referenced with acetone-d_6, –60 °C) 64.97, 68.91, 115.71, 118.22, 120.75, 123.29. ^{11}B NMR: (500 MHz, externally referenced with $BF_3{\cdot}OEt_3$, –60 °C) –11.22 (s). IR (KBr): 3063m, 2967w, 2789w, 1587w, 1512w, 1451m, 1408m, 1247m, 1213m, 1141m, 1001s, 983s, 912m, 801m, 755m, 736m, 658w, 632w, 611m, 575w, 517w, 465w.

$(CH_3)_2(B_{12}Br_{12})$ Enough n-hexane (less than 1 mL) was added to barely cover ~80 mg $(Et_3Si)_2(B_{12}Br_{12})$ that was chilled in a bath of copper shots cooled with liquid nitrogen. A couple of drops of methyl triflate were added. The slurry was stirred for 5 minutes and the solid collected. The off-white solid was washed with a minimal amount of chilled n-hexane. IR (KBr): 3062w, 2951w, 1596w, 1523w, 1453w, 1399b, 1287m, 1250m, 1216m, 1147m, 1000s, 983s, 617w, 523m.

$[(Et_3Si)Me_4N_2]_2[B_{12}Cl_{12}]$ A few drops of tetramethylhydrazine were added to a solution of $(Et_3Si)_2(B_{12}Cl_{12})$ in *ortho*-dichlorobenzene. The solution turned cloudy and white

precipitate formed. The solid was collected and washed with n-hexane. Crystals suitable for X-ray diffraction were grown from ODCB/n-hexane and the structure is shown in Figure 6.20.

$[Et_3SiN_2(CH_3)_4][Et_3Si(B_{12}Br_{12})]$ $(Et_3Si)_2(B_{12}Br_{12})$ was reacted with ~1 equivalent of tetramethylhydrazine in ODCB, the resultant solution was slightly cloudy. n-Hexane was added in attempts to precipitate out the product, but instead, a very waxy product formed. The solvent was therefore removed with a pipette and fresh ODCB was added to the waxy solid. Crystals suitable for x-ray diffraction were obtained when a small amount of the waxy material was removed and re-dissolved in ODCB, followed by layering with n-hexane. The structure is shown in Figure 6.22.

6.3 Results and Discussion

Reaction Schemes 6.1 (Synthetic Route A) and 6.2 (Synthetic Route B) were followed in the attempt to synthesize $[Me_6N_2][B_{12}X_{12}]$. In Synthetic Route A, the synthesis of $(CH_3)_2(B_{12}X_{12})$ was attempted in both chilled n-hexane and neat methyl triflate. The analogous methyl carborane, $CH_3(CHB_{11}Cl_{11})$, forms transiently in cold n-hexane but quickly reacts with the solvent.[6] $CH_3(CHB_{11}Cl_{11})$ has yet to be isolated due to its high reactivity, and the same reactivity was hypothesized to be the case with $(CH_3)_2(B_{12}X_{12})$.[6] Therefore, in attempts to isolate $(CH_3)_2(B_{12}X_{12})$, n-hexane was not the only solvent used. Neat methyl triflate was used as a solvent in the first reaction of Synthetic Route A.

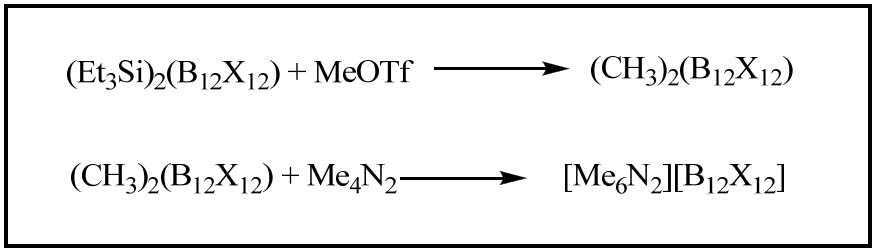

Reaction Scheme 6.1 Synthetic Route A to $[Me_6N_2][B_{12}X_{12}]$

In Reaction Scheme B, $(Et_3Si)_2(B_{12}X_{12})$ was first reacted with Me_4N_2 and then methyl triflate.

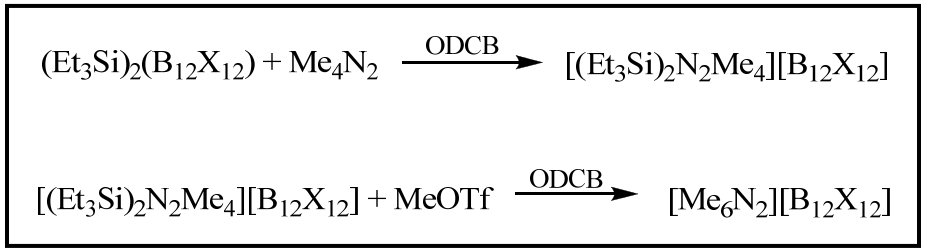

Reaction Scheme 6.2 Synthetic Route B to $[Me_6N_2][B_{12}X_{12}]$

The reaction of $(Et_3Si)_2(B_{12}Br_{12})$ in neat methyl triflate appears to result in the formation of $(CH_3)_2(B_{12}Br_{12})\cdot xCH_3OTf$. The white, solid compound was completely soluble in liquid SO_2. The ^{13}C NMR spectrum at –60 °C, Figure 6.1, compared to the ^{13}C NMR of methyl triflate in SO_2, Figure 6.2, indicates the presence of methyl triflate. There are only two other bands, at 69 and 80 ppm in the ^{13}C NMR of $(CH_3)_2(B_{12}Br_{12})$. When allowed to warm to 25 °C, another band appears at 52 ppm in the ^{13}C NMR spectrum (Figure 6.3). In comparison to $CH_3(CHB_{11}Me_5Br_6)$, the ^{13}C NMR chemical shifts for the methyl carbon were at 33 and 34 ppm for the two different isomers (12-isomer and 7-

isomer, respectively).[2] The ^{13}C NMR chemical shifts of the methyl carbon of $CH_3(CHB_{11}Me_5Cl_6)$ were at 46.8 and 46.6 ppm. Isomers are not expected with the $B_{12}X_{12}^{2-}$ di-anions, though, because the di-anion is symmetrical and it was expected that the methyl interactions with the di-anion are identical. The appearance of two bands, and then a third band when the sample was warmed to 25 °C, is puzzling and an area for future investigations.

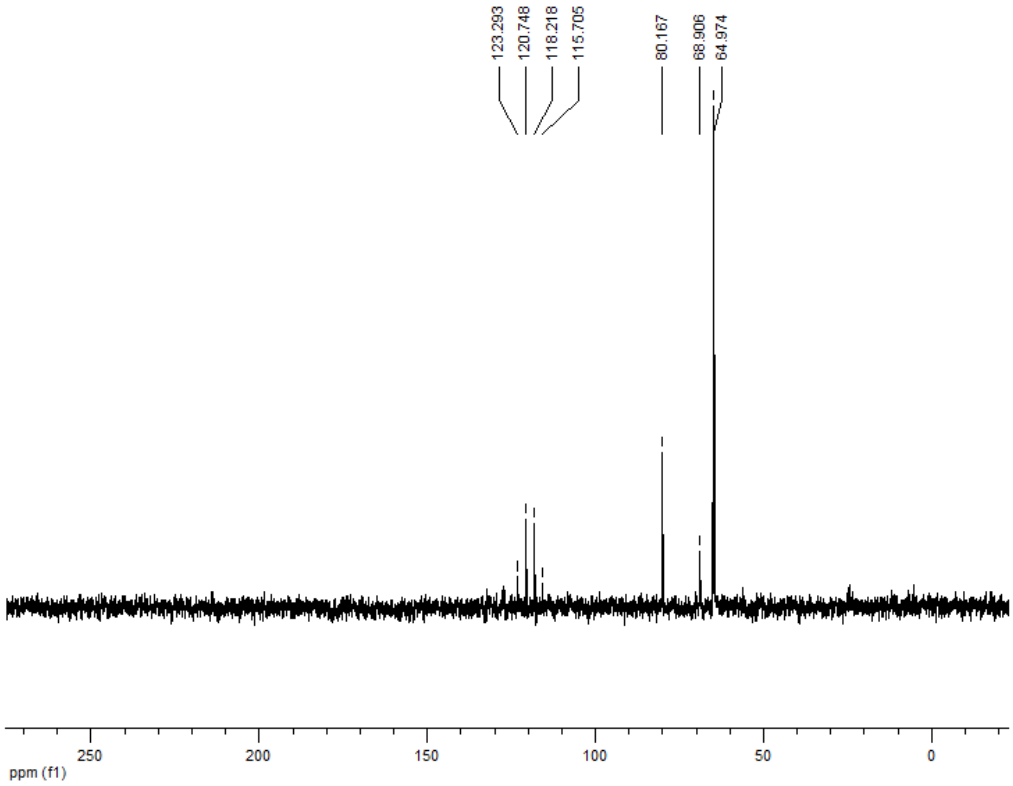

Figure 6.1 ^{13}C NMR spectrum of $(CH_3)_2(B_{12}Br_{12})$ containing excess methyl triflate in SO_2 at –60 °C

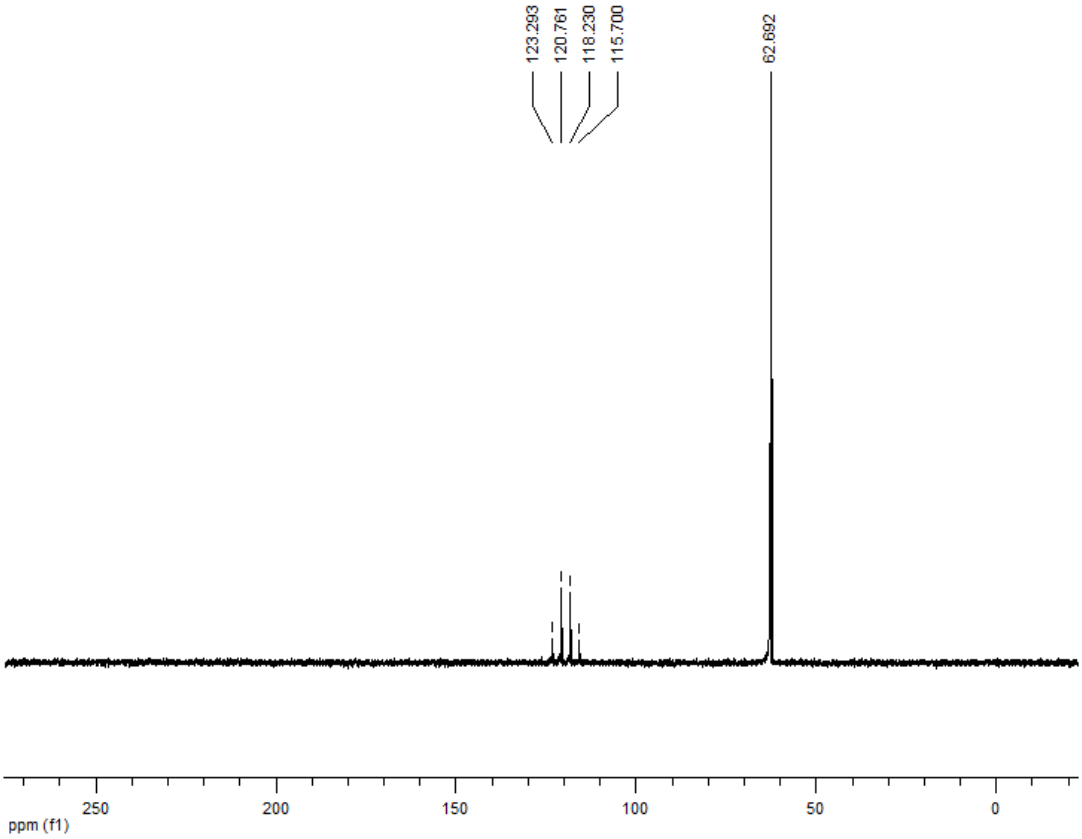

Figure 6.2 ^{13}C NMR spectrum of methyl triflate in SO_2

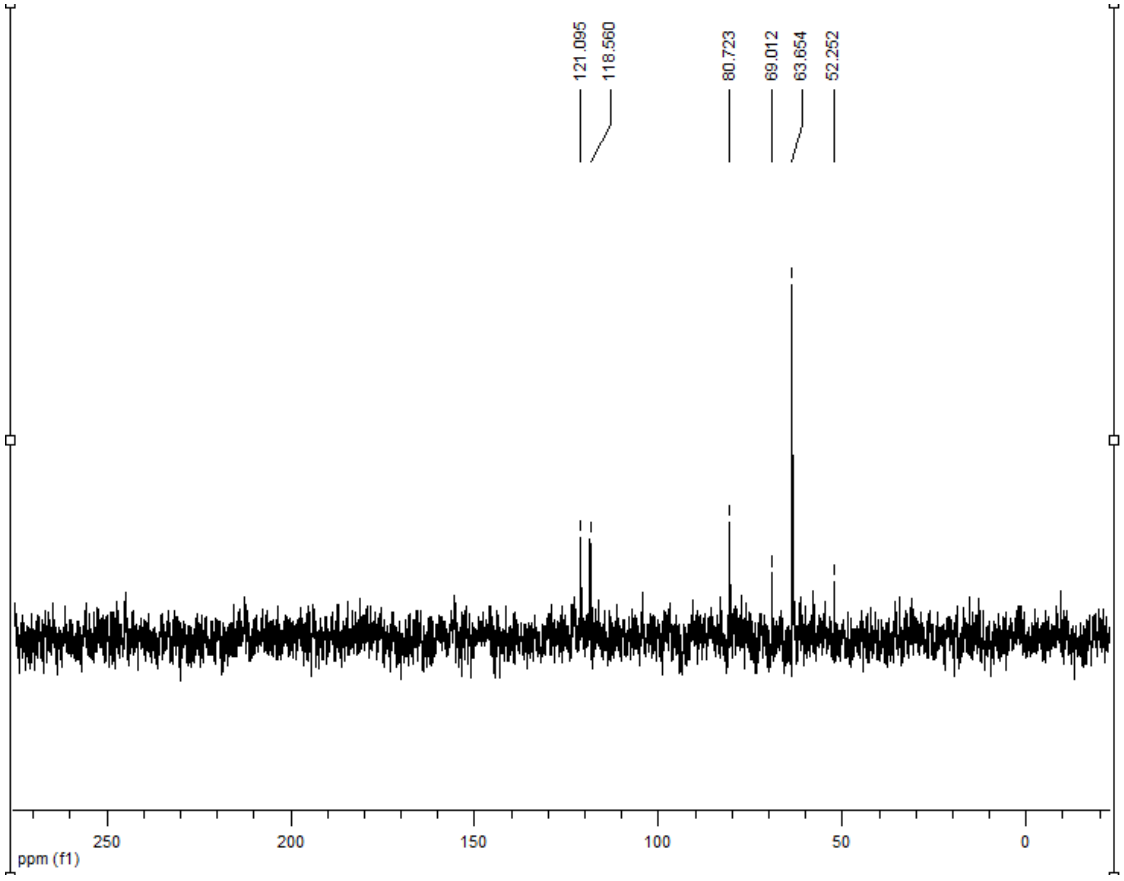

Figure 6.3 ^{13}C NMR spectrum of $(CH_3)_2(B_{12}Br_{12})$ containing excess methyl triflate in SO_2 at 25 °C

The ^{1}H NMR spectrum of $(CH_3)_2(B_{12}Br_{12})$ also was indicative of the presence of methyl triflate at an approximately 4:1 ratio as seen in Figure 6.4. There are also trace amounts of impurities. The entire ^{1}H NMR spectrum is shown in Figure 6.5. The ^{1}H NMR of methyl triflate in SO_2 is shown in Figure 6.6 for comparison. At 25 °C, the peaks sharpen in the ^{1}H NMR spectrum of $(CH_3)_2(B_{12}Br_{12})$ containing the exess methyl triflate (Figure 6.7). The peaks are all singlets which are indicative of methyl hydrogens. The ^{11}B NMR spectra at –60 °C and 25 °C contain only a singlet and are shown in Figures 6.8 and 6.9, respectively.

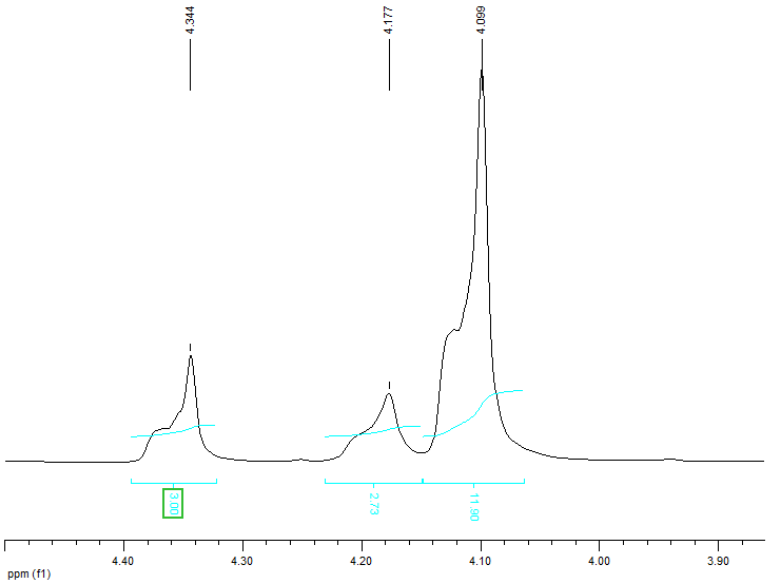

Figure 6.4 Partial ^{1}H NMR spectrum of $(CH_3)_2(B_{12}Br_{12})$ containing excess methyl triflate in SO_2 at –60 °C

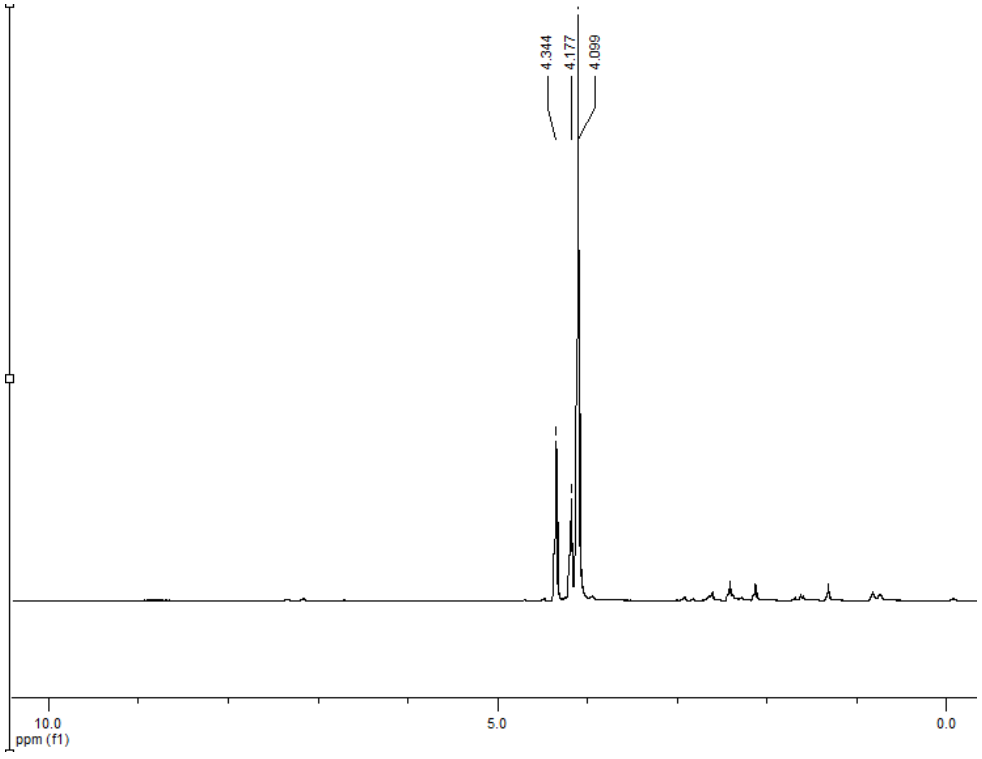

Figure 6.5 ^{1}H NMR spectrum of $(CH_3)_2(B_{12}Br_{12})$ containing excess methyl triflate in SO_2 at –60 °C

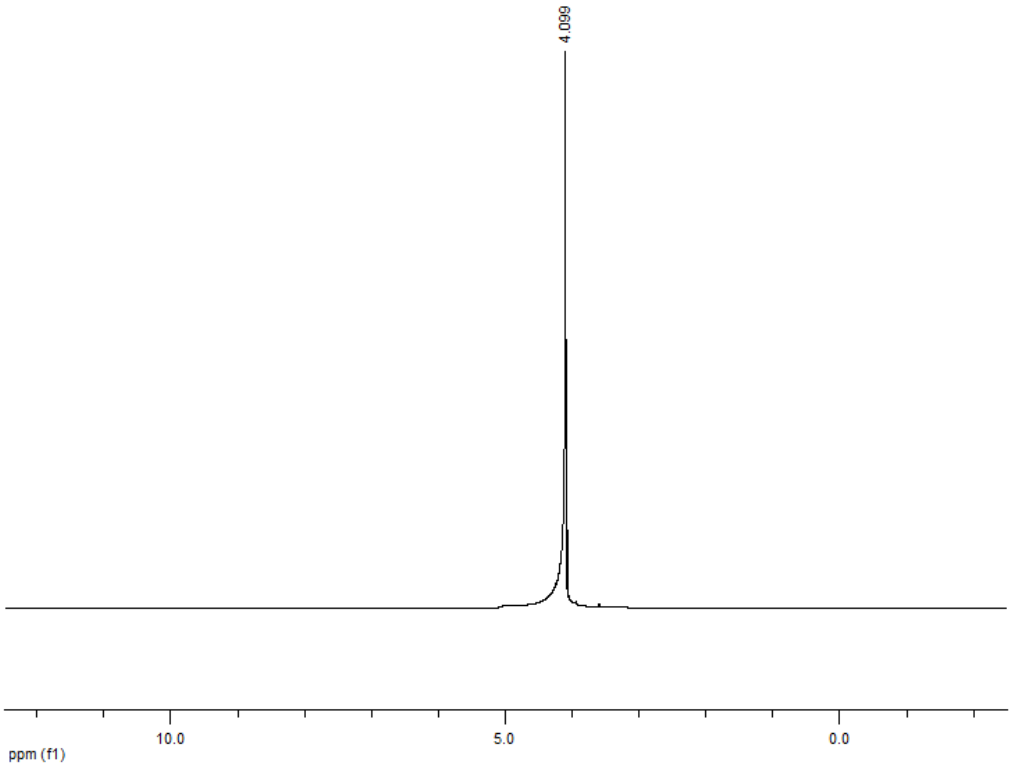

Figure 6.6 ^{1}H NMR spectrum of methyl triflate in SO_2

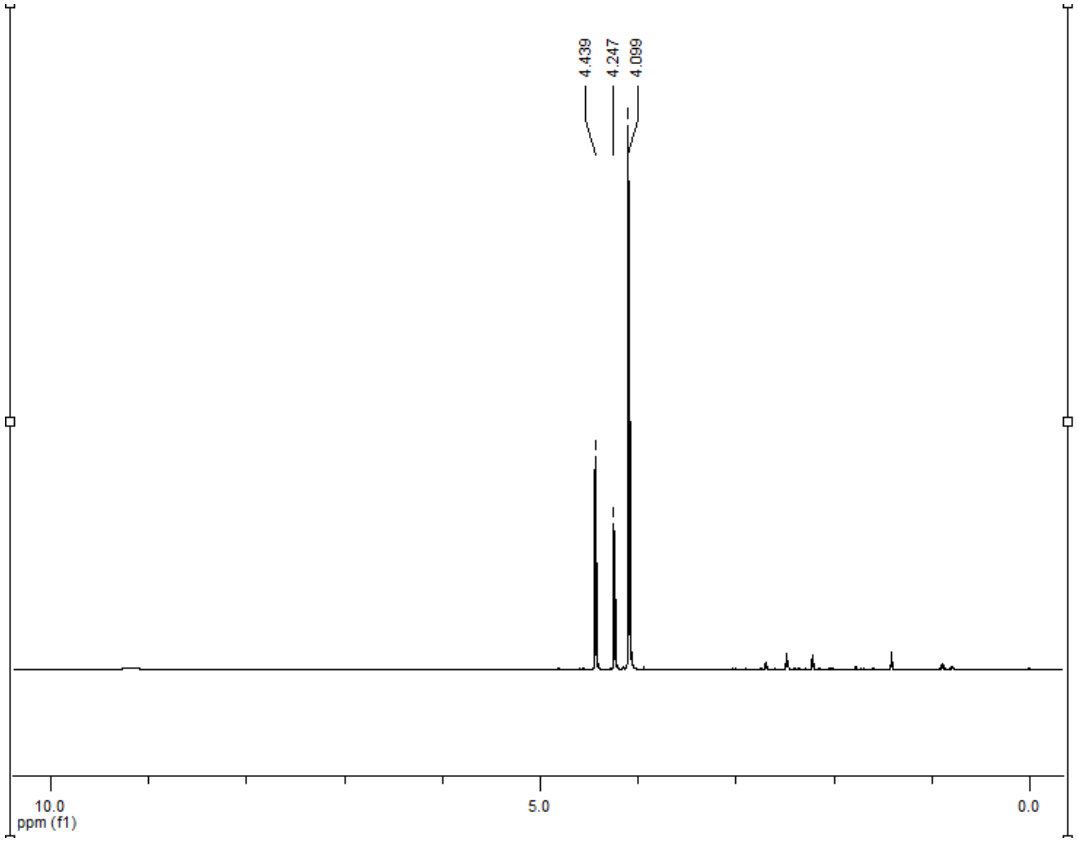

Figure 6.7 ^{1}H NMR spectrum of $(CH_3)_2(B_{12}Br_{12})$ containing excess methyl triflate in SO_2 at 25 °C

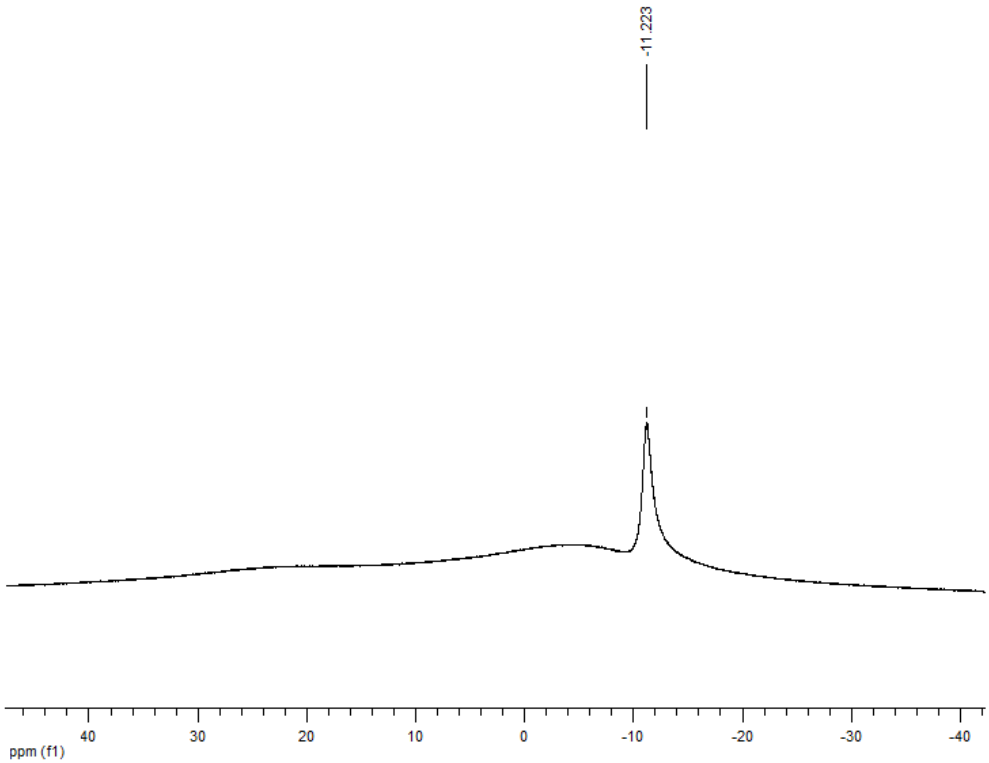

Figure 6.8 ^{11}B NMR spectrum of $(CH_3)_2(B_{12}Br_{12})$ containing excess methyl triflate in SO_2 at –60 °C (external reference $BF_3{\cdot}OEt_2$)

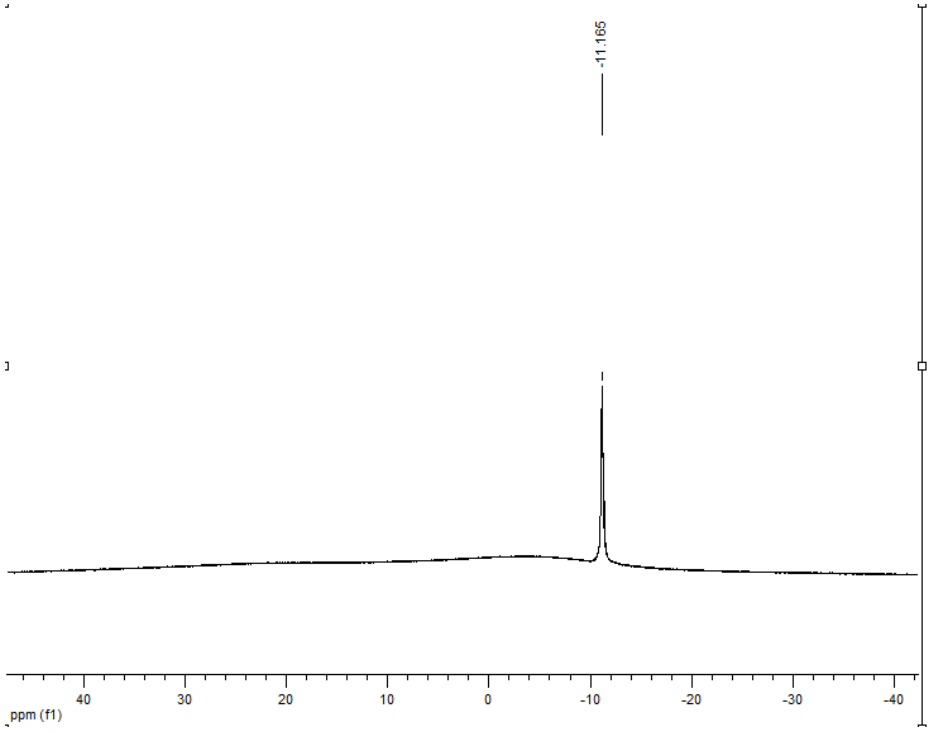

Figure 6.9 ^{11}B NMR spectrum of $(CH_3)_2(B_{12}Br_{12})$ containing excess methyl triflate in SO_2 at 25 °C

The reaction between $(Et_3Si)_2(B_{12}Br_{12})$ and approximately two equivalents of methyl triflate in chilled n-hexane resulted in a different product. A white solid was obtained, and found to be soluble in SO_2. This condition allowed for NMR spectroscopy. The ^{13}C NMR spectrum had three peaks at 214, 125, and 31 ppm as seen in Figure 6.10. As only one signal was expected, these peaks were found difficult to interpret. The ^{1}H NMR spectrum had a single peak, externally referenced at 2.3 ppm, shown in Figure 6.11. The ^{11}B NMR spectrum, Figure 6.12, contained a single peak at 11 ppm.

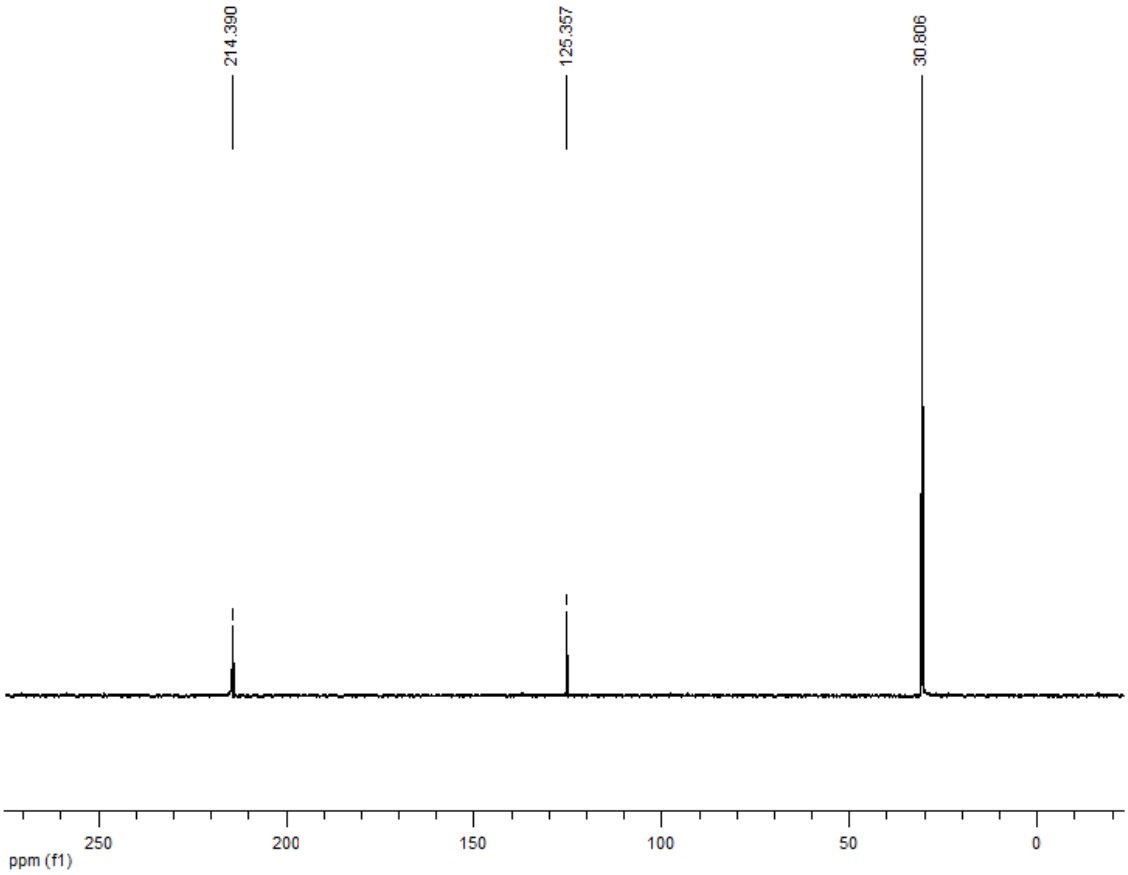

Figure 6.10 ^{13}C NMR spectrum of $(CH_3)_2(B_{12}Br_{12})$ at -60°C in SO_2 (external reference acetone)

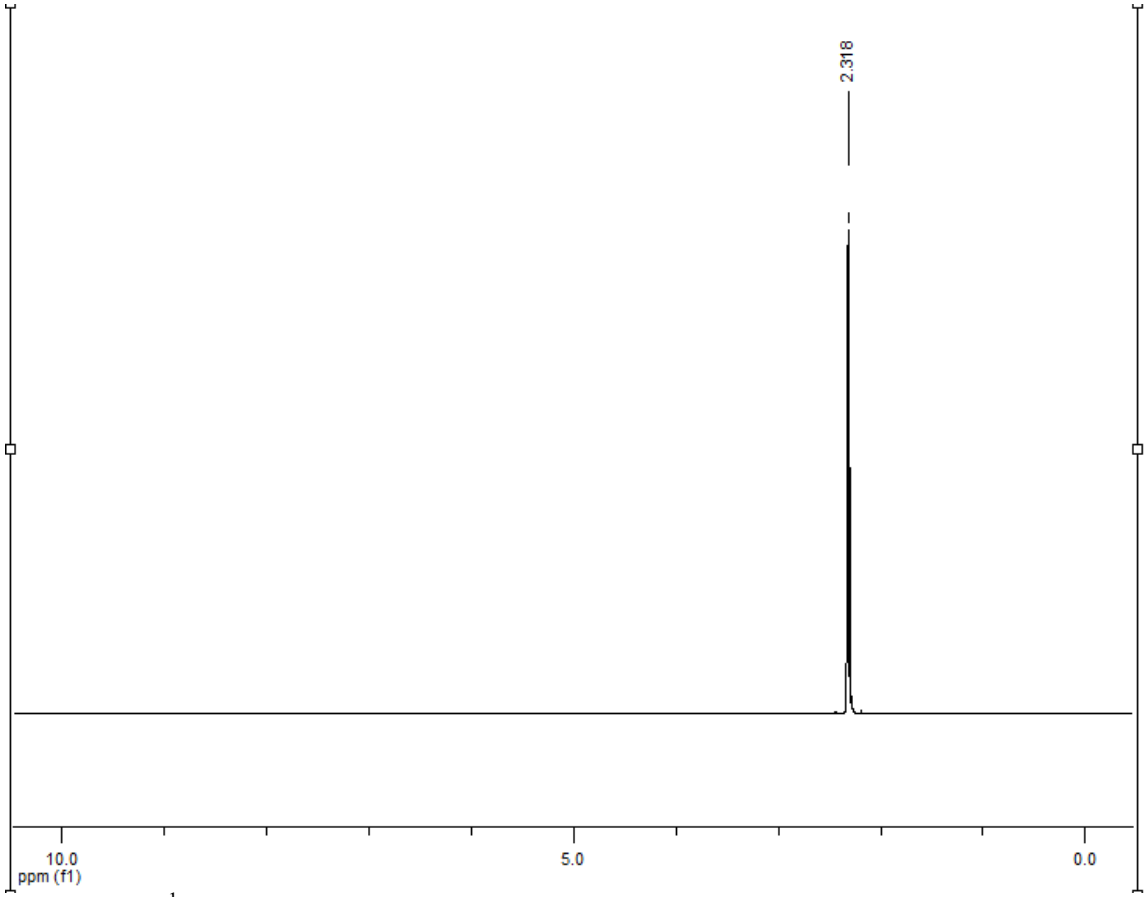

Figure 6.11 ^{1}H NMR spectrum of $(CH_3)_2(B_{12}Br_{12})$ in SO_2 at –60 °C (external reference d_6-acetone)

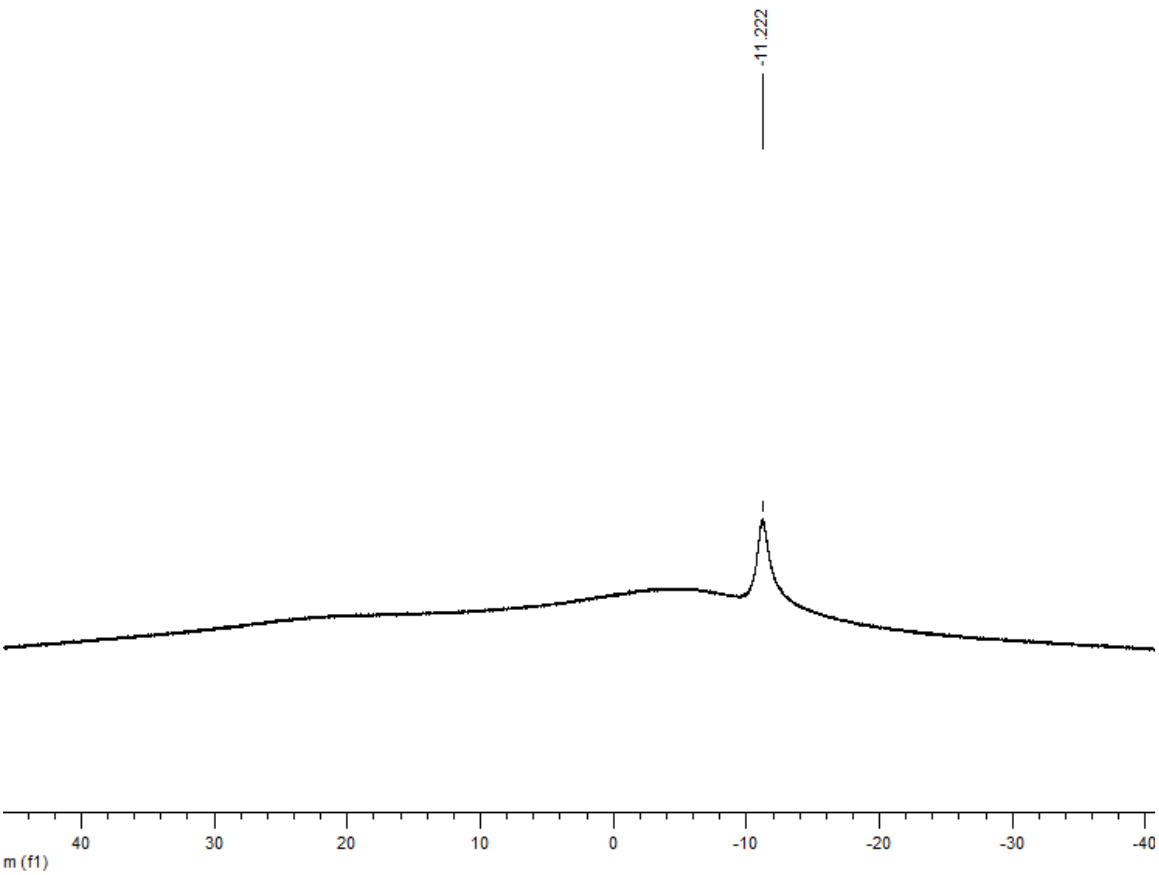

Figure 6.12 ^{11}B NMR spectrum of $(CH_3)_2(B_{12}Br_{12})$ in SO_2 at –60 °C (external reference $BF_3{\cdot}OEt_2$)

The FT-IR spectrum supports the preliminary determination that $(CH_3)_2(B_{12}Br_{12})$ is indeed a product. The spectrum indicates the presence of $(CH_3)_2(B_{12}Br_{12})$ and excess methyl triflate (Figure 6.13). The ATR spectrum of methyl triflate is shown in Figure 6.14 for comparison. Compared to $CH_3(CHB_{11}Me_5Br_6)$, there are several key vibrations due to the methyl group. As shown in Table 6.1, the stretching frequencies of the carborane analogue are higher than the stretching frequencies of methyl triflate, while the bending frequencies are lower.[7] These data were indicative that the positive charge on the methyl is higher in the carborane analogue than in methyl triflate. A similar pattern was

observed with the $B_{12}Br_{12}^{2-}$ derivative. The stretching frequency at 3078 cm^{-1} is observed as a shoulder in the FT-IR spectrum of $CH_3(CHB_{11}Me_5Br_6)$, and that frequency is at approximately 3075 cm^{-1} in both $(CH_3)_2(B_{12}Br_{12})\cdot xMeOTf$ and $(CH_3)_2(B_{12}Br_{12})$.

In regards to the removal of excess methyl triflate from the solid, $(CH_3)_2(B_{12}Br_{12})\cdot xMeOTf$ was placed under vacuum and some of the excess methyl triflate was removed by on the IR spectrum, but not entirely removed. The FT-IR spectrum is shown in Figure 6.16.

Table 6.1 Methyl Group Modes (cm^{-1})

Species	$\nu_3(E)$	$\nu_1(A_1)$	$\nu_4(E)$	$\nu_2(A_1)$
$CH_3(CHB_{11}Me_5Br_6)$[ref. 7]	3078	3063	1400	1292
$(CH_3)_2(B_{12}Br_{12})\cdot xMeOTf$	3075(shoulder)	3063	1451	--
$(CH_3)_2(B_{12}Br_{12})\cdot xMeOTf$ after pumping	3080(shoulder)	3061	1399	1287
$(CH_3)_2(B_{12}Br_{12})$	3075(shoulder)	3062	1399	1287
$CH_3CF_3SO_3$ (ATR)	3042 (vw)	2982	1447	--

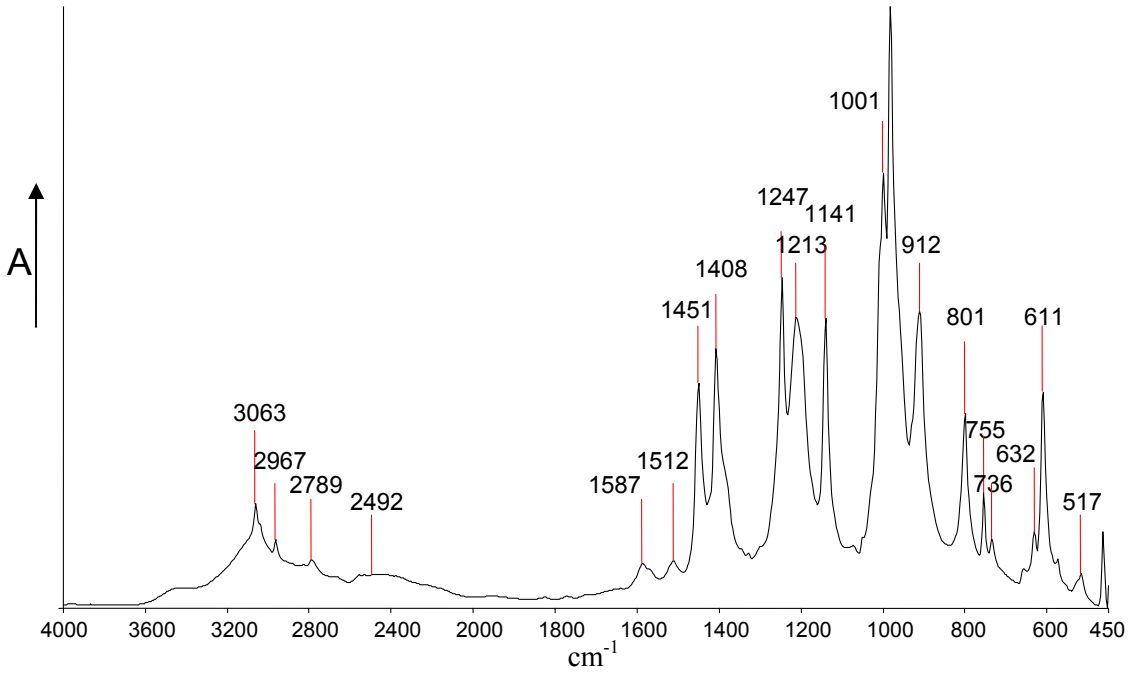

Figure 6.13 FT-IR spectrum of $(CH_3)_2(B_{12}Br_{12})$ containing excess methyl triflate

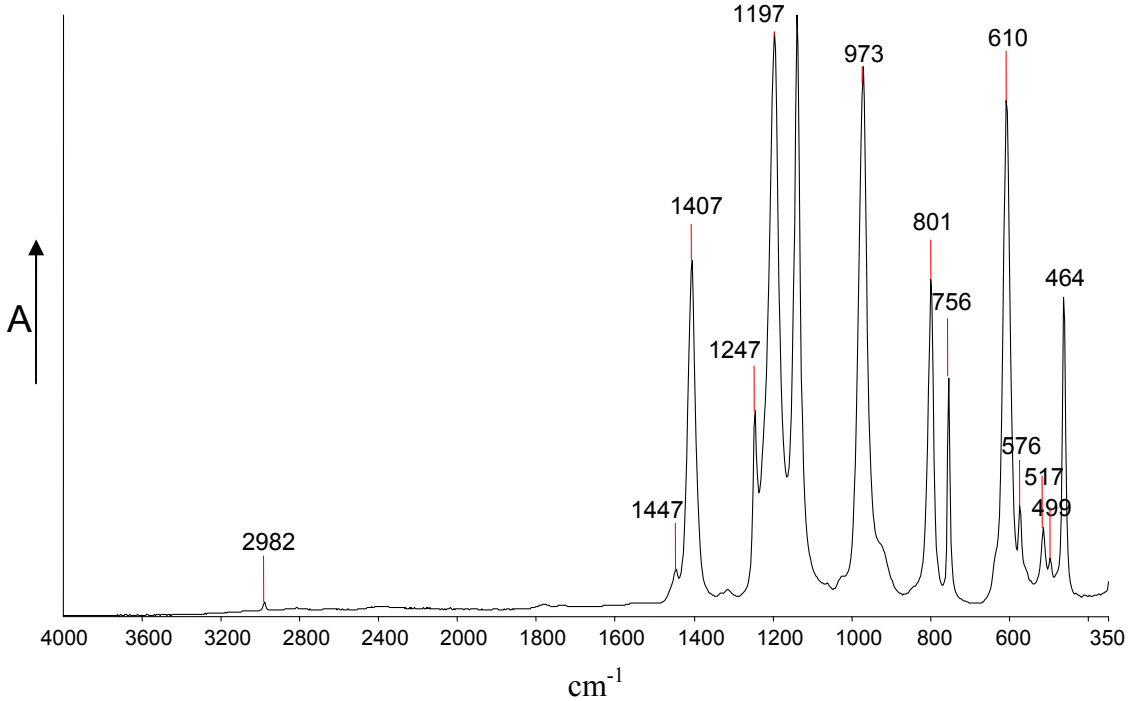

Figure 6.14 ATR of neat methyl triflate

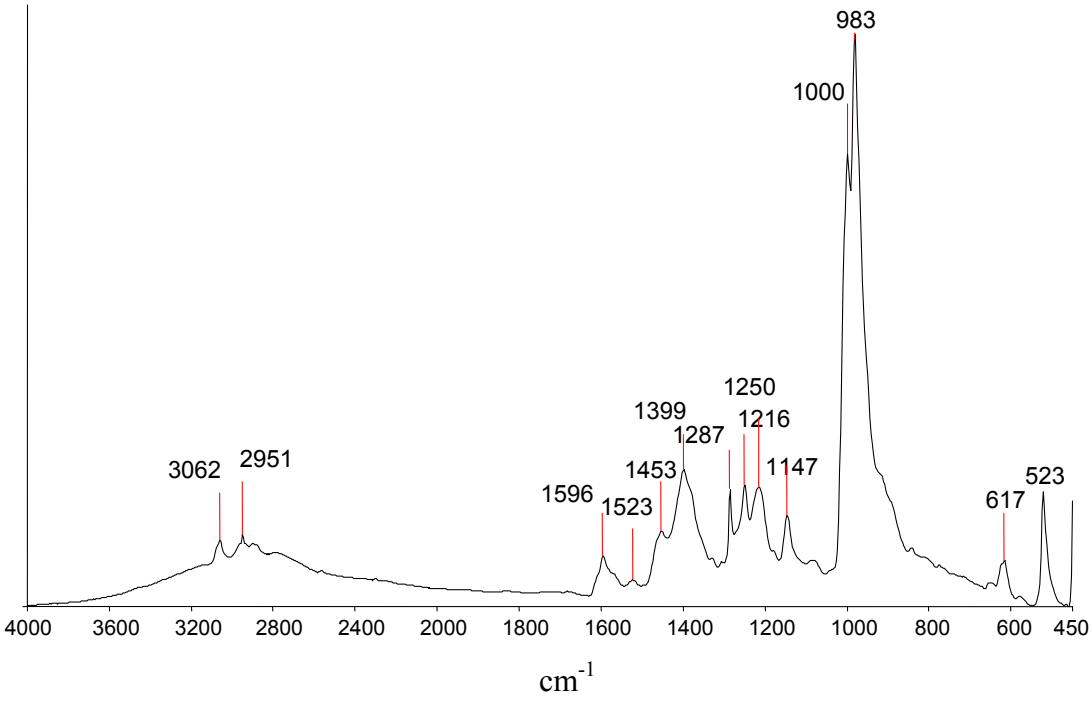

Figure 6.15 FT-IR spectrum of $(CH_3)_2(B_{12}Br_{12})$

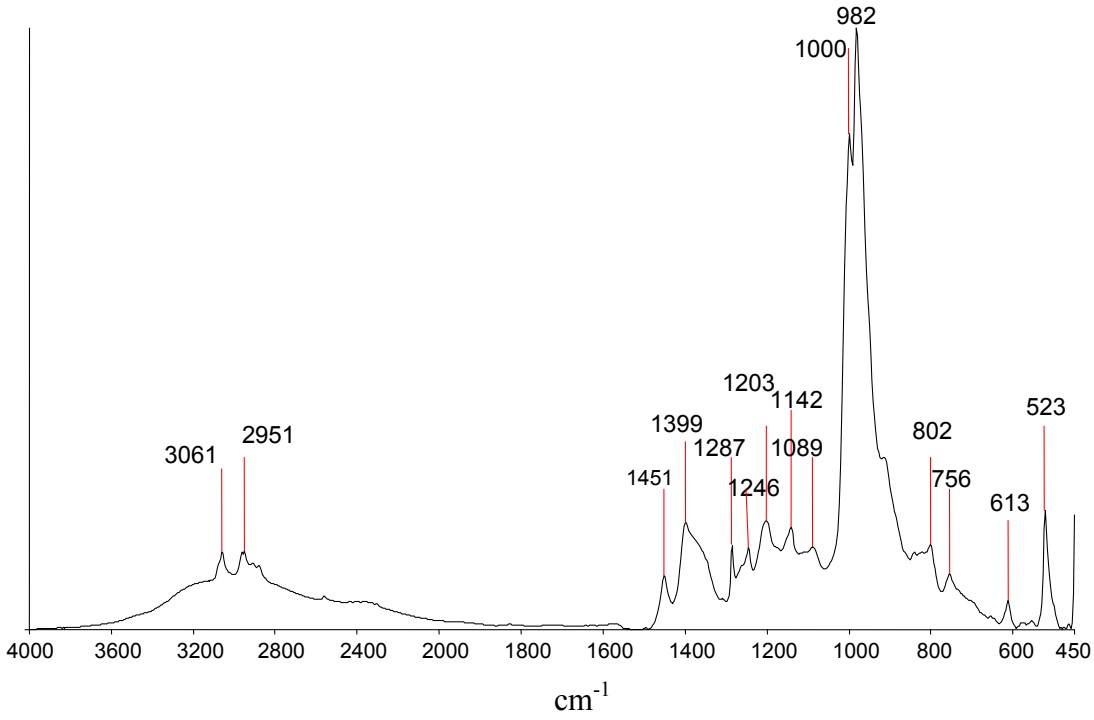

Figure 6.16 FT-IR spectrum of $(CH_3)_2(B_{12}Br_{12})$ with excess methyl triflate after vacuum

The data obtained for $(CH_3)_2(B_{12}Br_{12})$ was promising in that the di-methyl derivative is attainable. Though attempts were made to crystallize product from SO_2, crystals suitable for X-ray diffraction were not obtained.

When $(Et_3Si)_2(B_{12}Br_{12})$ was reacted with a slight excess of methyl triflate in n-hexane at room temperature, different ^{11}B NMR spectra were obtained what was observed in the spectra shown in Figures 6.8, 6.9 and 6.12. Specifically, there appears to be reaction with n-hexane and strong interaction with the di-anion, as the ^{11}B NMR

spectrum, shown in Figure 6.17, is no longer a singlet but instead splits. Therefore, all the borons of the cage are no longer symmetrical.

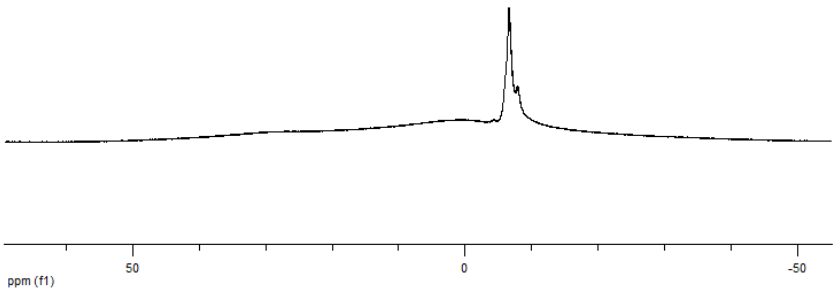

Figure 6.17 ^{11}B NMR spectrum (in SO_2 at –40 °C) of $Me_xB_{12}Br_{12}$ synthesized at 25 °C

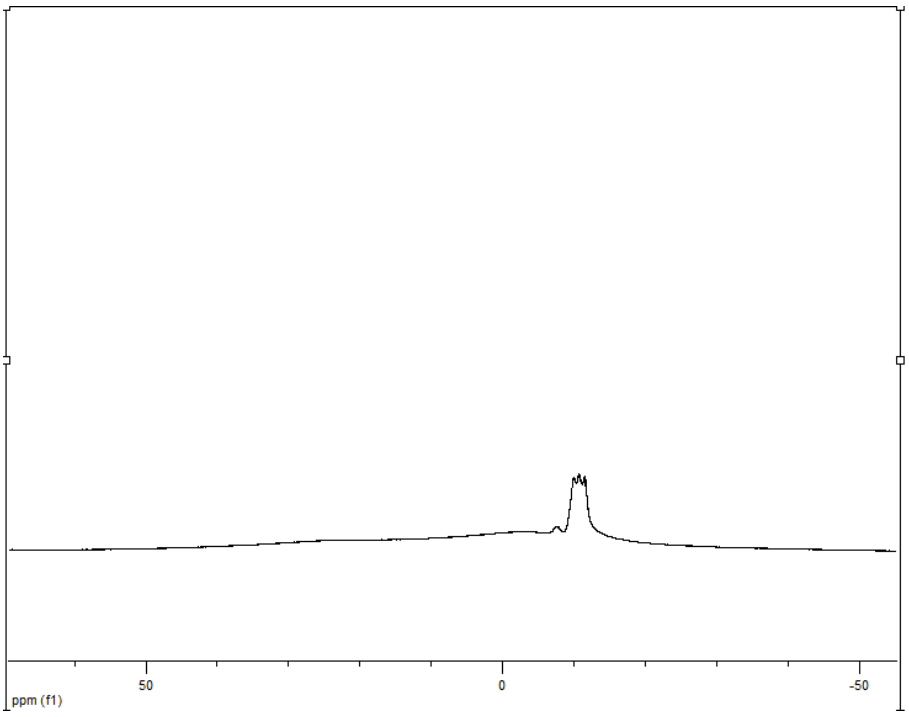

Figure 6.18 ^{11}B NMR spectrum (in SO_2 at –40 °C) of $Me_xB_{12}Cl_{12}$ synthesized at 25 °C

Reaction of $(Et_3Si)_2(B_{12}Cl_{12})$ with approximately two equivalents of methyl triflate in n-hexane resulted in the reaction with n-hexane, not the di-methylation of $B_{12}Cl_{12}^{2-}$. This result is in good agreement with what was observed with the carborane analogue. The compound, $CH_3(CHB_{11}Cl_{11})$, made in situ, immediately reacts with the alkane solvent.

When $(Et_3Si)_2(B_{12}Cl_{12})$ was reacted in neat methyl triflate at room temperature, the ATR spectrum was promising (Figure 6.19). The bands due to the methyl group were identified at 3063, 1411, and 1247 cm^{-1}. The band expected at ~1030 cm^{-1} due to the cage, though, was significantly changed. It was split and shifted to 1028 and 970 cm^{-1}. The split is indicative of the loss of symmetry.

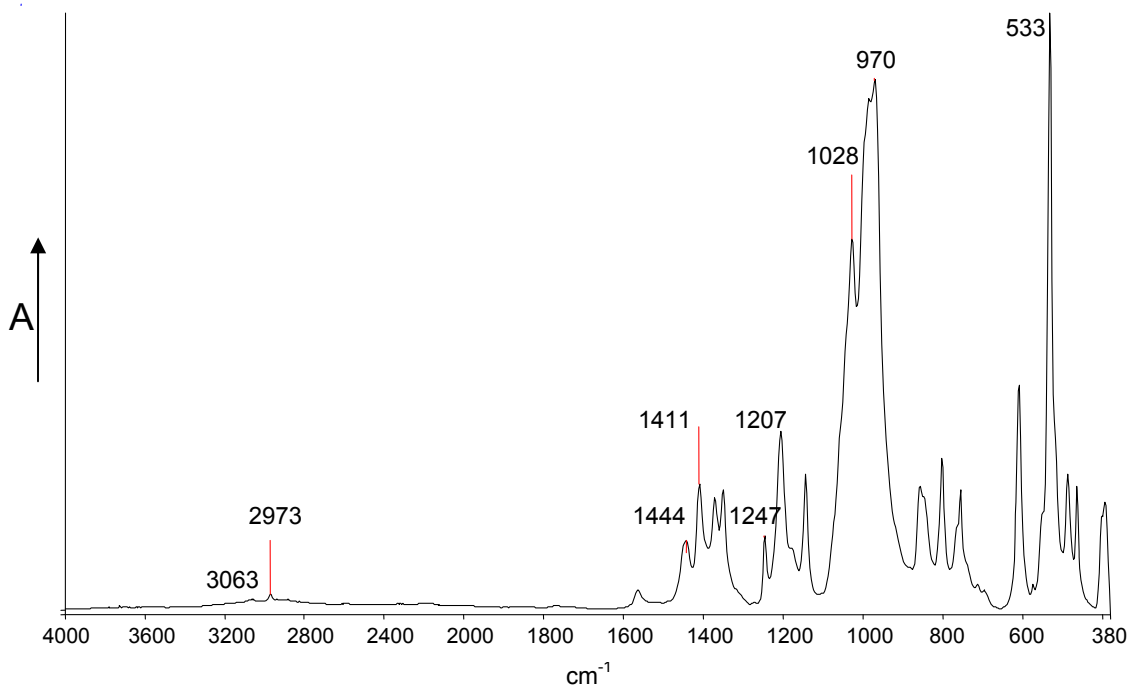

Figure 6.19 ATR of $(CH_3)_2(B_{12}Cl_{12})$ synthesized in neat methyl triflate

The material preliminarily assigned to be $(CH_3)_x(B_{12}X_2)$, X = Br or Cl was reacted with tetramethylhydrazine in ortho-dichlorobenzene. Unlike $(CH_3)_x(B_{12}X_2)$, the resultant solid was found to be insufficiently soluble in SO_2, deuterated methylene chloride, and deuterated ODCB to obtain NMR spectra.

Both $(Et_3Si)_2(B_{12}Cl_{12})$ and $(Et_3Si)_2(B_{12}Br_{12})$ were reacted with an excess of tetramethylhydrazine in ODCB, the white precipitate collected, and washed with n-hexane. Both compounds were found to be soluble in SO_2 but not in methylene chloride. The reaction resulted in the formation of the mono-silylated species, shown in Reaction Scheme 6.3. The mono-silylated compound with the $B_{12}Cl_{12}^{2-}$ di-anion was characterized via X-Ray diffraction, and the structure is shown in Figure 6.20.

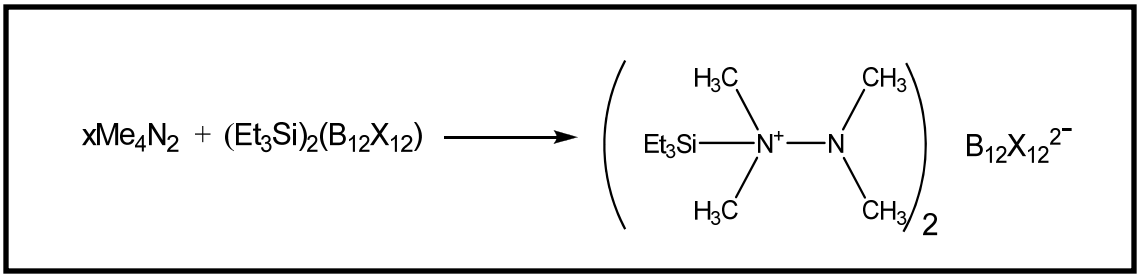

Reaction Scheme 6.3 Synthesis of $[(Et_3Si)Me_4N_2]_2[B_{12}X_{12}]$

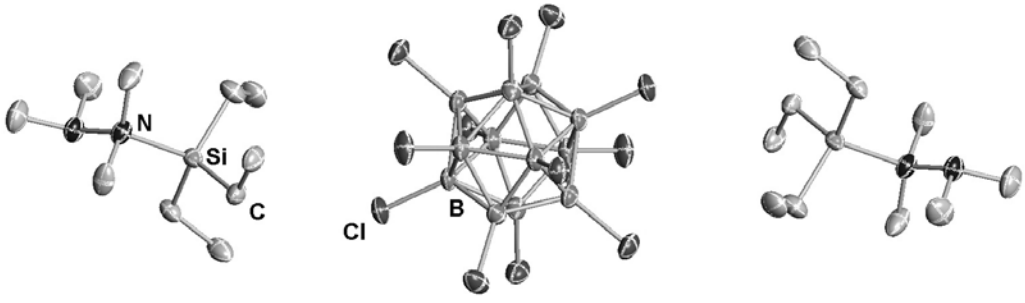

Figure 6.20 Thermal ellipsoid plot of $[(Et_3Si)Me_4N_2]_2[B_{12}Cl_{12}]\cdot$ODCB (solvent omitted; 50% probablility ellipsoids except for hydrogen atoms, which are not shown)

Table 6.2 Crystal structure and refinement data for $[(Et_3Si)Me_4N_2]_2[B_{12}Cl_{12}]\cdot$ODCB

Identification code	chr0617_final	
Empirical formula	C40 H88 B18 Cl21 N6 Si3	
Formula weight	1676.46	
Temperature	100(2) K	
Wavelength	0.71073 Å	
Crystal system	Triclinic	
Space group	P-1	
Unit cell dimensions	a = 12.8515(13) Å	α = 109.668(4)°.
	b = 16.5164(16) Å	β = 105.693(4)°.
	c = 20.4973(19) Å	γ = 93.815(4)°.
Volume	3884.2(7) $Å^3$	
Z	2	
Density (calculated)	1.433 Mg/m^3	
Absorption coefficient	0.820 mm^{-1}	
F(000)	1718	
Crystal size	102.00 x 0.26 x 0.17 mm^3	
Theta range for data collection	1.33 to 23.53°.	
Index ranges	-14<=h<=14, -18<=k<=18, -22<=l<=23	
Reflections collected	27567	
Independent reflections	11268 [R(int) = 0.0225]	
Completeness to theta = 23.53°	97.5 %	
Absorption correction	None	
Max. and min. transmission	0.8732 and 0.0089	
Refinement method	Full-matrix least-squares on F^2	
Data / restraints / parameters	11268 / 6 / 907	
Goodness-of-fit on F^2	1.024	
Final R indices [I>2sigma(I)]	R1 = 0.0521, wR2 = 0.1343	
R indices (all data)	R1 = 0.0642, wR2 = 0.1449	
Largest diff. peak and hole	1.165 and -0.831 $e.Å^{-3}$	

The mono-silylated species was reacted with excess methyl triflate in ODCB. The white precipitate that formed was also soluble in SO_2 and slightly soluble in methylene chloride. Crystals were obtained from a solution of deuterated methylene chloride and the precipitate that formed using the $B_{12}Br_{12}^{2-}$ di-anion. The structure did not contain mono- or di-methylated tetramethylhydrazine. Instead, the cation was mono-protonated tetramethylhydrazine as shown in Figure 6.21. The presence of trace amounts of water, as potential source of hydrogen, may be the reason this crystal was obtained.

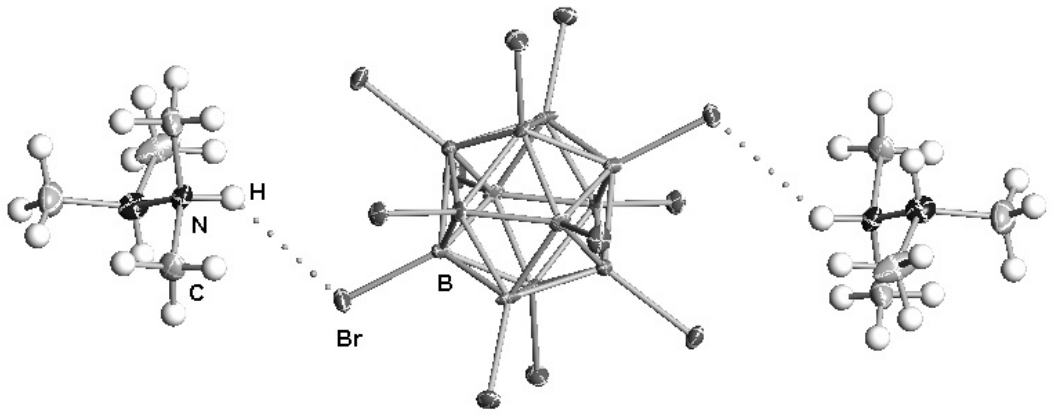

Figure 6.21 X-ray Structure $[(CH_3)_4NH]_2[B_{12}Br_{12}]\cdot 2CD_2Cl_2$ (solvent omitted)

Table 6.3 Crystal structure and refinement data for $[(CH_3)_4NH]_2[B_{12}Br_{12}]\cdot 2CD_2Cl_2$

Empirical formula	$C_5H_{14}B_6Br_6Cl_2N_2$	
Formula weight	717.40	
Temperature	293(2) K	
Wavelength	0.71073 Å	
Crystal system	Monoclinic	
Space group	P2(1)/c	
Unit cell dimensions	a = 10.5850(13) Å	α = 90°.
	b = 10.1142(12) Å	β = 105.037(3)°.
	c = 19.202(2) Å	γ = 90°.
Volume	1985.4(4) $Å^3$	
Z	4	
Density (calculated)	2.400 Mg/m^3	
Absorption coefficient	12.391 mm^{-1}	
F(000)	1328	
Crystal size	0.25 x 0.13 x 0.08 mm^3	
Theta range for data collection	1.99 to 23.28°	
Index ranges	-11<=h<=11, -11<=k<=10, -21<=l<=21	
Reflections collected	12659	
Independent reflections	2848 [R(int) = 0.0306]	
Completeness to theta = 23.28°	99.6 %	
Absorption correction	Sadabs	
Max. and min. transmission	0.4372 and 0.1477	
Refinement method	Full-matrix least-squares on F^2	
Data / restraints / parameters	2848 / 0 / 204	
Goodness-of-fit on F^2	1.065	
Final R indices [I>2sigma(I)]	R1 = 0.0312, wR2 = 0.0942	
R indices (all data)	R1 = 0.0348, wR2 = 0.0963	
Extinction coefficient	0.00019(16)	
Largest diff. peak and hole	1.509 and -0.558 $e.Å^{-3}$	

When $(Et_3Si)_2(B_{12}Br_{12})$ was reacted with ~1 equivalent of Me_4N_2 in ODCB, a structure was obtained that had only 1 silylium coordinating to Me_4N_2. The other silylium was found to coordinate to the di-anion rather than coordinate to Me_4N_2. The formation of this 1:1 salt, $[Et_3SiN_2(CH_3)_4][Et_3Si(B_{12}Br_{12})]$, instead of the 2 :1 salt, $[Et_3SiN_2(CH_3)_4]_2[B_{12}Br_{12}]$ does support more favorable lattice energies of 1 :1 salts versus 2 :1 salts.

After excess methyl triflate was added to the mixture, a white precipitate formed. The solid was found to be insoluble in SO_2 and methylene chloride and no NMR data or crystals could be obtained.

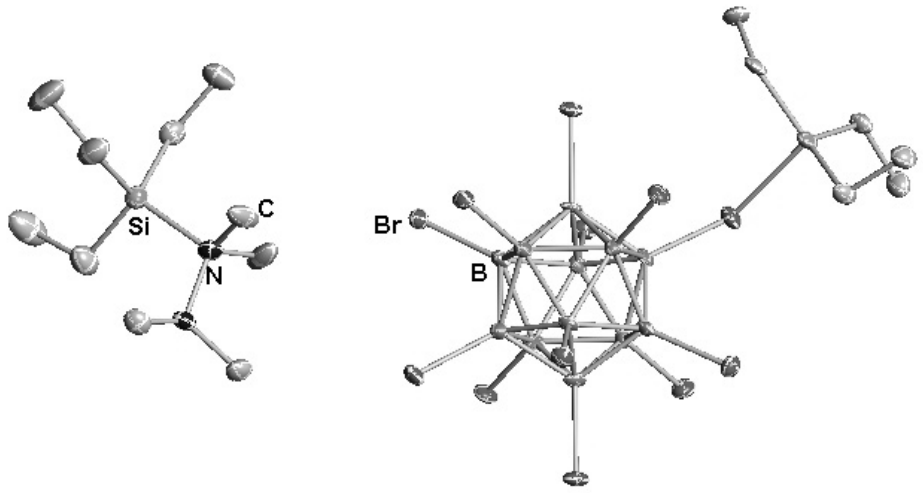

Figure 6.22 Structure of $[Et_3SiN_2(CH_3)_4][Et_3Si(B_{12}Br_{12})]\cdot CD_2Cl_2$ (solvent omitted)

Table 6.4 Crystal structure and refinement data for $[Et_3SiN_2(CH_3)_4][Et_3Si(B_{12}Br_{12})]\cdot CD_2Cl_2$

Empirical formula	$C_{22}H_{46}B_{12}Br_{12}Cl_2N_2Si_2$	
Formula weight	1554.33	
Temperature	100(2) K	
Wavelength	0.71073 Å	
Crystal system	Orthorhombic	
Space group	Pbca	
Unit cell dimensions	a = 18.917(2) Å	α = 90°
	b = 15.5947(17) Å	β = 90°
	c = 33.360(4) Å	γ = 90°
Volume	9841.4(19) $Å^3$	
Z	8	
Density (calculated)	2.098 Mg/m^3	
Absorption coefficient	9.948 mm^{-1}	
F(000)	5872	
Crystal size	0.32 x 0.17 x 0.14 mm^3	
Theta range for data collection	1.63 to 26.37°.	
Index ranges	-22<=h<=23, -19<=k<=19, -41<=l<=41	
Reflections collected	68706	
Independent reflections	10062 [R(int) = 0.1162]	
Completeness to theta = 26.37°	100.0 %	
Absorption correction	Sadabs	
Max. and min. transmission	0.3365 and 0.1430	
Refinement method	Full-matrix least-squares on F^2	
Data / restraints / parameters	10062 / 0 / 480	
Goodness-of-fit on F^2	1.021	
Final R indices [I>2sigma(I)]	R1 = 0.0455, wR2 = 0.0967	
R indices (all data)	R1 = 0.0783, wR2 = 0.1097	
Extinction coefficient	0.000012(13)	
Largest diff. peak and hole	1.371 and -1.337 $e.Å^{-3}$	

When $(Et_3Si)_2(B_{12}Cl_{12})$ was reacted with ~1 equivalent of tetramethylhydrazine in ODCB, a sticky product formed. After excess methyl triflate was added to the mixture, a white precipitate formed and was also found to be insufficiently soluble to obtain NMR spectra or for the formation of crystals.

6.4 Conclusions

The dimethylation of tetramethylhydrazine with the di-anions proved to be elusive. Preliminary data is promising for the synthesis of $(CH_3)_2(B_{12}X_{12})$, but conclusions cannot be made at this time about their alkylating ability. The crystals that were obtained in general were 2:1 salts. Tentatively, this finding does support the lower lattice energies associated to 2:1 salts; that is, they are able to dissolve and crystallize out of a solution. The only 1:1 salt obtained was $[Et_3SiN_2(CH_3)_4][Et_3Si(B_{12}Br_{12})]\cdot CD_2Cl_2$. Though there is a basic site remaining on $Et_3SiN_2(CH_3)_4$ for the second $Et_3Si^{\delta+}$, the site remains unsilylated in favor of the formation of the 1 :1 and minimized electrostaic repulsion. Further investigation into these topics and the identification of a suitable solvent for the analysis is potential future work.

6.5 References

1. "How to Overcome Coulomb Explosions in Labile Dications by Using the $[B_{12}Cl_{12}]^{2-}$ Dianion," Knapp, C.; Schulz, C. *Chem. Commun.* **2009**, 4991-4993.

2. "Relationship Among Ionic Lattice Energies, Molecular (Formula Unit) Volumes, and Thermochemical Radii," Jenkins, H.D.B.; Roobottom, H.K.; Pasmore, J.; Glasser, L. *Inorg. Chem.* **1999**, *38*, 3609-3620. "Predictive Thermodynamics for Condensed Phases," Glasser, L.; Jenkins, H.D.B. *Chem. Soc. Rev.* **2005**, *34*, 866-874.

3. "Can the hexamethylhydrazinium dication $[Me_3N\text{-}NMe_3]^{2+}$ be prepared?" Zhang, Y.; Reed, C.A. *Dalton Trans.* **2008**, 4392-4394.

4. "Structures and Stabilities of the Dimer Di-cation of First- and Second- Row Hydrides," Gill, P.M.W.; Radom, L. *J. Am. Chem. Soc.* **1989**, *111*, 4613-4622. "Hydrazinium Radical Cation ($NH_3NH_3^{+\cdot}$) and Di-cation ($NH_3NH_3^{2+\cdot}$): Prototypes for the Ionized Forms of Medium-Ring Bicyclic Compounds," *J. Am. Chem. Soc.* **1985**, *107*, 345-348.

5. "1,2-Dications in Organic Main Group Systems," Nenajdenko, V.G.; Shevchenko, N.E.; Balenkova, E.S.; Alabugin, I.V. *Chem. Rev.* **2003**, *103*, 229-282.

6. "Optimizing the Least Nucleophilic Anion. A New, Strong $Methyl^+$ Reagent," Stasko, D.; Reed, C.A. *J. Am. Chem. Soc*. **2002**, *124*, 1148-1149.

7. "Alkylating Agents Stronger than Alkyl Triflates," Kato, T.; Stoyanov, E.; Geier, J.; Grützmacher, H.; Reed, C.A. *J. Am. Chem. Soc.* **2004**, *126*, 12451-12457.

Appendix A. X-ray Structure Determination for $[Ph_3C]_2[B_{12}Br_{12}]\cdot 2$toluene

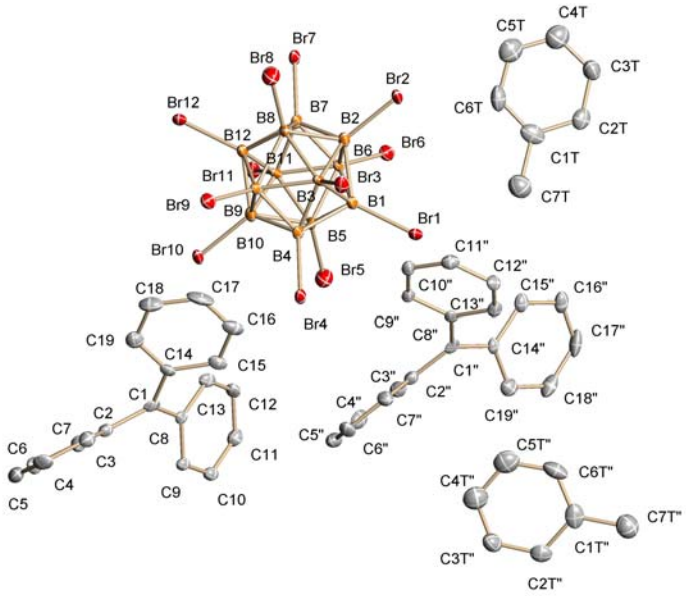

A.1 Experimental Details

A yellow thin plate fragment (0.07 x 0.06 x 0.01 mm^3) was used for the single crystal x-ray diffraction study of $[[C_6H_5]_3C]_2^+[B_{12}Br_{12}]^{2-}$ (sample cr215_0m). The crystal was coated with paratone oil and mounted on to a cryo-loop glass fiber. X-ray intensity data were collected at 100(2) K on a Bruker APEX2 (version 2.0-22, **ref. 1**) platform-CCD x-ray diffractometer system (Mo-radiation, λ = 0.71073 Å, 50KV/40mA power). The CCD detector was placed at a distance of 5.0400 cm from the crystal.

A total of 2400 frames were collected for a hemisphere of reflections (with scan width of 0.3° in ω, starting ω and 2θ angles at –30°, and ϕ angles of 0°, 90°, 180°, and 270° for every 600 frames, 60 sec/frame exposure time). The frames were integrated using the Bruker SAINT software package (version V7.23A, **ref. 2**) and using a narrow-frame integration algorithm. Based on a monoclinic crystal system, the integrated frames

yielded a total of 35065 reflections at a maximum 2θ angle of 52.74° (0.80 Å resolution), of which 6030 were independent reflections (R_{int} = 0.0956, R_{sig} = 0.0662, redundancy = 5.8, completeness = 100%) and 4184 (69.4%) reflections were greater than 2σ(I). The unit cell parameters were, **a** = 9.9080(4) Å, **b** = 15.7105(7) Å, **c** = 18.9333(8) Å, **β** = 90.6008(8)°, V = 2947.0(2) $Å^3$, Z = 4, calculated density D_c = 1.983 g/cm^3. Absorption corrections were applied (absorption coefficient μ = 8.192 mm^{-1}; max/min transmission = 0.9226/0.6180) to the raw intensity data using the SADABS program (version 2004/1, **ref. 1**).

The Bruker SHELXTL software package (Version 6.14, **ref. 4**) was used for phase determination and structure refinement. The distribution of intensities (E^2-1 = 0.920) and systematic absent reflections indicated one possible space group, P2(1)/n. The space group P2(1)/n (#14) was later determined to be correct. Direct methods of phase determination followed by two Fourier cycles of refinement led to an electron density map from which most of the non-hydrogen atoms were identified in the asymmetry unit of the unit cell. With subsequent isotropic refinement, all of the non-hydrogen atoms were identified. There were one cation of $[C_6H_5]_3C^+$, half an anion of $[B_{12}Br_{12}]^{2-}$ and one toluene solvent molecule present in the asymmetry unit of the unit cell. The anion $[B_{12}Br_{12}]^{2-}$ was located at the inversion center.

Atomic coordinates, isotropic and anisotropic displacement parameters of all the non-hydrogen atoms were refined by means of a full matrix least-squares procedure on F^2. The H-atoms were included in the refinement in calculated positions riding on the atoms to which they were attached. The refinement converged at R1 = 0.0461, wR2 =

0.0996, with intensity I>2σ (I). The largest peak/hole in the final difference map was 1.034/-1.943 e/Å^3.

A.2 Structure Data

A.2.1 Crystal structure and refinement data for $[Ph_3C]_2[B_{12}Br_{12}]$·2toluene

Identification code	cr215_0m	
Empirical formula	C26 H23 B6 Br6	
Formula weight	879.76	
Temperature	100(2) K	
Wavelength	0.71073 Å	
Crystal system	Monoclinic	
Space group	P2(1)/n	
Unit cell dimensions	a = 9.9081(4) Å	α = 90°.
	b = 15.7107(7) Å	β = 90.6020(10)°.
	c = 18.9335(9) Å	γ = 90°.
Volume	2947.1(2) Å^3	
Z	4	
Density (calculated)	1.983 Mg/m^3	
Absorption coefficient	8.192 mm^{-1}	
F(000)	1676	
Crystal size	0.07 x 0.06 x 0.01 mm^3	
Theta range for data collection	1.68 to 26.37°.	
Index ranges	-12<=h<=12, -19<=k<=19, -23<=l<=23	
Reflections collected	34988	
Independent reflections	6031 [R(int) = 0.0972]	
Completeness to theta = 26.37°	100.0 %	
Absorption correction	None	
Max. and min. transmission	0.9226 and 0.6180	
Refinement method	Full-matrix least-squares on F^2	
Data / restraints / parameters	6031 / 0 / 344	
Goodness-of-fit on F^2	1.026	
Final R indices [I>2sigma(I)]	R1 = 0.0463, wR2 = 0.0985	

R indices (all data)	R1 = 0.0824, wR2 = 0.1123
Largest diff. peak and hole	1.067 and -1.913 e.Å^{-3}

A.2.2 Atomic Coordinates

Atomic coordinates (x 10^4) and equivalent isotropic displacement parameters (Å^{2}x 10^3) for $[Ph_3C]_2[B_{12}Br_{12}]\cdot$2toluene. U(eq) is defined as one third of the trace of the orthogonalized U^{ij} tensor.

	x	y	z	U(eq)
B(1)	-347(8)	6053(5)	-90(4)	15(2)
B(2)	-1585(8)	5318(5)	225(4)	15(2)
B(3)	-703(8)	4499(5)	693(4)	15(2)
B(4)	1038(8)	4732(5)	672(4)	13(2)
B(5)	1269(8)	5696(5)	179(4)	12(2)
B(6)	-145(8)	5568(5)	752(4)	16(2)
Br(1)	-792(1)	7256(1)	-196(1)	18(1)
Br(2)	-3404(1)	5658(1)	460(1)	21(1)
Br(3)	-1505(1)	3934(1)	1506(1)	19(1)
Br(4)	2218(1)	4379(1)	1442(1)	30(1)
Br(5)	2735(1)	6491(1)	391(1)	21(1)
Br(6)	-291(1)	6204(1)	1640(1)	20(1)
C(1)	7287(7)	724(4)	1681(3)	15(2)
C(2)	7058(7)	-187(4)	1620(4)	17(2)
C(3)	5732(8)	-516(5)	1593(4)	21(2)
C(4)	5552(8)	-1384(5)	1528(4)	26(2)
C(5)	6644(8)	-1929(5)	1466(4)	27(2)
C(6)	7946(8)	-1603(5)	1483(4)	23(2)
C(7)	8154(8)	-742(5)	1562(4)	21(2)
C(8)	8494(7)	1024(4)	2046(3)	13(1)
C(9)	9000(7)	594(4)	2638(3)	15(1)
C(10)	10157(7)	884(4)	2966(4)	17(2)

C(11)	10842(7)	1574(5)	2706(4)	21(2)
C(12)	10363(7)	2004(4)	2114(4)	19(2)
C(13)	9183(7)	1746(4)	1789(4)	18(2)
C(14)	6359(7)	1321(4)	1371(4)	16(2)
C(15)	6191(7)	2135(4)	1674(4)	20(2)
C(16)	5320(8)	2713(5)	1372(4)	28(2)
C(17)	4635(8)	2523(5)	766(4)	32(2)
C(18)	4793(8)	1729(5)	445(4)	29(2)
C(19)	5640(7)	1138(5)	743(4)	24(2)
C(1T)	1787(8)	9068(5)	1380(5)	31(2)
C(2T)	2114(7)	9924(5)	1572(4)	28(2)
C(3T)	2135(8)	10543(5)	1056(4)	31(2)
C(4T)	1837(9)	10358(6)	377(5)	44(2)
C(5T)	1525(9)	9549(6)	178(5)	43(2)
C(6T)	1518(8)	8910(5)	669(5)	33(2)
C(7T)	1701(10)	8383(6)	1922(5)	44(2)

A.2.3 Bond Lengths and Angles

Bond lengths [Å] and angles [°] for $[Ph_3C]_2[B_{12}Br_{12}]\cdot 2$toluene.

B(1)-B(5)	1.766(11)
B(1)-B(6)	1.777(11)
B(1)-B(3)#1	1.778(10)
B(1)-B(4)#1	1.785(11)
B(1)-B(2)	1.791(11)
B(1)-Br(1)	1.950(7)
B(2)-B(6)	1.777(12)
B(2)-B(3)	1.786(11)
B(2)-B(4)#1	1.788(11)
B(2)-B(5)#1	1.796(10)
B(2)-Br(2)	1.937(8)

B(3)-B(4)	1.764(11)
B(3)-B(5)#1	1.766(11)
B(3)-B(6)	1.771(11)
B(3)-B(1)#1	1.778(10)
B(3)-Br(3)	1.953(7)
B(4)-B(6)	1.769(11)
B(4)-B(1)#1	1.785(11)
B(4)-B(2)#1	1.788(11)
B(4)-B(5)	1.795(10)
B(4)-Br(4)	1.940(7)
B(5)-B(3)#1	1.766(11)
B(5)-B(6)	1.792(11)
B(5)-B(2)#1	1.796(10)
B(5)-Br(5)	1.954(7)
B(6)-Br(6)	1.962(8)
C(1)-C(14)	1.434(9)
C(1)-C(8)	1.453(10)
C(1)-C(2)	1.454(10)
C(2)-C(7)	1.398(10)
C(2)-C(3)	1.413(10)
C(3)-C(4)	1.381(10)
C(4)-C(5)	1.386(11)
C(5)-C(6)	1.388(11)
C(6)-C(7)	1.375(10)
C(8)-C(9)	1.398(9)
C(8)-C(13)	1.413(9)
C(9)-C(10)	1.375(10)
C(10)-C(11)	1.373(10)
C(11)-C(12)	1.389(10)
C(12)-C(13)	1.376(10)
C(14)-C(19)	1.410(10)
C(14)-C(15)	1.413(10)
C(15)-C(16)	1.374(10)
C(16)-C(17)	1.361(12)

C(17)-C(18)	1.398(12)
C(18)-C(19)	1.369(11)
C(1T)-C(6T)	1.392(12)
C(1T)-C(2T)	1.430(11)
C(1T)-C(7T)	1.490(12)
C(2T)-C(3T)	1.380(11)
C(3T)-C(4T)	1.346(12)
C(4T)-C(5T)	1.361(13)
C(5T)-C(6T)	1.366(12)
B(5)-B(1)-B(6)	60.8(4)
B(5)-B(1)-B(3)#1	59.8(4)
B(6)-B(1)-B(3)#1	107.8(5)
B(5)-B(1)-B(4)#1	107.5(5)
B(6)-B(1)-B(4)#1	107.3(5)
B(3)#1-B(1)-B(4)#1	59.3(4)
B(5)-B(1)-B(2)	108.7(5)
B(6)-B(1)-B(2)	59.8(4)
B(3)#1-B(1)-B(2)	107.8(5)
B(4)#1-B(1)-B(2)	60.0(4)
B(5)-B(1)-Br(1)	122.7(5)
B(6)-B(1)-Br(1)	122.1(5)
B(3)#1-B(1)-Br(1)	122.6(5)
B(4)#1-B(1)-Br(1)	121.3(5)
B(2)-B(1)-Br(1)	120.3(5)
B(6)-B(2)-B(3)	59.6(4)
B(6)-B(2)-B(4)#1	107.1(5)
B(3)-B(2)-B(4)#1	106.8(5)
B(6)-B(2)-B(1)	59.7(4)
B(3)-B(2)-B(1)	107.2(6)
B(4)#1-B(2)-B(1)	59.8(4)
B(6)-B(2)-B(5)#1	107.0(5)
B(3)-B(2)-B(5)#1	59.1(4)
B(4)#1-B(2)-B(5)#1	60.1(4)
B(1)-B(2)-B(5)#1	107.9(5)

B(6)-B(2)-Br(2)	123.6(5)
B(3)-B(2)-Br(2)	122.5(5)
B(4)#1-B(2)-Br(2)	121.5(5)
B(1)-B(2)-Br(2)	122.7(5)
B(5)#1-B(2)-Br(2)	120.6(5)
B(4)-B(3)-B(5)#1	108.4(5)
B(4)-B(3)-B(6)	60.0(4)
B(5)#1-B(3)-B(6)	108.7(5)
B(4)-B(3)-B(1)#1	60.5(4)
B(5)#1-B(3)-B(1)#1	59.8(4)
B(6)-B(3)-B(1)#1	108.6(5)
B(4)-B(3)-B(2)	108.2(5)
B(5)#1-B(3)-B(2)	60.8(4)
B(6)-B(3)-B(2)	59.9(4)
B(1)#1-B(3)-B(2)	108.6(5)
B(4)-B(3)-Br(3)	121.2(5)
B(5)#1-B(3)-Br(3)	122.0(5)
B(6)-B(3)-Br(3)	120.7(5)
B(1)#1-B(3)-Br(3)	122.0(5)
B(2)-B(3)-Br(3)	121.2(5)
B(3)-B(4)-B(6)	60.2(4)
B(3)-B(4)-B(1)#1	60.1(4)
B(6)-B(4)-B(1)#1	108.4(5)
B(3)-B(4)-B(2)#1	108.6(5)
B(6)-B(4)-B(2)#1	108.8(5)
B(1)#1-B(4)-B(2)#1	60.2(4)
B(3)-B(4)-B(5)	108.5(5)
B(6)-B(4)-B(5)	60.4(4)
B(1)#1-B(4)-B(5)	108.2(5)
B(2)#1-B(4)-B(5)	60.2(4)
B(3)-B(4)-Br(4)	120.3(5)
B(6)-B(4)-Br(4)	122.8(5)
B(1)#1-B(4)-Br(4)	119.4(5)
B(2)#1-B(4)-Br(4)	121.0(5)

B(5)-B(4)-Br(4)	123.5(5)
B(3)#1-B(5)-B(1)	60.4(4)
B(3)#1-B(5)-B(6)	107.7(5)
B(1)-B(5)-B(6)	59.9(4)
B(3)#1-B(5)-B(4)	107.3(5)
B(1)-B(5)-B(4)	107.3(5)
B(6)-B(5)-B(4)	59.1(4)
B(3)#1-B(5)-B(2)#1	60.2(4)
B(1)-B(5)-B(2)#1	108.7(5)
B(6)-B(5)-B(2)#1	107.4(5)
B(4)-B(5)-B(2)#1	59.7(4)
B(3)#1-B(5)-Br(5)	122.1(5)
B(1)-B(5)-Br(5)	121.7(5)
B(6)-B(5)-Br(5)	122.1(5)
B(4)-B(5)-Br(5)	122.1(5)
B(2)#1-B(5)-Br(5)	121.5(5)
B(4)-B(6)-B(3)	59.8(4)
B(4)-B(6)-B(1)	108.0(5)
B(3)-B(6)-B(1)	108.5(5)
B(4)-B(6)-B(2)	108.4(5)
B(3)-B(6)-B(2)	60.4(4)
B(1)-B(6)-B(2)	60.5(4)
B(4)-B(6)-B(5)	60.5(4)
B(3)-B(6)-B(5)	108.3(5)
B(1)-B(6)-B(5)	59.3(4)
B(2)-B(6)-B(5)	108.2(5)
B(4)-B(6)-Br(6)	120.5(5)
B(3)-B(6)-Br(6)	120.8(5)
B(1)-B(6)-Br(6)	122.8(5)
B(2)-B(6)-Br(6)	121.9(5)
B(5)-B(6)-Br(6)	121.8(5)
C(14)-C(1)-C(8)	120.2(6)
C(14)-C(1)-C(2)	120.8(6)
C(8)-C(1)-C(2)	119.0(6)

C(7)-C(2)-C(3)	119.4(7)
C(7)-C(2)-C(1)	120.0(6)
C(3)-C(2)-C(1)	120.5(6)
C(4)-C(3)-C(2)	119.0(7)
C(3)-C(4)-C(5)	121.1(7)
C(4)-C(5)-C(6)	119.8(7)
C(7)-C(6)-C(5)	120.2(7)
C(6)-C(7)-C(2)	120.5(7)
C(9)-C(8)-C(13)	119.6(6)
C(9)-C(8)-C(1)	120.7(6)
C(13)-C(8)-C(1)	119.6(6)
C(10)-C(9)-C(8)	119.5(6)
C(11)-C(10)-C(9)	120.9(7)
C(10)-C(11)-C(12)	120.4(7)
C(13)-C(12)-C(11)	120.0(6)
C(12)-C(13)-C(8)	119.6(6)
C(19)-C(14)-C(15)	117.8(6)
C(19)-C(14)-C(1)	121.9(6)
C(15)-C(14)-C(1)	120.2(6)
C(16)-C(15)-C(14)	120.4(7)
C(17)-C(16)-C(15)	120.8(8)
C(16)-C(17)-C(18)	120.4(7)
C(19)-C(18)-C(17)	119.8(8)
C(18)-C(19)-C(14)	120.8(7)
C(6T)-C(1T)-C(2T)	117.0(7)
C(6T)-C(1T)-C(7T)	121.8(8)
C(2T)-C(1T)-C(7T)	121.2(8)
C(3T)-C(2T)-C(1T)	119.2(8)
C(4T)-C(3T)-C(2T)	121.3(8)
C(3T)-C(4T)-C(5T)	120.8(9)
C(4T)-C(5T)-C(6T)	120.1(9)
C(5T)-C(6T)-C(1T)	121.6(8)

Symmetry transformations used to generate equivalent atoms: #1 -x,-y+1,-z

A.2.4 Anisotropic Displacement Parameters

Anisotropic displacement parameters ($Å^2 x\ 10^3$) for $[Ph_3C]_2[B_{12}Br_{12}]\cdot 2$toluene. The anisotropic displacement factor exponent takes the form: $-2p^2[\ h^2a^{*2}U^{11} + ... + 2\ h\ k\ a^*\ b^*\ U^{12}\ ]$

	U^{11}	U^{22}	U^{33}	U^{23}	U^{13}	U^{12}
B(1)	18(4)	10(4)	18(4)	3(3)	3(3)	5(3)
B(2)	22(4)	9(4)	15(4)	-3(3)	7(3)	-1(3)
B(3)	21(4)	12(4)	12(4)	3(3)	8(3)	0(3)
B(4)	20(4)	10(4)	10(4)	2(3)	-4(3)	5(3)
B(5)	14(4)	9(4)	13(4)	-1(3)	2(3)	-3(3)
B(6)	23(4)	10(4)	15(4)	0(3)	5(3)	0(3)
Br(1)	29(1)	8(1)	18(1)	2(1)	5(1)	4(1)
Br(2)	21(1)	19(1)	22(1)	4(1)	8(1)	7(1)
Br(3)	30(1)	12(1)	16(1)	4(1)	10(1)	3(1)
Br(4)	34(1)	28(1)	27(1)	2(1)	-5(1)	1(1)
Br(5)	23(1)	16(1)	22(1)	-1(1)	1(1)	-4(1)
Br(6)	34(1)	13(1)	14(1)	-3(1)	6(1)	2(1)
C(1)	16(4)	21(4)	9(3)	2(3)	11(3)	2(3)
C(2)	19(4)	19(4)	13(3)	0(3)	2(3)	1(3)
C(3)	22(4)	23(4)	18(4)	0(3)	0(3)	2(3)
C(4)	29(5)	28(4)	22(4)	6(3)	5(3)	-14(4)
C(5)	41(5)	23(4)	18(4)	-2(3)	3(4)	-5(4)
C(6)	30(4)	17(4)	23(4)	-3(3)	7(3)	7(3)
C(7)	24(4)	20(4)	19(4)	-1(3)	-1(3)	1(3)
C(8)	15(4)	12(3)	12(3)	-2(3)	7(3)	2(3)
C(9)	19(4)	15(3)	12(3)	1(3)	6(3)	3(3)
C(10)	22(4)	15(4)	15(4)	1(3)	5(3)	4(3)
C(11)	18(4)	25(4)	19(4)	-4(3)	1(3)	0(3)
C(12)	23(4)	14(4)	20(4)	1(3)	6(3)	-6(3)
C(13)	18(4)	20(4)	16(4)	2(3)	8(3)	6(3)
C(14)	15(4)	13(3)	18(4)	6(3)	6(3)	0(3)

C(15)	18(4)	19(4)	24(4)	7(3)	6(3)	1(3)
C(16)	29(4)	24(4)	30(4)	12(3)	13(4)	5(4)
C(17)	22(4)	33(5)	41(5)	25(4)	3(4)	7(4)
C(18)	22(4)	40(5)	25(4)	14(4)	-4(3)	-3(4)
C(19)	24(4)	25(4)	24(4)	2(3)	6(3)	-2(3)
C(1T)	16(4)	33(5)	46(5)	10(4)	13(4)	5(3)
C(2T)	19(4)	33(5)	31(5)	-7(4)	6(3)	3(4)
C(3T)	38(5)	23(4)	33(5)	-2(4)	8(4)	-4(4)
C(4T)	40(6)	49(6)	42(6)	-4(5)	9(4)	0(5)
C(5T)	36(6)	54(6)	40(5)	-5(5)	10(4)	5(5)
C(6T)	27(5)	28(5)	43(5)	-15(4)	4(4)	-2(4)
C(7T)	43(6)	39(5)	50(6)	2(5)	7(5)	0(4)

A.2.5 Hydrogen Coordinates

Hydrogen coordinates (x 10^4) and isotropic displacement parameters (Å^{2}x 10^3) for $[Ph_3C]_2[B_{12}Br_{12}]\cdot 2$ toluene.

	x	y	z	U(eq)
H(3A)	4975	-146	1619	25
H(4A)	4663	-1612	1526	32
H(5A)	6503	-2523	1411	33
H(6A)	8697	-1975	1440	28
H(7A)	9048	-524	1578	26
H(9A)	8549	105	2813	18
H(10A)	10486	603	3377	21
H(11A)	11651	1758	2933	25
H(12A)	10849	2476	1933	22
H(13A)	8834	2052	1395	21
H(15A)	6684	2284	2089	24
H(16A)	5193	3252	1590	33

H(17A)	4046	2933	559	39
H(18A)	4315	1599	21	35
H(19A)	5744	598	524	29
H(2TA)	2316	10064	2050	33
H(3TA)	2363	11111	1181	37
H(4TA)	1844	10798	33	52
H(5TA)	1313	9427	-302	52
H(6TA)	1324	8345	520	39
H(7TA)	1711	7826	1689	66
H(7TB)	861	8447	2186	66
H(7TC)	2473	8426	2248	66

A.3 References

1. *APEX 2,* version 2.0-22, Bruker (2004), Bruker AXS Inc., Madison, Wisconsin, USA.

2. *SAINT,* version V7.23A, Bruker (2003), Bruker AXS Inc., Madison, Wisconsin, USA.

3. *SADABS,* version 2004/1, Bruker (2004), Bruker AXS Inc., Madison, Wisconsin, USA.

4. *SHELXTL,* version 6.14, Bruker (2008), Bruker AXS Inc., Madison, Wisconsin, USA.

Appendix B. X-Ray Structure Determination for $[Ph_3C]_2[B_{12}Cl_{12}]\cdot 2C_6H_4Cl_2$.

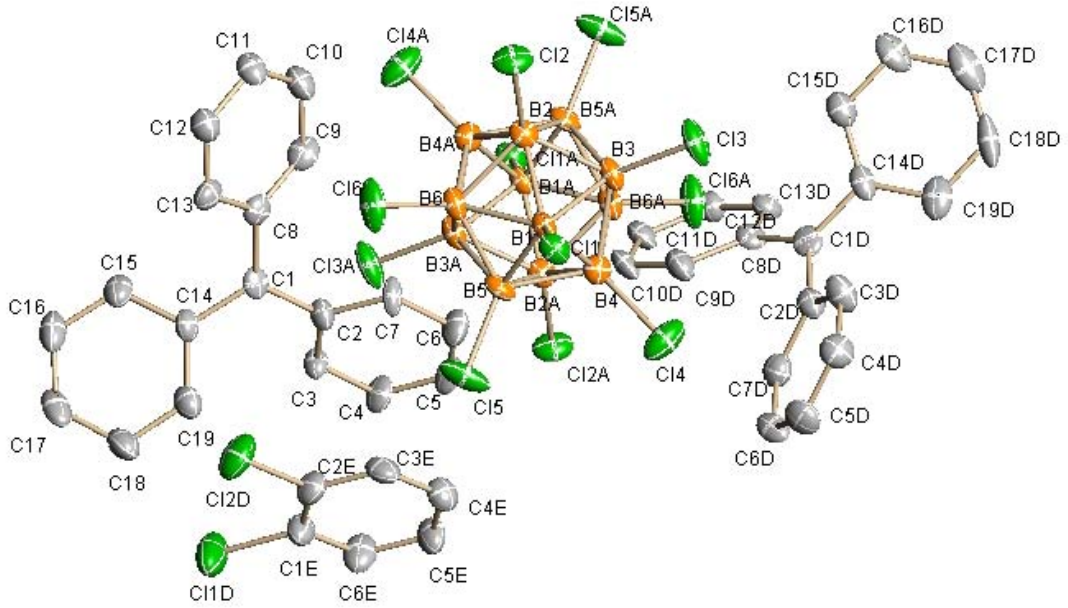

B.1 Experimental Details

A brown thin needle fragment (0.34 x 0.05 x 0.02 mm^3) was used for the single crystal x-ray diffraction study (sample cr303_0m). The crystal was coated with Paratone oil and mounted on to a cryo-loop glass fiber. X-ray intensity data were collected at 100(2) K on a Bruker APEX2 (version 2.0-22, **ref. 1**) platform-CCD x-ray diffractometer system (Mo-radiation, λ = 0.71073 Å, 50KV/40mA power). The CCD detector was placed at a distance of 5.0500 cm from the crystal.

A total of 3600 frames were collected for a sphere of reflections (with scan width of 0.3° in ω, starting ω and 2θ angles at –30°, and ϕ angles of 0°, 90°, 120°, 180°, 240°, and 270° for every 600 frames, 60 sec/frame exposure time). The frames were integrated using the Bruker SAINT software package (version V7.23A, **ref. 2**) and using a narrow-frame integration algorithm. Based on a monoclinic crystal system, the integrated frames

yielded a total of 44242 reflections at a maximum 2θ angle of 49.42° (0.85 Å resolution), of which 4931 were independent reflections (R_{int} = 0.0991, R_{sig} = 0.0507, redundancy = 9.0, completeness = 100%) and 3210 (65.1%) reflections were greater than 2σ(I). The unit cell parameters were, **a** = 30.6533(12) Å, **b** = 10.2904(4) Å, **c** = 19.7470(8) Å, **β** = 111.5814(7)°**,** V = 5792.2(4) Å^3, Z = 8, calculated density D_c = 1.532 g/cm^3. Absorption corrections were applied (absorption coefficient μ = 0.796 mm^{-1}; max/min transmission = 0.9843/0.7730) to the raw intensity data using the SADABS program (version 2004/1, **ref. 1**).

The Bruker SHELXTL software package (Version 6.14, **ref. 4**) was used for phase determination and structure refinement. The distribution of intensities (E^2-1 = 0.957) and systematic absent reflections indicated two possible space groups, C2/c and Cc. The space group C2/c (#15) was later determined to be correct. Direct methods of phase determination followed by two Fourier cycles of refinement led to an electron density map from which most of the non-hydrogen atoms were identified in the asymmetry unit of the unit cell. With subsequent isotropic refinement, all of the non-hydrogen atoms were identified. There is one disordered cation of $(C_6H_5)_3C^+$ (disordered site occupancy ratio was 53%/47%), half an anion of $B_{12}Cl_2^{2-}$, and one disordered solvent molecule of $C_6H_4Cl_2$ (disorder was modeled with 50%/50% site occupancy) present in the asymmetry unit of the unit cell. The FLAT, SADI, DELU and SIMU restraints were used on the cation and solvent molecule in the final least squares refinement.

Atomic coordinates, isotropic and anisotropic displacement parameters of all the non-hydrogen atoms were refined by means of a full matrix least-squares procedure on F^2. The H-atoms were included in the refinement in calculated positions riding on the atoms to which they were attached. The refinement converged at R1 = 0.0418, wR2 = 0.0806, with intensity I>2σ (I). The largest peak/hole in the final difference map was 0.878/-0.489 e/Å^3.

B.2 Structure Data

B.2.1 Crystal data and structure refinement for $[[C_6H_5]_3C]_2[B_{12}Cl_{12}].2[C_6H_4Cl_2]$

Identification code	cr303_0m	
Empirical formula	C25 H19 B6 Cl8	
Formula weight	667.86	
Temperature	100(2) K	
Wavelength	0.71073 Å	
Crystal system	Monoclinic	
Space group	C2/c (#15)	
Unit cell dimensions	a = 30.6533(12) Å	α = 90°.
	b = 10.2904(4) Å	β = 111.5814(7)°.
	c = 19.7470(8) Å	γ = 90°.
Volume	5792.2(4) Å^3	
Z	8	
Density (calculated)	1.532 Mg/m^3	
Absorption coefficient	0.796 mm^{-1}	
F(000)	2680	
Crystal size	0.34 x 0.05 x 0.02 mm^3	
Theta range for data collection	2.10 to 24.71°.	
Index ranges	-36<=h<=36, -12<=k<=12, -23<=l<=23	
Reflections collected	44242	
Independent reflections	4931 [R(int) = 0.0991]	

Completeness to theta = 24.71°	100.0 %
Absorption correction	Semi-empirical from equivalents
Max. and min. transmission	0.9843 and 0.7730
Refinement method	Full-matrix least-squares on F^2
Data / restraints / parameters	4931 / 1014 / 599
Goodness-of-fit on F^2	1.058
Final R indices [I>2sigma(I)]	R1 = 0.0418, wR2 = 0.0806
R indices (all data)	R1 = 0.0866, wR2 = 0.0987
Largest diff. peak and hole	0.878 and -0.489 e.$Å^{-3}$

B.2.2 Atomic Coordinates

Atomic coordinates (x 10^4) and equivalent isotropic displacement parameters ($Å^2$x 10^3) for $[[C_6H_5]_3C]_2[B_{12}Cl_{12}].2[C_6H_4Cl_2]$. U(eq) is defined as one third of the trace of the orthogonalized U^{ij} tensor.

	x	y	z	U(eq)
B(1)	2424(1)	6707(4)	4211(2)	22(1)
B(2)	2628(1)	8341(4)	4361(2)	24(1)
B(3)	2991(1)	7046(4)	4860(2)	25(1)
B(4)	2626(1)	5883(4)	5064(2)	25(1)
B(5)	2039(1)	6471(4)	4691(2)	26(1)
B(6)	2041(1)	7980(4)	4260(2)	25(1)
Cl(1)	2342(1)	5894(1)	3366(1)	28(1)
Cl(2)	2755(1)	9237(1)	3673(1)	37(1)
Cl(3)	3520(1)	6578(1)	4735(1)	42(1)
Cl(4)	2751(1)	4183(1)	5132(1)	49(1)
Cl(5)	1543(1)	5397(1)	4360(1)	48(1)
Cl(6)	1552(1)	8480(1)	3477(1)	48(1)
C(1)	938(2)	10058(8)	1635(5)	23(2)
C(2)	1221(5)	10981(14)	2174(10)	28(3)
C(3)	1075(7)	11393(17)	2737(10)	27(3)
C(4)	1343(7)	12274(19)	3259(11)	34(3)

C(5)	1760(7)	12745(19)	3222(9)	32(3)
C(6)	1904(6)	12351(18)	2664(9)	39(4)
C(7)	1640(5)	11466(17)	2141(10)	28(3)
C(8)	1151(4)	9153(8)	1287(5)	26(2)
C(9)	1601(5)	8649(13)	1644(8)	32(3)
C(10)	1784(4)	7748(14)	1293(6)	36(3)
C(11)	1524(3)	7337(11)	587(6)	32(3)
C(12)	1076(3)	7837(8)	226(5)	35(2)
C(13)	893(3)	8730(7)	578(5)	31(2)
C(14)	432(2)	10050(6)	1439(3)	28(2)
C(15)	175(2)	8895(7)	1281(3)	34(2)
C(16)	-310(2)	8898(8)	1083(3)	43(2)
C(17)	-539(3)	10070(7)	1041(4)	44(2)
C(18)	-298(2)	11237(7)	1194(3)	42(2)
C(19)	185(2)	11204(7)	1395(3)	33(2)
C(1D)	950(3)	9499(9)	1720(6)	27(2)
C(2D)	1164(6)	10629(17)	2143(11)	29(3)
C(3D)	1018(8)	11040(20)	2696(12)	39(4)
C(4D)	1261(8)	12040(20)	3148(13)	36(4)
C(5D)	1644(7)	12610(20)	3059(10)	39(4)
C(6D)	1789(7)	12218(19)	2509(10)	33(3)
C(7D)	1547(6)	11222(18)	2062(12)	34(3)
C(8D)	1204(4)	8697(9)	1394(6)	26(3)
C(9D)	1688(5)	8532(16)	1750(11)	36(3)
C(10D)	1946(4)	7810(16)	1434(7)	30(3)
C(11D)	1713(3)	7259(13)	757(7)	31(3)
C(12D)	1234(3)	7415(9)	396(5)	27(3)
C(13D)	974(4)	8127(8)	711(5)	28(2)
C(14D)	468(2)	9165(7)	1600(3)	30(2)
C(15D)	344(2)	7865(8)	1598(3)	34(2)
C(16D)	-115(2)	7524(8)	1481(3)	42(2)
C(17D)	-455(3)	8459(9)	1364(3)	51(2)
C(18D)	-332(3)	9753(10)	1365(4)	48(2)
C(19D)	125(2)	10112(9)	1486(3)	41(2)

C(1S)	223(2)	5039(4)	1282(3)	28(2)
C(2S)	468(2)	4478(4)	898(3)	28(2)
C(3S)	950(3)	4513(7)	1163(5)	32(3)
C(4S)	1187(3)	5116(9)	1819(5)	45(4)
C(5S)	944(3)	5675(8)	2206(5)	46(3)
C(6S)	462(2)	5640(6)	1942(3)	32(2)
Cl(1S)	-384(1)	5023(2)	958(1)	49(1)
Cl(2S)	178(1)	3705(2)	72(1)	45(1)
C(1E)	386(2)	4110(4)	1736(3)	38(2)
C(2E)	532(2)	3857(5)	1165(3)	35(2)
C(3E)	958(3)	4328(7)	1185(5)	36(3)
C(4E)	1234(3)	5052(9)	1775(5)	34(3)
C(5E)	1088(3)	5295(8)	2346(5)	40(3)
C(6E)	662(2)	4816(6)	2325(3)	46(2)
Cl(1D)	-152(1)	3540(2)	1734(1)	62(1)
Cl(2D)	191(1)	2944(2)	424(1)	53(1)

B.2.3 Bond Lengths and Angles

Bond lengths [Å] and angles [°] for $[[C_6H_5]_3C]_2[B_{12}Cl_{12}].2[C_6H_4Cl_2]$.

B(1)-B(3)	1.773(5)
B(1)-B(2)	1.780(5)
B(1)-B(4)	1.781(5)
B(1)-B(5)	1.783(5)
B(1)-B(6)	1.786(5)
B(1)-Cl(1)	1.799(4)
B(2)-B(6)	1.777(5)
B(2)-B(3)	1.782(6)
B(2)-B(5)#1	1.783(5)
B(2)-B(4)#1	1.787(5)
B(2)-Cl(2)	1.798(4)
B(3)-B(6)#1	1.777(5)

B(3)-B(4)	1.782(5)
B(3)-B(5)#1	1.784(5)
B(3)-Cl(3)	1.792(4)
B(4)-B(5)	1.782(5)
B(4)-Cl(4)	1.785(4)
B(4)-B(6)#1	1.787(5)
B(4)-B(2)#1	1.787(5)
B(5)-B(6)	1.772(6)
B(5)-B(2)#1	1.783(5)
B(5)-B(3)#1	1.784(5)
B(5)-Cl(5)	1.796(4)
B(6)-B(3)#1	1.777(5)
B(6)-B(4)#1	1.787(5)
B(6)-Cl(6)	1.789(4)
C(1)-C(8)	1.446(8)
C(1)-C(2)	1.451(8)
C(1)-C(14)	1.456(7)
C(2)-C(7)	1.401(8)
C(2)-C(3)	1.407(8)
C(3)-C(4)	1.392(8)
C(3)-H(3)	0.9500
C(3)-H(31)	1.40(8)
C(4)-C(5)	1.393(9)
C(4)-H(4)	0.9500
C(5)-C(6)	1.390(9)
C(5)-H(5)	0.9500
C(6)-C(7)	1.391(8)
C(6)-H(6)	0.9500
C(7)-H(7)	0.9500
C(8)-C(9)	1.398(7)
C(8)-C(13)	1.400(7)
C(9)-C(10)	1.394(7)
C(9)-H(9)	0.9500
C(10)-C(11)	1.392(7)

C(10)-H(10)	0.9500
C(11)-C(12)	1.393(7)
C(11)-H(11)	0.9500
C(12)-C(13)	1.388(7)
C(12)-H(12)	0.9500
C(13)-H(13)	0.9500
C(14)-C(19)	1.394(6)
C(14)-C(15)	1.395(6)
C(15)-C(16)	1.391(6)
C(15)-H(15)	0.9500
C(16)-C(17)	1.383(6)
C(16)-H(16)	0.9500
C(17)-C(18)	1.384(6)
C(17)-H(17)	0.9500
C(18)-C(19)	1.383(6)
C(18)-H(18)	0.9500
C(19)-H(19)	0.9500
C(1D)-C(8D)	1.440(8)
C(1D)-C(2D)	1.441(8)
C(1D)-C(14D)	1.449(8)
C(2D)-C(7D)	1.383(9)
C(2D)-C(3D)	1.392(9)
C(3D)-C(4D)	1.381(9)
C(3D)-H(31)	1.10(8)
C(4D)-C(5D)	1.380(9)
C(4D)-H(41)	0.9500
C(5D)-C(6D)	1.379(9)
C(5D)-H(51)	0.9500
C(6D)-C(7D)	1.378(9)
C(6D)-H(61)	0.9500
C(7D)-H(71)	0.9500
C(8D)-C(9D)	1.397(8)
C(8D)-C(13D)	1.400(7)
C(9D)-C(10D)	1.388(8)

C(9D)-H(91)	0.9500
C(10D)-C(11D)	1.386(8)
C(10D)-H(101)	0.9500
C(11D)-C(12D)	1.385(7)
C(11D)-H(111)	0.9500
C(12D)-C(13D)	1.387(7)
C(12D)-H(121)	0.9500
C(13D)-H(131)	0.9500
C(14D)-C(19D)	1.389(6)
C(14D)-C(15D)	1.391(7)
C(15D)-C(16D)	1.384(6)
C(15D)-H(151)	0.9500
C(16D)-C(17D)	1.375(7)
C(16D)-H(161)	0.9500
C(17D)-C(18D)	1.383(7)
C(17D)-H(171)	0.9500
C(18D)-C(19D)	1.382(7)
C(18D)-H(181)	0.9500
C(19D)-H(191)	0.9500
C(1S)-C(2S)	1.375(7)
C(1S)-C(6S)	1.384(8)
C(1S)-Cl(1S)	1.732(6)
C(2S)-C(3S)	1.373(7)
C(2S)-Cl(2S)	1.736(7)
C(3S)-C(4S)	1.379(7)
C(3S)-H(20)	0.9500
C(4S)-C(5S)	1.375(7)
C(4S)-H(21)	0.9500
C(5S)-C(6S)	1.374(7)
C(5S)-H(22)	0.9500
C(6S)-H(23)	0.9500
C(1E)-C(6E)	1.367(8)
C(1E)-C(2E)	1.383(7)
C(1E)-Cl(1D)	1.750(6)

C(2E)-C(3E)	1.380(7)
C(2E)-Cl(2D)	1.729(7)
C(3E)-C(4E)	1.379(7)
C(3E)-H(24)	0.9500
C(4E)-C(5E)	1.380(7)
C(4E)-H(25)	0.9500
C(5E)-C(6E)	1.383(7)
C(5E)-H(26)	0.9500
C(6E)-H(27)	0.9500

B(3)-B(1)-B(2)	60.2(2)
B(3)-B(1)-B(4)	60.2(2)
B(2)-B(1)-B(4)	108.3(3)
B(3)-B(1)-B(5)	107.9(2)
B(2)-B(1)-B(5)	107.5(3)
B(4)-B(1)-B(5)	60.0(2)
B(3)-B(1)-B(6)	107.8(3)
B(2)-B(1)-B(6)	59.8(2)
B(4)-B(1)-B(6)	107.8(2)
B(5)-B(1)-B(6)	59.5(2)
B(3)-B(1)-Cl(1)	121.8(2)
B(2)-B(1)-Cl(1)	120.9(2)
B(4)-B(1)-Cl(1)	122.4(3)
B(5)-B(1)-Cl(1)	122.4(2)
B(6)-B(1)-Cl(1)	121.4(2)
B(6)-B(2)-B(1)	60.3(2)
B(6)-B(2)-B(3)	107.8(3)
B(1)-B(2)-B(3)	59.7(2)
B(6)-B(2)-B(5)#1	107.8(2)
B(1)-B(2)-B(5)#1	107.9(3)
B(3)-B(2)-B(5)#1	60.1(2)
B(6)-B(2)-B(4)#1	60.2(2)
B(1)-B(2)-B(4)#1	108.6(3)
B(3)-B(2)-B(4)#1	108.2(2)

B(5)#1-B(2)-B(4)#1	59.9(2)
B(6)-B(2)-Cl(2)	121.0(2)
B(1)-B(2)-Cl(2)	121.3(2)
B(3)-B(2)-Cl(2)	122.4(2)
B(5)#1-B(2)-Cl(2)	122.6(2)
B(4)#1-B(2)-Cl(2)	121.2(3)
B(1)-B(3)-B(6)#1	108.2(2)
B(1)-B(3)-B(2)	60.1(2)
B(6)#1-B(3)-B(2)	107.7(3)
B(1)-B(3)-B(4)	60.1(2)
B(6)#1-B(3)-B(4)	60.3(2)
B(2)-B(3)-B(4)	108.1(3)
B(1)-B(3)-B(5)#1	108.1(3)
B(6)#1-B(3)-B(5)#1	59.7(2)
B(2)-B(3)-B(5)#1	60.0(2)
B(4)-B(3)-B(5)#1	108.1(2)
B(1)-B(3)-Cl(3)	122.9(2)
B(6)#1-B(3)-Cl(3)	120.6(2)
B(2)-B(3)-Cl(3)	122.4(2)
B(4)-B(3)-Cl(3)	121.7(3)
B(5)#1-B(3)-Cl(3)	120.8(2)
B(1)-B(4)-B(5)	60.1(2)
B(1)-B(4)-B(3)	59.7(2)
B(5)-B(4)-B(3)	107.5(3)
B(1)-B(4)-Cl(4)	121.9(2)
B(5)-B(4)-Cl(4)	121.4(3)
B(3)-B(4)-Cl(4)	122.7(2)
B(1)-B(4)-B(6)#1	107.4(3)
B(5)-B(4)-B(6)#1	107.4(3)
B(3)-B(4)-B(6)#1	59.7(2)
Cl(4)-B(4)-B(6)#1	122.5(3)
B(1)-B(4)-B(2)#1	107.9(3)
B(5)-B(4)-B(2)#1	59.9(2)
B(3)-B(4)-B(2)#1	107.5(3)

Cl(4)-B(4)-B(2)#1	121.4(2)
B(6)#1-B(4)-B(2)#1	59.6(2)
B(6)-B(5)-B(4)	108.3(3)
B(6)-B(5)-B(2)#1	108.0(3)
B(4)-B(5)-B(2)#1	60.2(2)
B(6)-B(5)-B(1)	60.3(2)
B(4)-B(5)-B(1)	59.9(2)
B(2)#1-B(5)-B(1)	108.0(3)
B(6)-B(5)-B(3)#1	60.0(2)
B(4)-B(5)-B(3)#1	108.3(3)
B(2)#1-B(5)-B(3)#1	60.0(2)
B(1)-B(5)-B(3)#1	108.3(3)
B(6)-B(5)-Cl(5)	121.1(3)
B(4)-B(5)-Cl(5)	122.1(3)
B(2)#1-B(5)-Cl(5)	122.0(2)
B(1)-B(5)-Cl(5)	121.8(2)
B(3)#1-B(5)-Cl(5)	121.1(2)
B(5)-B(6)-B(2)	108.2(3)
B(5)-B(6)-B(3)#1	60.3(2)
B(2)-B(6)-B(3)#1	108.2(2)
B(5)-B(6)-B(1)	60.1(2)
B(2)-B(6)-B(1)	60.0(2)
B(3)#1-B(6)-B(1)	108.4(3)
B(5)-B(6)-B(4)#1	108.4(3)
B(2)-B(6)-B(4)#1	60.2(2)
B(3)#1-B(6)-B(4)#1	60.0(2)
B(1)-B(6)-B(4)#1	108.3(3)
B(5)-B(6)-Cl(6)	121.2(3)
B(2)-B(6)-Cl(6)	122.0(2)
B(3)#1-B(6)-Cl(6)	121.3(2)
B(1)-B(6)-Cl(6)	121.6(2)
B(4)#1-B(6)-Cl(6)	121.6(3)
C(8)-C(1)-C(2)	121.2(8)
C(8)-C(1)-C(14)	119.5(7)

C(2)-C(1)-C(14)	119.3(8)
C(7)-C(2)-C(3)	119.5(11)
C(7)-C(2)-C(1)	120.6(10)
C(3)-C(2)-C(1)	119.9(9)
C(4)-C(3)-C(2)	120.6(11)
C(4)-C(3)-H(3)	119.7
C(2)-C(3)-H(3)	119.7
C(4)-C(3)-H(31)	125(3)
C(2)-C(3)-H(31)	112(3)
H(3)-C(3)-H(31)	17.1
C(3)-C(4)-C(5)	119.4(12)
C(3)-C(4)-H(4)	120.3
C(5)-C(4)-H(4)	120.3
C(6)-C(5)-C(4)	120.3(12)
C(6)-C(5)-H(5)	119.8
C(4)-C(5)-H(5)	119.8
C(5)-C(6)-C(7)	120.7(12)
C(5)-C(6)-H(6)	119.6
C(7)-C(6)-H(6)	119.6
C(6)-C(7)-C(2)	119.5(11)
C(6)-C(7)-H(7)	120.2
C(2)-C(7)-H(7)	120.2
C(9)-C(8)-C(13)	118.5(9)
C(9)-C(8)-C(1)	122.2(8)
C(13)-C(8)-C(1)	119.2(8)
C(10)-C(9)-C(8)	119.9(11)
C(10)-C(9)-H(9)	120.0
C(8)-C(9)-H(9)	120.0
C(11)-C(10)-C(9)	120.9(10)
C(11)-C(10)-H(10)	119.6
C(9)-C(10)-H(10)	119.6
C(10)-C(11)-C(12)	119.6(8)
C(10)-C(11)-H(11)	120.2
C(12)-C(11)-H(11)	120.2

C(13)-C(12)-C(11)	119.4(8)
C(13)-C(12)-H(12)	120.3
C(11)-C(12)-H(12)	120.3
C(12)-C(13)-C(8)	121.6(8)
C(12)-C(13)-H(13)	119.2
C(8)-C(13)-H(13)	119.2
C(19)-C(14)-C(15)	117.6(6)
C(19)-C(14)-C(1)	120.9(5)
C(15)-C(14)-C(1)	121.5(6)
C(16)-C(15)-C(14)	121.1(7)
C(16)-C(15)-H(15)	119.4
C(14)-C(15)-H(15)	119.4
C(17)-C(16)-C(15)	119.1(7)
C(17)-C(16)-H(16)	120.5
C(15)-C(16)-H(16)	120.5
C(16)-C(17)-C(18)	121.6(7)
C(16)-C(17)-H(17)	119.2
C(18)-C(17)-H(17)	119.2
C(19)-C(18)-C(17)	118.1(7)
C(19)-C(18)-H(18)	121.0
C(17)-C(18)-H(18)	121.0
C(18)-C(19)-C(14)	122.5(6)
C(18)-C(19)-H(19)	118.7
C(14)-C(19)-H(19)	118.7
C(8D)-C(1D)-C(2D)	121.0(9)
C(8D)-C(1D)-C(14D)	118.6(8)
C(2D)-C(1D)-C(14D)	120.5(9)
C(7D)-C(2D)-C(3D)	119.2(14)
C(7D)-C(2D)-C(1D)	121.0(12)
C(3D)-C(2D)-C(1D)	119.4(12)
C(4D)-C(3D)-C(2D)	118.7(14)
C(4D)-C(3D)-H(31)	118(4)
C(2D)-C(3D)-H(31)	123(4)
C(5D)-C(4D)-C(3D)	121.1(14)

C(5D)-C(4D)-H(41)	119.4
C(3D)-C(4D)-H(41)	119.4
C(6D)-C(5D)-C(4D)	120.7(14)
C(6D)-C(5D)-H(51)	119.7
C(4D)-C(5D)-H(51)	119.7
C(7D)-C(6D)-C(5D)	118.0(13)
C(7D)-C(6D)-H(61)	121.0
C(5D)-C(6D)-H(61)	121.0
C(6D)-C(7D)-C(2D)	122.3(15)
C(6D)-C(7D)-H(71)	118.9
C(2D)-C(7D)-H(71)	118.9
C(9D)-C(8D)-C(13D)	120.0(11)
C(9D)-C(8D)-C(1D)	119.6(10)
C(13D)-C(8D)-C(1D)	120.4(9)
C(10D)-C(9D)-C(8D)	120.9(14)
C(10D)-C(9D)-H(91)	119.6
C(8D)-C(9D)-H(91)	119.6
C(11D)-C(10D)-C(9D)	118.4(13)
C(11D)-C(10D)-H(101)	120.8
C(9D)-C(10D)-H(101)	120.8
C(12D)-C(11D)-C(10D)	121.4(11)
C(12D)-C(11D)-H(111)	119.3
C(10D)-C(11D)-H(111)	119.3
C(11D)-C(12D)-C(13D)	120.4(10)
C(11D)-C(12D)-H(121)	119.8
C(13D)-C(12D)-H(121)	119.8
C(12D)-C(13D)-C(8D)	119.0(8)
C(12D)-C(13D)-H(131)	120.5
C(8D)-C(13D)-H(131)	120.5
C(19D)-C(14D)-C(15D)	119.0(7)
C(19D)-C(14D)-C(1D)	121.7(7)
C(15D)-C(14D)-C(1D)	119.3(6)
C(16D)-C(15D)-C(14D)	120.3(7)
C(16D)-C(15D)-H(151)	119.9

C(14D)-C(15D)-H(151)	119.9
C(17D)-C(16D)-C(15D)	120.8(8)
C(17D)-C(16D)-H(161)	119.6
C(15D)-C(16D)-H(161)	119.6
C(16D)-C(17D)-C(18D)	119.0(9)
C(16D)-C(17D)-H(171)	120.5
C(18D)-C(17D)-H(171)	120.5
C(19D)-C(18D)-C(17D)	121.0(9)
C(19D)-C(18D)-H(181)	119.5
C(17D)-C(18D)-H(181)	119.5
C(18D)-C(19D)-C(14D)	119.9(8)
C(18D)-C(19D)-H(191)	120.0
C(14D)-C(19D)-H(191)	120.0
C(2S)-C(1S)-C(6S)	120.0(4)
C(2S)-C(1S)-Cl(1S)	121.5(5)
C(6S)-C(1S)-Cl(1S)	118.5(4)
C(3S)-C(2S)-C(1S)	120.4(5)
C(3S)-C(2S)-Cl(2S)	118.6(5)
C(1S)-C(2S)-Cl(2S)	121.0(5)
C(2S)-C(3S)-C(4S)	119.5(4)
C(2S)-C(3S)-H(20)	120.2
C(4S)-C(3S)-H(20)	120.2
C(5S)-C(4S)-C(3S)	120.2(4)
C(5S)-C(4S)-H(21)	119.9
C(3S)-C(4S)-H(21)	119.9
C(6S)-C(5S)-C(4S)	120.3(5)
C(6S)-C(5S)-H(22)	119.8
C(4S)-C(5S)-H(22)	119.8
C(5S)-C(6S)-C(1S)	119.5(4)
C(5S)-C(6S)-H(23)	120.3
C(1S)-C(6S)-H(23)	120.3
C(6E)-C(1E)-C(2E)	120.6(4)
C(6E)-C(1E)-Cl(1D)	117.9(4)
C(2E)-C(1E)-Cl(1D)	121.5(5)

C(3E)-C(2E)-C(1E)	119.8(5)
C(3E)-C(2E)-Cl(2D)	119.1(5)
C(1E)-C(2E)-Cl(2D)	121.1(5)
C(4E)-C(3E)-C(2E)	119.6(4)
C(4E)-C(3E)-H(24)	120.2
C(2E)-C(3E)-H(24)	120.2
C(3E)-C(4E)-C(5E)	120.4(4)
C(3E)-C(4E)-H(25)	119.8
C(5E)-C(4E)-H(25)	119.8
C(4E)-C(5E)-C(6E)	119.8(5)
C(4E)-C(5E)-H(26)	120.1
C(6E)-C(5E)-H(26)	120.1
C(1E)-C(6E)-C(5E)	119.8(4)
C(1E)-C(6E)-H(27)	120.1
C(5E)-C(6E)-H(27)	120.1

Symmetry transformations used to generate equivalent atoms:
#1 -x+1/2,-y+3/2,-z+1

B.2.4 Anisotropic Displacement Parameters

Anisotropic displacement parameters ($Å^2 x\ 10^3$) for $[[C_6H_5]_3C]_2[B_{12}Cl_{12}].2[C_6H_4Cl_2]$. The anisotropic displacement factor exponent takes the form: $-2p^2[\ h^2a^{*2}U^{11} + ... + 2\ h\ k\ a^*\ b^*\ U^{12}\ ]$

	U^{11}	U^{22}	U^{33}	U^{23}	U^{13}	U^{12}
B(1)	17(2)	32(2)	17(2)	0(2)	6(2)	-1(2)
B(2)	27(2)	32(2)	16(2)	-4(2)	11(2)	-2(2)
B(3)	16(2)	44(3)	14(2)	-5(2)	5(2)	2(2)
B(4)	29(2)	29(2)	21(2)	-3(2)	13(2)	2(2)
B(5)	23(2)	36(2)	23(2)	-5(2)	14(2)	-9(2)
B(6)	19(2)	40(2)	16(2)	-4(2)	6(2)	4(2)

Cl(1)	28(1)	39(1)	19(1)	-8(1)	11(1)	-4(1)
Cl(2)	57(1)	38(1)	27(1)	0(1)	26(1)	-8(1)
Cl(3)	20(1)	84(1)	22(1)	-8(1)	9(1)	10(1)
Cl(4)	88(1)	31(1)	36(1)	4(1)	33(1)	16(1)
Cl(5)	45(1)	73(1)	34(1)	-25(1)	24(1)	-38(1)
Cl(6)	36(1)	86(1)	17(1)	-2(1)	2(1)	29(1)
C(1)	25(3)	30(5)	17(4)	9(4)	12(3)	-5(3)
C(2)	21(5)	37(8)	24(5)	-3(5)	6(4)	-5(4)
C(3)	25(6)	36(8)	21(5)	-11(5)	12(5)	-8(5)
C(4)	38(7)	39(7)	20(6)	-10(4)	5(5)	-13(5)
C(5)	41(9)	35(6)	15(6)	-6(4)	3(6)	-13(5)
C(6)	38(8)	43(6)	35(8)	-16(5)	12(7)	-15(5)
C(7)	24(6)	44(7)	15(6)	-2(5)	8(5)	-18(4)
C(8)	32(4)	24(6)	24(4)	7(4)	12(3)	-4(4)
C(9)	44(7)	37(6)	20(5)	-4(4)	16(5)	-6(5)
C(10)	24(7)	50(6)	32(6)	-1(5)	10(5)	0(5)
C(11)	28(8)	47(5)	23(6)	-6(4)	13(6)	-1(6)
C(12)	31(6)	41(6)	32(5)	-1(4)	11(4)	-2(4)
C(13)	37(5)	23(5)	36(4)	-1(4)	19(4)	-7(4)
C(14)	24(3)	36(4)	27(4)	-1(3)	12(3)	-8(3)
C(15)	35(4)	39(4)	33(4)	-13(3)	18(3)	-8(3)
C(16)	38(4)	58(5)	41(5)	-21(4)	23(4)	-21(4)
C(17)	27(4)	70(5)	40(5)	-27(4)	20(4)	-8(4)
C(18)	27(4)	51(4)	47(4)	-10(4)	14(3)	4(3)
C(19)	26(3)	44(4)	29(4)	-7(3)	9(3)	-3(3)
C(1D)	32(4)	39(6)	11(4)	10(4)	9(3)	3(4)
C(2D)	26(6)	38(8)	24(6)	6(5)	11(5)	1(4)
C(3D)	28(7)	56(12)	32(6)	-9(6)	9(5)	-1(7)
C(4D)	41(9)	43(9)	30(8)	-2(6)	18(7)	0(7)
C(5D)	32(9)	49(8)	26(8)	-7(6)	1(7)	-8(6)
C(6D)	29(8)	49(9)	18(7)	12(6)	5(6)	-6(5)
C(7D)	34(8)	36(8)	29(6)	3(5)	7(6)	5(5)
C(8D)	29(5)	34(7)	21(5)	4(5)	16(4)	-3(5)
C(9D)	24(5)	48(8)	35(7)	8(5)	10(4)	-1(5)

C(10D)	15(6)	51(6)	23(5)	6(5)	5(4)	-5(5)
C(11D)	21(7)	41(6)	33(7)	2(5)	10(6)	-6(5)
C(12D)	25(7)	33(6)	22(6)	-1(4)	7(5)	2(5)
C(13D)	25(4)	32(6)	28(5)	-4(4)	14(4)	-6(4)
C(14D)	23(4)	49(5)	19(4)	4(4)	11(3)	6(4)
C(15D)	29(4)	49(5)	26(4)	-2(4)	12(3)	2(4)
C(16D)	33(4)	68(5)	31(4)	-8(4)	20(4)	-6(4)
C(17D)	32(5)	97(6)	28(5)	-17(5)	15(4)	0(4)
C(18D)	27(4)	92(6)	20(5)	3(5)	5(4)	29(5)
C(19D)	45(4)	58(6)	20(4)	8(4)	13(4)	16(4)
C(1S)	33(3)	21(4)	33(4)	-1(3)	18(3)	-7(3)
C(2S)	41(4)	25(5)	23(4)	-1(3)	16(3)	-5(4)
C(3S)	36(5)	35(6)	30(6)	10(5)	18(5)	-3(5)
C(4S)	27(6)	56(9)	45(8)	6(7)	4(5)	-4(6)
C(5S)	52(5)	51(7)	29(5)	-6(4)	8(4)	-19(6)
C(6S)	45(4)	28(4)	30(4)	2(3)	20(3)	-8(4)
Cl(1S)	33(1)	74(2)	45(1)	-8(1)	20(1)	-7(1)
Cl(2S)	49(1)	56(1)	31(1)	-16(1)	14(1)	-12(1)
C(1E)	32(4)	40(4)	52(4)	-14(4)	26(3)	-7(3)
C(2E)	40(4)	33(5)	31(4)	-10(3)	11(4)	-8(4)
C(3E)	32(5)	43(6)	35(6)	-9(5)	14(5)	9(5)
C(4E)	31(6)	45(8)	31(6)	-1(6)	16(5)	-1(5)
C(5E)	32(5)	52(7)	36(5)	-19(5)	12(4)	-10(5)
C(6E)	52(5)	54(5)	41(5)	-20(4)	30(4)	-14(4)
Cl(1D)	56(1)	66(2)	80(2)	-30(1)	45(1)	-26(1)
Cl(2D)	76(2)	47(1)	39(1)	-15(1)	22(1)	-24(1)

B.2.5 Hydrogen Coordinates

Hydrogen coordinates (x 10^4) and isotropic displacement parameters (Å^{2}x 10^3) for $[[C_6H_5]_3C]_2[B_{12}Cl_{12}].2[C_6H_4Cl_2]$.

	x	y	z	U(eq)
H(3)	791	11066	2761	32
H(4)	1243	12553	3636	41
H(5)	1946	13339	3580	39
H(6)	2187	12688	2640	47
H(7)	1742	11194	1765	33
H(9)	1782	8921	2126	39
H(10)	2090	7409	1538	43
H(11)	1651	6719	354	38
H(12)	896	7569	-257	42
H(13)	586	9063	332	37
H(15)	335	8093	1309	41
H(16)	-481	8106	978	52
H(17)	-870	10074	904	52
H(18)	-458	12037	1162	50
H(19)	354	11998	1508	40
H(31)	730(30)	10560(70)	2820(40)	47
H(41)	1164	12328	3526	44
H(51)	1808	13284	3381	46
H(61)	2048	12622	2440	39
H(71)	1647	10932	1685	41
H(91)	1842	8918	2214	43
H(101)	2274	7697	1677	36
H(111)	1885	6763	534	38
H(121)	1082	7032	-70	32
H(131)	645	8226	468	33
H(151)	575	7208	1677	41

H(161)	-196	6632	1481	50
H(171)	-769	8221	1283	61
H(181)	-566	10404	1281	57
H(191)	204	11005	1491	49
H(20)	1118	4124	896	38
H(21)	1521	5146	2004	54
H(22)	1110	6088	2659	55
H(23)	295	6025	2211	39
H(24)	1061	4156	795	44
H(25)	1526	5385	1789	41
H(26)	1280	5790	2752	48
H(27)	561	4978	2718	55

B.3 References

1. *APEX 2,* version 2.0-22, Bruker (2004), Bruker AXS Inc., Madison, Wisconsin, USA.

2. *SAINT,* version V7.23A, Bruker (2003), Bruker AXS Inc., Madison, Wisconsin, USA.

3. *SADABS,* version 2004/1, Bruker (2004), Bruker AXS Inc., Madison, Wisconsin, USA.

4. *SHELXTL,* version 6.14, Bruker (2008), Bruker AXS Inc., Madison, Wisconsin, USA.

Appendix C. X-Ray Structure Determination for $((C_2H_5)_3Si)_2(B_{12}Br_{12})\cdot ODCB$

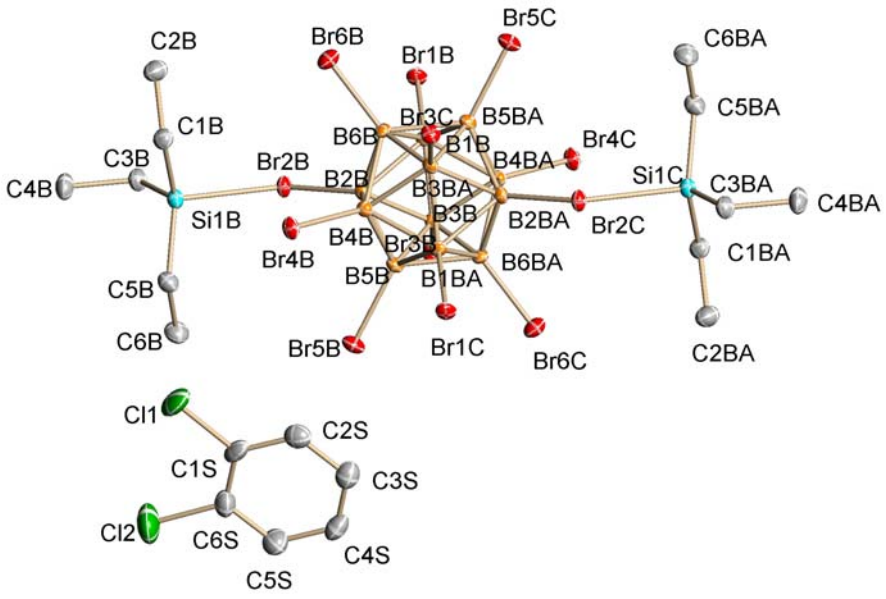

C.1 Experimental Details

The Bruker X8-APEX (**ref. 1**) X-ray diffraction instrument with Mo-radiation was used for data collection**.** All data frames were collected at low temperatures (T = 100 K) using an ω, φ-scan mode (0.5^o ω-scan width, hemisphere of reflections) and integrated using a Bruker SAINTPLUS software package (**ref. 2**). The intensity data were corrected for Lorentzian polarization. Absorption corrections were performed using the SADABS program (**ref. 3**). The SIR97 (**ref. 4**) was used for direct methods of phase determination, and Bruker SHELXTL software package (**ref. 5**) include in the WINGX package (**ref. 6)** for structure refinement and difference Fourier maps. Atomic coordinates, isotropic and anisotropic displacement parameters of all the non-hydrogen atoms were refined by means of a full matrix least-squares procedure on F^2. All H-atoms

were included in the refinement in calculated positions riding on the C atoms. Drawings of molecules were performed using Ortep 3 (**ref. 7**). Further details on the Crystal Structure Investigation, are available on request from the Director of the Cambridge Crystallographic Data centre, 12 Union Road, GB-Cambridge CB21EZ UK.

Crystal and structure parameters of $C_{18}H_{33}B_{12}Br_{12}Cl_2Si_2$:

size 0.32 x 0.09 x 0.07 mm^3, orthorhombic, space group P2(1)/c , **a** = 18.3119(4) Å, **b** = 11.9561(2) Å, **c** = 21.0939(4) Å, $\alpha = \gamma = 90.0^o$ **,** β = 110.9080(10)° , V = 10.692(13) $Å^3$, ρ_{calcd} = 2.256 g/cm^3, Mo-radiation (λ = 0.71073 Å), T = 100(2) K, reflections collected = 41588, independent reflections = 8810 (R_{int} = 0.0234), absorption coefficient μ = 11.338 mm^{-1}; max/min transmission = 0.2811 and 0.1057, 422 parameters were refined and converged at R1 = 0.0217, wR2 = 0.0547, with intensity I>2σ(I).

C.2 Structure Data

C.2.1 Crystal structure and refinement data for $((C_2H_5)_3Si)_2(B_{12}Br_{12})\cdot$ODCB

Empirical formula	$C_{18}H_{33}B_{12}Br_{12}Cl_2Si_2$	
Formula weight	1465.16	
Temperature	100(2) K	
Wavelength	0.71073 Å	
Crystal system	Monoclinic	
Space group	P2(1)/c	
Unit cell dimensions	a = 18.3119(4) Å	α = 90°
	b = 11.9561(2) Å	β = 110.9080(10)°
	c = 21.0939(4) Å	γ = 90°
Volume	4314.18(14) $Å^3$	

Z	4
Density (calculated)	2.256 Mg/m^3
Absorption coefficient	11.338 mm^{-1}
F(000)	2732
Crystal size	0.36 x 0.19 x 0.15 mm^3
Theta range for data collection	1.98 to 26.37°
Index ranges	-22<=h<=22, -14<=k<=14, -26<=l<=26
Reflections collected	41588
Independent reflections	8810 [R(int) = 0.0234]
Completeness to theta = 26.37°	100.0 %
Absorption correction	Sadabs
Max. and min. transmission	0.2811 and 0.1057
Refinement method	Full-matrix least-squares on F^2
Data / restraints / parameters	8810 / 0 / 422
Goodness-of-fit on F^2	1.042
Final R indices [I>2sigma(I)]	R1 = 0.0217, wR2 = 0.0547
R indices (all data)	R1 = 0.0262, wR2 = 0.0563
Extinction coefficient	0.000016(19)
Largest diff. peak and hole	1.088 and -1.040 $e.Å^{-3}$

C.2.2 Atomic Coordinates

Atomic coordinates (x 10^4) and equivalent isotropic displacement parameters ($Å^2$x 10^3) for $((C_2H_5)_3Si)_2(B_{12}Br_{12})$·ODCB. U(eq) is defined as one third of the trace of the orthogonalized U^{ij} tensor.

	x	y	z	U(eq)
Si(1A)	968(1)	6254(1)	4043(1)	14(1)
C(1A)	1514(2)	5728(3)	4905(2)	18(1)
C(2A)	1074(2)	4914(3)	5203(2)	23(1)

C(3A)	337(2)	5184(3)	3471(2)	19(1)
C(4A)	860(2)	4252(3)	3355(2)	25(1)
C(5A)	1485(2)	7187(3)	3647(2)	18(1)
C(6A)	1059(2)	7373(3)	2888(2)	30(1)
Br(1A)	-1461(1)	9734(1)	3304(1)	15(1)
Br(2A)	-143(1)	7360(1)	4088(1)	14(1)
Br(3A)	668(1)	10125(1)	3564(1)	18(1)
Br(4A)	490(1)	7476(1)	6034(1)	16(1)
Br(5A)	1921(1)	8778(1)	5291(1)	16(1)
Br(6A)	-1623(1)	8100(1)	4809(1)	15(1)
B(1A)	-688(2)	9880(3)	4206(2)	12(1)
B(2A)	-1(2)	8803(3)	4597(2)	10(1)
B(3A)	327(2)	10059(3)	4335(2)	12(1)
B(4A)	223(2)	8816(3)	5490(2)	11(1)
B(5A)	888(2)	9412(3)	5126(2)	12(1)
B(6A)	-754(2)	9108(3)	4921(2)	11(1)
Si(1B)	4009(1)	4886(1)	2224(1)	16(1)
C(1B)	3468(2)	6201(3)	2195(2)	20(1)
C(2B)	3860(2)	7273(3)	2088(2)	27(1)
C(3B)	4654(2)	4900(3)	1718(2)	20(1)
C(4B)	4147(2)	4867(3)	955(2)	28(1)
C(5B)	3458(2)	3577(3)	2178(2)	21(1)
C(6B)	3895(2)	2482(3)	2187(2)	27(1)
Br(1B)	6581(1)	6457(1)	4674(1)	17(1)
Br(2B)	5130(1)	4823(1)	3310(1)	15(1)
Br(3B)	6515(1)	3257(1)	4767(1)	16(1)
Br(4B)	3078(1)	4944(1)	3653(1)	18(1)
Br(5B)	4397(1)	2344(1)	4120(1)	20(1)
Br(6B)	4469(1)	7519(1)	3973(1)	21(1)
B(1B)	5736(2)	5690(3)	4849(2)	13(1)
B(2B)	4999(2)	4912(3)	4211(2)	12(1)
B(3B)	5713(2)	4184(3)	4896(2)	12(1)
B(4B)	4109(2)	4988(3)	4360(2)	12(1)
B(5B)	4708(2)	3751(3)	4588(2)	12(1)

B(6B)	4745(2)	6182(3)	4515(2)	12(1)
C(1S)	2257(2)	1096(3)	3034(2)	28(1)
C(2S)	2465(2)	1383(3)	3708(2)	30(1)
C(3S)	2832(2)	600(3)	4204(2)	31(1)
C(4S)	2999(2)	-447(3)	4030(2)	31(1)
C(5S)	2791(2)	-735(3)	3352(2)	34(1)
C(6S)	2420(2)	45(3)	2854(2)	31(1)
Cl(1)	1789(1)	2090(1)	2432(1)	46(1)
Cl(2)	2147(1)	-341(1)	2011(1)	61(1)

C.2.3 Bond Lengths and Angles

Bond lengths [Å] and angles [°] for $((C_2H_5)_3Si)_2(B_{12}Br_{12})\cdot$ODCB.

Si(1A)-C(1A)	1.844(3)
Si(1A)-C(5A)	1.845(3)
Si(1A)-C(3A)	1.853(3)
Si(1A)-Br(2A)	2.4558(8)
C(1A)-C(2A)	1.533(4)
C(3A)-C(4A)	1.546(4)
C(5A)-C(6A)	1.527(5)
Br(1A)-B(1A)	1.932(3)
Br(2A)-B(2A)	2.000(3)
Br(3A)-B(3A)	1.941(3)
Br(4A)-B(4A)	1.931(3)
Br(5A)-B(5A)	1.949(3)
Br(6A)-B(6A)	1.942(3)
B(1A)-B(4A)#1	1.782(4)
B(1A)-B(2A)	1.784(5)
B(1A)-B(5A)#1	1.790(5)
B(1A)-B(3A)	1.793(4)

B(1A)-B(6A)	1.809(5)
B(2A)-B(5A)	1.769(4)
B(2A)-B(3A)	1.777(5)
B(2A)-B(4A)	1.779(5)
B(2A)-B(6A)	1.782(4)
B(3A)-B(6A)#1	1.787(5)
B(3A)-B(5A)	1.793(5)
B(3A)-B(4A)#1	1.796(5)
B(4A)-B(1A)#1	1.782(4)
B(4A)-B(3A)#1	1.796(5)
B(4A)-B(6A)	1.798(4)
B(4A)-B(5A)	1.802(4)
B(5A)-B(6A)#1	1.785(5)
B(5A)-B(1A)#1	1.790(5)
B(6A)-B(5A)#1	1.785(5)
B(6A)-B(3A)#1	1.787(5)
Si(1B)-C(5B)	1.846(3)
Si(1B)-C(1B)	1.848(3)
Si(1B)-C(3B)	1.855(3)
Si(1B)-Br(2B)	2.4727(9)
C(1B)-C(2B)	1.525(5)
C(3B)-C(4B)	1.544(5)
C(5B)-C(6B)	1.531(4)
Br(1B)-B(1B)	1.944(3)
Br(2B)-B(2B)	2.002(3)
Br(3B)-B(3B)	1.936(3)
Br(4B)-B(4B)	1.945(3)
Br(5B)-B(5B)	1.931(3)
Br(6B)-B(6B)	1.925(3)
B(1B)-B(4B)#2	1.784(5)
B(1B)-B(2B)	1.788(5)
B(1B)-B(5B)#2	1.791(5)
B(1B)-B(6B)	1.795(5)
B(1B)-B(3B)	1.805(5)

B(2B)-B(4B)	1.769(4)
B(2B)-B(6B)	1.773(5)
B(2B)-B(5B)	1.775(5)
B(2B)-B(3B)	1.790(5)
B(3B)-B(4B)#2	1.784(5)
B(3B)-B(6B)#2	1.784(5)
B(3B)-B(5B)	1.796(4)
B(4B)-B(3B)#2	1.784(5)
B(4B)-B(1B)#2	1.784(5)
B(4B)-B(6B)	1.798(5)
B(4B)-B(5B)	1.801(5)
B(5B)-B(1B)#2	1.791(5)
B(5B)-B(6B)#2	1.799(5)
B(6B)-B(3B)#2	1.784(5)
B(6B)-B(5B)#2	1.799(5)
C(1S)-C(6S)	1.376(5)
C(1S)-C(2S)	1.378(5)
C(1S)-Cl(1)	1.727(4)
C(2S)-C(3S)	1.386(5)
C(3S)-C(4S)	1.369(6)
C(4S)-C(5S)	1.386(6)
C(5S)-C(6S)	1.387(5)
C(6S)-Cl(2)	1.730(4)
C(1A)-Si(1A)-C(5A)	117.80(14)
C(1A)-Si(1A)-C(3A)	113.53(15)
C(5A)-Si(1A)-C(3A)	115.11(15)
C(1A)-Si(1A)-Br(2A)	108.14(11)
C(5A)-Si(1A)-Br(2A)	104.96(11)
C(3A)-Si(1A)-Br(2A)	93.67(10)
C(2A)-C(1A)-Si(1A)	116.2(2)
C(4A)-C(3A)-Si(1A)	108.8(2)
C(6A)-C(5A)-Si(1A)	114.2(2)
B(2A)-Br(2A)-Si(1A)	122.29(9)
B(4A)#1-B(1A)-B(2A)	107.3(2)

B(4A)#1-B(1A)-B(5A)#1 60.57(18)
B(2A)-B(1A)-B(5A)#1 106.6(2)
B(4A)#1-B(1A)-B(3A) 60.30(18)
B(2A)-B(1A)-B(3A) 59.56(18)
B(5A)#1-B(1A)-B(3A) 108.4(2)
B(4A)#1-B(1A)-B(6A) 108.1(2)
B(2A)-B(1A)-B(6A) 59.45(18)
B(5A)#1-B(1A)-B(6A) 59.45(18)
B(3A)-B(1A)-B(6A) 107.9(2)
B(4A)#1-B(1A)-Br(1A) 121.5(2)
B(2A)-B(1A)-Br(1A) 122.6(2)
B(5A)#1-B(1A)-Br(1A) 122.3(2)
B(3A)-B(1A)-Br(1A) 121.1(2)
B(6A)-B(1A)-Br(1A) 122.1(2)
B(5A)-B(2A)-B(3A) 60.76(18)
B(5A)-B(2A)-B(4A) 61.04(18)
B(3A)-B(2A)-B(4A) 110.2(2)
B(5A)-B(2A)-B(6A) 109.8(2)
B(3A)-B(2A)-B(6A) 109.9(2)
B(4A)-B(2A)-B(6A) 60.66(18)
B(5A)-B(2A)-B(1A) 109.5(2)
B(3A)-B(2A)-B(1A) 60.47(18)
B(4A)-B(2A)-B(1A) 110.0(2)
B(6A)-B(2A)-B(1A) 60.96(18)
B(5A)-B(2A)-Br(2A) 127.4(2)
B(3A)-B(2A)-Br(2A) 123.8(2)
B(4A)-B(2A)-Br(2A) 120.9(2)
B(6A)-B(2A)-Br(2A) 114.35(19)
B(1A)-B(2A)-Br(2A) 116.04(19)
B(2A)-B(3A)-B(6A)#1 106.8(2)
B(2A)-B(3A)-B(1A) 59.97(18)
B(6A)#1-B(3A)-B(1A) 107.8(2)
B(2A)-B(3A)-B(5A) 59.41(18)
B(6A)#1-B(3A)-B(5A) 59.80(18)

B(1A)-B(3A)-B(5A)	108.0(2)
B(2A)-B(3A)-B(4A)#1	107.0(2)
B(6A)#1-B(3A)-B(4A)#1	60.24(18)
B(1A)-B(3A)-B(4A)#1	59.56(18)
B(5A)-B(3A)-B(4A)#1	108.0(2)
B(2A)-B(3A)-Br(3A)	122.8(2)
B(6A)#1-B(3A)-Br(3A)	122.8(2)
B(1A)-B(3A)-Br(3A)	120.2(2)
B(5A)-B(3A)-Br(3A)	123.3(2)
B(4A)#1-B(3A)-Br(3A)	120.9(2)
B(2A)-B(4A)-B(1A)#1	106.8(2)
B(2A)-B(4A)-B(3A)#1	106.9(2)
B(1A)#1-B(4A)-B(3A)#1	60.14(18)
B(2A)-B(4A)-B(6A)	59.75(18)
B(1A)#1-B(4A)-B(6A)	107.8(2)
B(3A)#1-B(4A)-B(6A)	59.63(18)
B(2A)-B(4A)-B(5A)	59.22(18)
B(1A)#1-B(4A)-B(5A)	59.94(18)
B(3A)#1-B(4A)-B(5A)	107.8(2)
B(6A)-B(4A)-B(5A)	107.6(2)
B(2A)-B(4A)-Br(4A)	122.4(2)
B(1A)#1-B(4A)-Br(4A)	121.6(2)
B(3A)#1-B(4A)-Br(4A)	122.8(2)
B(6A)-B(4A)-Br(4A)	122.62(19)
B(5A)-B(4A)-Br(4A)	121.0(2)
B(2A)-B(5A)-B(6A)#1	107.2(2)
B(2A)-B(5A)-B(1A)#1	106.9(2)
B(6A)#1-B(5A)-B(1A)#1	60.78(18)
B(2A)-B(5A)-B(3A)	59.83(18)
B(6A)#1-B(5A)-B(3A)	59.91(18)
B(1A)#1-B(5A)-B(3A)	108.5(2)
B(2A)-B(5A)-B(4A)	59.74(18)
B(6A)#1-B(5A)-B(4A)	108.3(2)
B(1A)#1-B(5A)-B(4A)	59.49(18)

B(3A)-B(5A)-B(4A)	108.4(2)
B(2A)-B(5A)-Br(5A)	124.7(2)
B(6A)#1-B(5A)-Br(5A)	120.05(19)
B(1A)#1-B(5A)-Br(5A)	120.1(2)
B(3A)-B(5A)-Br(5A)	122.1(2)
B(4A)-B(5A)-Br(5A)	122.1(2)
B(2A)-B(6A)-B(5A)#1	107.0(2)
B(2A)-B(6A)-B(3A)#1	107.1(2)
B(5A)#1-B(6A)-B(3A)#1	60.28(18)
B(2A)-B(6A)-B(4A)	59.59(18)
B(5A)#1-B(6A)-B(4A)	108.3(2)
B(3A)#1-B(6A)-B(4A)	60.13(18)
B(2A)-B(6A)-B(1A)	59.59(18)
B(5A)#1-B(6A)-B(1A)	59.77(18)
B(3A)#1-B(6A)-B(1A)	108.0(2)
B(4A)-B(6A)-B(1A)	108.0(2)
B(2A)-B(6A)-Br(6A)	122.6(2)
B(5A)#1-B(6A)-Br(6A)	121.21(19)
B(3A)#1-B(6A)-Br(6A)	122.4(2)
B(4A)-B(6A)-Br(6A)	122.5(2)
B(1A)-B(6A)-Br(6A)	120.8(2)
C(5B)-Si(1B)-C(1B)	116.33(15)
C(5B)-Si(1B)-C(3B)	115.18(15)
C(1B)-Si(1B)-C(3B)	114.70(15)
C(5B)-Si(1B)-Br(2B)	106.31(11)
C(1B)-Si(1B)-Br(2B)	108.35(11)
C(3B)-Si(1B)-Br(2B)	92.55(11)
C(2B)-C(1B)-Si(1B)	116.4(2)
C(4B)-C(3B)-Si(1B)	109.3(2)
C(6B)-C(5B)-Si(1B)	116.8(2)
B(2B)-Br(2B)-Si(1B)	122.47(9)
B(4B)#2-B(1B)-B(2B)	107.0(2)
B(4B)#2-B(1B)-B(5B)#2	60.51(19)
B(2B)-B(1B)-B(5B)#2	107.1(2)

B(4B)#2-B(1B)-B(6B)	108.5(2)
B(2B)-B(1B)-B(6B)	59.29(18)
B(5B)#2-B(1B)-B(6B)	60.23(18)
B(4B)#2-B(1B)-B(3B)	59.61(18)
B(2B)-B(1B)-B(3B)	59.77(18)
B(5B)#2-B(1B)-B(3B)	108.1(2)
B(6B)-B(1B)-B(3B)	107.9(2)
B(4B)#2-B(1B)-Br(1B)	121.4(2)
B(2B)-B(1B)-Br(1B)	122.7(2)
B(5B)#2-B(1B)-Br(1B)	122.0(2)
B(6B)-B(1B)-Br(1B)	122.1(2)
B(3B)-B(1B)-Br(1B)	121.2(2)
B(4B)-B(2B)-B(6B)	61.01(18)
B(4B)-B(2B)-B(5B)	61.10(18)
B(6B)-B(2B)-B(5B)	110.4(2)
B(4B)-B(2B)-B(1B)	109.6(2)
B(6B)-B(2B)-B(1B)	60.54(18)
B(5B)-B(2B)-B(1B)	109.7(2)
B(4B)-B(2B)-B(3B)	109.6(2)
B(6B)-B(2B)-B(3B)	109.6(2)
B(5B)-B(2B)-B(3B)	60.49(18)
B(1B)-B(2B)-B(3B)	60.56(18)
B(4B)-B(2B)-Br(2B)	127.0(2)
B(6B)-B(2B)-Br(2B)	121.6(2)
B(5B)-B(2B)-Br(2B)	122.7(2)
B(1B)-B(2B)-Br(2B)	115.3(2)
B(3B)-B(2B)-Br(2B)	116.12(19)
B(4B)#2-B(3B)-B(6B)#2	60.51(18)
B(4B)#2-B(3B)-B(2B)	106.9(2)
B(6B)#2-B(3B)-B(2B)	107.0(2)
B(4B)#2-B(3B)-B(5B)	108.7(2)
B(6B)#2-B(3B)-B(5B)	60.34(18)
B(2B)-B(3B)-B(5B)	59.33(18)
B(4B)#2-B(3B)-B(1B)	59.63(18)

B(6B)#2-B(3B)-B(1B)	108.1(2)
B(2B)-B(3B)-B(1B)	59.67(18)
B(5B)-B(3B)-B(1B)	108.0(2)
B(4B)#2-B(3B)-Br(3B)	122.2(2)
B(6B)#2-B(3B)-Br(3B)	121.8(2)
B(2B)-B(3B)-Br(3B)	122.4(2)
B(5B)-B(3B)-Br(3B)	121.0(2)
B(1B)-B(3B)-Br(3B)	122.0(2)
B(2B)-B(4B)-B(3B)#2	107.0(2)
B(2B)-B(4B)-B(1B)#2	107.1(2)
B(3B)#2-B(4B)-B(1B)#2	60.76(19)
B(2B)-B(4B)-B(6B)	59.59(18)
B(3B)#2-B(4B)-B(6B)	59.75(18)
B(1B)#2-B(4B)-B(6B)	108.3(2)
B(2B)-B(4B)-B(5B)	59.61(18)
B(3B)#2-B(4B)-B(5B)	108.5(2)
B(1B)#2-B(4B)-B(5B)	59.92(18)
B(6B)-B(4B)-B(5B)	108.1(2)
B(2B)-B(4B)-Br(4B)	124.5(2)
B(3B)#2-B(4B)-Br(4B)	120.8(2)
B(1B)#2-B(4B)-Br(4B)	119.5(2)
B(6B)-B(4B)-Br(4B)	123.3(2)
B(5B)-B(4B)-Br(4B)	121.0(2)
B(2B)-B(5B)-B(1B)#2	106.6(2)
B(2B)-B(5B)-B(3B)	60.18(18)
B(1B)#2-B(5B)-B(3B)	107.6(2)
B(2B)-B(5B)-B(6B)#2	107.0(2)
B(1B)#2-B(5B)-B(6B)#2	60.01(18)
B(3B)-B(5B)-B(6B)#2	59.52(18)
B(2B)-B(5B)-B(4B)	59.30(18)
B(1B)#2-B(5B)-B(4B)	59.57(18)
B(3B)-B(5B)-B(4B)	107.9(2)
B(6B)#2-B(5B)-B(4B)	107.6(2)
B(2B)-B(5B)-Br(5B)	122.2(2)

B(1B)#2-B(5B)-Br(5B)	123.0(2)
B(3B)-B(5B)-Br(5B)	120.9(2)
B(6B)#2-B(5B)-Br(5B)	121.9(2)
B(4B)-B(5B)-Br(5B)	122.6(2)
B(2B)-B(6B)-B(3B)#2	106.9(2)
B(2B)-B(6B)-B(1B)	60.16(18)
B(3B)#2-B(6B)-B(1B)	107.9(2)
B(2B)-B(6B)-B(4B)	59.39(18)
B(3B)#2-B(6B)-B(4B)	59.73(18)
B(1B)-B(6B)-B(4B)	108.0(2)
B(2B)-B(6B)-B(5B)#2	107.4(2)
B(3B)#2-B(6B)-B(5B)#2	60.14(18)
B(1B)-B(6B)-B(5B)#2	59.76(18)
B(4B)-B(6B)-B(5B)#2	107.9(2)
B(2B)-B(6B)-Br(6B)	123.0(2)
B(3B)#2-B(6B)-Br(6B)	121.9(2)
B(1B)-B(6B)-Br(6B)	121.3(2)
B(4B)-B(6B)-Br(6B)	122.4(2)
B(5B)#2-B(6B)-Br(6B)	121.2(2)
C(6S)-C(1S)-C(2S)	120.3(3)
C(6S)-C(1S)-Cl(1)	121.7(3)
C(2S)-C(1S)-Cl(1)	118.0(3)
C(1S)-C(2S)-C(3S)	119.5(4)
C(4S)-C(3S)-C(2S)	120.6(4)
C(3S)-C(4S)-C(5S)	119.9(4)
C(4S)-C(5S)-C(6S)	119.6(4)
C(1S)-C(6S)-C(5S)	120.1(4)
C(1S)-C(6S)-Cl(2)	121.0(3)
C(5S)-C(6S)-Cl(2)	118.9(3)

Symmetry transformations used to generate equivalent atoms: #1 -x,-y+2,-z+1 #2 -x+1,-y+1,-z+1

C.2.4 Anisotropic Displacement Parameters

Anisotropic displacement parameters for $((C_2H_5)_3Si)_2(B_{12}Br_{12})\cdot ODCB$ ($Å^2 x\ 10^3$). The anisotropic displacement factor exponent takes the form: $-2p^2[h^2a^{*2}U^{11} + ... + 2\ h\ k\ a^*\ b^*\ U^{12}\ ]$

	U^{11}	U^{22}	U^{33}	U^{23}	U^{13}	U^{12}
Si(1A)	14(1)	11(1)	15(1)	-2(1)	5(1)	1(1)
C(1A)	17(2)	14(2)	20(2)	2(1)	3(1)	1(1)
C(2A)	30(2)	16(2)	20(2)	2(1)	7(1)	-3(1)
C(3A)	19(2)	15(2)	22(2)	-4(1)	8(1)	-2(1)
C(4A)	28(2)	19(2)	30(2)	-11(2)	13(2)	-3(1)
C(5A)	19(2)	19(2)	17(2)	0(1)	7(1)	-4(1)
C(6A)	39(2)	30(2)	20(2)	1(2)	10(2)	-5(2)
Br(1A)	14(1)	16(1)	13(1)	-2(1)	1(1)	0(1)
Br(2A)	11(1)	10(1)	18(1)	-5(1)	4(1)	0(1)
Br(3A)	20(1)	20(1)	18(1)	0(1)	10(1)	-1(1)
Br(4A)	22(1)	10(1)	16(1)	3(1)	5(1)	0(1)
Br(5A)	11(1)	16(1)	20(1)	-4(1)	4(1)	2(1)
Br(6A)	13(1)	12(1)	22(1)	-3(1)	8(1)	-5(1)
B(1A)	12(2)	10(2)	12(2)	0(1)	4(1)	-1(1)
B(2A)	12(1)	8(2)	11(2)	-3(1)	4(1)	-1(1)
B(3A)	12(2)	10(2)	13(2)	-1(1)	5(1)	-2(1)
B(4A)	12(1)	7(1)	12(2)	2(1)	3(1)	-1(1)
B(5A)	10(1)	11(2)	14(2)	1(1)	4(1)	0(1)
B(6A)	12(1)	9(2)	12(2)	-2(1)	4(1)	-1(1)
Si(1B)	15(1)	18(1)	13(1)	-1(1)	3(1)	1(1)
C(1B)	17(2)	21(2)	20(2)	2(1)	4(1)	2(1)
C(2B)	34(2)	22(2)	27(2)	2(2)	12(2)	0(2)
C(3B)	22(2)	24(2)	16(2)	-2(1)	7(1)	1(1)
C(4B)	34(2)	32(2)	16(2)	0(2)	5(2)	5(2)
C(5B)	19(2)	21(2)	22(2)	-3(1)	6(1)	0(1)

C(6B)	31(2)	21(2)	28(2)	-4(2)	10(2)	3(1)
Br(1B)	13(1)	18(1)	20(1)	1(1)	8(1)	-4(1)
Br(2B)	12(1)	22(1)	11(1)	0(1)	4(1)	1(1)
Br(3B)	13(1)	17(1)	18(1)	-1(1)	6(1)	4(1)
Br(4B)	10(1)	25(1)	15(1)	-1(1)	2(1)	1(1)

	U^{11}	U^{22}	U^{33}	U^{23}	U^{13}	U^{12}
Br(5B)	20(1)	16(1)	24(1)	-6(1)	8(1)	-4(1)
Br(6B)	24(1)	18(1)	22(1)	6(1)	9(1)	4(1)
B(1B)	11(2)	13(2)	15(2)	2(1)	4(1)	-1(1)
B(2B)	10(1)	15(2)	11(2)	-1(1)	2(1)	-1(1)
B(3B)	9(1)	12(2)	13(2)	-1(1)	3(1)	-1(1)
B(4B)	10(2)	13(2)	13(2)	0(1)	3(1)	1(1)
B(5B)	11(1)	13(2)	13(2)	-3(1)	6(1)	-2(1)
B(6B)	14(2)	9(2)	13(2)	2(1)	5(1)	1(1)
C(1S)	19(2)	27(2)	32(2)	14(2)	2(1)	-2(1)
C(2S)	23(2)	28(2)	37(2)	0(2)	8(2)	-1(2)
C(3S)	27(2)	38(2)	28(2)	5(2)	9(2)	1(2)
C(4S)	28(2)	33(2)	29(2)	13(2)	9(2)	5(2)
C(5S)	33(2)	31(2)	33(2)	2(2)	7(2)	5(2)
C(6S)	28(2)	37(2)	22(2)	2(2)	4(2)	-1(2)
Cl(1)	39(1)	40(1)	45(1)	24(1)	-1(1)	2(1)
Cl(2)	73(1)	72(1)	25(1)	-4(1)	3(1)	10(1)

C.2.5 Hydrogen Coordinates

Hydrogen coordinates (x 10^4) and isotropic displacement parameters (Å^{2}x 10^3).

	x	y	z	U(eq)
H(1A1)	1992	5351	4898	22

H(1A2)	1682	6378	5214	22
H(2A1)	658	5316	5298	34
H(2A2)	1439	4594	5625	34
H(2A3)	845	4313	4876	34
H(3A1)	-25	4863	3678	22
H(3A2)	21	5530	3033	22
H(4A1)	1205	4571	3138	37
H(4A2)	531	3673	3061	37
H(4A3)	1177	3922	3792	37
H(5A)	1975	7522	3894	22
H(6A1)	1000	6657	2649	44
H(6A2)	1362	7889	2717	44
H(6A3)	542	7694	2811	44
H(1B1)	2952	6140	1825	24
H(1B2)	3371	6272	2626	24
H(2B1)	4347	7389	2474	41
H(2B2)	3509	7908	2050	41
H(2B3)	3976	7209	1670	41
H(3B1)	4979	5585	1820	25
H(3B2)	5007	4244	1837	25
H(4B1)	3842	4174	854	42
H(4B2)	4486	4897	686	42
H(4B3)	3792	5511	842	42
H(5B1)	3271	3565	2564	25
H(5B2)	2990	3595	1756	25
H(6B1)	4105	2489	1819	40
H(6B2)	3535	1850	2123	40
H(6B3)	4326	2405	2623	40
H(2S)	2357	2111	3832	36
H(3S)	2969	791	4669	37
H(4S)	3258	-974	4373	37
H(5S)	2901	-1463	3229	41

C.3 References

1. Bruker (2005). APEX 2 version 2.0-2. Bruker AXS Inc., Madison, Wisconsin, U.S.A.

2 Bruker (2005). SAINT version V7.21A. Bruker AXS Inc., Madison, Wisconsin, USA.

3 Bruker (2004). SADABS version 2004/1. Bruker Analytical X-Ray System, Inc., Madison, Wisconsin, USA.

4 Altomare, A., Burla, M.C., Carnalli, M. Cascarano, G. Giacovazzo, C., Guagliardi, A.; Moliterni, A.G.G.; Polidori, G. Spagan, R. SIR 97 (1999) J. Appl. Cryst. 32, 115-122.

5 Bruker (2003). SHELXTL Software Version 6.14, Dec, Bruker Analytical X-Ray System, Inc.,Madison, Wisconsin, USA.

6 WinGX - L. J. Farrugia (1999) J. Appl. Cryst. 32, 837 -838.

7 ORTEP3 for Windows - L. J. Farrugia, J. Appl. Crystallogr. 1997, 30, 565.

Appendix D. X-Ray Structure Determination for $((C_2H_5)_3Si)_2(B_{12}Cl_2)$

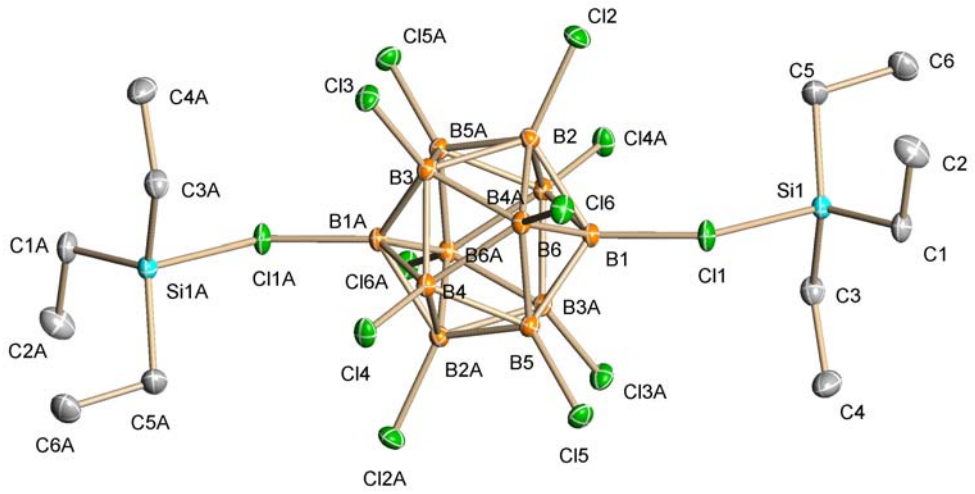

D.1 Experimental Details

A colorless prism fragment (0.41 x 0.25 x 0.09 mm^3) was used for the single crystal x-ray diffraction study of $[[C_2H_5]_3Si]^+_2[B_{12}Cl_{12}]^{2-}$ (sample cr306_0m). The crystal was coated with paratone oil and mounted on to a cryo-loop glass fiber. X-ray intensity data were collected at 100(2) K on a Bruker APEX2 (version 2.0-22) platform-CCD x-ray diffractometer system (Mo-radiation, λ = 0.71073 Å, 50KV/40mA power).[1] The CCD detector was placed at a distance of 5.0375 cm from the crystal.

A total of 3600 frames were collected for a sphere of reflections (with scan width of 0.3° in ω, starting ω and 2θ angles at –30°, and ϕ angles of 0°, 90°, 120°, 180°, 240°, and 270° for every 600 frames, 20 sec/frame exposure time). The frames were integrated using the Bruker SAINT software package (version V7.23A) and using a narrow-frame integration algorithm.[2] Based on a monoclinic crystal system, the integrated frames yielded a total of 39414 reflections at a maximum 2θ angle of 61.02° (0.70 Å resolution),

of which 5118 were independent reflections (R_{int} = 0.0239, R_{sig} = 0.0129, redundancy = 7.7, completeness = 99.9%) and 4757 (92.9%) reflections were greater than 2σ(I). The unit cell parameters were, **a** = 9.1338(7) Å, **b** = 19.3255(14) Å, **c** = 9.5172(7) Å, **β** = 93.0356(10)°**,** V = 1677.6(2) $Å^3$, Z = 2, calculated density D_c = 1.555 g/cm^3. Absorption corrections were applied (absorption coefficient μ = 1.072 mm^{-1}; max/min transmission = 0.9087/0.6676) to the raw intensity data using the SADABS program (version 2004/1).[3]

The Bruker SHELXTL software package (Version 6.14) was used for phase determination and structure refinement.[4] The distribution of intensities (E^2-1 = 0.939) and systematic absent reflections indicated two possible space groups, P2(1)/n. The space group P2(1)/n (#14) was later determined to be correct. Direct methods of phase determination followed by two Fourier cycles of refinement led to an electron density map from which most of the non-hydrogen atoms were identified in the asymmetry unit of the unit cell. With subsequent isotropic refinement, all of the non-hydrogen atoms were identified. There was one cation of $[[C_2H_5]_3Si]^+$, and half an anion of $[B_{12}Cl_{12}]^-$ present in the asymmetry unit of the unit cell.

Atomic coordinates, isotropic and anisotropic displacement parameters of all the non-hydrogen atoms were refined by means of a full matrix least-squares procedure on F^2. The H-atoms were included in the refinement in calculated positions riding on the atoms to which they were attached. The refinement converged at R1 = 0.0181, wR2 = 0.0495, with intensity I>2σ (I). The largest peak/hole in the final difference map was 0.481/-0.283 e/$Å^3$.

D.2 Structure Data

D.2.1 Crystal data and structure refinement for $((C_2H_5)_3Si)_2(B_{12}Cl_{12})$

Identification code	cr306_0m	
Empirical formula	C12 H30 B12 Cl12 Si2	
Formula weight	785.66	
Temperature	100(2) K	
Wavelength	0.71073 Å	
Crystal system	Monoclinic (#14)	
Space group	P2(1)/n	
Unit cell dimensions	a = 9.1338(7) Å	α = 90°.
	b = 19.3255(14) Å	β = 93.0356(10)°.
	c = 9.5172(7) Å	γ = 90°.
Volume	1677.6(2) $Å^3$	
Z	2	
Density (calculated)	1.555 Mg/m^3	
Absorption coefficient	1.072 mm^{-1}	
F(000)	788	
Crystal size	0.41 x 0.25 x 0.09 mm^3	
Theta range for data collection	2.11 to 30.51°.	
Index ranges	-12<=h<=13, -27<=k<=27, -13<=l<=13	
Reflections collected	39414	
Independent reflections	5118 [R(int) = 0.0239]	
Completeness to theta = 30.51°	99.9 %	
Absorption correction	Semi-empirical from equivalents	
Max. and min. transmission	0.9087 and 0.6676	
Refinement method	Full-matrix least-squares on F^2	
Data / restraints / parameters	5118 / 0 / 175	
Goodness-of-fit on F^2	1.052	
Final R indices [I>2sigma(I)]	R1 = 0.0181, wR2 = 0.0495	
R indices (all data)	R1 = 0.0202, wR2 = 0.0508	
Largest diff. peak and hole	0.481 and -0.283 $e.Å^{-3}$	

D.2.2 Atomic Coordinates

Atomic coordinates (x 10^4) and equivalent isotropic displacement parameters ($Å^2$x 10^3) for $((C_2H_5)_3Si)_2(B_{12}Cl_{12})$. U(eq) is defined as one third of the trace of the orthogonalized U^{ij} tensor.

	x	y	z	U(eq)
B(1)	1438(1)	355(1)	864(1)	11(1)
B(2)	302(1)	-238(1)	1727(1)	11(1)
B(3)	-380(1)	-835(1)	414(1)	11(1)
B(4)	364(1)	-610(1)	-1238(1)	11(1)
B(5)	1508(1)	135(1)	-950(1)	12(1)
B(6)	1459(1)	-531(1)	368(1)	11(1)
Cl(1)	3177(1)	650(1)	1740(1)	15(1)
Cl(2)	628(1)	-481(1)	3513(1)	18(1)
Cl(3)	-763(1)	-1708(1)	869(1)	16(1)
Cl(4)	743(1)	-1259(1)	-2501(1)	16(1)
Cl(5)	3114(1)	291(1)	-1882(1)	16(1)
Cl(6)	3015(1)	-1070(1)	749(1)	15(1)
Si(1)	3505(1)	1610(1)	3169(1)	13(1)
C(1)	5501(1)	1452(1)	3418(1)	17(1)
C(2)	5913(1)	882(1)	4486(1)	26(1)
C(3)	2926(1)	2339(1)	2026(1)	18(1)
C(4)	3889(1)	2476(1)	786(1)	26(1)
C(5)	2501(1)	1465(1)	4771(1)	21(1)
C(6)	3058(1)	1990(1)	5901(1)	25(1)

D.2.3 Bond Lengths and Angles

Bond lengths [Å] and angles [°] for $((C_2H_5)_3Si)_2(B_{12}Cl_{12})$

B(1)-B(4)#1	1.7725(14)

B(1)-B(3)#1	1.7750(13)
B(1)-B(2)	1.7761(14)
B(1)-B(6)	1.7772(13)
B(1)-B(5)	1.7818(14)
B(1)-Cl(1)	1.8451(10)
B(2)-Cl(2)	1.7739(10)
B(2)-B(5)#1	1.7861(14)
B(2)-B(3)	1.7883(14)
B(2)-B(4)#1	1.8007(14)
B(2)-B(6)	1.8043(14)
B(3)-B(1)#1	1.7750(13)
B(3)-Cl(3)	1.7800(10)
B(3)-B(6)	1.7817(14)
B(3)-B(5)#1	1.7914(14)
B(3)-B(4)	1.7994(14)
B(4)-B(1)#1	1.7725(14)
B(4)-Cl(4)	1.7827(10)
B(4)-B(6)	1.7882(14)
B(4)-B(5)	1.7916(14)
B(4)-B(2)#1	1.8007(14)
B(5)-Cl(5)	1.7796(10)
B(5)-B(2)#1	1.7861(14)
B(5)-B(3)#1	1.7914(14)
B(5)-B(6)	1.7999(14)
B(6)-Cl(6)	1.7832(10)
Cl(1)-Si(1)	2.3109(3)
Si(1)-C(3)	1.8402(10)
Si(1)-C(5)	1.8421(10)
Si(1)-C(1)	1.8516(10)
C(1)-C(2)	1.5327(15)
C(1)-H(1A)	0.9900
C(1)-H(1B)	0.9900
C(2)-H(2A)	0.9800
C(2)-H(2B)	0.9800

C(2)-H(2C)	0.9800
C(3)-C(4)	1.5316(15)
C(3)-H(3A)	0.9900
C(3)-H(3B)	0.9900
C(4)-H(4A)	0.9800
C(4)-H(4B)	0.9800
C(4)-H(4C)	0.9800
C(5)-C(6)	1.5446(14)
C(5)-H(5A)	0.9900
C(5)-H(5B)	0.9900
C(6)-H(6A)	0.9800
C(6)-H(6B)	0.9800
C(6)-H(6C)	0.9800

B(4)#1-B(1)-B(3)#1	60.96(5)
B(4)#1-B(1)-B(2)	60.99(5)
B(3)#1-B(1)-B(2)	110.13(7)
B(4)#1-B(1)-B(6)	110.16(7)
B(3)#1-B(1)-B(6)	109.60(7)
B(2)-B(1)-B(6)	61.03(5)
B(4)#1-B(1)-B(5)	110.04(7)
B(3)#1-B(1)-B(5)	60.48(5)
B(2)-B(1)-B(5)	110.24(7)
B(6)-B(1)-B(5)	60.76(5)
B(4)#1-B(1)-Cl(1)	127.58(6)
B(3)#1-B(1)-Cl(1)	124.96(6)
B(2)-B(1)-Cl(1)	120.01(6)
B(6)-B(1)-Cl(1)	113.35(6)
B(5)-B(1)-Cl(1)	115.92(6)
Cl(2)-B(2)-B(1)	122.79(6)
Cl(2)-B(2)-B(5)#1	122.09(6)
B(1)-B(2)-B(5)#1	106.69(7)
Cl(2)-B(2)-B(3)	122.22(6)
B(1)-B(2)-B(3)	106.48(7)

B(5)#1-B(2)-B(3)	60.15(5)
Cl(2)-B(2)-B(4)#1	121.73(6)
B(1)-B(2)-B(4)#1	59.41(5)
B(5)#1-B(2)-B(4)#1	59.93(5)
B(3)-B(2)-B(4)#1	107.86(6)
Cl(2)-B(2)-B(6)	121.91(6)
B(1)-B(2)-B(6)	59.51(5)
B(5)#1-B(2)-B(6)	107.62(6)
B(3)-B(2)-B(6)	59.46(5)
B(4)#1-B(2)-B(6)	107.68(6)
B(1)#1-B(3)-Cl(3)	123.72(6)
B(1)#1-B(3)-B(6)	106.88(7)
Cl(3)-B(3)-B(6)	121.05(6)
B(1)#1-B(3)-B(2)	107.33(6)
Cl(3)-B(3)-B(2)	120.48(6)
B(6)-B(3)-B(2)	60.72(5)
B(1)#1-B(3)-B(5)#1	59.95(5)
Cl(3)-B(3)-B(5)#1	121.53(6)
B(6)-B(3)-B(5)#1	108.38(6)
B(2)-B(3)-B(5)#1	59.86(5)
B(1)#1-B(3)-B(4)	59.45(5)
Cl(3)-B(3)-B(4)	121.99(6)
B(6)-B(3)-B(4)	59.91(5)
B(2)-B(3)-B(4)	108.71(6)
B(5)#1-B(3)-B(4)	108.39(6)
B(1)#1-B(4)-Cl(4)	123.12(6)
B(1)#1-B(4)-B(6)	106.71(7)
Cl(4)-B(4)-B(6)	121.10(6)
B(1)#1-B(4)-B(5)	106.61(6)
Cl(4)-B(4)-B(5)	122.40(6)
B(6)-B(4)-B(5)	60.37(5)
B(1)#1-B(4)-B(3)	59.59(5)
Cl(4)-B(4)-B(3)	121.00(6)
B(6)-B(4)-B(3)	59.55(5)

B(5)-B(4)-B(3)	107.73(6)
B(1)#1-B(4)-B(2)#1	59.61(5)
Cl(4)-B(4)-B(2)#1	122.72(6)
B(6)-B(4)-B(2)#1	108.02(6)
B(5)-B(4)-B(2)#1	59.63(5)
B(3)-B(4)-B(2)#1	107.93(6)
Cl(5)-B(5)-B(1)	121.03(6)
Cl(5)-B(5)-B(2)#1	122.95(6)
B(1)-B(5)-B(2)#1	107.13(7)
Cl(5)-B(5)-B(3)#1	121.05(6)
B(1)-B(5)-B(3)#1	59.57(5)
B(2)#1-B(5)-B(3)#1	59.98(5)
Cl(5)-B(5)-B(4)	123.29(6)
B(1)-B(5)-B(4)	106.83(7)
B(2)#1-B(5)-B(4)	60.44(5)
B(3)#1-B(5)-B(4)	108.13(7)
Cl(5)-B(5)-B(6)	121.34(6)
B(1)-B(5)-B(6)	59.49(5)
B(2)#1-B(5)-B(6)	108.15(7)
B(3)#1-B(5)-B(6)	107.84(7)
B(4)-B(5)-B(6)	59.72(5)
B(1)-B(6)-B(3)	106.72(7)
B(1)-B(6)-Cl(6)	121.88(6)
B(3)-B(6)-Cl(6)	123.02(6)
B(1)-B(6)-B(4)	107.18(6)
B(3)-B(6)-B(4)	60.54(5)
Cl(6)-B(6)-B(4)	121.85(6)
B(1)-B(6)-B(5)	59.75(5)
B(3)-B(6)-B(5)	108.15(7)
Cl(6)-B(6)-B(5)	120.66(6)
B(4)-B(6)-B(5)	59.91(5)
B(1)-B(6)-B(2)	59.46(5)
B(3)-B(6)-B(2)	59.82(5)
Cl(6)-B(6)-B(2)	121.92(6)

B(4)-B(6)-B(2)	108.50(6)
B(5)-B(6)-B(2)	108.16(6)
B(1)-Cl(1)-Si(1)	126.55(3)
C(3)-Si(1)-C(5)	117.74(5)
C(3)-Si(1)-C(1)	116.88(5)
C(5)-Si(1)-C(1)	113.52(5)
C(3)-Si(1)-Cl(1)	104.04(3)
C(5)-Si(1)-Cl(1)	108.09(4)
C(1)-Si(1)-Cl(1)	92.25(3)
C(2)-C(1)-Si(1)	114.11(7)
C(2)-C(1)-H(1A)	108.7
Si(1)-C(1)-H(1A)	108.7
C(2)-C(1)-H(1B)	108.7
Si(1)-C(1)-H(1B)	108.7
H(1A)-C(1)-H(1B)	107.6
C(1)-C(2)-H(2A)	109.5
C(1)-C(2)-H(2B)	109.5
H(2A)-C(2)-H(2B)	109.5
C(1)-C(2)-H(2C)	109.5
H(2A)-C(2)-H(2C)	109.5
H(2B)-C(2)-H(2C)	109.5
C(4)-C(3)-Si(1)	115.40(7)
C(4)-C(3)-H(3A)	108.4
Si(1)-C(3)-H(3A)	108.4
C(4)-C(3)-H(3B)	108.4
Si(1)-C(3)-H(3B)	108.4
H(3A)-C(3)-H(3B)	107.5
C(3)-C(4)-H(4A)	109.5
C(3)-C(4)-H(4B)	109.5
H(4A)-C(4)-H(4B)	109.5
C(3)-C(4)-H(4C)	109.5
H(4A)-C(4)-H(4C)	109.5
H(4B)-C(4)-H(4C)	109.5
C(6)-C(5)-Si(1)	108.45(7)

C(6)-C(5)-H(5A)	110.0
Si(1)-C(5)-H(5A)	110.0
C(6)-C(5)-H(5B)	110.0
Si(1)-C(5)-H(5B)	110.0
H(5A)-C(5)-H(5B)	108.4
C(5)-C(6)-H(6A)	109.5
C(5)-C(6)-H(6B)	109.5
H(6A)-C(6)-H(6B)	109.5
C(5)-C(6)-H(6C)	109.5
H(6A)-C(6)-H(6C)	109.5
H(6B)-C(6)-H(6C)	109.5

Symmetry transformations used to generate equivalent atoms:
#1 -x,-y,-z

D.2.4 Anisotropic Displacement Parameters

Anisotropic displacement parameters ($Å^2 x\ 10^3$) for $((C_2H_5)_3Si)_2(B_{12}Cl_{12})$. The anisotropic displacement factor exponent takes the form: $-2p^2[\ h^2a^{*2}U^{11} + ... + 2\ h\ k\ a^*\ b^*\ U^{12}\ ]$

	U^{11}	U^{22}	U^{33}	U^{23}	U^{13}	U^{12}
B(1)	9(1)	10(1)	12(1)	-1(1)	-2(1)	0(1)
B(2)	11(1)	12(1)	11(1)	0(1)	-1(1)	0(1)
B(3)	11(1)	9(1)	14(1)	0(1)	0(1)	0(1)
B(4)	10(1)	11(1)	13(1)	-2(1)	0(1)	1(1)
B(5)	10(1)	12(1)	13(1)	0(1)	1(1)	0(1)
B(6)	10(1)	10(1)	13(1)	0(1)	-1(1)	1(1)
Cl(1)	10(1)	14(1)	20(1)	-5(1)	-3(1)	0(1)
Cl(2)	19(1)	23(1)	12(1)	3(1)	-2(1)	0(1)
Cl(3)	17(1)	11(1)	20(1)	2(1)	-1(1)	-1(1)
Cl(4)	14(1)	16(1)	18(1)	-7(1)	1(1)	1(1)
Cl(5)	12(1)	19(1)	18(1)	0(1)	5(1)	-1(1)

Cl(6)	11(1)	13(1)	22(1)	1(1)	-2(1)	3(1)
Si(1)	12(1)	13(1)	13(1)	-1(1)	0(1)	-1(1)
C(1)	13(1)	16(1)	22(1)	-2(1)	-3(1)	-1(1)
C(2)	26(1)	31(1)	22(1)	1(1)	-2(1)	11(1)
C(3)	18(1)	14(1)	21(1)	0(1)	-3(1)	0(1)
C(4)	24(1)	29(1)	25(1)	9(1)	-2(1)	-7(1)
C(5)	19(1)	26(1)	16(1)	-2(1)	3(1)	-5(1)
C(6)	26(1)	31(1)	18(1)	-6(1)	4(1)	-1(1)

D.2.5 Hydrogen Coordinates

Hydrogen coordinates (x 10^4) and isotropic displacement parameters (Å^{2}x 10^3) for $((C_2H_5)_3Si)_2(B_{12}Cl_{12})$.

	x	y	z	U(eq)
H(1A)	5887	1325	2500	21
H(1B)	5987	1888	3733	21
H(2A)	5616	1021	5419	40
H(2B)	6975	807	4518	40
H(2C)	5410	452	4204	40
H(3A)	1912	2251	1650	21
H(3B)	2906	2763	2608	21
H(4A)	4894	2575	1142	39
H(4B)	3502	2873	246	39
H(4C)	3888	2067	177	39
H(5A)	1436	1529	4563	25
H(5B)	2667	987	5117	25
H(6A)	4120	1936	6072	37
H(6B)	2569	1905	6777	37
H(6C)	2840	2461	5572	37

D.3 References

1. *APEX 2,* version 2.0-22, Bruker (2004), Bruker AXS Inc., Madison, Wisconsin, USA.

2. *SAINT,* version V7.23A, Bruker (2003), Bruker AXS Inc., Madison, Wisconsin, USA.

3. *SADABS,* version 2004/1, Bruker (2004), Bruker AXS Inc., Madison, Wisconsin, USA.

4. *SHELXTL,* version 6.14, Bruker (2003), Bruker AXS Inc., Madison, Wisconsin, USA.

Appendix E. X-Ray Structure Determination for $[H(C_4H_8O)_2[B_{12}Br_{12}]\cdot C_6H_6$

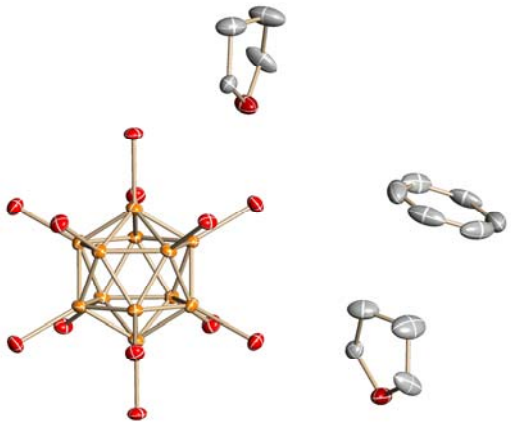

E.1 Experimental Details

A brown prism fragment (0.10 x 0.09 x 0.08 mm^3) was used for the single crystal x-ray diffraction study of $[C_4H_8OH]^+_2[B_{12}Br_{12}]^{-2}$ (sample cr317_0m-4). The crystal was coated with paratone oil and mounted on to a cryo-loop glass fiber. X-ray intensity data were collected at 100(2) K on a Bruker APEX2 (**ref. 1**) platform-CCD x-ray diffractometer system (Mo-radiation, λ = 0.71073 Å, 50 KV and 40 mA power). The CCD detector was placed at a distance of 5.0550 cm from the crystal.

A total of 2400 frames were collected for a hemisphere of reflections (with scan width of 0.3° in ω, starting ω and 2θ angles at –30°, and ϕ angles of 0°, 90°, 180°, and 270° for every 600 frames, 40 sec/frame exposure time). The frames were integrated using the Bruker SAINT software package (**ref. 2**) and using a narrow-frame integration algorithm. Based on a monoclinic crystal system, the integrated frames yielded a total of 12357 reflections at a maximum 2θ angle of 60.06° (0.71 Å resolution), of which 5244 were independent reflections (R_{int} = 0.0431, R_{sig} = 0.0274, redundancy = 2.4,

completeness = 100%) and 4233 (80.7%) reflections were greater than 2σ(I). The unit cell parameters were, **a** = 17.0638(9) Å, **b** = 12.0666(7) Å, **c** = 18.5359(10) Å, **β** = 110.2597(8)°**,** V = 3580.5(3) $Å^3$, Z = 4, calculated density D_c = 2.436 g/cm^3. Absorption corrections were applied (absorption coefficient μ = 13.442 mm^{-1}; max/min transmission = 0.4127/0.3467) to the raw intensity data using the SADABS program (**ref. 3**).

The Bruker SHELXTL software package (**ref. 4**) was used for phase determination and structure refinement. The distribution of intensities (E^2-1 = 0.940) and systematic absent reflections indicated two possible space groups, I2/a and Ia. The space group I2/a (#15) was later determined to be correct. Direct methods of phase determination followed by two Fourier cycles of refinement led to an electron density map from which most of the non-hydrogen atoms were identified in the asymmetry unit of the unit cell. With subsequent isotropic refinement, all of the non-hydrogen atoms were identified. There were one disordered cation of $[C_4H_8OH]^+$, half an anion of $[B_{12}Br_{12}]^{2-}$, and half a benzene solvent molecule present in the asymmetry unit of the unit cell. The cation disordered, C4/C4D, site occupancy factor ratio was 81%/19%. The possible O-H…Br hydrogen bonding distances and angles were given in Table 7.

Atomic coordinates, isotropic and anisotropic displacement parameters of all the non-hydrogen atoms were refined by means of a full matrix least-squares procedure on F^2. The H-atoms not involved in hydrogen bonding were included in the refinement in calculated positions riding on the atoms to which they were attached. The refinement converged at R1 = 0.0318, wR2 = 0.0696, with intensity I>2σ (I). The largest peak/hole in the final difference map was 1.099/-0.719 e/$Å^3$.

E.2 Structure Data

E.2.1 Crystal structure and refinement data for $[H(C_4H_8O)_2[B_{12}Br_{12}]\cdot C_6H_6$

Identification code	cr317_0m-4	
Empirical formula	C14 H24 B12 Br12 O2	
Formula weight	1312.97	
Temperature	100(2) K	
Wavelength	0.71073 Å	
Crystal system	Monoclinic	
Space group	I2/a	
Unit cell dimensions	a = 17.0638(9) Å	a= 90°.
	b = 12.0666(7) Å	b= 110.2597(8)°.
	c = 18.5359(10) Å	g = 90°.
Volume	3580.5(3) $Å^3$	
Z	4	
Density (calculated)	2.436 Mg/m^3	
Absorption coefficient	13.442 mm^{-1}	
F(000)	2416	
Crystal size	0.10 x 0.09 x 0.08 mm^3	
Theta range for data collection	2.05 to 30.03°.	
Index ranges	-24<=h<=22, 0<=k<=16, 0<=l<=26	
Reflections collected	12357	
Independent reflections	5244 [R(int) = 0.0431]	
Completeness to theta = 30.03°	100.0 %	
Absorption correction	Semi-empirical from equivalents	
Max. and min. transmission	0.4127 and 0.3467	
Refinement method	Full-matrix least-squares on F^2	
Data / restraints / parameters	5244 / 69 / 194	
Goodness-of-fit on F^2	1.061	
Final R indices [I>2sigma(I)]	R1 = 0.0318, wR2 = 0.0696	
R indices (all data)	R1 = 0.0467, wR2 = 0.0735	
Largest diff. peak and hole	1.099 and -0.719 $e.Å^{-3}$	

E.2.2 Atomic Coordinates

Atomic coordinates (x 10^4) and equivalent isotropic displacement parameters ($Å^2$x 10^3) for $[H(C_4H_8O]_2[B_{12}Br_{12}]\cdot C_6H_6$. U(eq) is defined as one third of the trace of the orthogonalized U^{ij} tensor.

	x	y	z	U(eq)
B(1)	7916(2)	7836(3)	1821(2)	18(1)
B(2)	7146(2)	6767(3)	1664(2)	15(1)
B(3)	6477(2)	7134(3)	2182(2)	15(1)
B(4)	6828(2)	8427(3)	2646(2)	15(1)
B(5)	7710(2)	8864(3)	2424(2)	16(1)
B(6)	6867(2)	8185(3)	1709(2)	18(1)
Br(1)	8394(1)	8198(1)	1036(1)	21(1)
Br(2)	6770(1)	5920(1)	716(1)	23(1)
Br(3)	5302(1)	6717(1)	1827(1)	22(1)
Br(4)	6042(1)	9476(1)	2824(1)	21(1)
Br(5)	7947(1)	10425(1)	2333(1)	22(1)
Br(6)	6148(1)	8983(1)	811(1)	22(1)
O(1)	9730(2)	2144(3)	3360(2)	33(1)
C(2)	9838(2)	1321(3)	3999(2)	26(1)
C(3)	9425(3)	1862(4)	4497(3)	43(1)
C(5)	9233(3)	3113(4)	3467(3)	47(1)
C(4)	8820(4)	2649(5)	3991(4)	37(2)
C(4D)	9210(19)	3024(10)	4252(8)	41(5)
C(6)	7807(3)	1728(4)	5352(3)	45(1)
C(7)	8116(3)	2694(5)	5705(3)	47(1)
C(8)	7819(3)	3682(4)	5357(3)	53(2)

E.2.3 Bond Lengths and Angles

Bond lengths [Å] and angles [°] for $[H(C_4H_8O]_2[B_{12}Br_{12}]\cdot C_6H_6$.

B(1)-B(3)#1	1.778(5)
B(1)-B(6)	1.779(5)
B(1)-B(5)	1.784(5)
B(1)-B(4)#1	1.785(5)
B(1)-B(2)	1.791(5)
B(1)-Br(1)	1.950(4)
B(2)-B(3)	1.784(5)
B(2)-B(6)	1.786(5)
B(2)-B(4)#1	1.789(5)
B(2)-B(5)#1	1.791(5)
B(2)-Br(2)	1.941(4)
B(3)-B(1)#1	1.778(5)
B(3)-B(4)	1.781(5)
B(3)-B(5)#1	1.791(5)
B(3)-B(6)	1.795(5)
B(3)-Br(3)	1.947(4)
B(4)-B(5)	1.773(5)
B(4)-B(1)#1	1.785(5)
B(4)-B(6)	1.786(5)
B(4)-B(2)#1	1.789(5)
B(4)-Br(4)	1.953(4)
B(5)-B(6)	1.783(5)
B(5)-B(2)#1	1.791(5)
B(5)-B(3)#1	1.791(5)
B(5)-Br(5)	1.946(4)
B(6)-Br(6)	1.947(4)
O(1)-C(5)	1.497(5)
O(1)-C(2)	1.508(5)
O(1)-H(1)	1.05(5)

C(2)-C(3)	1.491(5)
C(2)-H(2A)	0.9900
C(2)-H(2B)	0.9900
C(3)-C(4)	1.475(6)
C(3)-C(4D)	1.481(9)
C(3)-H(3A)	0.9900
C(3)-H(3B)	0.9900
C(3)-H(3C)	0.9885
C(3)-H(3D)	0.9889
C(5)-C(4D)	1.474(9)
C(5)-C(4)	1.494(6)
C(5)-H(5A)	0.9900
C(5)-H(5B)	0.9900
C(5)-H(5C)	0.9890
C(5)-H(5D)	0.9886
C(4)-H(4A)	0.9900
C(4)-H(4B)	0.9900
C(4D)-H(4DA)	0.9900
C(4D)-H(4DB)	0.9900
C(6)-C(7)	1.351(7)
C(6)-C(6)#2	1.363(11)
C(6)-H(6)	0.9500
C(7)-C(8)	1.366(7)
C(7)-H(7)	0.9500
C(8)-C(8)#2	1.392(12)
C(8)-H(8)	0.9500

B(3)#1-B(1)-B(6)	108.5(2)
B(3)#1-B(1)-B(5)	60.4(2)
B(6)-B(1)-B(5)	60.0(2)
B(3)#1-B(1)-B(4)#1	60.0(2)
B(6)-B(1)-B(4)#1	108.1(3)
B(5)-B(1)-B(4)#1	108.1(3)
B(3)#1-B(1)-B(2)	108.3(3)

B(6)-B(1)-B(2)	60.0(2)
B(5)-B(1)-B(2)	108.1(2)
B(4)#1-B(1)-B(2)	60.0(2)
B(3)#1-B(1)-Br(1)	121.8(2)
B(6)-B(1)-Br(1)	121.6(2)
B(5)-B(1)-Br(1)	122.4(2)
B(4)#1-B(1)-Br(1)	121.2(2)
B(2)-B(1)-Br(1)	120.9(2)
B(3)-B(2)-B(6)	60.4(2)
B(3)-B(2)-B(4)#1	107.4(2)
B(6)-B(2)-B(4)#1	107.6(3)
B(3)-B(2)-B(1)	107.7(3)
B(6)-B(2)-B(1)	59.7(2)
B(4)#1-B(2)-B(1)	59.8(2)
B(3)-B(2)-B(5)#1	60.1(2)
B(6)-B(2)-B(5)#1	108.4(2)
B(4)#1-B(2)-B(5)#1	59.4(2)
B(1)-B(2)-B(5)#1	107.4(3)
B(3)-B(2)-Br(2)	123.0(2)
B(6)-B(2)-Br(2)	122.4(2)
B(4)#1-B(2)-Br(2)	120.9(2)
B(1)-B(2)-Br(2)	121.4(2)
B(5)#1-B(2)-Br(2)	121.7(2)
B(1)#1-B(3)-B(4)	60.2(2)
B(1)#1-B(3)-B(2)	108.2(3)
B(4)-B(3)-B(2)	107.9(2)
B(1)#1-B(3)-B(5)#1	60.0(2)
B(4)-B(3)-B(5)#1	108.0(3)
B(2)-B(3)-B(5)#1	60.1(2)
B(1)#1-B(3)-B(6)	108.2(3)
B(4)-B(3)-B(6)	59.9(2)
B(2)-B(3)-B(6)	59.9(2)
B(5)#1-B(3)-B(6)	107.9(3)
B(1)#1-B(3)-Br(3)	121.2(2)

B(4)-B(3)-Br(3)	121.6(2)
B(2)-B(3)-Br(3)	122.0(2)
B(5)#1-B(3)-Br(3)	121.7(2)
B(6)-B(3)-Br(3)	122.0(2)
B(5)-B(4)-B(3)	108.6(2)
B(5)-B(4)-B(1)#1	108.5(3)
B(3)-B(4)-B(1)#1	59.8(2)
B(5)-B(4)-B(6)	60.1(2)
B(3)-B(4)-B(6)	60.4(2)
B(1)#1-B(4)-B(6)	108.3(3)
B(5)-B(4)-B(2)#1	60.4(2)
B(3)-B(4)-B(2)#1	108.2(3)
B(1)#1-B(4)-B(2)#1	60.1(2)
B(6)-B(4)-B(2)#1	108.5(2)
B(5)-B(4)-Br(4)	122.3(2)
B(3)-B(4)-Br(4)	120.9(2)
B(1)#1-B(4)-Br(4)	120.7(2)
B(6)-B(4)-Br(4)	121.9(2)
B(2)#1-B(4)-Br(4)	121.6(2)
B(4)-B(5)-B(6)	60.3(2)
B(4)-B(5)-B(1)	107.8(3)
B(6)-B(5)-B(1)	59.8(2)
B(4)-B(5)-B(2)#1	60.3(2)
B(6)-B(5)-B(2)#1	108.5(3)
B(1)-B(5)-B(2)#1	107.6(3)
B(4)-B(5)-B(3)#1	107.8(3)
B(6)-B(5)-B(3)#1	107.8(3)
B(1)-B(5)-B(3)#1	59.7(2)
B(2)#1-B(5)-B(3)#1	59.7(2)
B(4)-B(5)-Br(5)	121.8(2)
B(6)-B(5)-Br(5)	121.3(2)
B(1)-B(5)-Br(5)	121.8(2)
B(2)#1-B(5)-Br(5)	121.9(2)
B(3)#1-B(5)-Br(5)	122.1(2)

B(1)-B(6)-B(5)	60.1(2)
B(1)-B(6)-B(2)	60.3(2)
B(5)-B(6)-B(2)	108.4(3)
B(1)-B(6)-B(4)	107.4(3)
B(5)-B(6)-B(4)	59.6(2)
B(2)-B(6)-B(4)	107.6(3)
B(1)-B(6)-B(3)	107.7(3)
B(5)-B(6)-B(3)	107.6(3)
B(2)-B(6)-B(3)	59.8(2)
B(4)-B(6)-B(3)	59.7(2)
B(1)-B(6)-Br(6)	121.9(2)
B(5)-B(6)-Br(6)	121.0(2)
B(2)-B(6)-Br(6)	122.3(2)
B(4)-B(6)-Br(6)	121.8(2)
B(3)-B(6)-Br(6)	122.4(2)
C(5)-O(1)-C(2)	109.4(3)
C(5)-O(1)-H(1)	110(3)
C(2)-O(1)-H(1)	115(3)
C(3)-C(2)-O(1)	104.1(3)
C(3)-C(2)-H(2A)	110.9
O(1)-C(2)-H(2A)	110.9
C(3)-C(2)-H(2B)	110.9
O(1)-C(2)-H(2B)	110.9
H(2A)-C(2)-H(2B)	109.0
C(4)-C(3)-C(4D)	31.8(10)
C(4)-C(3)-C(2)	105.4(4)
C(4D)-C(3)-C(2)	110.2(6)
C(4)-C(3)-H(3A)	110.7
C(4D)-C(3)-H(3A)	131.2
C(2)-C(3)-H(3A)	110.7
C(4)-C(3)-H(3B)	110.7
C(4D)-C(3)-H(3B)	80.0
C(2)-C(3)-H(3B)	110.7
H(3A)-C(3)-H(3B)	108.8

C(4)-C(3)-H(3C)	137.3
C(4D)-C(3)-H(3C)	110.5
C(2)-C(3)-H(3C)	109.5
H(3A)-C(3)-H(3C)	79.1
H(3B)-C(3)-H(3C)	33.1
C(4)-C(3)-H(3D)	81.6
C(4D)-C(3)-H(3D)	108.6
C(2)-C(3)-H(3D)	109.8
H(3A)-C(3)-H(3D)	31.1
H(3B)-C(3)-H(3D)	132.2
H(3C)-C(3)-H(3D)	108.2
C(4D)-C(5)-C(4)	31.7(10)
C(4D)-C(5)-O(1)	106.5(6)
C(4)-C(5)-O(1)	102.1(4)
C(4D)-C(5)-H(5A)	80.9
C(4)-C(5)-H(5A)	111.4
O(1)-C(5)-H(5A)	111.4
C(4D)-C(5)-H(5B)	132.8
C(4)-C(5)-H(5B)	111.4
O(1)-C(5)-H(5B)	111.4
H(5A)-C(5)-H(5B)	109.2
C(4D)-C(5)-H(5C)	111.3
C(4)-C(5)-H(5C)	138.1
O(1)-C(5)-H(5C)	110.9
H(5A)-C(5)-H(5C)	32.4
H(5B)-C(5)-H(5C)	80.3
C(4D)-C(5)-H(5D)	109.1
C(4)-C(5)-H(5D)	82.0
O(1)-C(5)-H(5D)	110.3
H(5A)-C(5)-H(5D)	131.8
H(5B)-C(5)-H(5D)	30.9
H(5C)-C(5)-H(5D)	108.7
C(3)-C(4)-C(5)	105.7(4)
C(3)-C(4)-H(4A)	110.6

C(5)-C(4)-H(4A)	110.6
C(3)-C(4)-H(4B)	110.6
C(5)-C(4)-H(4B)	110.6
H(4A)-C(4)-H(4B)	108.7
C(5)-C(4D)-C(3)	106.4(7)
C(5)-C(4D)-H(4DA)	110.4
C(3)-C(4D)-H(4DA)	110.4
C(5)-C(4D)-H(4DB)	110.4
C(3)-C(4D)-H(4DB)	110.4
H(4DA)-C(4D)-H(4DB)	108.6
C(7)-C(6)-C(6)#2	120.4(3)
C(7)-C(6)-H(6)	119.8
C(6)#2-C(6)-H(6)	119.8
C(6)-C(7)-C(8)	120.3(5)
C(6)-C(7)-H(7)	119.8
C(8)-C(7)-H(7)	119.8
C(7)-C(8)-C(8)#2	119.3(3)
C(7)-C(8)-H(8)	120.4
C(8)#2-C(8)-H(8)	120.4

Symmetry transformations used to generate equivalent atoms:
#1 -x+3/2,-y+3/2,-z+1/2 #2 -x+3/2,y,-z+1

E.2.4 Anisotropic Displacement Parameters

Anisotropic displacement parameters ($Å^2 x\ 10^3$) for $[H(C_4H_8O]_2[B_{12}Br_{12}]\cdot C_6H_6$. The anisotropic displacement factor exponent takes the form: $-2\pi^2[\ h^2\ a^{*2}U^{11} + ...\ + 2\ h\ k\ a^*\ b^*\ U^{12}\ ]$

	U^{11}	U^{22}	U^{33}	U^{23}	U^{13}	U^{12}
B(1)	17(2)	21(2)	18(2)	-1(1)	11(1)	-1(1)
B(2)	17(2)	17(2)	12(2)	-3(1)	4(1)	-1(1)
B(3)	16(2)	16(2)	16(2)	0(1)	8(1)	-2(1)

B(4)	14(2)	16(2)	19(2)	0(1)	9(1)	0(1)
B(5)	15(2)	15(2)	19(2)	1(1)	9(1)	0(1)
B(6)	15(2)	21(2)	16(2)	2(1)	5(1)	1(1)
Br(1)	25(1)	25(1)	20(1)	3(1)	15(1)	1(1)
Br(2)	28(1)	25(1)	16(1)	-6(1)	7(1)	-2(1)
Br(3)	15(1)	27(1)	26(1)	-1(1)	7(1)	-4(1)
Br(4)	23(1)	21(1)	25(1)	1(1)	15(1)	5(1)
Br(5)	26(1)	18(1)	24(1)	0(1)	10(1)	-3(1)
Br(6)	23(1)	25(1)	17(1)	3(1)	5(1)	3(1)
O(1)	31(2)	39(2)	36(2)	11(1)	21(1)	8(1)
C(2)	27(2)	26(2)	24(2)	1(2)	9(2)	-1(2)
C(3)	60(3)	39(2)	43(3)	-6(2)	37(2)	-5(2)
C(5)	37(2)	35(2)	82(4)	23(2)	36(3)	17(2)
C(4)	35(3)	39(3)	47(4)	-3(3)	26(3)	0(3)
C(4D)	22(12)	42(9)	59(10)	-18(9)	16(10)	5(9)
C(6)	49(3)	38(2)	64(3)	18(2)	41(2)	22(2)
C(7)	29(2)	79(4)	31(2)	-1(2)	9(2)	10(2)
C(8)	70(4)	40(3)	72(4)	-29(2)	55(3)	-27(3)

E.2.5 Hydrogen Coordinates

Hydrogen coordinates (x 10^4) and isotropic displacement parameters (Å^{2}x 10^3) for $[H(C_4H_8O]_2[B_{12}Br_{12}]\cdot C_6H_6$.

	x	y	z	U(eq)
H(1)	10290(30)	2420(40)	3300(30)	39
H(2A)	9564	608	3794	31
H(2B)	10437	1185	4288	31
H(3A)	9136	1305	4707	51
H(3B)	9841	2257	4930	51
H(3C)	9801	1833	5039	51

H(3D)	8906	1460	4455	51
H(5A)	9600	3747	3706	57
H(5B)	8817	3354	2971	57
H(5C)	9491	3819	3393	57
H(5D)	8657	3080	3093	57
H(4A)	8689	3246	4298	44
H(4B)	8296	2264	3693	44
H(4DA)	8645	3208	4255	49
H(4DB)	9618	3539	4603	49
H(6)	8019	1045	5597	54
H(7)	8542	2687	6198	56
H(8)	8047	4361	5598	63

E.2.6 Hydrogen Bonds

Hydrogen bonds for $[H(C_4H_8O]_2[B_{12}Br_{12}]\cdot C_6H_6$ [Å and °].

D-H...A	d(D-H)	d(H...A)	d(D...A)	<(DHA)
O(1)-H(1)...Br(3)#3	1.05(5)	2.94(5)	3.582(3)	120(3)
O(1)-H(1)...Br(1)#4	1.05(5)	2.35(5)	3.262(3)	144(4)

Symmetry transformations used to generate equivalent atoms:

#1 -x+3/2,-y+3/2,-z+1/2 #2 -x+3/2,y,-z+1 #3 x+1/2,-y+1,z #4 -x+2,y-1/2,-z+1/2

E.3 References

1. *APEX 2,* version 2009.5-1, Bruker (2009), Bruker AXS Inc., Madison, Wisconsin, USA.

2. *SAINT,* version V7.60A, Bruker (2009), Bruker AXS Inc., Madison, Wisconsin, USA.

3. *SADABS,* version 2008/1, Bruker (2008), Bruker AXS Inc., Madison, Wisconsin, USA.

4. *SHELXTL,* version 2008/4, Bruker (2008), Bruker AXS Inc., Madison, Wisconsin, USA.

Appendix F. X Ray Structure Determination for C27 H47 Ag0.01 B18 Cl18 Si

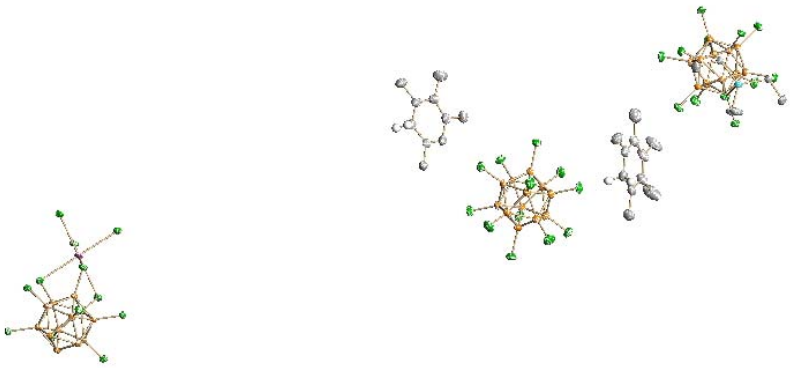

F.1 Experimental Details

An orange prism fragment (0.16 x 0.13 x 0.09 mm^3) was used for the single crystal x-ray diffraction study of $(C_6H_2[CH_3]_5^+).(C_6H_3[CH_3]_4^+).([C_2H_5]_3SiB_{12}Cl_{12}]^-).([B_{12}Cl_{12}]^{2+})_{0.5}$ (sample cr308_0m). The crystal was coated with paratone oil and mounted on to a glass fiber. X-ray intensity data were collected at 100(2) K on a Bruker APEX2 (**ref. 1**) platform-CCD x-ray diffractometer system (Mo-radiation, λ = 0.71073 Å, 50KV/40mA power). The CCD detector was placed at a distance of 5.0375 cm from the crystal.

A total of 2400 frames were collected for a hemisphere of reflections (with scan width of 0.3° in ω, starting ω and 2θ angles at –30°, ϕ angles of 0°, 90°, 180°, and 270° for every 600 frames, 60 sec/frame exposure time). The frames were integrated using the Bruker SAINT software package (**ref. 2**) and using a narrow-frame integration algorithm. Based on a trigonal crystal system, the integrated frames yielded a total of 165029 reflections at a maximum 2θ angle of 56.56° (0.75 Å resolution), of which 13039 were independent reflections (R_{int} = 0.0668, R_{sig} = 0.0305, redundancy = 12.7, completeness =

99.9%) and 9716 (74.5%) reflections were greater than $2\sigma(I)$. The unit cell parameters were, **a** = **b** = 31.6284(8) Å, **c** = 9.1064(2) Å, $\alpha = \beta = 90^{o}$, $\gamma = 120^{o}$, V = 7889.2(3) $Å^3$, Z = 6, calculated density D_c = 1.557 g/cm^3. Absorption corrections were applied (absorption coefficient μ = 0.988 mm^{-1}; max/min transmission = 0.9189/0.8571) to the raw intensity data using the SADABS program (**ref. 3**).

The Bruker SHELXTL software package (**ref. 4**) was used for phase determination and structure refinement. The distribution of intensities (E^2-1 = 0.979) and systematic absent reflections indicated two possible space groups, P-3 and P3. The space group P-3 was later determined to be correct. Direct methods of phase determination followed by two Fourier cycles of refinement led to an electron density map from which most of the non-hydrogen atoms were identified in the asymmetry unit of the unit cell. With subsequent isotropic refinement, all of the non-hydrogen atoms were identified. There were one cation of ($C_6H_2[CH_3]_5^+$), one cation of ($C_6H_3[CH_3]_4^+$), 1/6 anion of $[B_{12}Cl_{12}]^{2-}$ (where the anion was located at the 3-fold inversion axis parallel to the **c**-axis), and 1/3 anion of $[B_{12}Cl_{12}]^{2-}$ (where the anion was located at the 3-fold rotation axis parallel to the **c**-axis) present in the asymmetry unit of the unit cell. A 0.5% of Ag ion was co-crystallized as impurity and was located at the 3-fold inversion axis parallel to the **c**-axis. The carbo-cation protons were located from the difference electron density map and refined unrestrained.

Atomic coordinates, isotropic and anisotropic displacement parameters of all the non-hydrogen atoms were refined by means of a full matrix least-squares procedure on F^2. The H-atoms were included in the refinement in calculated positions riding on the

atoms to which they were attached, except the carbo-cation protons. The refinement converged at R1 = 0.0452, wR2 = 0.1102, with intensity, I>2σ(I). The largest peak/hole in the final difference map was 1.128/-0.573 e/Å^3. The high difference electron density peak/hole near the Cl-atoms were probably due to absorption correction error.

F.2 Structure Data

F.2.1 Crystal data and structure refinement for C27 H47 Ag0.01 B18 Cl18 Si.

Identification code	cr308_0m	
Empirical formula	C27 H47 Ag0.01 B18 Cl18 Si	
Formula weight	1232.96	
Temperature	100(2) K	
Wavelength	0.71073 Å	
Crystal system	Trigonal	
Space group	P-3	
Unit cell dimensions	a = 31.6284(8) Å	α = 90°.
	b = 31.6284(8) Å	β = 90°.
	c = 9.1064(2) Å	γ = 120°.
Volume	7889.2(3) Å^3	
Z	6	
Density (calculated)	1.557 Mg/m^3	
Absorption coefficient	0.988 mm^{-1}	
F(000)	3715	
Crystal size	0.16 x 0.13 x 0.09 mm^3	
Theta range for data collection	1.29 to 28.28°.	
Index ranges	-42<=h<=42, -42<=k<=42, -12<=l<=12	
Reflections collected	165029	
Independent reflections	13039 [R(int) = 0.0668]	
Completeness to theta = 28.28°	99.9 %	
Absorption correction	Semi-empirical from equivalents	
Max. and min. transmission	0.9189 and 0.8571	

Refinement method	Full-matrix least-squares on F^2
Data / restraints / parameters	13039 / 0 / 603
Goodness-of-fit on F^2	1.063
Final R indices [I>2sigma(I)]	R1 = 0.0452, wR2 = 0.1102
R indices (all data)	R1 = 0.0706, wR2 = 0.1254
Largest diff. peak and hole	1.128 and -0.573 e.Å^{-3}

F.2.2 Atomic Coordinates

Atomic coordinates (x 10^4) and equivalent isotropic displacement parameters (Å^{2}x 10^3) for cr308_0m. U(eq) is defined as one third of the trace of the orthogonalized U^{ij} tensor.

	x	y	z	U(eq)
Ag(1)	10000	0	5000	19(5)
C(1A)	8601(1)	3911(1)	3361(4)	34(1)
C(2A)	8491(1)	3675(1)	4793(4)	35(1)
C(3A)	8698(1)	3951(1)	6032(4)	38(1)
C(4A)	9038(2)	4456(1)	5860(4)	45(1)
C(5A)	9165(2)	4695(1)	4480(4)	42(1)
C(6A)	8942(1)	4434(1)	3240(4)	36(1)
C(7A)	8159(2)	3137(1)	4827(5)	48(1)
C(8A)	8565(2)	3739(2)	7545(5)	67(1)
C(9A)	9274(2)	4752(2)	7210(5)	68(2)
C(10A)	9531(2)	5225(2)	4394(6)	89(2)
C(11A)	9033(2)	4656(2)	1737(4)	49(1)
C(1B)	4394(1)	2557(1)	2737(4)	32(1)
C(2B)	3960(1)	2191(1)	3458(4)	33(1)
C(3B)	3956(1)	2164(1)	5052(4)	34(1)
C(4B)	4359(1)	2485(1)	5862(4)	40(1)
C(5B)	4755(1)	2875(1)	5126(4)	38(1)
C(6B)	4776(1)	2903(1)	3572(4)	35(1)
C(7B)	4422(1)	2565(1)	1107(4)	37(1)
C(8B)	3504(1)	1784(1)	5783(4)	41(1)

C(9B)	4374(2)	2403(2)	7489(5)	59(1)
C(10B)	5172(1)	3271(2)	5973(5)	47(1)
B(1)	9868(1)	2845(1)	9116(3)	18(1)
B(2)	9510(1)	3131(1)	8954(3)	21(1)
B(3)	10166(1)	3493(1)	9080(4)	22(1)
B(4)	10370(1)	3190(1)	10304(3)	19(1)
B(5)	9847(1)	2646(1)	10946(3)	17(1)
B(6)	9315(1)	2608(1)	10115(3)	18(1)
B(7)	9268(1)	3116(1)	10723(4)	22(1)
B(8)	9793(1)	3664(1)	10087(4)	23(1)
B(9)	10320(1)	3699(1)	10923(4)	21(1)
B(10)	10126(1)	3181(1)	12076(3)	20(1)
B(11)	9476(1)	2820(1)	11966(3)	20(1)
B(12)	9765(1)	3470(1)	11944(4)	22(1)
Cl(1)	9913(1)	2560(1)	7400(1)	23(1)
Cl(2)	9200(1)	3100(1)	7281(1)	31(1)
Cl(3)	10530(1)	3833(1)	7542(1)	30(1)
Cl(4)	10945(1)	3216(1)	10078(1)	24(1)
Cl(5)	9884(1)	2117(1)	11419(1)	21(1)
Cl(6)	8784(1)	2036(1)	9706(1)	25(1)
Cl(7)	8681(1)	3068(1)	10924(1)	31(1)
Cl(8)	9774(1)	4207(1)	9665(1)	35(1)
Cl(9)	10845(1)	4276(1)	11332(1)	32(1)
Cl(10)	10447(1)	3208(1)	13725(1)	28(1)
Cl(11)	9123(1)	2472(1)	13497(1)	28(1)
Cl(12)	9697(1)	3794(1)	13449(1)	32(1)
Si(1)	9954(1)	1847(1)	7236(1)	21(1)
C(1)	10556(1)	2029(1)	8048(3)	25(1)
C(2)	10992(1)	2426(1)	7206(4)	33(1)
C(3)	9927(1)	1854(1)	5201(3)	29(1)
C(4)	9911(2)	1404(1)	4525(3)	39(1)
C(5)	9396(1)	1371(1)	8137(3)	23(1)
C(6)	8921(1)	1210(1)	7288(4)	34(1)
B(13)	6549(1)	2758(1)	-53(4)	25(1)

B(14)	6952(1)	3263(1)	-1193(4)	27(1)
B(15)	7124(1)	3215(1)	640(4)	22(1)
B(16)	6591(1)	2977(1)	1778(4)	22(1)
Cl(13)	6423(1)	2146(1)	-388(1)	34(1)
Cl(14)	7250(1)	3195(1)	-2764(1)	42(1)
Cl(15)	7606(1)	3086(1)	989(1)	32(1)
Cl(16)	6505(1)	2605(1)	3354(1)	31(1)
B(17)	9685(1)	19(1)	1478(3)	16(1)
B(18)	10028(1)	541(1)	352(3)	16(1)
Cl(17)	9360(1)	38(1)	3064(1)	22(1)
Cl(18)	10059(1)	1109(1)	743(1)	23(1)

F.2.3 Bond Length and Angles

Bond lengths [Å] and angles [°] for cr308_0m.

Ag(1)-Cl(17)#1	2.7325(7)
Ag(1)-Cl(17)#2	2.7325(7)
Ag(1)-Cl(17)	2.7325(7)
Ag(1)-Cl(17)#3	2.7325(7)
Ag(1)-Cl(17)#4	2.7325(7)
Ag(1)-Cl(17)#5	2.7325(7)
C(1A)-C(2A)	1.456(5)
C(1A)-C(6A)	1.459(5)
C(1A)-H(11A)	1.01(4)
C(1A)-H(12A)	0.92(4)
C(2A)-C(3A)	1.375(5)
C(2A)-C(7A)	1.487(5)
C(3A)-C(4A)	1.421(6)
C(3A)-C(8A)	1.497(6)
C(4A)-C(5A)	1.417(6)
C(4A)-C(9A)	1.499(5)
C(5A)-C(6A)	1.368(5)

C(5A)-C(10A)	1.487(6)
C(6A)-C(11A)	1.499(5)
C(7A)-H(71A)	0.9800
C(7A)-H(72A)	0.9800
C(7A)-H(73A)	0.9800
C(8A)-H(81A)	0.9800
C(8A)-H(82A)	0.9800
C(8A)-H(83A)	0.9800
C(9A)-H(91A)	0.9800
C(9A)-H(92A)	0.9800
C(9A)-H(93A)	0.9800
C(10A)-H(101)	0.9800
C(10A)-H(102)	0.9800
C(10A)-H(103)	0.9800
C(11A)-H(111)	0.9800
C(11A)-H(112)	0.9800
C(11A)-H(113)	0.9800
C(1B)-C(6B)	1.384(5)
C(1B)-C(2B)	1.437(5)
C(1B)-C(7B)	1.486(5)
C(2B)-C(3B)	1.454(5)
C(2B)-H(11B)	0.97(4)
C(2B)-H(12B)	0.98(4)
C(3B)-C(4B)	1.380(5)
C(3B)-C(8B)	1.488(5)
C(4B)-C(5B)	1.412(5)
C(4B)-C(9B)	1.509(5)
C(5B)-C(6B)	1.418(5)
C(5B)-C(10B)	1.500(5)
C(6B)-H(61B)	0.9500
C(7B)-H(71B)	0.9800
C(7B)-H(72B)	0.9800
C(7B)-H(73B)	0.9800
C(8B)-H(81B)	0.9800

C(8B)-H(83B)	0.9800
C(8B)-H(82B)	0.9800
C(9B)-H(91B)	0.9800
C(9B)-H(92B)	0.9800
C(9B)-H(93B)	0.9800
C(10B)-H(104)	0.9800
C(10B)-H(105)	0.9800
C(10B)-H(106)	0.9800
B(1)-B(5)	1.771(4)
B(1)-B(6)	1.773(4)
B(1)-B(4)	1.775(4)
B(1)-B(2)	1.775(4)
B(1)-B(3)	1.779(4)
B(1)-Cl(1)	1.845(3)
B(2)-B(7)	1.774(5)
B(2)-B(8)	1.788(5)
B(2)-Cl(2)	1.788(3)
B(2)-B(6)	1.793(4)
B(2)-B(3)	1.805(5)
B(3)-B(9)	1.778(5)
B(3)-B(8)	1.779(5)
B(3)-B(4)	1.788(4)
B(3)-Cl(3)	1.790(3)
B(4)-B(10)	1.782(4)
B(4)-B(9)	1.786(4)
B(4)-B(5)	1.788(4)
B(4)-Cl(4)	1.790(3)
B(5)-B(11)	1.786(4)
B(5)-Cl(5)	1.787(3)
B(5)-B(10)	1.791(4)
B(5)-B(6)	1.794(4)
B(6)-B(7)	1.775(4)
B(6)-Cl(6)	1.786(3)
B(6)-B(11)	1.792(4)

B(7)-B(12)	1.788(5)
B(7)-B(11)	1.792(5)
B(7)-B(8)	1.793(5)
B(7)-Cl(7)	1.793(3)
B(8)-B(9)	1.784(5)
B(8)-B(12)	1.785(5)
B(8)-Cl(8)	1.791(3)
B(9)-B(10)	1.778(5)
B(9)-Cl(9)	1.788(3)
B(9)-B(12)	1.789(5)
B(10)-B(11)	1.786(4)
B(10)-Cl(10)	1.791(3)
B(10)-B(12)	1.792(4)
B(11)-Cl(11)	1.782(3)
B(11)-B(12)	1.785(5)
B(12)-Cl(12)	1.786(3)
Cl(1)-Si(1)	2.3263(10)
Si(1)-C(5)	1.842(3)
Si(1)-C(1)	1.848(3)
Si(1)-C(3)	1.856(3)
C(1)-C(2)	1.528(4)
C(1)-H(1A)	0.9900
C(1)-H(1B)	0.9900
C(2)-H(2A)	0.9800
C(2)-H(2B)	0.9800
C(2)-H(2C)	0.9800
C(3)-C(4)	1.528(4)
C(3)-H(3A)	0.9900
C(3)-H(3B)	0.9900
C(4)-H(4A)	0.9800
C(4)-H(4B)	0.9800
C(4)-H(4C)	0.9800
C(5)-C(6)	1.533(4)
C(5)-H(5A)	0.9900

C(5)-H(5B)	0.9900
C(6)-H(6A)	0.9800
C(6)-H(6B)	0.9800
C(6)-H(6C)	0.9800
B(13)-B(15)	1.779(5)
B(13)-B(14)#6	1.779(5)
B(13)-B(15)#6	1.781(5)
B(13)-B(16)	1.785(5)
B(13)-B(14)	1.794(5)
B(13)-Cl(13)	1.798(3)
B(14)-B(13)#7	1.779(5)
B(14)-B(15)	1.785(5)
B(14)-Cl(14)	1.785(3)
B(14)-B(14)#6	1.788(6)
B(14)-B(14)#7	1.788(6)
B(15)-B(16)#7	1.780(4)
B(15)-B(13)#7	1.781(5)
B(15)-Cl(15)	1.792(3)
B(15)-B(16)	1.792(5)
B(16)-B(15)#6	1.780(4)
B(16)-B(16)#7	1.782(5)
B(16)-B(16)#6	1.782(5)
B(16)-Cl(16)	1.789(3)
B(17)-B(18)	1.778(4)
B(17)-B(17)#5	1.779(5)
B(17)-B(17)#2	1.779(5)
B(17)-B(18)#8	1.785(4)
B(17)-B(18)#2	1.786(4)
B(17)-Cl(17)	1.792(3)
B(18)-B(17)#9	1.785(4)
B(18)-Cl(18)	1.786(3)
B(18)-B(17)#5	1.786(4)
B(18)-B(18)#8	1.787(3)
B(18)-B(18)#9	1.787(3)

Cl(17)#1-Ag(1)-Cl(17)#2 180.00(2)
Cl(17)#1-Ag(1)-Cl(17) 97.136(19)
Cl(17)#2-Ag(1)-Cl(17) 82.864(19)
Cl(17)#1-Ag(1)-Cl(17)#3 82.864(19)
Cl(17)#2-Ag(1)-Cl(17)#3 97.136(19)
Cl(17)-Ag(1)-Cl(17)#3 180.00(3)
Cl(17)#1-Ag(1)-Cl(17)#4 82.864(19)
Cl(17)#2-Ag(1)-Cl(17)#4 97.136(19)
Cl(17)-Ag(1)-Cl(17)#4 97.136(19)
Cl(17)#3-Ag(1)-Cl(17)#4 82.864(19)
Cl(17)#1-Ag(1)-Cl(17)#5 97.136(19)
Cl(17)#2-Ag(1)-Cl(17)#5 82.864(19)
Cl(17)-Ag(1)-Cl(17)#5 82.864(19)
Cl(17)#3-Ag(1)-Cl(17)#5 97.136(19)
Cl(17)#4-Ag(1)-Cl(17)#5 180.00(5)
C(2A)-C(1A)-C(6A) 120.0(3)
C(2A)-C(1A)-H(11A) 109(2)
C(6A)-C(1A)-H(11A) 106(2)
C(2A)-C(1A)-H(12A) 112(2)
C(6A)-C(1A)-H(12A) 103(2)
H(11A)-C(1A)-H(12A) 106(3)
C(3A)-C(2A)-C(1A) 119.6(3)
C(3A)-C(2A)-C(7A) 123.2(3)
C(1A)-C(2A)-C(7A) 117.1(3)
C(2A)-C(3A)-C(4A) 118.4(3)
C(2A)-C(3A)-C(8A) 122.2(4)
C(4A)-C(3A)-C(8A) 119.4(4)
C(5A)-C(4A)-C(3A) 123.5(3)
C(5A)-C(4A)-C(9A) 118.3(4)
C(3A)-C(4A)-C(9A) 118.2(4)
C(6A)-C(5A)-C(4A) 119.1(3)
C(6A)-C(5A)-C(10A) 120.9(4)
C(4A)-C(5A)-C(10A) 120.1(4)

C(5A)-C(6A)-C(1A)	119.3(3)
C(5A)-C(6A)-C(11A)	123.4(3)
C(1A)-C(6A)-C(11A)	117.4(3)
C(2A)-C(7A)-H(71A)	109.5
C(2A)-C(7A)-H(72A)	109.5
H(71A)-C(7A)-H(72A)	109.5
C(2A)-C(7A)-H(73A)	109.5
H(71A)-C(7A)-H(73A)	109.5
H(72A)-C(7A)-H(73A)	109.5
C(3A)-C(8A)-H(81A)	109.5
C(3A)-C(8A)-H(82A)	109.5
H(81A)-C(8A)-H(82A)	109.5
C(3A)-C(8A)-H(83A)	109.5
H(81A)-C(8A)-H(83A)	109.5
H(82A)-C(8A)-H(83A)	109.5
C(4A)-C(9A)-H(91A)	109.5
C(4A)-C(9A)-H(92A)	109.5
H(91A)-C(9A)-H(92A)	109.5
C(4A)-C(9A)-H(93A)	109.5
H(91A)-C(9A)-H(93A)	109.5
H(92A)-C(9A)-H(93A)	109.5
C(5A)-C(10A)-H(101)	109.5
C(5A)-C(10A)-H(102)	109.5
H(101)-C(10A)-H(102)	109.5
C(5A)-C(10A)-H(103)	109.5
H(101)-C(10A)-H(103)	109.5
H(102)-C(10A)-H(103)	109.5
C(6A)-C(11A)-H(111)	109.5
C(6A)-C(11A)-H(112)	109.5
H(111)-C(11A)-H(112)	109.5
C(6A)-C(11A)-H(113)	109.5
H(111)-C(11A)-H(113)	109.5
H(112)-C(11A)-H(113)	109.5
C(6B)-C(1B)-C(2B)	119.4(3)

C(6B)-C(1B)-C(7B)	121.0(3)
C(2B)-C(1B)-C(7B)	119.6(3)
C(1B)-C(2B)-C(3B)	118.7(3)
C(1B)-C(2B)-H(11B)	111(2)
C(3B)-C(2B)-H(11B)	118(2)
C(1B)-C(2B)-H(12B)	110(2)
C(3B)-C(2B)-H(12B)	105(2)
H(11B)-C(2B)-H(12B)	89(3)
C(4B)-C(3B)-C(2B)	120.8(3)
C(4B)-C(3B)-C(8B)	121.0(3)
C(2B)-C(3B)-C(8B)	118.1(3)
C(3B)-C(4B)-C(5B)	118.6(3)
C(3B)-C(4B)-C(9B)	119.7(4)
C(5B)-C(4B)-C(9B)	121.7(4)
C(4B)-C(5B)-C(6B)	121.5(3)
C(4B)-C(5B)-C(10B)	120.7(3)
C(6B)-C(5B)-C(10B)	117.8(3)
C(1B)-C(6B)-C(5B)	120.3(3)
C(1B)-C(6B)-H(61B)	119.9
C(5B)-C(6B)-H(61B)	119.9
C(1B)-C(7B)-H(71B)	109.5
C(1B)-C(7B)-H(72B)	109.5
H(71B)-C(7B)-H(72B)	109.5
C(1B)-C(7B)-H(73B)	109.5
H(71B)-C(7B)-H(73B)	109.5
H(72B)-C(7B)-H(73B)	109.5
C(3B)-C(8B)-H(81B)	109.5
C(3B)-C(8B)-H(83B)	109.5
H(81B)-C(8B)-H(83B)	109.5
C(3B)-C(8B)-H(82B)	109.5
H(81B)-C(8B)-H(82B)	109.5
H(83B)-C(8B)-H(82B)	109.5
C(4B)-C(9B)-H(91B)	109.5
C(4B)-C(9B)-H(92B)	109.5

H(91B)-C(9B)-H(92B)	109.5
C(4B)-C(9B)-H(93B)	109.5
H(91B)-C(9B)-H(93B)	109.5
H(92B)-C(9B)-H(93B)	109.5
C(5B)-C(10B)-H(104)	109.5
C(5B)-C(10B)-H(105)	109.5
H(104)-C(10B)-H(105)	109.5
C(5B)-C(10B)-H(106)	109.5
H(104)-C(10B)-H(106)	109.5
H(105)-C(10B)-H(106)	109.5
B(5)-B(1)-B(6)	60.84(17)
B(5)-B(1)-B(4)	60.56(17)
B(6)-B(1)-B(4)	109.7(2)
B(5)-B(1)-B(2)	109.8(2)
B(6)-B(1)-B(2)	60.73(18)
B(4)-B(1)-B(2)	109.8(2)
B(5)-B(1)-B(3)	109.4(2)
B(6)-B(1)-B(3)	109.8(2)
B(4)-B(1)-B(3)	60.40(18)
B(2)-B(1)-B(3)	61.03(18)
B(5)-B(1)-Cl(1)	128.5(2)
B(6)-B(1)-Cl(1)	122.0(2)
B(4)-B(1)-Cl(1)	123.6(2)
B(2)-B(1)-Cl(1)	113.82(19)
B(3)-B(1)-Cl(1)	114.91(19)
B(7)-B(2)-B(1)	106.8(2)
B(7)-B(2)-B(8)	60.46(18)
B(1)-B(2)-B(8)	106.6(2)
B(7)-B(2)-Cl(2)	123.7(2)
B(1)-B(2)-Cl(2)	121.0(2)
B(8)-B(2)-Cl(2)	123.1(2)
B(7)-B(2)-B(6)	59.70(17)
B(1)-B(2)-B(6)	59.57(17)
B(8)-B(2)-B(6)	108.0(2)

Cl(2)-B(2)-B(6)	121.7(2)
B(7)-B(2)-B(3)	107.7(2)
B(1)-B(2)-B(3)	59.59(17)
B(8)-B(2)-B(3)	59.35(18)
Cl(2)-B(2)-B(3)	120.9(2)
B(6)-B(2)-B(3)	107.8(2)
B(9)-B(3)-B(8)	60.19(18)
B(9)-B(3)-B(1)	107.1(2)
B(8)-B(3)-B(1)	106.9(2)
B(9)-B(3)-B(4)	60.12(18)
B(8)-B(3)-B(4)	108.2(2)
B(1)-B(3)-B(4)	59.68(17)
B(9)-B(3)-Cl(3)	122.9(2)
B(8)-B(3)-Cl(3)	123.1(2)
B(1)-B(3)-Cl(3)	121.2(2)
B(4)-B(3)-Cl(3)	121.0(2)
B(9)-B(3)-B(2)	108.0(2)
B(8)-B(3)-B(2)	59.85(18)
B(1)-B(3)-B(2)	59.37(17)
B(4)-B(3)-B(2)	107.9(2)
Cl(3)-B(3)-B(2)	121.4(2)
B(1)-B(4)-B(10)	107.2(2)
B(1)-B(4)-B(9)	107.0(2)
B(10)-B(4)-B(9)	59.77(18)
B(1)-B(4)-B(5)	59.60(17)
B(10)-B(4)-B(5)	60.24(17)
B(9)-B(4)-B(5)	108.0(2)
B(1)-B(4)-B(3)	59.91(17)
B(10)-B(4)-B(3)	107.7(2)
B(9)-B(4)-B(3)	59.66(18)
B(5)-B(4)-B(3)	108.2(2)
B(1)-B(4)-Cl(4)	122.2(2)
B(10)-B(4)-Cl(4)	121.8(2)
B(9)-B(4)-Cl(4)	122.8(2)

B(5)-B(4)-Cl(4)	120.8(2)
B(3)-B(4)-Cl(4)	122.2(2)
B(1)-B(5)-B(11)	107.1(2)
B(1)-B(5)-Cl(5)	123.44(19)
B(11)-B(5)-Cl(5)	121.65(19)
B(1)-B(5)-B(4)	59.84(17)
B(11)-B(5)-B(4)	107.8(2)
Cl(5)-B(5)-B(4)	121.2(2)
B(1)-B(5)-B(10)	106.9(2)
B(11)-B(5)-B(10)	59.91(17)
Cl(5)-B(5)-B(10)	120.9(2)
B(4)-B(5)-B(10)	59.72(17)
B(1)-B(5)-B(6)	59.64(17)
B(11)-B(5)-B(6)	60.07(17)
Cl(5)-B(5)-B(6)	122.5(2)
B(4)-B(5)-B(6)	108.2(2)
B(10)-B(5)-B(6)	108.0(2)
B(1)-B(6)-B(7)	106.8(2)
B(1)-B(6)-Cl(6)	123.4(2)
B(7)-B(6)-Cl(6)	121.4(2)
B(1)-B(6)-B(11)	106.7(2)
B(7)-B(6)-B(11)	60.30(18)
Cl(6)-B(6)-B(11)	121.6(2)
B(1)-B(6)-B(2)	59.70(17)
B(7)-B(6)-B(2)	59.60(18)
Cl(6)-B(6)-B(2)	121.8(2)
B(11)-B(6)-B(2)	107.8(2)
B(1)-B(6)-B(5)	59.52(16)
B(7)-B(6)-B(5)	108.0(2)
Cl(6)-B(6)-B(5)	122.1(2)
B(11)-B(6)-B(5)	59.73(17)
B(2)-B(6)-B(5)	107.9(2)
B(2)-B(7)-B(6)	60.70(17)
B(2)-B(7)-B(12)	108.4(2)

B(6)-B(7)-B(12)	108.5(2)
B(2)-B(7)-B(11)	108.7(2)
B(6)-B(7)-B(11)	60.30(17)
B(12)-B(7)-B(11)	59.81(18)
B(2)-B(7)-B(8)	60.17(19)
B(6)-B(7)-B(8)	108.6(2)
B(12)-B(7)-B(8)	59.79(19)
B(11)-B(7)-B(8)	107.7(2)
B(2)-B(7)-Cl(7)	120.6(2)
B(6)-B(7)-Cl(7)	120.3(2)
B(12)-B(7)-Cl(7)	122.5(2)
B(11)-B(7)-Cl(7)	121.7(2)
B(8)-B(7)-Cl(7)	122.4(2)
B(3)-B(8)-B(9)	59.88(18)
B(3)-B(8)-B(12)	108.2(2)
B(9)-B(8)-B(12)	60.18(18)
B(3)-B(8)-B(2)	60.80(18)
B(9)-B(8)-B(2)	108.5(2)
B(12)-B(8)-B(2)	107.9(2)
B(3)-B(8)-Cl(8)	121.8(2)
B(9)-B(8)-Cl(8)	120.7(2)
B(12)-B(8)-Cl(8)	120.8(2)
B(2)-B(8)-Cl(8)	122.6(2)
B(3)-B(8)-B(7)	108.0(2)
B(9)-B(8)-B(7)	107.9(2)
B(12)-B(8)-B(7)	59.98(19)
B(2)-B(8)-B(7)	59.38(18)
Cl(8)-B(8)-B(7)	122.4(2)
B(10)-B(9)-B(3)	108.4(2)
B(10)-B(9)-B(8)	108.3(2)
B(3)-B(9)-B(8)	59.92(18)
B(10)-B(9)-B(4)	60.01(17)
B(3)-B(9)-B(4)	60.22(18)
B(8)-B(9)-B(4)	108.1(2)

B(10)-B(9)-Cl(9)	122.3(2)
B(3)-B(9)-Cl(9)	121.0(2)
B(8)-B(9)-Cl(9)	121.0(2)
B(4)-B(9)-Cl(9)	122.0(2)
B(10)-B(9)-B(12)	60.31(18)
B(3)-B(9)-B(12)	108.0(2)
B(8)-B(9)-B(12)	59.95(18)
B(4)-B(9)-B(12)	108.2(2)
Cl(9)-B(9)-B(12)	121.8(2)
B(9)-B(10)-B(4)	60.23(18)
B(9)-B(10)-B(11)	108.1(2)
B(4)-B(10)-B(11)	108.1(2)
B(9)-B(10)-Cl(10)	121.7(2)
B(4)-B(10)-Cl(10)	121.9(2)
B(11)-B(10)-Cl(10)	121.4(2)
B(9)-B(10)-B(5)	108.2(2)
B(4)-B(10)-B(5)	60.03(17)
B(11)-B(10)-B(5)	59.88(17)
Cl(10)-B(10)-B(5)	121.8(2)
B(9)-B(10)-B(12)	60.16(18)
B(4)-B(10)-B(12)	108.2(2)
B(11)-B(10)-B(12)	59.85(18)
Cl(10)-B(10)-B(12)	121.6(2)
B(5)-B(10)-B(12)	107.8(2)
Cl(11)-B(11)-B(12)	121.5(2)
Cl(11)-B(11)-B(5)	121.4(2)
B(12)-B(11)-B(5)	108.3(2)
Cl(11)-B(11)-B(10)	121.1(2)
B(12)-B(11)-B(10)	60.23(18)
B(5)-B(11)-B(10)	60.21(17)
Cl(11)-B(11)-B(7)	122.5(2)
B(12)-B(11)-B(7)	60.00(18)
B(5)-B(11)-B(7)	107.6(2)
B(10)-B(11)-B(7)	108.0(2)

Cl(11)-B(11)-B(6)	122.1(2)
B(12)-B(11)-B(6)	107.9(2)
B(5)-B(11)-B(6)	60.20(17)
B(10)-B(11)-B(6)	108.3(2)
B(7)-B(11)-B(6)	59.40(17)
B(11)-B(12)-B(8)	108.3(2)
B(11)-B(12)-Cl(12)	120.9(2)
B(8)-B(12)-Cl(12)	122.1(2)
B(11)-B(12)-B(7)	60.19(18)
B(8)-B(12)-B(7)	60.24(19)
Cl(12)-B(12)-B(7)	121.1(2)
B(11)-B(12)-B(9)	107.7(2)
B(8)-B(12)-B(9)	59.87(18)
Cl(12)-B(12)-B(9)	122.8(2)
B(7)-B(12)-B(9)	107.9(2)
B(11)-B(12)-B(10)	59.92(17)
B(8)-B(12)-B(10)	107.6(2)
Cl(12)-B(12)-B(10)	122.1(2)
B(7)-B(12)-B(10)	107.8(2)
B(9)-B(12)-B(10)	59.53(18)
B(1)-Cl(1)-Si(1)	125.65(10)
C(5)-Si(1)-C(1)	119.53(13)
C(5)-Si(1)-C(3)	115.11(14)
C(1)-Si(1)-C(3)	116.25(15)
C(5)-Si(1)-Cl(1)	105.67(10)
C(1)-Si(1)-Cl(1)	102.70(10)
C(3)-Si(1)-Cl(1)	91.51(10)
C(2)-C(1)-Si(1)	114.9(2)
C(2)-C(1)-H(1A)	108.5
Si(1)-C(1)-H(1A)	108.5
C(2)-C(1)-H(1B)	108.5
Si(1)-C(1)-H(1B)	108.5
H(1A)-C(1)-H(1B)	107.5
C(1)-C(2)-H(2A)	109.5

C(1)-C(2)-H(2B)	109.5
H(2A)-C(2)-H(2B)	109.5
C(1)-C(2)-H(2C)	109.5
H(2A)-C(2)-H(2C)	109.5
H(2B)-C(2)-H(2C)	109.5
C(4)-C(3)-Si(1)	111.7(2)
C(4)-C(3)-H(3A)	109.3
Si(1)-C(3)-H(3A)	109.3
C(4)-C(3)-H(3B)	109.3
Si(1)-C(3)-H(3B)	109.3
H(3A)-C(3)-H(3B)	107.9
C(3)-C(4)-H(4A)	109.5
C(3)-C(4)-H(4B)	109.5
H(4A)-C(4)-H(4B)	109.5
C(3)-C(4)-H(4C)	109.5
H(4A)-C(4)-H(4C)	109.5
H(4B)-C(4)-H(4C)	109.5
C(6)-C(5)-Si(1)	115.1(2)
C(6)-C(5)-H(5A)	108.5
Si(1)-C(5)-H(5A)	108.5
C(6)-C(5)-H(5B)	108.5
Si(1)-C(5)-H(5B)	108.5
H(5A)-C(5)-H(5B)	107.5
C(5)-C(6)-H(6A)	109.5
C(5)-C(6)-H(6B)	109.5
H(6A)-C(6)-H(6B)	109.5
C(5)-C(6)-H(6C)	109.5
H(6A)-C(6)-H(6C)	109.5
H(6B)-C(6)-H(6C)	109.5
B(15)-B(13)-B(14)#6	108.2(2)
B(15)-B(13)-B(15)#6	108.2(3)
B(14)#6-B(13)-B(15)#6	60.18(19)
B(15)-B(13)-B(16)	60.38(19)
B(14)#6-B(13)-B(16)	108.4(2)

B(15)#6-B(13)-B(16)	59.92(18)
B(15)-B(13)-B(14)	59.95(19)
B(14)#6-B(13)-B(14)	60.1(3)
B(15)#6-B(13)-B(14)	108.1(2)
B(16)-B(13)-B(14)	108.3(2)
B(15)-B(13)-Cl(13)	121.3(2)
B(14)#6-B(13)-Cl(13)	122.2(2)
B(15)#6-B(13)-Cl(13)	121.4(2)
B(16)-B(13)-Cl(13)	120.6(2)
B(14)-B(13)-Cl(13)	122.4(2)
B(13)#7-B(14)-B(15)	59.94(19)
B(13)#7-B(14)-Cl(14)	121.7(2)
B(15)-B(14)-Cl(14)	122.5(2)
B(13)#7-B(14)-B(14)#6	108.1(2)
B(15)-B(14)-B(14)#6	107.59(17)
Cl(14)-B(14)-B(14)#6	121.41(17)
B(13)#7-B(14)-B(14)#7	60.4(2)
B(15)-B(14)-B(14)#7	108.11(16)
Cl(14)-B(14)-B(14)#7	121.00(17)
B(14)#6-B(14)-B(14)#7	60.000(1)
B(13)#7-B(14)-B(13)	107.5(3)
B(15)-B(14)-B(13)	59.60(19)
Cl(14)-B(14)-B(13)	122.7(2)
B(14)#6-B(14)-B(13)	59.6(2)
B(14)#7-B(14)-B(13)	107.5(2)
B(13)-B(15)-B(16)#7	108.1(2)
B(13)-B(15)-B(13)#7	108.1(3)
B(16)#7-B(15)-B(13)#7	60.16(18)
B(13)-B(15)-B(14)	60.5(2)
B(16)#7-B(15)-B(14)	108.3(2)
B(13)#7-B(15)-B(14)	59.88(19)
B(13)-B(15)-Cl(15)	121.3(2)
B(16)#7-B(15)-Cl(15)	122.1(2)
B(13)#7-B(15)-Cl(15)	121.8(2)

B(14)-B(15)-Cl(15)	120.9(2)
B(13)-B(15)-B(16)	59.98(19)
B(16)#7-B(15)-B(16)	59.8(2)
B(13)#7-B(15)-B(16)	107.9(2)
B(14)-B(15)-B(16)	108.4(2)
Cl(15)-B(15)-B(16)	122.0(2)
B(15)#6-B(16)-B(16)#7	108.20(18)
B(15)#6-B(16)-B(16)#6	60.4(2)
B(16)#7-B(16)-B(16)#6	60.000(1)
B(15)#6-B(16)-B(13)	59.92(18)
B(16)#7-B(16)-B(13)	107.71(17)
B(16)#6-B(16)-B(13)	108.15(16)
B(15)#6-B(16)-Cl(16)	121.4(2)
B(16)#7-B(16)-Cl(16)	121.48(15)
B(16)#6-B(16)-Cl(16)	120.79(15)
B(13)-B(16)-Cl(16)	122.5(2)
B(15)#6-B(16)-B(15)	107.6(3)
B(16)#7-B(16)-B(15)	59.8(2)
B(16)#6-B(16)-B(15)	107.69(18)
B(13)-B(16)-B(15)	59.64(18)
Cl(16)-B(16)-B(15)	122.8(2)
B(18)-B(17)-B(17)#5	60.28(19)
B(18)-B(17)-B(17)#2	108.32(17)
B(17)#5-B(17)-B(17)#2	60.000(1)
B(18)-B(17)-B(18)#8	60.19(12)
B(17)#5-B(17)-B(18)#8	108.24(15)
B(17)#2-B(17)-B(18)#8	107.96(15)
B(18)-B(17)-B(18)#2	108.3(2)
B(17)#5-B(17)-B(18)#2	107.95(17)
B(17)#2-B(17)-B(18)#2	59.82(19)
B(18)#8-B(17)-B(18)#2	60.03(12)
B(18)-B(17)-Cl(17)	121.88(19)
B(17)#5-B(17)-Cl(17)	120.88(14)
B(17)#2-B(17)-Cl(17)	120.79(14)

B(18)#8-B(17)-Cl(17)	122.69(19)
B(18)#2-B(17)-Cl(17)	121.89(19)
B(17)-B(18)-B(17)#9	107.9(2)
B(17)-B(18)-Cl(18)	121.37(19)
B(17)#9-B(18)-Cl(18)	122.52(19)
B(17)-B(18)-B(17)#5	59.9(2)
B(17)#9-B(18)-B(17)#5	107.6(2)
Cl(18)-B(18)-B(17)#5	121.29(18)
B(17)-B(18)-B(18)#8	60.12(14)
B(17)#9-B(18)-B(18)#8	60.01(18)
Cl(18)-B(18)-B(18)#8	122.13(19)
B(17)#5-B(18)-B(18)#8	107.88(15)
B(17)-B(18)-B(18)#9	107.97(15)
B(17)#9-B(18)-B(18)#9	59.70(18)
Cl(18)-B(18)-B(18)#9	121.73(19)
B(17)#5-B(18)-B(18)#9	59.96(14)
B(18)#8-B(18)-B(18)#9	107.88(18)
B(17)-Cl(17)-Ag(1)	93.88(10)

Symmetry transformations used to generate equivalent atoms:
#1 y+1,-x+y+1,-z+1 #2 -y+1,x-y-1,z #3 -x+2,-y,-z+1
#4 x-y,x-1,-z+1 #5 -x+y+2,-x+1,z #6 -x+y+1,-x+1,z
#7 -y+1,x-y,z #8 x-y,x-1,-z #9 y+1,-x+y+1,-z

F.2.4 Anisotropic Displacement Parameters

Anisotropic displacement parameters ($Å^2 x\ 10^3$) for cr308_0m. The anisotropic displacement factor exponent takes the form: $-2p^2[\ h^2\ a^{*2}U^{11} + ...\ + 2\ h\ k\ a^*\ b^*\ U^{12}\ ]$

	U^{11}	U^{22}	U^{33}	U^{23}	U^{13}	U^{12}
Ag(1)	27(7)	27(7)	4(7)	0	0	13(3)
C(1A)	31(2)	38(2)	35(2)	-12(1)	-4(1)	20(2)
C(2A)	31(2)	41(2)	40(2)	-7(2)	0(1)	23(2)

C(3A)	50(2)	42(2)	36(2)	-5(2)	-3(2)	34(2)
C(4A)	66(3)	42(2)	45(2)	-15(2)	-20(2)	41(2)
C(5A)	55(2)	30(2)	44(2)	-8(2)	-18(2)	25(2)
C(6A)	35(2)	39(2)	41(2)	-8(2)	-8(2)	23(2)
C(7A)	46(2)	39(2)	49(2)	-4(2)	8(2)	14(2)
C(8A)	69(3)	80(3)	67(3)	-9(3)	-5(2)	47(3)
C(9A)	122(4)	53(3)	49(2)	-22(2)	-40(3)	58(3)
C(10A)	131(5)	39(3)	83(4)	-11(2)	-51(4)	31(3)
C(11A)	50(2)	54(2)	40(2)	0(2)	-6(2)	24(2)
C(1B)	31(2)	35(2)	39(2)	6(1)	0(1)	24(2)
C(2B)	28(2)	30(2)	41(2)	0(1)	-1(1)	16(1)
C(3B)	38(2)	31(2)	39(2)	6(1)	8(1)	22(2)
C(4B)	41(2)	46(2)	34(2)	6(2)	4(2)	24(2)
C(5B)	36(2)	49(2)	38(2)	-1(2)	-3(2)	28(2)
C(6B)	26(2)	38(2)	39(2)	6(2)	2(1)	16(1)
C(7B)	30(2)	45(2)	36(2)	6(2)	1(1)	20(2)
C(8B)	45(2)	36(2)	41(2)	9(2)	14(2)	20(2)
C(9B)	79(3)	67(3)	41(2)	-2(2)	5(2)	43(3)
C(10B)	38(2)	59(3)	46(2)	-7(2)	-5(2)	25(2)
B(1)	22(2)	19(1)	15(1)	-1(1)	0(1)	11(1)
B(2)	25(2)	23(2)	19(1)	0(1)	-1(1)	14(1)
B(3)	21(2)	20(2)	25(2)	3(1)	3(1)	11(1)
B(4)	17(1)	17(1)	21(1)	-1(1)	1(1)	8(1)
B(5)	20(1)	18(1)	16(1)	2(1)	1(1)	11(1)
B(6)	17(1)	19(1)	18(1)	-1(1)	-1(1)	9(1)
B(7)	18(2)	25(2)	27(2)	-5(1)	-1(1)	14(1)
B(8)	25(2)	20(2)	28(2)	-1(1)	0(1)	16(1)
B(9)	19(2)	16(1)	27(2)	-4(1)	0(1)	7(1)
B(10)	20(2)	21(2)	19(1)	-4(1)	0(1)	11(1)
B(11)	19(1)	23(2)	18(1)	-3(1)	0(1)	11(1)
B(12)	22(2)	22(2)	25(2)	-6(1)	-1(1)	13(1)
Cl(1)	34(1)	24(1)	15(1)	1(1)	2(1)	18(1)
Cl(2)	39(1)	35(1)	25(1)	-1(1)	-9(1)	25(1)
Cl(3)	35(1)	25(1)	28(1)	10(1)	9(1)	14(1)

Cl(4)	18(1)	26(1)	30(1)	-2(1)	2(1)	12(1)
Cl(5)	28(1)	20(1)	18(1)	1(1)	-1(1)	14(1)
Cl(6)	19(1)	22(1)	29(1)	-4(1)	-3(1)	6(1)
Cl(7)	21(1)	36(1)	41(1)	-9(1)	-2(1)	18(1)
Cl(8)	42(1)	24(1)	46(1)	0(1)	-3(1)	22(1)
Cl(9)	25(1)	20(1)	45(1)	-8(1)	-1(1)	6(1)
Cl(10)	29(1)	33(1)	21(1)	-6(1)	-8(1)	16(1)
Cl(11)	27(1)	34(1)	21(1)	2(1)	8(1)	12(1)
Cl(12)	32(1)	33(1)	32(1)	-14(1)	-1(1)	19(1)
Si(1)	25(1)	22(1)	16(1)	-1(1)	1(1)	12(1)
C(1)	24(1)	25(2)	23(1)	-1(1)	2(1)	12(1)
C(2)	25(2)	36(2)	31(2)	-4(1)	7(1)	11(1)
C(3)	44(2)	29(2)	16(1)	-1(1)	-1(1)	20(2)
C(4)	75(3)	41(2)	17(1)	2(1)	4(2)	41(2)
C(5)	23(1)	22(1)	22(1)	-2(1)	-1(1)	10(1)
C(6)	26(2)	39(2)	34(2)	-10(1)	-8(1)	13(1)
B(13)	25(2)	21(2)	31(2)	-4(1)	-4(1)	12(1)
B(14)	29(2)	28(2)	24(2)	-5(1)	2(1)	15(2)
B(15)	21(2)	21(2)	28(2)	-4(1)	-1(1)	12(1)
B(16)	23(2)	20(2)	24(2)	1(1)	-2(1)	12(1)
Cl(13)	35(1)	23(1)	45(1)	-9(1)	-7(1)	15(1)
Cl(14)	44(1)	47(1)	34(1)	-8(1)	10(1)	23(1)
Cl(15)	24(1)	31(1)	49(1)	-7(1)	-6(1)	18(1)
Cl(16)	34(1)	29(1)	32(1)	8(1)	-2(1)	17(1)
B(17)	19(1)	21(1)	9(1)	0(1)	1(1)	10(1)
B(18)	22(1)	17(1)	11(1)	-2(1)	-1(1)	11(1)
Cl(17)	24(1)	30(1)	13(1)	-1(1)	3(1)	15(1)
Cl(18)	31(1)	21(1)	20(1)	-2(1)	-1(1)	16(1)

F.2.5 Hydrogen Coordinates

Hydrogen coordinates (x 10^4) and isotropic displacement parameters ($Å^2$x 10^3) for cr308_0m.

	x	y	z	U(eq)
H(11A)	8735(14)	3749(14)	2710(40)	40
H(12A)	8327(15)	3875(14)	2900(40)	40
H(71A)	7977	3045	5754	71
H(72A)	8351	2973	4747	71
H(73A)	7929	3039	4004	71
H(81A)	8347	3385	7478	101
H(82A)	8400	3886	8070	101
H(83A)	8862	3808	8077	101
H(91A)	9047	4619	8039	102
H(92A)	9360	5092	7040	102
H(93A)	9571	4739	7433	102
H(101)	9602	5323	3362	133
H(102)	9833	5287	4887	133
H(103)	9402	5413	4876	133
H(111)	8987	4941	1755	74
H(112)	8803	4415	1039	74
H(113)	9368	4758	1435	74
H(11B)	3808(14)	1889(14)	2910(40)	38
H(12B)	3685(14)	2235(13)	3200(40)	38
H(61B)	5054	3161	3102	42
H(71B)	4763	2767	799	56
H(72B)	4228	2701	708	56
H(73B)	4293	2231	740	56
H(81B)	3412	1934	6570	61
H(83B)	3564	1532	6199	61
H(82B)	3239	1635	5062	61

H(91B)	4267	2059	7671	89
H(92B)	4157	2491	8003	89
H(93B)	4708	2607	7850	89
H(104)	5044	3395	6737	71
H(105)	5382	3537	5305	71
H(106)	5362	3139	6429	71
H(1A)	10564	2145	9062	29
H(1B)	10594	1737	8111	29
H(2A)	11295	2505	7720	49
H(2B)	10962	2720	7145	49
H(2C)	10998	2310	6214	49
H(3A)	9633	1867	4897	34
H(3B)	10217	2152	4826	34
H(4A)	9880	1413	3456	59
H(4B)	9630	1109	4917	59
H(4C)	10212	1403	4768	59
H(5A)	9432	1081	8300	28
H(5B)	9368	1493	9113	28
H(6A)	8643	973	7875	52
H(6B)	8931	1060	6357	52
H(6C)	8886	1496	7090	52

F.3 References

1. *APEX 2,* version 2009.5-1, Bruker (2009), Bruker AXS Inc., Madison, Wisconsin, USA.

2. *SAINT,* version V7.60A, Bruker (2009), Bruker AXS Inc., Madison, Wisconsin, USA.

3. *SADABS,* version 2008/1, Bruker (2008), Bruker AXS Inc., Madison, Wisconsin, USA.

4. *SHELXTL,* version 2008/4, Bruker (2008), Bruker AXS Inc., Madison, Wisconsin, USA.

Appendix G. X-ray Structure Determination for $[(Et_3Si)Me_4N_2]_2[B_{12}Cl_{12}]\cdot ODCB$

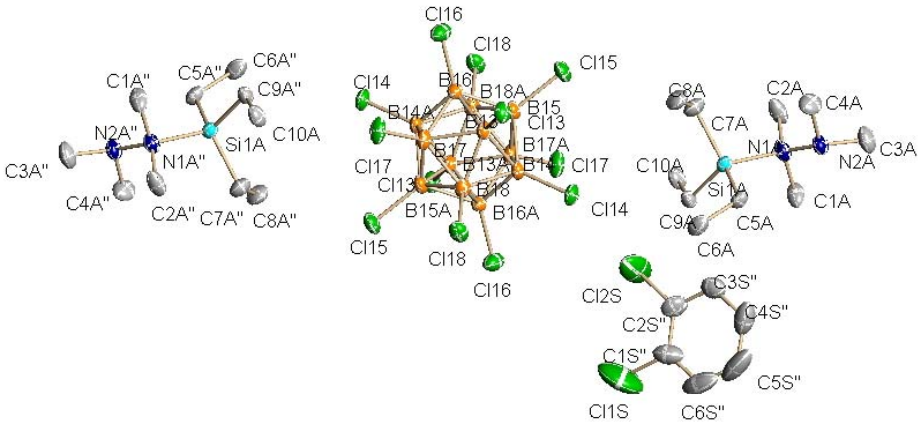

G.1 Experimental Details

The Bruker X8-APEX (**ref. 1**) X-ray diffraction instrument with Mo-radiation was used for data collection**.** All data frames were collected at low temperatures (T = 100 K) using an ω, φ-scan mode (0.5° ω-scan width, hemisphere of reflections) and integrated using a Bruker SAINTPLUS software package (**ref. 2**). The intensity data were corrected for Lorentzian polarization. Absorption corrections were applied for all data using the SADABS program (**ref. 3**) in the SAINTPLUS software (**ref. 2**). The Bruker SHELXTL (Version 6.10) software (**ref. 5**) in the APEX 2 package (**ref. 1**) was used for phase determination and structure refinement. Direct methods of phase determination followed by some subsequent difference Fourier map led to an electron density map from which most of the non-hydrogen atoms were identified in the asymmetry unit of the unit cell. With subsequent isotropic refinement, all of the non-hydrogen atoms were identified. Atomic coordinates, isotropic and anisotropic displacement parameters of all the non-hydrogen atoms were refined by means of a full matrix least-squares procedure on F^2. The H-atoms

were included in the refinement in calculated positions riding on the atoms to which they were attached.

G.2 Structure Details

G.2.1 Crystal structure and refinement data for $[(Et_3Si)Me_4N_2]_2[B_{12}Cl_{12}]\cdot$ODCB.

Identification code	chr0617_final	
Empirical formula	C40 H88 B18 Cl21 N6 Si3	
Formula weight	1676.46	
Temperature	100(2) K	
Wavelength	0.71073 Å	
Crystal system	Triclinic	
Space group	P-1	
Unit cell dimensions	a = 12.8515(13) Å	□= 109.668(4)°.
	b = 16.5164(16) Å	□= 105.693(4)°.
	c = 20.4973(19) Å	□ = 93.815(4)°.
Volume	3884.2(7) Å^3	
Z	2	
Density (calculated)	1.433 Mg/m^3	
Absorption coefficient	0.820 mm^{-1}	
F(000)	1718	
Crystal size	102.00 x 0.26 x 0.17 mm^3	
Theta range for data collection	1.33 to 23.53°.	
Index ranges	-14<=h<=14, -18<=k<=18, -22<=l<=23	
Reflections collected	27567	
Independent reflections	11268 [R(int) = 0.0225]	
Completeness to theta = 23.53°	97.5 %	
Absorption correction	None	
Max. and min. transmission	0.8732 and 0.0089	
Refinement method	Full-matrix least-squares on F^2	
Data / restraints / parameters	11268 / 6 / 907	

Goodness-of-fit on F^2	1.024
Final R indices [I>2sigma(I)]	R1 = 0.0521, wR2 = 0.1343
R indices (all data)	R1 = 0.0642, wR2 = 0.1449
Largest diff. peak and hole	1.165 and -0.831 e.$Å^{-3}$

G.2.2 Atomic Coordinates

Atomic coordinates (x 10^4) and equivalent isotropic displacement parameters ($Å^2$x 10^3) for $[(Et_3Si)Me_4N_2]_2[B_{12}Cl_{12}]\cdot$ODCB. U(eq) is defined as one third of the trace of the orthogonalized U^{ij} tensor.

	x	y	z	U(eq)
Si(1A)	9243(1)	2215(1)	9780(1)	22(1)
N(1A)	10782(3)	2163(2)	9955(2)	27(1)
N(2A)	11023(3)	1361(2)	10100(2)	29(1)
C(1A)	11012(4)	2061(4)	9251(3)	39(1)
C(2A)	11468(4)	2989(3)	10538(3)	42(1)
C(3A)	12156(4)	1234(3)	10164(3)	45(1)
C(4A)	10782(5)	1379(4)	10764(3)	45(1)
C(5A)	8526(4)	1063(3)	9300(2)	28(1)
C(6A)	7304(4)	969(3)	8909(3)	38(1)
C(7A)	9027(4)	2805(3)	10677(3)	36(1)
C(8A)	8125(4)	2350(4)	10846(3)	42(1)
C(9A)	8898(4)	2861(3)	9185(2)	28(1)
C(10A)	9496(4)	3799(3)	9449(3)	36(1)
Si(1B)	5733(3)	3526(3)	3443(2)	30(1)
N(1B)	6789(11)	4216(7)	3226(5)	29(3)
N(2B)	7298(6)	5037(6)	3895(6)	37(2)
C(1B)	6113(8)	4514(7)	2666(5)	47(2)
C(2B)	7584(8)	3716(5)	2963(5)	40(2)
C(3B)	8076(11)	5603(7)	3750(6)	81(4)
C(4B)	7869(8)	4856(5)	4527(4)	53(2)

C(5B)	5010(7)	4311(6)	3998(5)	55(2)
C(6B)	3906(9)	4465(8)	3584(8)	90(4)
C(7B)	4730(6)	2811(5)	2559(4)	44(2)
C(8B)	5089(11)	2125(9)	2011(9)	49(4)
C(9B)	6510(20)	2910(20)	3920(18)	65(10)
C(10B)	5760(20)	2065(9)	3836(9)	48(5)
Si(1D)	5940(8)	3458(7)	3228(5)	36(2)
N(1D)	6910(20)	4522(16)	3520(12)	31(5)
N(2D)	8036(12)	4371(9)	3594(7)	52(4)
C(1D)	6570(20)	5014(15)	3018(14)	66(6)
C(2D)	6898(19)	5132(11)	4263(11)	54(5)
C(3D)	8155(18)	3945(13)	2865(12)	59(5)
C(4D)	8850(20)	5120(15)	4005(14)	88(8)
C(5D)	4615(14)	3754(11)	3369(9)	46(4)
C(6D)	3860(20)	4111(16)	2830(14)	87(8)
C(7D)	5685(13)	2744(13)	2271(8)	38(4)
C(8D)	4620(20)	2010(30)	1941(18)	65(10)
C(10D)	5980(50)	2120(40)	3820(30)	100(20)
C(9D)	6520(20)	2900(20)	3960(20)	11(8)
Si(1C)	4574(1)	8022(1)	3490(1)	28(1)
N(1C)	5624(3)	8673(2)	3253(2)	30(1)
N(2C)	5021(3)	9071(2)	2742(2)	32(1)
C(1C)	6469(4)	9305(3)	3933(3)	36(1)
C(2C)	6214(4)	8027(3)	2836(3)	37(1)
C(3C)	4411(4)	9706(3)	3090(3)	35(1)
C(4C)	5738(4)	9486(4)	2448(3)	44(1)
C(5C)	5296(4)	7196(3)	3789(3)	40(1)
C(6C)	4769(5)	6826(4)	4225(3)	52(2)
C(7C)	4217(4)	8779(3)	4288(2)	33(1)
C(8C)	3047(4)	8513(3)	4261(3)	37(1)
C(9C)	3420(4)	7524(3)	2621(2)	32(1)
C(10C)	2745(4)	6688(3)	2545(3)	40(1)
Cl(1)	2487(1)	1292(1)	2529(1)	31(1)
Cl(2)	2646(1)	3074(1)	4236(1)	53(1)

Cl(3)	391(1)	2722(1)	2573(1)	39(1)
Cl(4)	-461(1)	340(1)	1569(1)	25(1)
Cl(5)	1326(1)	-745(1)	2611(1)	27(1)
Cl(6)	3220(1)	964(1)	4272(1)	43(1)
Cl(7)	-1337(1)	1198(1)	4377(1)	37(1)
Cl(8)	-2056(1)	1519(1)	2665(1)	28(1)
Cl(9)	-166(1)	3221(1)	4322(1)	41(1)
Cl(10)	1574(1)	2124(1)	5360(1)	60(1)
Cl(11)	799(1)	-204(1)	4375(1)	51(1)
Cl(12)	-1436(1)	-616(1)	2678(1)	34(1)
Cl(13)	4419(1)	3400(1)	674(1)	30(1)
Cl(14)	5882(1)	3019(1)	-677(1)	30(1)
Cl(15)	7206(1)	4585(1)	1199(1)	35(1)
Cl(16)	5050(1)	5738(1)	1815(1)	37(1)
Cl(17)	2494(1)	4896(1)	342(1)	38(1)
Cl(18)	2994(1)	3200(1)	-1209(1)	34(1)
B(1)	1507(4)	1274(3)	3009(3)	23(1)
B(2)	1585(4)	2141(3)	3838(3)	29(1)
B(3)	492(4)	1963(3)	3024(3)	24(1)
B(4)	98(4)	812(3)	2541(2)	20(1)
B(5)	955(4)	283(3)	3051(2)	21(1)
B(6)	1860(4)	1101(4)	3849(3)	30(1)
B(7)	-341(4)	1211(4)	3913(3)	28(1)
B(8)	-688(4)	1387(3)	3078(2)	22(1)
B(9)	221(4)	2209(3)	3878(3)	27(1)
B(10)	1065(4)	1676(4)	4386(3)	33(1)
B(11)	680(4)	527(4)	3900(3)	30(1)
B(12)	-402(4)	350(3)	3090(3)	24(1)
B(13)	4711(4)	4225(3)	325(3)	24(1)
B(14)	5437(4)	4042(3)	-328(3)	24(1)
B(15)	6067(4)	4797(3)	583(3)	25(1)
B(16)	5044(4)	5356(3)	887(3)	24(1)
B(17)	3773(4)	4939(3)	159(3)	26(1)
B(18)	4020(4)	4131(3)	-583(3)	25(1)

Cl(1S)	1335(2)	5397(2)	3809(1)	129(1)
Cl(2S)	243(2)	4730(1)	2104(1)	95(1)
C(1S)	687(5)	6069(4)	3403(3)	56(2)
C(2S)	208(5)	5764(3)	2655(3)	46(1)
C(3S)	-335(4)	6300(4)	2335(3)	48(1)
C(4S)	-354(5)	7134(4)	2779(4)	68(2)
C(5S)	130(6)	7408(5)	3513(5)	90(3)
C(6S)	625(6)	6882(6)	3821(4)	78(2)
C(7S)	3607(7)	251(6)	8990(5)	95(3)
C(8S)	4289(8)	1096(6)	9432(5)	97(3)
C(9S)	5319(4)	399(3)	10213(2)	26(1)
C(10S)	5057(15)	1303(12)	10112(10)	39(7)
C(11S)	6506(12)	587(9)	10895(7)	22(4)
Cl(3S)	5075(3)	1242(2)	9988(2)	26(1)
Cl(4S)	6343(3)	548(3)	10962(2)	41(1)

G.2.3 Bond Lengths and Angles

Bond lengths [Å] and angles [°] for $[(Et_3Si)Me_4N_2]_2[B_{12}Cl_{12}]\cdot$ODCB.

Si(1A)-C(5A)	1.858(4)
Si(1A)-C(9A)	1.863(4)
Si(1A)-C(7A)	1.874(5)
Si(1A)-N(1A)	1.926(4)
N(1A)-N(2A)	1.487(5)
N(1A)-C(2A)	1.497(6)
N(1A)-C(1A)	1.508(6)
N(2A)-C(3A)	1.461(6)
N(2A)-C(4A)	1.467(6)
C(5A)-C(6A)	1.529(6)
C(7A)-C(8A)	1.518(7)
C(9A)-C(10A)	1.528(6)
Si(1B)-C(9B)	1.80(3)

Si(1B)-C(7B)	1.853(9)
Si(1B)-C(5B)	1.892(9)
Si(1B)-N(1B)	1.949(14)
N(1B)-C(2B)	1.458(15)
N(1B)-C(1B)	1.487(14)
N(1B)-N(2B)	1.514(10)
N(2B)-C(4B)	1.442(12)
N(2B)-C(3B)	1.478(12)
C(5B)-C(6B)	1.529(14)
C(7B)-C(8B)	1.501(17)
C(9B)-C(10B)	1.58(4)
Si(1D)-C(7D)	1.841(18)
Si(1D)-C(5D)	1.872(17)
Si(1D)-N(1D)	1.89(3)
Si(1D)-C(9D)	2.02(4)
N(1D)-N(2D)	1.47(3)
N(1D)-C(1D)	1.51(3)
N(1D)-C(2D)	1.52(2)
N(2D)-C(4D)	1.41(2)
N(2D)-C(3D)	1.48(2)
C(5D)-C(6D)	1.56(3)
C(7D)-C(8D)	1.59(3)
C(10D)-C(9D)	1.32(8)
Si(1C)-C(9C)	1.863(4)
Si(1C)-C(5C)	1.877(5)
Si(1C)-C(7C)	1.885(5)
Si(1C)-N(1C)	1.930(4)
N(1C)-N(2C)	1.490(5)
N(1C)-C(1C)	1.504(6)
N(1C)-C(2C)	1.512(5)
N(2C)-C(3C)	1.461(6)
N(2C)-C(4C)	1.476(6)
C(5C)-C(6C)	1.508(8)
C(7C)-C(8C)	1.520(7)

C(9C)-C(10C)	1.519(7)
Cl(1)-B(1)	1.800(5)
Cl(2)-B(2)	1.780(5)
Cl(3)-B(3)	1.783(5)
Cl(4)-B(4)	1.790(5)
Cl(5)-B(5)	1.798(5)
Cl(6)-B(6)	1.795(5)
Cl(7)-B(7)	1.792(5)
Cl(8)-B(8)	1.797(5)
Cl(9)-B(9)	1.790(5)
Cl(10)-B(10)	1.789(5)
Cl(11)-B(11)	1.778(5)
Cl(12)-B(12)	1.797(5)
Cl(13)-B(13)	1.801(5)
Cl(14)-B(14)	1.797(5)
Cl(15)-B(15)	1.796(5)
Cl(16)-B(16)	1.790(5)
Cl(17)-B(17)	1.785(5)
Cl(18)-B(18)	1.799(5)
B(1)-B(5)	1.779(7)
B(1)-B(4)	1.779(7)
B(1)-B(6)	1.783(7)
B(1)-B(3)	1.787(7)
B(1)-B(2)	1.788(7)
B(2)-B(6)	1.783(8)
B(2)-B(3)	1.785(7)
B(2)-B(9)	1.786(7)
B(2)-B(10)	1.795(8)
B(3)-B(8)	1.785(7)
B(3)-B(4)	1.785(6)
B(3)-B(9)	1.794(7)
B(4)-B(8)	1.776(6)
B(4)-B(12)	1.779(7)
B(4)-B(5)	1.786(6)

B(5)-B(6)	1.769(7)
B(5)-B(12)	1.775(6)
B(5)-B(11)	1.786(7)
B(6)-B(11)	1.781(8)
B(6)-B(10)	1.785(7)
B(7)-B(8)	1.775(7)
B(7)-B(10)	1.779(8)
B(7)-B(12)	1.781(7)
B(7)-B(9)	1.787(8)
B(7)-B(11)	1.788(6)
B(8)-B(9)	1.775(7)
B(8)-B(12)	1.783(6)
B(9)-B(10)	1.780(7)
B(10)-B(11)	1.781(8)
B(11)-B(12)	1.773(7)
B(13)-B(15)	1.776(7)
B(13)-B(18)	1.780(7)
B(13)-B(16)	1.782(7)
B(13)-B(14)	1.786(7)
B(13)-B(17)	1.787(6)
B(14)-B(16)#1	1.775(7)
B(14)-B(17)#1	1.782(7)
B(14)-B(15)	1.783(7)
B(14)-B(18)	1.783(7)
B(15)-B(17)#1	1.775(7)
B(15)-B(18)#1	1.782(6)
B(15)-B(16)	1.784(7)
B(16)-B(14)#1	1.775(7)
B(16)-B(18)#1	1.781(7)
B(16)-B(17)	1.791(7)
B(17)-B(18)	1.774(7)
B(17)-B(15)#1	1.775(7)
B(17)-B(14)#1	1.782(7)
B(18)-B(16)#1	1.781(7)

B(18)-B(15)#1	1.782(6)
Cl(1S)-C(1S)	1.729(7)
Cl(2S)-C(2S)	1.713(5)
C(1S)-C(6S)	1.350(10)
C(1S)-C(2S)	1.383(8)
C(2S)-C(3S)	1.387(8)
C(3S)-C(4S)	1.378(8)
C(4S)-C(5S)	1.362(11)
C(5S)-C(6S)	1.336(12)
C(7S)-Cl(4S)#2	1.361(9)
C(7S)-C(8S)	1.447(12)
C(7S)-C(11S)#2	1.485(16)
C(8S)-Cl(3S)	1.240(10)
C(8S)-C(10S)	1.39(2)
C(9S)-C(9S)#2	1.366(9)
C(9S)-C(10S)	1.621(19)
C(9S)-Cl(3S)	1.632(6)
C(9S)-Cl(4S)	1.662(6)
C(9S)-C(11S)	1.694(14)
C(11S)-C(7S)#2	1.485(16)
Cl(4S)-C(7S)#2	1.361(9)

C(5A)-Si(1A)-C(9A)	111.4(2)
C(5A)-Si(1A)-C(7A)	115.5(2)
C(9A)-Si(1A)-C(7A)	109.4(2)
C(5A)-Si(1A)-N(1A)	105.37(18)
C(9A)-Si(1A)-N(1A)	106.45(18)
C(7A)-Si(1A)-N(1A)	108.2(2)
N(2A)-N(1A)-C(2A)	114.0(3)
N(2A)-N(1A)-C(1A)	106.0(3)
C(2A)-N(1A)-C(1A)	108.9(4)
N(2A)-N(1A)-Si(1A)	110.2(2)
C(2A)-N(1A)-Si(1A)	110.8(3)
C(1A)-N(1A)-Si(1A)	106.6(3)

C(3A)-N(2A)-C(4A)	109.5(4)
C(3A)-N(2A)-N(1A)	113.0(3)
C(4A)-N(2A)-N(1A)	110.3(3)
C(6A)-C(5A)-Si(1A)	113.7(3)
C(8A)-C(7A)-Si(1A)	115.9(3)
C(10A)-C(9A)-Si(1A)	119.6(3)
C(9B)-Si(1B)-C(7B)	112.3(10)
C(9B)-Si(1B)-C(5B)	113.7(11)
C(7B)-Si(1B)-C(5B)	109.5(4)
C(9B)-Si(1B)-N(1B)	106.3(10)
C(7B)-Si(1B)-N(1B)	107.0(4)
C(5B)-Si(1B)-N(1B)	107.5(5)
C(2B)-N(1B)-C(1B)	111.6(8)
C(2B)-N(1B)-N(2B)	114.1(10)
C(1B)-N(1B)-N(2B)	105.4(9)
C(2B)-N(1B)-Si(1B)	112.4(8)
C(1B)-N(1B)-Si(1B)	104.9(8)
N(2B)-N(1B)-Si(1B)	107.8(7)
C(4B)-N(2B)-C(3B)	108.8(8)
C(4B)-N(2B)-N(1B)	112.8(8)
C(3B)-N(2B)-N(1B)	110.1(10)
C(6B)-C(5B)-Si(1B)	117.1(8)
C(8B)-C(7B)-Si(1B)	120.5(7)
C(10B)-C(9B)-Si(1B)	111.1(16)
C(7D)-Si(1D)-C(5D)	109.4(9)
C(7D)-Si(1D)-N(1D)	113.9(9)
C(5D)-Si(1D)-N(1D)	106.6(10)
C(7D)-Si(1D)-C(9D)	114.6(12)
C(5D)-Si(1D)-C(9D)	104.4(11)
N(1D)-Si(1D)-C(9D)	107.3(12)
N(2D)-N(1D)-C(1D)	110.7(17)
N(2D)-N(1D)-C(2D)	107.1(18)
C(1D)-N(1D)-C(2D)	105.3(19)
N(2D)-N(1D)-Si(1D)	110.6(16)

C(1D)-N(1D)-Si(1D)	113.0(17)
C(2D)-N(1D)-Si(1D)	109.8(15)
C(4D)-N(2D)-N(1D)	115.0(18)
C(4D)-N(2D)-C(3D)	110.2(17)
N(1D)-N(2D)-C(3D)	109.8(14)
C(6D)-C(5D)-Si(1D)	119.0(14)
C(8D)-C(7D)-Si(1D)	114.7(16)
C(10D)-C(9D)-Si(1D)	116(3)
C(9C)-Si(1C)-C(5C)	113.4(2)
C(9C)-Si(1C)-C(7C)	115.8(2)
C(5C)-Si(1C)-C(7C)	107.9(2)
C(9C)-Si(1C)-N(1C)	104.1(2)
C(5C)-Si(1C)-N(1C)	106.1(2)
C(7C)-Si(1C)-N(1C)	109.1(2)
N(2C)-N(1C)-C(1C)	115.1(3)
N(2C)-N(1C)-C(2C)	106.3(3)
C(1C)-N(1C)-C(2C)	107.7(3)
N(2C)-N(1C)-Si(1C)	108.9(3)
C(1C)-N(1C)-Si(1C)	111.0(3)
C(2C)-N(1C)-Si(1C)	107.6(3)
C(3C)-N(2C)-C(4C)	109.4(4)
C(3C)-N(2C)-N(1C)	111.0(3)
C(4C)-N(2C)-N(1C)	113.4(3)
C(6C)-C(5C)-Si(1C)	114.1(3)
C(8C)-C(7C)-Si(1C)	112.3(3)
C(10C)-C(9C)-Si(1C)	114.3(3)
B(5)-B(1)-B(4)	60.3(3)
B(5)-B(1)-B(6)	59.6(3)
B(4)-B(1)-B(6)	107.5(3)
B(5)-B(1)-B(3)	108.4(3)
B(4)-B(1)-B(3)	60.1(3)
B(6)-B(1)-B(3)	107.8(3)
B(5)-B(1)-B(2)	107.8(3)
B(4)-B(1)-B(2)	107.7(3)

B(6)-B(1)-B(2)	59.9(3)
B(3)-B(1)-B(2)	59.9(3)
B(5)-B(1)-Cl(1)	121.0(3)
B(4)-B(1)-Cl(1)	121.9(3)
B(6)-B(1)-Cl(1)	121.7(3)
B(3)-B(1)-Cl(1)	122.2(3)
B(2)-B(1)-Cl(1)	122.2(3)
Cl(2)-B(2)-B(6)	121.4(3)
Cl(2)-B(2)-B(3)	122.1(4)
B(6)-B(2)-B(3)	107.9(3)
Cl(2)-B(2)-B(9)	122.3(3)
B(6)-B(2)-B(9)	107.5(4)
B(3)-B(2)-B(9)	60.3(3)
Cl(2)-B(2)-B(1)	121.6(3)
B(6)-B(2)-B(1)	59.9(3)
B(3)-B(2)-B(1)	60.0(3)
B(9)-B(2)-B(1)	108.1(3)
Cl(2)-B(2)-B(10)	121.6(3)
B(6)-B(2)-B(10)	59.9(3)
B(3)-B(2)-B(10)	108.0(4)
B(9)-B(2)-B(10)	59.6(3)
B(1)-B(2)-B(10)	107.8(4)
Cl(3)-B(3)-B(8)	122.2(3)
Cl(3)-B(3)-B(4)	122.5(3)
B(8)-B(3)-B(4)	59.7(3)
Cl(3)-B(3)-B(2)	121.7(3)
B(8)-B(3)-B(2)	107.2(4)
B(4)-B(3)-B(2)	107.6(3)
Cl(3)-B(3)-B(1)	122.3(3)
B(8)-B(3)-B(1)	107.3(3)
B(4)-B(3)-B(1)	59.7(3)
B(2)-B(3)-B(1)	60.1(3)
Cl(3)-B(3)-B(9)	121.5(3)
B(8)-B(3)-B(9)	59.5(3)

B(4)-B(3)-B(9)	107.4(3)
B(2)-B(3)-B(9)	59.9(3)
B(1)-B(3)-B(9)	107.7(3)
B(8)-B(4)-B(12)	60.2(3)
B(8)-B(4)-B(1)	108.0(3)
B(12)-B(4)-B(1)	107.8(3)
B(8)-B(4)-B(3)	60.2(3)
B(12)-B(4)-B(3)	108.4(3)
B(1)-B(4)-B(3)	60.2(3)
B(8)-B(4)-B(5)	107.8(3)
B(12)-B(4)-B(5)	59.7(3)
B(1)-B(4)-B(5)	59.9(3)
B(3)-B(4)-B(5)	108.2(3)
B(8)-B(4)-Cl(4)	120.7(3)
B(12)-B(4)-Cl(4)	120.2(3)
B(1)-B(4)-Cl(4)	123.3(3)
B(3)-B(4)-Cl(4)	122.2(3)
B(5)-B(4)-Cl(4)	122.0(3)
B(6)-B(5)-B(12)	107.6(3)
B(6)-B(5)-B(1)	60.3(3)
B(12)-B(5)-B(1)	108.0(3)
B(6)-B(5)-B(4)	107.8(3)
B(12)-B(5)-B(4)	59.9(3)
B(1)-B(5)-B(4)	59.9(3)
B(6)-B(5)-B(11)	60.1(3)
B(12)-B(5)-B(11)	59.7(3)
B(1)-B(5)-B(11)	108.6(3)
B(4)-B(5)-B(11)	107.9(3)
B(6)-B(5)-Cl(5)	122.5(3)
B(12)-B(5)-Cl(5)	121.1(3)
B(1)-B(5)-Cl(5)	122.1(3)
B(4)-B(5)-Cl(5)	121.6(3)
B(11)-B(5)-Cl(5)	121.3(3)
B(5)-B(6)-B(11)	60.4(3)

B(5)-B(6)-B(2)	108.5(3)
B(11)-B(6)-B(2)	108.6(3)
B(5)-B(6)-B(1)	60.1(3)
B(11)-B(6)-B(1)	108.7(3)
B(2)-B(6)-B(1)	60.2(3)
B(5)-B(6)-B(10)	108.4(4)
B(11)-B(6)-B(10)	59.9(3)
B(2)-B(6)-B(10)	60.4(3)
B(1)-B(6)-B(10)	108.5(3)
B(5)-B(6)-Cl(6)	122.1(3)
B(11)-B(6)-Cl(6)	121.4(3)
B(2)-B(6)-Cl(6)	120.9(4)
B(1)-B(6)-Cl(6)	121.8(3)
B(10)-B(6)-Cl(6)	120.9(3)
B(8)-B(7)-B(10)	107.5(4)
B(8)-B(7)-B(12)	60.2(3)
B(10)-B(7)-B(12)	107.4(3)
B(8)-B(7)-B(9)	59.8(3)
B(10)-B(7)-B(9)	59.9(3)
B(12)-B(7)-B(9)	107.8(3)
B(8)-B(7)-B(11)	107.8(3)
B(10)-B(7)-B(11)	59.9(3)
B(12)-B(7)-B(11)	59.6(3)
B(9)-B(7)-B(11)	107.9(4)
B(8)-B(7)-Cl(7)	120.7(3)
B(10)-B(7)-Cl(7)	122.4(3)
B(12)-B(7)-Cl(7)	122.5(4)
B(9)-B(7)-Cl(7)	120.5(3)
B(11)-B(7)-Cl(7)	123.4(3)
B(7)-B(8)-B(9)	60.4(3)
B(7)-B(8)-B(4)	108.6(3)
B(9)-B(8)-B(4)	108.6(3)
B(7)-B(8)-B(12)	60.1(3)
B(9)-B(8)-B(12)	108.3(3)

B(4)-B(8)-B(12)	60.0(3)
B(7)-B(8)-B(3)	109.1(3)
B(9)-B(8)-B(3)	60.5(3)
B(4)-B(8)-B(3)	60.2(3)
B(12)-B(8)-B(3)	108.3(3)
B(7)-B(8)-Cl(8)	120.7(3)
B(9)-B(8)-Cl(8)	122.0(3)
B(4)-B(8)-Cl(8)	121.3(3)
B(12)-B(8)-Cl(8)	120.8(3)
B(3)-B(8)-Cl(8)	122.0(3)
B(8)-B(9)-B(10)	107.5(4)
B(8)-B(9)-B(2)	107.6(3)
B(10)-B(9)-B(2)	60.4(3)
B(8)-B(9)-B(7)	59.8(3)
B(10)-B(9)-B(7)	59.8(3)
B(2)-B(9)-B(7)	108.2(3)
B(8)-B(9)-Cl(9)	122.1(3)
B(10)-B(9)-Cl(9)	121.4(3)
B(2)-B(9)-Cl(9)	122.0(4)
B(7)-B(9)-Cl(9)	121.1(3)
B(8)-B(9)-B(3)	60.0(3)
B(10)-B(9)-B(3)	108.2(3)
B(2)-B(9)-B(3)	59.8(3)
B(7)-B(9)-B(3)	108.2(3)
Cl(9)-B(9)-B(3)	122.1(3)
B(7)-B(10)-B(9)	60.3(3)
B(7)-B(10)-B(11)	60.3(3)
B(9)-B(10)-B(11)	108.5(3)
B(7)-B(10)-B(6)	107.9(4)
B(9)-B(10)-B(6)	107.7(3)
B(11)-B(10)-B(6)	59.9(3)
B(7)-B(10)-Cl(10)	121.4(3)
B(9)-B(10)-Cl(10)	121.9(3)
B(11)-B(10)-Cl(10)	121.1(4)

B(6)-B(10)-Cl(10)	121.9(3)
B(7)-B(10)-B(2)	108.2(3)
B(9)-B(10)-B(2)	60.0(3)
B(11)-B(10)-B(2)	108.1(3)
B(6)-B(10)-B(2)	59.7(3)
Cl(10)-B(10)-B(2)	122.1(4)
B(12)-B(11)-Cl(11)	123.2(4)
B(12)-B(11)-B(6)	107.2(3)
Cl(11)-B(11)-B(6)	121.4(3)
B(12)-B(11)-B(10)	107.6(3)
Cl(11)-B(11)-B(10)	120.6(3)
B(6)-B(11)-B(10)	60.2(3)
B(12)-B(11)-B(5)	59.8(3)
Cl(11)-B(11)-B(5)	122.7(3)
B(6)-B(11)-B(5)	59.4(3)
B(10)-B(11)-B(5)	107.7(4)
B(12)-B(11)-B(7)	60.0(3)
Cl(11)-B(11)-B(7)	121.7(3)
B(6)-B(11)-B(7)	107.7(4)
B(10)-B(11)-B(7)	59.8(3)
B(5)-B(11)-B(7)	107.9(3)
B(11)-B(12)-B(5)	60.5(3)
B(11)-B(12)-B(4)	108.8(3)
B(5)-B(12)-B(4)	60.3(3)
B(11)-B(12)-B(7)	60.4(3)
B(5)-B(12)-B(7)	108.7(3)
B(4)-B(12)-B(7)	108.2(3)
B(11)-B(12)-B(8)	108.1(4)
B(5)-B(12)-B(8)	108.0(3)
B(4)-B(12)-B(8)	59.8(3)
B(7)-B(12)-B(8)	59.7(3)
B(11)-B(12)-Cl(12)	121.3(3)
B(5)-B(12)-Cl(12)	120.2(3)
B(4)-B(12)-Cl(12)	120.7(3)

B(7)-B(12)-Cl(12)	122.7(3)
B(8)-B(12)-Cl(12)	122.7(3)
B(15)-B(13)-B(18)	108.1(3)
B(15)-B(13)-B(16)	60.2(3)
B(18)-B(13)-B(16)	107.9(3)
B(15)-B(13)-B(14)	60.1(3)
B(18)-B(13)-B(14)	60.0(3)
B(16)-B(13)-B(14)	108.1(3)
B(15)-B(13)-B(17)	108.3(3)
B(18)-B(13)-B(17)	59.6(3)
B(16)-B(13)-B(17)	60.3(3)
B(14)-B(13)-B(17)	107.8(3)
B(15)-B(13)-Cl(13)	121.0(3)
B(18)-B(13)-Cl(13)	122.1(3)
B(16)-B(13)-Cl(13)	121.6(3)
B(14)-B(13)-Cl(13)	121.4(3)
B(17)-B(13)-Cl(13)	122.2(3)
B(16)#1-B(14)-B(17)#1	60.5(3)
B(16)#1-B(14)-B(15)	108.1(3)
B(17)#1-B(14)-B(15)	59.7(3)
B(16)#1-B(14)-B(18)	60.1(3)
B(17)#1-B(14)-B(18)	108.2(3)
B(15)-B(14)-B(18)	107.7(3)
B(16)#1-B(14)-B(13)	108.0(3)
B(17)#1-B(14)-B(13)	107.6(3)
B(15)-B(14)-B(13)	59.7(3)
B(18)-B(14)-B(13)	59.8(3)
B(16)#1-B(14)-Cl(14)	121.7(3)
B(17)#1-B(14)-Cl(14)	122.4(3)
B(15)-B(14)-Cl(14)	122.2(3)
B(18)-B(14)-Cl(14)	121.2(3)
B(13)-B(14)-Cl(14)	121.4(3)
B(17)#1-B(15)-B(13)	108.4(3)
B(17)#1-B(15)-B(18)#1	59.8(3)

B(13)-B(15)-B(18)#1	108.0(3)
B(17)#1-B(15)-B(14)	60.1(3)
B(13)-B(15)-B(14)	60.2(3)
B(18)#1-B(15)-B(14)	107.8(3)
B(17)#1-B(15)-B(16)	108.0(3)
B(13)-B(15)-B(16)	60.1(3)
B(18)#1-B(15)-B(16)	59.9(3)
B(14)-B(15)-B(16)	108.2(3)
B(17)#1-B(15)-Cl(15)	121.0(3)
B(13)-B(15)-Cl(15)	122.1(3)
B(18)#1-B(15)-Cl(15)	121.5(3)
B(14)-B(15)-Cl(15)	121.6(3)
B(16)-B(15)-Cl(15)	122.0(3)
B(14)#1-B(16)-B(18)#1	60.2(3)
B(14)#1-B(16)-B(13)	108.1(3)
B(18)#1-B(16)-B(13)	107.8(3)
B(14)#1-B(16)-B(15)	108.2(3)
B(18)#1-B(16)-B(15)	60.0(3)
B(13)-B(16)-B(15)	59.7(3)
B(14)#1-B(16)-Cl(16)	120.3(3)
B(18)#1-B(16)-Cl(16)	122.6(3)
B(13)-B(16)-Cl(16)	122.0(3)
B(15)-B(16)-Cl(16)	123.5(3)
B(14)#1-B(16)-B(17)	60.0(3)
B(18)#1-B(16)-B(17)	107.9(3)
B(13)-B(16)-B(17)	60.0(3)
B(15)-B(16)-B(17)	107.8(3)
Cl(16)-B(16)-B(17)	120.2(3)
B(18)-B(17)-B(15)#1	60.3(3)
B(18)-B(17)-B(14)#1	108.2(3)
B(15)#1-B(17)-B(14)#1	60.2(3)
B(18)-B(17)-Cl(17)	122.9(3)
B(15)#1-B(17)-Cl(17)	122.0(3)
B(14)#1-B(17)-Cl(17)	120.7(3)

B(18)-B(17)-B(13)	60.0(3)
B(15)#1-B(17)-B(13)	108.0(3)
B(14)#1-B(17)-B(13)	107.5(3)
Cl(17)-B(17)-B(13)	122.4(3)
B(18)-B(17)-B(16)	107.8(3)
B(15)#1-B(17)-B(16)	107.7(3)
B(14)#1-B(17)-B(16)	59.6(3)
Cl(17)-B(17)-B(16)	121.0(3)
B(13)-B(17)-B(16)	59.7(3)
B(17)-B(18)-B(13)	60.4(3)
B(17)-B(18)-B(16)#1	108.2(3)
B(13)-B(18)-B(16)#1	107.9(3)
B(17)-B(18)-B(15)#1	59.9(3)
B(13)-B(18)-B(15)#1	108.0(3)
B(16)#1-B(18)-B(15)#1	60.1(3)
B(17)-B(18)-B(14)	108.6(3)
B(13)-B(18)-B(14)	60.2(3)
B(16)#1-B(18)-B(14)	59.7(3)
B(15)#1-B(18)-B(14)	107.9(3)
B(17)-B(18)-Cl(18)	122.2(3)
B(13)-B(18)-Cl(18)	121.9(3)
B(16)#1-B(18)-Cl(18)	121.1(3)
B(15)#1-B(18)-Cl(18)	122.1(3)
B(14)-B(18)-Cl(18)	120.9(3)
C(6S)-C(1S)-C(2S)	120.3(7)
C(6S)-C(1S)-Cl(1S)	119.7(6)
C(2S)-C(1S)-Cl(1S)	120.0(5)
C(1S)-C(2S)-C(3S)	119.7(5)
C(1S)-C(2S)-Cl(2S)	121.9(5)
C(3S)-C(2S)-Cl(2S)	118.4(4)
C(4S)-C(3S)-C(2S)	118.3(6)
C(5S)-C(4S)-C(3S)	120.1(7)
C(6S)-C(5S)-C(4S)	121.4(7)
C(5S)-C(6S)-C(1S)	120.2(7)

Cl(4S)#2-C(7S)-C(8S)	131.7(8)
Cl(4S)#2-C(7S)-C(11S)#2	10.8(6)
C(8S)-C(7S)-C(11S)#2	132.8(10)
Cl(3S)-C(8S)-C(10S)	8.8(8)
Cl(3S)-C(8S)-C(7S)	124.6(8)
C(10S)-C(8S)-C(7S)	125.3(11)
C(9S)#2-C(9S)-C(10S)	124.0(8)
C(9S)#2-C(9S)-Cl(3S)	119.5(5)
C(10S)-C(9S)-Cl(3S)	8.8(7)
C(9S)#2-C(9S)-Cl(4S)	122.2(5)
C(10S)-C(9S)-Cl(4S)	113.2(7)
Cl(3S)-C(9S)-Cl(4S)	118.2(3)
C(9S)#2-C(9S)-C(11S)	125.6(6)
C(10S)-C(9S)-C(11S)	110.3(8)
Cl(3S)-C(9S)-C(11S)	114.0(6)
Cl(4S)-C(9S)-C(11S)	10.0(5)
C(8S)-C(10S)-C(9S)	108.1(12)
C(7S)#2-C(11S)-C(9S)	99.3(9)
C(8S)-Cl(3S)-C(9S)	115.5(5)
C(7S)#2-Cl(4S)-C(9S)	106.4(5)

Symmetry transformations used to generate equivalent atoms:
#1 -x+1,-y+1,-z #2 -x+1,-y,-z+2

G.2.4 Anisotropic Displacement Parameters

Anisotropic displacement parameters ($Å^2 x\ 10^3$) for $[(Et_3Si)Me_4N_2]_2[B_{12}Cl_{12}]\cdot ODCB$. The anisotropic displacement factor exponent takes the form: $-2p^2[\ h^2\ a^{*2}U^{11} + ...\ + 2\ h\ k\ a^*\ b^*\ U^{12}\ ]$

	U^{11}	U^{22}	U^{33}	U^{23}	U^{13}	U^{12}
Si(1A)	21(1)	20(1)	22(1)	5(1)	8(1)	2(1)
N(1A)	22(2)	26(2)	35(2)	16(2)	5(2)	3(2)

N(2A)	29(2)	29(2)	35(2)	19(2)	10(2)	9(2)
C(1A)	34(3)	56(3)	51(3)	38(3)	27(2)	20(2)
C(2A)	27(3)	30(3)	58(3)	16(2)	-6(2)	1(2)
C(3A)	35(3)	41(3)	63(4)	29(3)	9(3)	15(2)
C(4A)	64(4)	47(3)	38(3)	28(3)	19(3)	20(3)
C(5A)	29(2)	22(2)	31(3)	3(2)	15(2)	2(2)
C(6A)	30(3)	30(3)	40(3)	-3(2)	12(2)	-3(2)
C(7A)	46(3)	29(2)	31(3)	3(2)	17(2)	8(2)
C(8A)	45(3)	52(3)	34(3)	10(2)	23(2)	13(3)
C(9A)	25(2)	27(2)	28(2)	10(2)	3(2)	7(2)
C(10A)	36(3)	27(2)	42(3)	18(2)	3(2)	9(2)
Si(1B)	31(2)	26(1)	32(2)	10(1)	10(1)	1(1)
N(1B)	38(4)	26(6)	17(6)	9(4)	-4(5)	4(4)
N(2B)	43(5)	29(4)	33(5)	8(4)	8(4)	3(4)
C(1B)	44(6)	57(6)	46(6)	33(5)	5(4)	14(5)
C(2B)	49(5)	33(4)	41(5)	10(4)	22(4)	13(4)
C(3B)	101(9)	50(6)	70(7)	11(5)	19(6)	-39(6)
C(4B)	67(6)	33(4)	32(5)	2(4)	-12(4)	8(4)
C(5B)	54(6)	43(5)	74(7)	19(5)	32(5)	10(4)
C(6B)	79(8)	86(8)	146(12)	68(9)	62(8)	47(7)
C(7B)	38(4)	40(4)	51(5)	20(4)	8(4)	2(4)
C(8B)	53(10)	36(6)	37(6)	3(5)	-2(8)	0(7)
C(9B)	88(15)	64(11)	54(13)	24(8)	29(9)	30(9)
C(10B)	90(13)	16(5)	33(7)	11(5)	10(7)	2(6)
Si(1D)	41(4)	45(4)	46(5)	33(4)	28(3)	20(3)
N(1D)	38(13)	48(19)	12(14)	12(11)	13(13)	15(14)
N(2D)	53(9)	49(9)	38(8)	15(7)	-4(7)	-7(7)
C(1D)	82(18)	63(15)	100(20)	54(14)	60(16)	36(13)
C(2D)	89(15)	30(9)	35(11)	-5(8)	28(11)	9(9)
C(3D)	63(14)	51(12)	76(15)	19(10)	44(12)	30(11)
C(4D)	78(16)	64(14)	92(18)	-7(13)	34(14)	-20(13)
C(5D)	45(10)	45(10)	49(11)	11(9)	21(8)	24(8)
C(6D)	104(19)	102(18)	91(17)	57(15)	48(15)	78(16)
C(7D)	31(9)	74(13)	26(8)	28(9)	19(7)	30(9)

C(8D)	38(17)	110(20)	25(12)	-2(12)	8(14)	-14(15)
C(10D)	70(20)	140(50)	110(40)	80(30)	10(20)	60(30)
C(9D)	12(8)	11(9)	10(9)	6(5)	0(5)	3(5)
Si(1C)	25(1)	28(1)	25(1)	4(1)	2(1)	9(1)
N(1C)	24(2)	28(2)	28(2)	2(2)	3(2)	10(2)
N(2C)	24(2)	36(2)	33(2)	10(2)	8(2)	11(2)
C(1C)	22(2)	34(3)	36(3)	2(2)	-2(2)	4(2)
C(2C)	32(3)	33(3)	40(3)	3(2)	14(2)	16(2)
C(3C)	27(3)	38(3)	38(3)	11(2)	8(2)	14(2)
C(4C)	32(3)	50(3)	54(3)	20(3)	18(2)	10(2)
C(5C)	37(3)	30(3)	38(3)	2(2)	0(2)	15(2)
C(6C)	68(4)	41(3)	43(3)	19(3)	3(3)	27(3)
C(7C)	32(3)	35(3)	27(2)	7(2)	5(2)	13(2)
C(8C)	35(3)	42(3)	32(3)	12(2)	11(2)	11(2)
C(9C)	27(2)	35(3)	26(2)	5(2)	3(2)	7(2)
C(10C)	34(3)	44(3)	27(3)	8(2)	-1(2)	-5(2)
Cl(1)	26(1)	40(1)	26(1)	10(1)	12(1)	2(1)
Cl(2)	34(1)	44(1)	47(1)	-14(1)	2(1)	-4(1)
Cl(3)	56(1)	26(1)	38(1)	16(1)	13(1)	8(1)
Cl(4)	28(1)	31(1)	14(1)	7(1)	4(1)	8(1)
Cl(5)	29(1)	32(1)	28(1)	14(1)	14(1)	18(1)
Cl(6)	28(1)	72(1)	20(1)	7(1)	3(1)	29(1)
Cl(7)	38(1)	60(1)	31(1)	25(1)	23(1)	31(1)
Cl(8)	25(1)	32(1)	22(1)	6(1)	1(1)	15(1)
Cl(9)	38(1)	37(1)	28(1)	-6(1)	2(1)	17(1)
Cl(10)	47(1)	111(1)	12(1)	8(1)	4(1)	50(1)
Cl(11)	63(1)	86(1)	48(1)	55(1)	40(1)	55(1)
Cl(12)	30(1)	31(1)	52(1)	20(1)	23(1)	11(1)
Cl(13)	33(1)	26(1)	40(1)	19(1)	15(1)	9(1)
Cl(14)	33(1)	22(1)	40(1)	12(1)	17(1)	12(1)
Cl(15)	29(1)	33(1)	41(1)	18(1)	1(1)	10(1)
Cl(16)	56(1)	31(1)	28(1)	12(1)	17(1)	15(1)
Cl(17)	28(1)	34(1)	65(1)	24(1)	26(1)	12(1)
Cl(18)	28(1)	25(1)	40(1)	10(1)	2(1)	0(1)

B(1)	23(3)	31(3)	15(2)	7(2)	6(2)	6(2)
B(2)	22(3)	36(3)	18(3)	-1(2)	-1(2)	3(2)
B(3)	26(3)	21(2)	20(3)	5(2)	3(2)	5(2)
B(4)	23(2)	23(2)	15(2)	7(2)	5(2)	9(2)
B(5)	23(3)	29(3)	15(2)	11(2)	8(2)	13(2)
B(6)	28(3)	46(3)	15(3)	9(2)	7(2)	21(2)
B(7)	30(3)	46(3)	20(3)	19(2)	12(2)	25(2)
B(8)	24(3)	28(3)	14(2)	7(2)	3(2)	13(2)
B(9)	27(3)	34(3)	15(2)	4(2)	2(2)	15(2)
B(10)	29(3)	58(4)	13(2)	12(2)	5(2)	28(3)
B(11)	33(3)	50(3)	21(3)	21(2)	15(2)	28(3)
B(12)	23(3)	30(3)	25(3)	16(2)	12(2)	13(2)
B(13)	24(3)	22(2)	30(3)	13(2)	11(2)	8(2)
B(14)	22(3)	19(2)	31(3)	10(2)	9(2)	8(2)
B(15)	23(3)	21(2)	32(3)	12(2)	6(2)	7(2)
B(16)	28(3)	23(2)	23(3)	11(2)	9(2)	8(2)
B(17)	22(3)	22(2)	38(3)	13(2)	13(2)	7(2)
B(18)	25(3)	18(2)	31(3)	8(2)	7(2)	3(2)
Cl(1S)	137(2)	157(2)	86(2)	83(2)	-16(2)	-3(2)
Cl(2S)	124(2)	33(1)	77(1)	-5(1)	-16(1)	16(1)
C(1S)	51(4)	72(4)	34(3)	14(3)	7(3)	-11(3)
C(2S)	51(3)	30(3)	42(3)	0(2)	13(3)	-9(2)
C(3S)	38(3)	54(3)	41(3)	13(3)	6(2)	0(3)
C(4S)	47(4)	46(4)	102(6)	9(4)	29(4)	13(3)
C(5S)	56(5)	73(5)	98(7)	-34(5)	43(5)	-7(4)
C(6S)	48(4)	103(6)	48(4)	-17(4)	26(3)	-23(4)

G.2.5 Hydrogen Coordinates

Hydrogen coordinates (x 10^4) and isotropic displacement parameters ($Å^2$x 10^3) for $[(Et_3Si)Me_4N_2]_2[B_{12}Cl_{12}]\cdot$ODCB.

	x	y	z	U(eq)
H(1A1)	11801	2079	9325	58
H(1A2)	10778	2538	9095	58
H(1A3)	10607	1501	8874	58
H(2A1)	11433	3005	11014	64
H(2A2)	11189	3491	10447	64
H(2A3)	12231	3011	10535	64
H(3A1)	12658	1740	10560	67
H(3A2)	12297	1173	9705	67
H(3A3)	12272	706	10271	67
H(4A1)	10799	803	10800	68
H(4A2)	10052	1530	10745	68
H(4A3)	11333	1816	11191	68
H(5A1)	8884	756	8939	34
H(5A2)	8610	774	9659	34
H(6A1)	6940	1265	9263	57
H(6A2)	6975	349	8674	57
H(6A3)	7213	1233	8539	57
H(7A1)	9724	2902	11070	43
H(7A2)	8858	3385	10690	43
H(8A1)	7421	2269	10473	64
H(8A2)	8082	2708	11325	64
H(8A3)	8289	1780	10848	64
H(9A1)	9019	2533	8717	33
H(9A2)	8103	2878	9077	33
H(10A)	9477	4122	9943	53
H(10B)	9134	4081	9120	53
H(10C)	10261	3795	9454	53

H(1B1)	5588	4846	2859	71
H(1B2)	5714	4006	2228	71
H(1B3)	6592	4887	2543	71
H(2B1)	8006	3522	3341	60
H(2B2)	8083	4084	2849	60
H(2B3)	7197	3206	2523	60
H(3B1)	7698	5726	3319	121
H(3B2)	8688	5305	3663	121
H(3B3)	8357	6152	4172	121
H(4B1)	7360	4483	4629	79
H(4B2)	8157	5406	4948	79
H(4B3)	8477	4558	4433	79
H(5B1)	4892	4093	4372	66
H(5B2)	5509	4881	4259	66
H(6B1)	3602	4865	3930	134
H(6B2)	3397	3908	3322	134
H(6B3)	4013	4722	3234	134
H(7B1)	4145	2510	2669	53
H(7B2)	4385	3196	2316	53
H(8B1)	4452	1798	1586	73
H(8B2)	5425	1725	2231	73
H(8B3)	5626	2405	1858	73
H(9B1)	7119	2748	3724	79
H(9B2)	6827	3284	4443	79
H(10D)	6182	1773	4135	72
H(10E)	5506	1670	3323	72
H(10F)	5124	2226	3996	72
H(1D1)	6534	4647	2523	99
H(1D2)	7103	5549	3188	99
H(1D3)	5842	5164	3018	99
H(2D1)	7122	4852	4619	81
H(2D2)	6156	5260	4233	81
H(2D3)	7410	5677	4417	81
H(3D1)	7645	3388	2607	88

H(3D2)	8910	3840	2918	88
H(3D3)	7990	4326	2586	88
H(4D1)	8780	5386	4492	132
H(4D2)	8767	5540	3760	132
H(4D3)	9579	4954	4047	132
H(5D1)	4181	3229	3357	55
H(5D2)	4790	4199	3867	55
H(6D1)	3174	4194	2951	130
H(6D2)	3688	3692	2330	130
H(6D3)	4233	4671	2873	130
H(7D1)	5615	3110	1971	46
H(7D2)	6332	2458	2234	46
H(8D1)	4557	1651	1437	97
H(8D2)	3971	2284	1950	97
H(8D3)	4683	1640	2232	97
H(10G)	6433	1831	4111	150
H(10H)	5808	1766	3301	150
H(10I)	5297	2182	3944	150
H(9D1)	7296	2848	3996	13
H(9D2)	6513	3293	4446	13
H(1C1)	7033	9585	3800	54
H(1C2)	6811	8990	4241	54
H(1C3)	6115	9750	4202	54
H(2C1)	5691	7633	2372	55
H(2C2)	6539	7688	3125	55
H(2C3)	6795	8343	2742	55
H(3C1)	4922	10173	3517	52
H(3C2)	3882	9417	3242	52
H(3C3)	4018	9956	2743	52
H(4C1)	5305	9772	2146	67
H(4C2)	6061	9040	2151	67
H(4C3)	6325	9921	2852	67
H(5C1)	5317	6711	3352	47
H(5C2)	6063	7473	4087	47

H(6C1)	4786	7296	4676	78
H(6C2)	5171	6385	4345	78
H(6C3)	4005	6556	3938	78
H(7C1)	4730	8781	4746	40
H(7C2)	4312	9380	4291	40
H(8C1)	2534	8540	3821	55
H(8C2)	2905	8912	4693	55
H(8C3)	2946	7916	4253	55
H(9C1)	2929	7955	2584	39
H(9C2)	3723	7399	2208	39
H(10G)	3225	6258	2585	59
H(10H)	2176	6454	2068	59
H(10I)	2400	6812	2931	59
H(3S)	-686	6096	1824	57
H(4S)	-705	7518	2572	82
H(5S)	114	7986	3813	108
H(6S)	935	7081	4336	94
H(7S)	3138	228	8535	114
H(8S)	4203	1547	9240	116
H(11S)	7076	1082	11133	26
HL3S	5507	1806	10264	32

G.3 References

2. Bruker (2005). APEX 2 version 2.0-2. Bruker AXS Inc., Madison, Wisconsin, U.S.A.

2. Bruker (2005). SAINT version V7.21A. Bruker AXS Inc., Madison, Wisconsin, USA.

3. Bruker (2004). SADABS version 2004/1. Bruker Analytical X-Ray System, Inc., Madison, Wisconsin, USA.

4. Altomare, A., Burla, M.C., Carnalli, M. Cascarano, G. Giacovazzo, C., Guagliardi, A.; Moliterni, A.G.G.; Polidori, G. Spagan, R. SIR 97 (1999) J. Appl. Cryst. 32, 115-122.

5. Bruker (2003). SHELXTL Software Version 6.14, Dec, Bruker Analytical X-Ray System, Inc.,Madison, Wisconsin, USA .

Appendix H. X-ray Structure Determination for $[(CH_3)_4NH]_2[B_{12}Br_{12}]\cdot 2CD_2Cl_2$

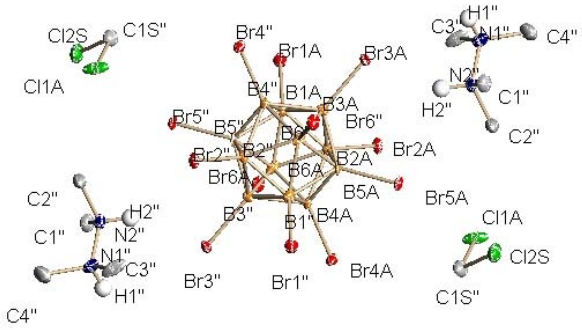

H.1 Experimental Details

The Bruker X8-APEX (**ref. 1**) X-ray diffraction instrument with Mo-radiation was used for data collection**.** All data frames were collected at low temperatures (T = 100 K) using an ω, φ-scan mode (0.5^o ω-scan width, hemisphere of reflections) and integrated using a Bruker SAINTPLUS software package (**ref. 2**). The intensity data were corrected for Lorentzian polarization. Absorption corrections were applied for all data using the SADABS program (**ref. 3**) in the SAINTPLUS software (**ref. 2**). The Bruker SHELXTL (Version 6.10) software (**ref. 5**) in the APEX 2 package (**ref. 1**) was used for phase determination and structure refinement. Direct methods of phase determination followed by some subsequent difference Fourier map led to an electron density map from which most of the non-hydrogen atoms were identified in the asymmetry unit of the unit cell. With subsequent isotropic refinement, all of the non-hydrogen atoms were identified. Atomic coordinates, isotropic and anisotropic displacement parameters of all the non-hydrogen atoms were refined by means of a full matrix least-squares procedure on F^2. The H-atoms were included in the refinement in calculated positions riding on the atoms to which they were attached.

H.2 Structure Details

H.2.1 Crystal Structure and Refinement Data for $[(CH_3)_4NH]_2[B_{12}Br_{12}]\cdot 2CD_2Cl_2$

Empirical formula	$C_5H_{14}B_6Br_6Cl_2N_2$	
Formula weight	717.40	
Temperature	293(2) K	
Wavelength	0.71073 Å	
Crystal system	Monoclinic	
Space group	P2(1)/c	
Unit cell dimensions	a = 10.5850(13) Å	α = 90°.
	b = 10.1142(12) Å	β = 105.037(3)°.
	c = 19.202(2) Å	γ = 90°.
Volume	1985.4(4) $Å^3$	
Z	4	
Density (calculated)	2.400 Mg/m^3	
Absorption coefficient	12.391 mm^{-1}	
F(000)	1328	
Crystal size	0.25 x 0.13 x 0.08 mm^3	
Theta range for data collection	1.99 to 23.28°	
Index ranges	-11<=h<=11, -11<=k<=10, -21<=l<=21	
Reflections collected	12659	
Independent reflections	2848 [R(int) = 0.0306]	
Completeness to theta = 23.28°	99.6 %	
Absorption correction	Sadabs	
Max. and min. transmission	0.4372 and 0.1477	
Refinement method	Full-matrix least-squares on F^2	
Data / restraints / parameters	2848 / 0 / 204	
Goodness-of-fit on F^2	1.065	
Final R indices [I>2sigma(I)]	R1 = 0.0312, wR2 = 0.0942	
R indices (all data)	R1 = 0.0348, wR2 = 0.0963	
Extinction coefficient	0.00019(16)	
Largest diff. peak and hole	1.509 and -0.558 $e.Å^{-3}$	

H.2.2 Atomic Coordinates

Atomic coordinates (x 10^4) and equivalent isotropic displacement parameters ($Å^2$x 10^3) for $[(CH_3)_4NH]_2[B_{12}Br_{12}]\cdot 2CD_2Cl_2$. U(eq) is defined as one third of the trace of the orthogonalized U^{ij} tensor.

	x	y	z	U(eq)
N(1)	1354(6)	5210(6)	1027(3)	23(1)
N(2)	1319(6)	6663(6)	1067(3)	18(1)
C(1)	101(7)	7163(8)	553(4)	22(2)
C(2)	1497(8)	7268(8)	1803(4)	25(2)
C(3)	2674(9)	4762(8)	1387(4)	35(2)
C(4)	380(8)	4623(8)	1349(5)	33(2)
B(1)	5622(7)	8438(7)	97(4)	12(2)
B(2)	4833(7)	9138(8)	715(4)	11(2)
B(3)	3910(7)	8732(7)	-164(4)	12(2)
B(4)	5118(7)	10875(7)	775(4)	10(2)
B(5)	3600(7)	10240(8)	248(4)	12(2)
B(6)	6383(7)	9767(8)	681(4)	13(2)
Br(1)	6324(1)	6647(1)	219(1)	19(1)
Br(2)	4616(1)	8154(1)	1560(1)	16(1)
Br(3)	2668(1)	7274(1)	-359(1)	16(1)
Br(4)	5250(1)	11870(1)	1650(1)	16(1)
Br(5)	1999(1)	10498(1)	554(1)	15(1)
Br(6)	7954(1)	9506(1)	1453(1)	17(1)

	x	y	z	U(eq)
C(1S)	2515(7)	11263(8)	2572(4)	24(2)
Cl(1A)	3050(14)	9765(14)	3042(5)	29(2)
Cl(1B)	2940(30)	9880(30)	3068(12)	69(8)
Cl(2S)	830(2)	11226(2)	2118(1)	29(1)

H.2.3 Bond Lengths and Angles

Bond lengths [Å] and angles [°] for $[(CH_3)_4NH]_2[B_{12}Br_{12}]\cdot 2CD_2Cl_2$.

N(1)-C(4)	1.459(10)	N(1)-C(3)	1.461(10)
N(1)-N(2)	1.472(8)	N(2)-C(1)	1.494(9)
N(2)-C(2)	1.508(9)	B(1)-B(2)	1.767(10)
B(1)-B(3)	1.775(10)	B(1)-B(5)#1	1.785(10)
B(1)-B(4)#1	1.793(9)	B(1)-B(6)	1.801(10)
B(1)-Br(1)	1.949(7)	B(2)-B(3)	1.766(10)
B(2)-B(5)	1.773(10)	B(2)-B(6)	1.777(10)
B(2)-B(4)	1.782(11)	B(2)-Br(2)	1.966(7)
B(3)-B(5)	1.788(11)	B(3)-B(4)#1	1.794(10)
B(3)-B(6)#1	1.797(10)	B(3)-Br(3)	1.946(8)
B(4)-B(5)	1.781(10)	B(4)-B(6)	1.791(10)
B(4)-B(1)#1	1.793(9)	B(4)-B(3)#1	1.794(10)
B(4)-Br(4)	1.933(7)	B(5)-B(1)#1	1.785(10)
B(5)-B(6)#1	1.789(10)	B(5)-Br(5)	1.950(7)
B(6)-B(5)#1	1.789(10)	B(6)-B(3)#1	1.797(10)
B(6)-Br(6)	1.937(7)		

C(1S)-Cl(1B)	1.69(3)	C(1S)-Cl(2S)	1.771(7)
C(1S)-Cl(1A)	1.779(15)		

C(4)-N(1)-C(3)	111.6(6)	C(4)-N(1)-N(2)	110.8(6)
C(3)-N(1)-N(2)	108.6(6)	N(1)-N(2)-C(1)	109.4(5)
N(1)-N(2)-C(2)	117.0(5)	C(1)-N(2)-C(2)	111.0(6)
B(2)-B(1)-B(3)	59.8(4)	B(2)-B(1)-B(5)#1	107.1(5)
B(3)-B(1)-B(5)#1	107.8(5)	B(2)-B(1)-B(4)#1	107.7(5)
B(3)-B(1)-B(4)#1	60.4(4)	B(5)#1-B(1)-B(4)#1	59.7(4)
B(2)-B(1)-B(6)	59.7(4)	B(3)-B(1)-B(6)	108.0(5)
B(5)#1-B(1)-B(6)	59.8(4)	B(4)#1-B(1)-B(6)	108.0(5)
B(2)-B(1)-Br(1)	121.5(5)	B(3)-B(1)-Br(1)	121.2(5)

B(5)#1-B(1)-Br(1)	122.9(5)	B(4)#1-B(1)-Br(1)	122.2(5)
B(6)-B(1)-Br(1)	121.6(4)	B(3)-B(2)-B(1)	60.3(4)
B(3)-B(2)-B(5)	60.7(4)	B(1)-B(2)-B(5)	109.0(5)
B(3)-B(2)-B(6)	109.6(5)	B(1)-B(2)-B(6)	61.1(4)
B(5)-B(2)-B(6)	108.8(5)	B(3)-B(2)-B(4)	109.4(5)
B(1)-B(2)-B(4)	109.7(5)	B(5)-B(2)-B(4)	60.1(4)
B(6)-B(2)-B(4)	60.4(4)	B(3)-B(2)-Br(2)	121.1(5)
B(1)-B(2)-Br(2)	121.9(5)	B(5)-B(2)-Br(2)	120.4(5)
B(6)-B(2)-Br(2)	121.2(4)	B(4)-B(2)-Br(2)	120.0(4)
B(2)-B(3)-B(1)	59.9(4)	B(2)-B(3)-B(5)	59.9(4)
B(1)-B(3)-B(5)	108.0(5)	B(2)-B(3)-B(4)#1	107.7(5)
B(1)-B(3)-B(4)#1	60.3(4)	B(5)-B(3)-B(4)#1	107.6(5)
B(2)-B(3)-B(6)#1	107.8(5)	B(1)-B(3)-B(6)#1	108.3(5)
B(5)-B(3)-B(6)#1	59.9(4)	B(4)#1-B(3)-B(6)#1	59.8(4)
B(2)-B(3)-Br(3)	122.6(5)	B(1)-B(3)-Br(3)	121.1(5)
B(5)-B(3)-Br(3)	122.6(5)	B(4)#1-B(3)-Br(3)	121.1(5)
B(6)#1-B(3)-Br(3)	121.5(5)	B(5)-B(4)-B(2)	59.7(4)
B(5)-B(4)-B(6)	107.8(5)	B(2)-B(4)-B(6)	59.6(4)
B(5)-B(4)-B(1)#1	59.9(4)	B(2)-B(4)-B(1)#1	107.3(5)
B(6)-B(4)-B(1)#1	107.8(5)	B(5)-B(4)-B(3)#1	107.2(5)
B(2)-B(4)-B(3)#1	107.0(5)	B(6)-B(4)-B(3)#1	60.2(4)
B(1)#1-B(4)-B(3)#1	59.3(4)	B(5)-B(4)-Br(4)	122.2(5)
B(2)-B(4)-Br(4)	122.8(4)	B(6)-B(4)-Br(4)	121.7(4)
B(1)#1-B(4)-Br(4)	121.7(5)	B(3)#1-B(4)-Br(4)	121.9(5)
B(2)-B(5)-B(4)	60.2(4)	B(2)-B(5)-B(1)#1	108.0(5)
B(4)-B(5)-B(1)#1	60.4(4)	B(2)-B(5)-B(3)	59.4(4)
B(4)-B(5)-B(3)	108.5(5)	B(1)#1-B(5)-B(3)	108.6(5)
B(2)-B(5)-B(6)#1	107.8(5)	B(4)-B(5)-B(6)#1	109.1(5)
B(1)#1-B(5)-B(6)#1	60.5(4)	B(3)-B(5)-B(6)#1	60.3(4)
B(2)-B(5)-Br(5)	121.0(5)	B(4)-B(5)-Br(5)	120.5(5)
B(1)#1-B(5)-Br(5)	122.2(5)	B(3)-B(5)-Br(5)	121.4(5)
B(6)#1-B(5)-Br(5)	122.4(5)	B(2)-B(6)-B(5)#1	106.5(5)
B(2)-B(6)-B(4)	59.9(4)	B(5)#1-B(6)-B(4)	107.7(5)

B(2)-B(6)-B(3)#1	107.1(5)	B(5)#1-B(6)-B(3)#1	59.8(4)
B(4)-B(6)-B(3)#1	60.0(4)	B(2)-B(6)-B(1)	59.2(4)
B(5)#1-B(6)-B(1)	59.6(4)	B(4)-B(6)-B(1)	107.7(5)
B(3)#1-B(6)-B(1)	107.5(5)	B(2)-B(6)-Br(6)	122.7(5)
B(5)#1-B(6)-Br(6)	122.3(5)	B(4)-B(6)-Br(6)	121.6(4)
B(3)#1-B(6)-Br(6)	121.9(5)	B(1)-B(6)-Br(6)	122.1(5)
Cl(1B)-C(1S)-Cl(2S)	110.1(11)	Cl(1B)-C(1S)-Cl(1A)	5.2(15)
Cl(2S)-C(1S)-Cl(1A)	112.3(6)		

Symmetry transformations used to generate equivalent atoms: #1 -x+1,-y+2,-z

H.2.4 Anisotropic Displacement Parameters

Anisotropic displacement parameters ($Å^2 x\ 10^3$) for $[(CH_3)_4NH]_2[B_{12}Br_{12}]\cdot 2CD_2Cl_2$. The anisotropic displacement factor exponent takes the form: $-2p^2[\ h^2\ a^{*2}U^{11} + ...\ + 2\ h\ k\ a^*\ b^*\ U^{12}\ ]$

	U^{11}	U^{22}	U^{33}	U^{23}	U^{13}	U^{12}
N(1)	27(4)	20(3)	24(3)	-3(3)	9(3)	4(3)
N(2)	20(3)	17(3)	18(3)	2(2)	8(3)	1(2)
C(1)	16(4)	27(4)	26(4)	3(3)	7(3)	4(3)
C(2)	27(4)	25(4)	27(4)	-8(3)	14(3)	-10(3)
C(3)	55(6)	28(5)	23(4)	4(3)	10(4)	27(4)
C(4)	41(5)	25(5)	36(5)	0(4)	14(4)	-10(4)
B(1)	11(4)	13(4)	10(4)	5(3)	3(3)	5(3)
B(2)	8(4)	17(4)	9(3)	1(3)	1(3)	-2(3)
B(3)	15(4)	12(4)	9(4)	2(3)	1(3)	-1(3)
B(4)	11(4)	13(4)	7(3)	1(3)	4(3)	-1(3)
B(5)	7(4)	19(4)	13(4)	5(3)	7(3)	0(3)
B(6)	14(4)	18(4)	6(3)	1(3)	1(3)	6(3)
Br(1)	19(1)	15(1)	24(1)	2(1)	9(1)	3(1)
Br(2)	15(1)	22(1)	14(1)	6(1)	7(1)	0(1)

Br(3)	15(1)	17(1)	18(1)	-4(1)	8(1)	-7(1)
Br(4)	16(1)	21(1)	14(1)	-6(1)	7(1)	-3(1)
Br(5)	10(1)	20(1)	16(1)	0(1)	8(1)	1(1)
Br(6)	11(1)	25(1)	13(1)	2(1)	0(1)	1(1)

	U^{11}	U^{22}	U^{33}	U^{23}	U^{13}	U^{12}
C(1S)	15(4)	27(4)	30(4)	-3(3)	4(3)	-2(3)
Cl(1A)	48(5)	18(4)	11(3)	-3(3)	-10(3)	12(3)
Cl(1B)	87(12)	35(8)	82(12)	-6(6)	16(8)	19(7)
Cl(2S)	20(1)	40(1)	30(1)	-2(1)	12(1)	-2(1)

H.2.5 Hydrogen Coordinates

Hydrogen coordinates (x 10^4) and isotropic displacement parameters (Å^{2}x 10^3) for $[(CH_3)_4NH]_2[B_{12}Br_{12}]\cdot 2CD_2Cl_2$.

	x	y	z	U(eq)
H(1A)	-44	6692	105	34
H(1B)	193	8089	469	34
H(1C)	-629	7028	755	34
H(2A)	740	7087	1975	38
H(2B)	1607	8206	1774	38
H(2C)	2257	6895	2130	38
H(3A)	3297	5229	1195	53
H(3B)	2744	3831	1308	53
H(3C)	2848	4931	1895	53
H(4A)	360	3683	1276	50
H(4B)	-465	4988	1126	50
H(4C)	605	4810	1856	50

	x	y	z	U(eq)
H(1S1)	2678	11991	2912	29
H(1S2)	3019	11419	2224	29

H.3 References

1. Bruker (2005). APEX 2 version 2.0-2. Bruker AXS Inc., Madison, Wisconsin, U.S.A.

2. Bruker (2005). SAINT version V7.21A. Bruker AXS Inc., Madison, Wisconsin, USA.

3. Bruker (2004). SADABS version 2004/1. Bruker Analytical X-Ray System, Inc., Madison, Wisconsin, USA.

4. Altomare, A., Burla, M.C., Carnalli, M. Cascarano, G. Giacovazzo, C., Guagliardi, A.; Moliterni, A.G.G.; Polidori, G. Spagan, R. SIR 97 (1999) J. Appl. Cryst. 32, 115-122.

5. Bruker (2003). SHELXTL Software Version 6.14, Dec, Bruker Analytical X-Ray System, Inc., Madison, Wisconsin, USA .

Appendix I. X-ray Structure Determination for $[Et_3SiN_2(CH_3)_4][Et_3Si(B_{12}Br_{12})]\cdot CD_2Cl_2$

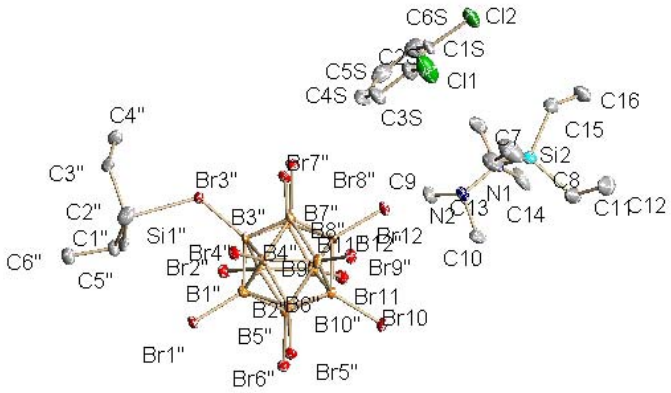

I.1 Experimental Details

The Bruker X8-APEX (**ref. 1**) X-ray diffraction instrument with Mo-radiation was used for data collection**.** All data frames were collected at low temperatures (T = 100 K) using an ω, φ-scan mode (0.5^o ω-scan width, hemisphere of reflections) and integrated using a Bruker SAINTPLUS software package (**ref. 2**). The intensity data were corrected for Lorentzian polarization. Absorption corrections were applied for all data using the SADABS program (**ref. 3**) in the SAINTPLUS software (**ref. 2**). The Bruker SHELXTL (Version 6.10) software (**ref. 5**) in the APEX 2 package (**ref. 1**) was used for phase determination and structure refinement. Direct methods of phase determination followed by some subsequent difference Fourier map led to an electron density map from which most of the non-hydrogen atoms were identified in the asymmetry unit of the unit cell. With subsequent isotropic refinement, all of the non-hydrogen atoms were identified. Atomic coordinates, isotropic and anisotropic displacement parameters of all the non-hydrogen atoms were refined by means of a full matrix least-squares procedure

on F^2. The H-atoms were included in the refinement in calculated positions riding on the atoms to which they were attached.

I.2 Structure Details

I.2.1 Crystal Structure and Refinement Data for $[Et_3SiN_2(CH_3)_4][Et_3Si(B_{12}Br_{12})]\cdot CD_2Cl_2$

Empirical formula	$C_{22}H_{46}B_{12}Br_{12}Cl_2N_2Si_2$	
Formula weight	1554.33	
Temperature	100(2) K	
Wavelength	0.71073 Å	
Crystal system	Orthorhombic	
Space group	Pbca	
Unit cell dimensions	a = 18.917(2) Å	α = 90°
	b = 15.5947(17) Å	β = 90°
	c = 33.360(4) Å	γ = 90°
Volume	9841.4(19) $Å^3$	
Z	8	
Density (calculated)	2.098 Mg/m^3	
Absorption coefficient	9.948 mm^{-1}	
F(000)	5872	
Crystal size	0.32 x 0.17 x 0.14 mm^3	
Theta range for data collection	1.63 to 26.37°.	
Index ranges	-22<=h<=23, -19<=k<=19, -41<=l<=41	
Reflections collected	68706	
Independent reflections	10062 [R(int) = 0.1162]	
Completeness to theta = 26.37°	100.0 %	
Absorption correction	Sadabs	
Max. and min. transmission	0.3365 and 0.1430	
Refinement method	Full-matrix least-squares on F^2	
Data / restraints / parameters	10062 / 0 / 480	
Goodness-of-fit on F^2	1.021	

Final R indices [I>2sigma(I)]	R1 = 0.0455, wR2 = 0.0967
R indices (all data)	R1 = 0.0783, wR2 = 0.1097
Extinction coefficient	0.000012(13)
Largest diff. peak and hole	1.371 and -1.337 e.Å^{-3}

I.2.2 Atomic Coordinates

Atomic coordinates (x 10^4) and equivalent isotropic displacement parameters (Å^{2}x 10^3) for $[Et_3SiN_2(CH_3)_4][Et_3Si(B_{12}Br_{12})]\cdot CD_2Cl_2$. U(eq) is defined as one third of the trace of the orthogonalized U^{ij} tensor.

	x	y	z	U(eq)
Si(1)	7856(1)	333(1)	1799(1)	18(1)
C(1)	7282(4)	1200(4)	1605(2)	21(2)
C(2)	7092(4)	1137(4)	1160(2)	29(2)
C(3)	7764(4)	-691(4)	1528(2)	22(2)
C(4)	8295(4)	-1414(4)	1622(2)	28(2)
C(5)	7969(4)	260(4)	2343(2)	23(2)
C(6)	7300(4)	-76(4)	2547(2)	27(2)
Si(2)	661(1)	7278(1)	5641(1)	21(1)
N(1)	738(3)	7929(3)	6130(2)	24(1)
N(2)	1420(3)	7698(3)	6326(2)	22(1)
C(7)	785(5)	8850(4)	6013(3)	47(2)
C(8)	100(4)	7830(6)	6400(2)	40(2)
C(9)	1623(4)	8294(4)	6647(2)	28(2)
C(10)	1398(4)	6823(4)	6497(2)	27(2)
C(11)	150(5)	6276(5)	5753(3)	40(2)
C(12)	-109(5)	5821(5)	5383(3)	54(3)
C(13)	1584(4)	7150(5)	5465(2)	38(2)
C(14)	1649(5)	6755(7)	5048(3)	58(3)
C(15)	145(4)	7917(4)	5277(2)	27(2)
C(16)	-629(4)	8130(5)	5360(3)	38(2)
B(1)	9323(4)	2591(4)	1928(2)	14(2)

B(2)	10039(4)	1915(4)	2088(2)	16(2)
B(3)	9584(4)	1701(4)	1642(2)	13(2)
B(4)	9359(4)	2661(4)	1392(2)	13(2)
B(5)	9697(4)	3512(4)	1692(2)	14(2)
B(6)	10111(4)	3054(4)	2120(2)	14(2)
B(7)	10517(4)	1571(4)	1656(2)	15(2)
B(8)	10105(4)	2035(4)	1228(2)	13(2)
B(9)	10171(4)	3178(5)	1262(2)	17(2)
B(10)	10631(4)	3414(4)	1713(2)	14(2)

	x	y	z	U(eq)
B(11)	10845(4)	2424(4)	1957(2)	15(2)
B(12)	10888(4)	2492(4)	1430(2)	14(2)
Br(1)	8434(1)	2658(1)	2223(1)	17(1)
Br(2)	9951(1)	1158(1)	2552(1)	19(1)
Br(3)	9050(1)	605(1)	1539(1)	19(1)
Br(4)	8520(1)	2774(1)	1064(1)	18(1)
Br(5)	9249(1)	4636(1)	1710(1)	18(1)
Br(6)	10112(1)	3656(1)	2637(1)	18(1)
Br(7)	10960(1)	450(1)	1644(1)	19(1)
Br(8)	10082(1)	1441(1)	714(1)	18(1)
Br(9)	10239(1)	3886(1)	785(1)	19(1)
Br(10)	11258(1)	4400(1)	1754(1)	20(1)
Br(11)	11692(1)	2309(1)	2289(1)	20(1)
Br(12)	11778(1)	2458(1)	1134(1)	20(1)

	x	y	z	U(eq)
C(1S)	2034(4)	9680(4)	5033(2)	24(2)
C(2S)	2648(4)	9202(5)	5014(2)	32(2)
C(3S)	3115(4)	9208(5)	5327(2)	38(2)

C(4S)	2976(5)	9694(5)	5662(2)	43(2)
C(5S)	2363(5)	10194(5)	5678(3)	43(2)
C(6S)	1901(4)	10188(5)	5360(3)	38(2)
Cl(1)	2833(1)	8579(2)	4593(1)	62(1)
Cl(2)	1417(1)	9633(1)	4648(1)	45(1)

I.2.3 Bond Lengths and Angles

Bond lengths [Å] and angles [°]for $[Et_3SiN_2(CH_3)_4][Et_3Si(B_{12}Br_{12})]\cdot CD_2Cl_2$.

Si(1)-C(5)	1.831(7)	Si(1)-C(3)	1.843(6)
Si(1)-C(1)	1.852(7)	Si(1)-Br(3)	2.4554(19)
C(1)-C(2)	1.532(9)	C(3)-C(4)	1.542(9)
C(5)-C(6)	1.530(9)	Si(2)-C(15)	1.851(7)
Si(2)-C(13)	1.853(8)	Si(2)-C(11)	1.876(8)
Si(2)-N(1)	1.925(6)	N(1)-N(2)	1.492(7)
N(1)-C(7)	1.491(9)	N(1)-C(8)	1.514(9)
N(2)-C(9)	1.468(8)	N(2)-C(10)	1.480(8)
C(11)-C(12)	1.506(10)	C(13)-C(14)	1.524(11)
C(15)-C(16)	1.528(10)	B(1)-B(3)	1.756(10)
B(1)-B(6)	1.776(10)	B(1)-B(5)	1.785(10)
B(1)-B(4)	1.795(11)	B(1)-B(2)	1.798(10)
B(1)-Br(1)	1.950(7)	B(2)-B(3)	1.750(10)
B(2)-B(11)	1.774(10)	B(2)-B(7)	1.784(11)
B(2)-B(6)	1.784(10)	B(2)-Br(2)	1.953(7)
B(3)-B(4)	1.767(10)	B(3)-B(8)	1.775(10)
B(3)-B(7)	1.778(10)	B(3)-Br(3)	2.014(7)
B(4)-B(5)	1.781(10)	B(4)-B(9)	1.786(10)
B(4)-B(8)	1.800(10)	B(4)-Br(4)	1.937(7)
B(5)-B(9)	1.769(11)	B(5)-B(10)	1.776(10)
B(5)-B(6)	1.779(10)	B(5)-Br(5)	1.948(7)
B(6)-B(10)	1.768(10)	B(6)-B(11)	1.785(10)
B(6)-Br(6)	1.964(7)	B(7)-B(12)	1.767(10)

B(7)-B(11)	1.777(10)	B(7)-B(8)	1.780(10)
B(7)-Br(7)	1.940(7)	B(8)-B(12)	1.776(10)
B(8)-B(9)	1.790(10)	B(8)-Br(8)	1.952(7)
B(9)-B(10)	1.776(10)	B(9)-B(12)	1.815(10)
B(9)-Br(9)	1.943(8)	B(10)-B(12)	1.787(9)
B(10)-B(11)	1.791(10)	B(10)-Br(10)	1.946(7)
B(11)-B(12)	1.763(11)	B(11)-Br(11)	1.956(7)
B(12)-Br(12)	1.954(7)		

C(1S)-C(6S)	1.370(10)	C(1S)-C(2S)	1.382(10)
C(1S)-Cl(2)	1.737(7)	C(2S)-C(3S)	1.369(10)
C(2S)-Cl(1)	1.741(8)	C(3S)-C(4S)	1.374(11)
C(4S)-C(5S)	1.398(12)	C(5S)-C(6S)	1.376(11)

C(5)-Si(1)-C(3)	116.2(3)	C(5)-Si(1)-C(1)	117.4(3)
C(3)-Si(1)-C(1)	114.0(3)	C(5)-Si(1)-Br(3)	104.7(2)
C(3)-Si(1)-Br(3)	93.7(2)	C(1)-Si(1)-Br(3)	106.9(2)
C(2)-C(1)-Si(1)	115.4(5)	C(4)-C(3)-Si(1)	118.3(5)
C(6)-C(5)-Si(1)	111.4(5)	C(15)-Si(2)-C(13)	110.3(4)
C(15)-Si(2)-C(11)	107.9(3)	C(13)-Si(2)-C(11)	117.3(4)
C(15)-Si(2)-N(1)	108.2(3)	C(13)-Si(2)-N(1)	104.7(3)
C(11)-Si(2)-N(1)	108.0(3)	N(2)-N(1)-C(7)	107.2(5)
N(2)-N(1)-C(8)	113.8(5)	C(7)-N(1)-C(8)	107.6(6)
N(2)-N(1)-Si(2)	108.1(4)	C(7)-N(1)-Si(2)	106.9(5)
C(8)-N(1)-Si(2)	112.9(4)	C(9)-N(2)-C(10)	108.2(5)
C(9)-N(2)-N(1)	113.2(5)	C(10)-N(2)-N(1)	111.5(5)
C(12)-C(11)-Si(2)	113.3(6)	C(14)-C(13)-Si(2)	114.1(6)
C(16)-C(15)-Si(2)	120.2(5)	B(3)-B(1)-B(6)	106.3(5)
B(3)-B(1)-B(5)	106.5(5)	B(6)-B(1)-B(5)	59.9(4)
B(3)-B(1)-B(4)	59.7(4)	B(6)-B(1)-B(4)	107.6(5)
B(5)-B(1)-B(4)	59.7(4)	B(3)-B(1)-B(2)	59.0(4)
B(6)-B(1)-B(2)	59.9(4)	B(5)-B(1)-B(2)	107.7(5)
B(4)-B(1)-B(2)	107.6(5)	B(3)-B(1)-Br(1)	124.0(4)
B(6)-B(1)-Br(1)	121.4(5)	B(5)-B(1)-Br(1)	121.4(4)

B(4)-B(1)-Br(1)	122.2(4)	B(2)-B(1)-Br(1)	122.1(5)
B(3)-B(2)-B(11)	107.4(5)	B(3)-B(2)-B(7)	60.4(4)
B(11)-B(2)-B(7)	59.9(4)	B(3)-B(2)-B(6)	106.1(5)
B(11)-B(2)-B(6)	60.2(4)	B(7)-B(2)-B(6)	107.9(5)
B(3)-B(2)-B(1)	59.3(4)	B(11)-B(2)-B(1)	108.2(5)
B(7)-B(2)-B(1)	108.6(5)	B(6)-B(2)-B(1)	59.4(4)
B(3)-B(2)-Br(2)	121.1(4)	B(11)-B(2)-Br(2)	122.6(5)
B(7)-B(2)-Br(2)	120.1(4)	B(6)-B(2)-Br(2)	124.1(5)
B(1)-B(2)-Br(2)	121.7(5)	B(2)-B(3)-B(1)	61.7(4)
B(2)-B(3)-B(4)	111.0(5)	B(1)-B(3)-B(4)	61.3(4)
B(2)-B(3)-B(8)	109.4(5)	B(1)-B(3)-B(8)	110.3(5)
B(4)-B(3)-B(8)	61.1(4)	B(2)-B(3)-B(7)	60.7(4)
B(1)-B(3)-B(7)	110.8(5)	B(4)-B(3)-B(7)	110.3(5)
B(8)-B(3)-B(7)	60.1(4)	B(2)-B(3)-Br(3)	123.6(4)
B(1)-B(3)-Br(3)	128.5(5)	B(4)-B(3)-Br(3)	121.2(5)
B(8)-B(3)-Br(3)	113.3(4)	B(7)-B(3)-Br(3)	114.0(4)
B(3)-B(4)-B(5)	106.2(5)	B(3)-B(4)-B(9)	106.8(5)
B(5)-B(4)-B(9)	59.4(4)	B(3)-B(4)-B(1)	59.1(4)
B(5)-B(4)-B(1)	59.9(4)	B(9)-B(4)-B(1)	107.5(5)
B(3)-B(4)-B(8)	59.7(4)	B(5)-B(4)-B(8)	107.1(5)
B(9)-B(4)-B(8)	59.9(4)	B(1)-B(4)-B(8)	107.4(5)
B(3)-B(4)-Br(4)	122.7(4)	B(5)-B(4)-Br(4)	123.0(4)
B(9)-B(4)-Br(4)	121.9(5)	B(1)-B(4)-Br(4)	122.5(4)
B(8)-B(4)-Br(4)	121.4(4)	B(9)-B(5)-B(10)	60.1(4)
B(9)-B(5)-B(6)	107.9(5)	B(10)-B(5)-B(6)	59.7(4)
B(9)-B(5)-B(4)	60.4(4)	B(10)-B(5)-B(4)	108.4(5)
B(6)-B(5)-B(4)	108.0(5)	B(9)-B(5)-B(1)	108.8(5)
B(10)-B(5)-B(1)	107.9(5)	B(6)-B(5)-B(1)	59.8(4)
B(4)-B(5)-B(1)	60.4(4)	B(9)-B(5)-Br(5)	120.8(5)
B(10)-B(5)-Br(5)	120.6(4)	B(6)-B(5)-Br(5)	121.9(4)
B(4)-B(5)-Br(5)	122.2(5)	B(1)-B(5)-Br(5)	122.5(5)
B(10)-B(6)-B(1)	108.7(5)	B(10)-B(6)-B(5)	60.1(4)
B(1)-B(6)-B(5)	60.3(4)	B(10)-B(6)-B(2)	108.3(5)
B(1)-B(6)-B(2)	60.6(4)	B(5)-B(6)-B(2)	108.6(5)

B(10)-B(6)-B(11)	60.6(4)	B(1)-B(6)-B(11)	108.7(5)
B(5)-B(6)-B(11)	108.6(5)	B(2)-B(6)-B(11)	59.6(4)
B(10)-B(6)-Br(6)	121.5(4)	B(1)-B(6)-Br(6)	120.7(5)
B(5)-B(6)-Br(6)	120.9(4)	B(2)-B(6)-Br(6)	121.9(5)
B(11)-B(6)-Br(6)	122.0(4)	B(12)-B(7)-B(11)	59.7(4)
B(12)-B(7)-B(3)	106.9(5)	B(11)-B(7)-B(3)	106.0(5)
B(12)-B(7)-B(8)	60.1(4)	B(11)-B(7)-B(8)	107.5(5)
B(3)-B(7)-B(8)	59.8(4)	B(12)-B(7)-B(2)	107.6(5)
B(11)-B(7)-B(2)	59.7(4)	B(3)-B(7)-B(2)	58.9(4)
B(8)-B(7)-B(2)	107.6(5)	B(12)-B(7)-Br(7)	123.5(5)
B(11)-B(7)-Br(7)	122.4(5)	B(3)-B(7)-Br(7)	122.0(4)
B(8)-B(7)-Br(7)	122.6(4)	B(2)-B(7)-Br(7)	120.5(4)
B(3)-B(8)-B(12)	106.6(5)	B(3)-B(8)-B(7)	60.0(4)
B(12)-B(8)-B(7)	59.6(4)	B(3)-B(8)-B(9)	106.4(5)
B(12)-B(8)-B(9)	61.2(4)	B(7)-B(8)-B(9)	108.8(5)
B(3)-B(8)-B(4)	59.3(4)	B(12)-B(8)-B(4)	108.7(5)
B(7)-B(8)-B(4)	108.7(5)	B(9)-B(8)-B(4)	59.7(4)
B(3)-B(8)-Br(8)	122.2(4)	B(12)-B(8)-Br(8)	122.8(5)
B(7)-B(8)-Br(8)	121.5(4)	B(9)-B(8)-Br(8)	122.0(5)
B(4)-B(8)-Br(8)	120.4(4)	B(5)-B(9)-B(10)	60.1(4)
B(5)-B(9)-B(4)	60.1(4)	B(10)-B(9)-B(4)	108.1(5)
B(5)-B(9)-B(8)	108.0(5)	B(10)-B(9)-B(8)	107.1(5)
B(4)-B(9)-B(8)	60.4(4)	B(5)-B(9)-B(12)	107.6(5)
B(10)-B(9)-B(12)	59.7(4)	B(4)-B(9)-B(12)	107.6(5)
B(8)-B(9)-B(12)	59.0(4)	B(5)-B(9)-Br(9)	122.0(5)
B(10)-B(9)-Br(9)	122.9(4)	B(4)-B(9)-Br(9)	120.7(5)
B(8)-B(9)-Br(9)	121.3(5)	B(12)-B(9)-Br(9)	122.6(5)
B(6)-B(10)-B(9)	108.1(5)	B(6)-B(10)-B(5)	60.2(4)
B(9)-B(10)-B(5)	59.7(4)	B(6)-B(10)-B(12)	107.5(5)
B(9)-B(10)-B(12)	61.3(4)	B(5)-B(10)-B(12)	108.6(5)
B(6)-B(10)-B(11)	60.2(4)	B(9)-B(10)-B(11)	108.4(5)
B(5)-B(10)-B(11)	108.5(5)	B(12)-B(10)-B(11)	59.0(4)
B(6)-B(10)-Br(10)	122.4(4)	B(9)-B(10)-Br(10)	121.5(4)
B(5)-B(10)-Br(10)	122.7(4)	B(12)-B(10)-Br(10)	120.5(5)

B(11)-B(10)-Br(10)	120.8(5)	B(12)-B(11)-B(2)	108.2(5)
B(12)-B(11)-B(7)	59.9(4)	B(2)-B(11)-B(7)	60.3(4)
B(12)-B(11)-B(6)	107.8(5)	B(2)-B(11)-B(6)	60.2(4)
B(7)-B(11)-B(6)	108.2(5)	B(12)-B(11)-B(10)	60.4(4)
B(2)-B(11)-B(10)	107.7(5)	B(7)-B(11)-B(10)	108.0(5)
B(6)-B(11)-B(10)	59.3(4)	B(12)-B(11)-Br(11)	122.1(5)
B(2)-B(11)-Br(11)	121.6(5)	B(7)-B(11)-Br(11)	122.4(5)
B(6)-B(11)-Br(11)	121.0(5)	B(10)-B(11)-Br(11)	121.4(4)
B(11)-B(12)-B(7)	60.5(4)	B(11)-B(12)-B(8)	108.4(5)
B(7)-B(12)-B(8)	60.3(4)	B(11)-B(12)-B(10)	60.6(4)
B(7)-B(12)-B(10)	108.7(5)	B(8)-B(12)-B(10)	107.3(5)
B(11)-B(12)-B(9)	107.9(5)	B(7)-B(12)-B(9)	108.3(5)
B(8)-B(12)-B(9)	59.8(4)	B(10)-B(12)-B(9)	59.1(4)
B(11)-B(12)-Br(12)	122.9(5)	B(7)-B(12)-Br(12)	122.4(4)
B(8)-B(12)-Br(12)	121.1(5)	B(10)-B(12)-Br(12)	121.5(4)
B(9)-B(12)-Br(12)	120.3(5)	B(3)-Br(3)-Si(1)	123.2(2)
C(6S)-C(1S)-C(2S)	120.2(7)	C(6S)-C(1S)-Cl(2)	119.3(6)
C(2S)-C(1S)-Cl(2)	120.5(6)	C(3S)-C(2S)-C(1S)	120.1(7)
C(3S)-C(2S)-Cl(1)	119.4(6)	C(1S)-C(2S)-Cl(1)	120.5(6)
C(2S)-C(3S)-C(4S)	120.0(8)	C(3S)-C(4S)-C(5S)	120.0(8)
C(6S)-C(5S)-C(4S)	119.4(8)	C(1S)-C(6S)-C(5S)	120.2(8)

I.2.4 Anisotropic Displacement Parameters

Anisotropic displacement parameters ($Å^2 x\ 10^3$) for $[Et_3SiN_2(CH_3)_4][Et_3Si(B_{12}Br_{12})]\cdot CD_2Cl_2$. The anisotropic displacement factor exponent takes the form: $-2p^2[\ h^2\ a^{*2}U^{11} + ...\ + 2\ h\ k\ a^*\ b^*\ U^{12}\ ]$

	U^{11}	U^{22}	U^{33}	U^{23}	U^{13}	U^{12}
Si(1)	11(1)	22(1)	20(1)	1(1)	-1(1)	-4(1)
C(1)	10(3)	23(3)	29(4)	-1(3)	-3(3)	-6(3)

C(2)	29(4)	30(4)	29(5)	5(3)	-18(3)	-2(3)
C(3)	18(4)	20(3)	29(4)	-3(3)	-5(3)	-3(3)
C(4)	26(4)	20(3)	38(5)	-1(3)	0(4)	0(3)
C(5)	20(4)	34(4)	15(4)	3(3)	-1(3)	-6(3)
C(6)	19(4)	34(4)	27(4)	2(3)	0(3)	-2(3)
Si(2)	24(1)	22(1)	16(1)	1(1)	-1(1)	1(1)
N(1)	22(3)	26(3)	22(3)	-1(3)	-8(3)	3(3)
N(2)	16(3)	27(3)	22(3)	-1(2)	-4(3)	4(2)
C(7)	65(6)	25(4)	49(6)	-6(4)	-39(5)	4(4)
C(8)	26(5)	72(6)	22(5)	-14(4)	-6(3)	13(4)
C(9)	28(4)	35(4)	23(4)	-6(3)	-8(3)	2(3)
C(10)	29(4)	32(4)	19(4)	5(3)	-1(3)	4(3)
C(11)	50(6)	29(4)	42(6)	2(4)	-19(4)	-4(4)
C(12)	77(7)	34(4)	51(6)	-4(4)	-31(5)	-16(5)
C(13)	35(5)	47(5)	31(5)	-4(4)	2(4)	11(4)
C(14)	43(6)	101(8)	29(5)	-3(5)	4(4)	26(6)
C(15)	32(5)	31(4)	17(4)	-1(3)	-1(3)	-2(3)
C(16)	28(5)	42(4)	44(6)	8(4)	-7(4)	7(4)
B(1)	12(4)	16(3)	16(4)	3(3)	0(3)	1(3)
B(2)	12(4)	13(3)	22(4)	1(3)	-6(3)	-3(3)
B(3)	8(4)	18(3)	14(4)	1(3)	2(3)	-4(3)
B(4)	6(4)	22(3)	11(4)	-4(3)	-4(3)	1(3)
B(5)	11(4)	14(3)	15(4)	-1(3)	-1(3)	-1(3)
B(6)	12(4)	18(3)	12(4)	-4(3)	-4(3)	-3(3)
B(7)	17(4)	14(3)	13(4)	1(3)	-1(3)	-3(3)
B(8)	11(4)	14(3)	15(4)	-1(3)	3(3)	-1(3)
B(9)	13(4)	20(3)	19(4)	1(3)	-3(3)	-5(3)
B(10)	13(4)	13(3)	16(4)	-1(3)	-3(3)	1(3)

	U^{11}	U^{22}	U^{33}	U^{23}	U^{13}	U^{12}
B(11)	11(4)	23(4)	10(4)	1(3)	-4(3)	1(3)
B(12)	6(4)	18(3)	18(4)	-4(3)	2(3)	4(3)

Br(1)	11(1)	21(1)	20(1)	-2(1)	4(1)	0(1)
Br(2)	21(1)	18(1)	16(1)	4(1)	1(1)	1(1)
Br(3)	15(1)	18(1)	23(1)	-4(1)	3(1)	-4(1)
Br(4)	11(1)	23(1)	19(1)	0(1)	-4(1)	0(1)
Br(5)	15(1)	16(1)	24(1)	-1(1)	-2(1)	2(1)
Br(6)	19(1)	20(1)	15(1)	-4(1)	-1(1)	-1(1)
Br(7)	17(1)	18(1)	21(1)	-1(1)	0(1)	6(1)
Br(8)	17(1)	23(1)	14(1)	-4(1)	0(1)	0(1)
Br(9)	17(1)	23(1)	17(1)	5(1)	0(1)	-3(1)
Br(10)	16(1)	21(1)	22(1)	0(1)	-3(1)	-8(1)
Br(11)	12(1)	28(1)	20(1)	-1(1)	-5(1)	2(1)
Br(12)	10(1)	28(1)	22(1)	-1(1)	3(1)	-1(1)

	U^{11}	U^{22}	U^{33}	U^{23}	U^{13}	U^{12}
C(1S)	16(4)	33(4)	25(4)	4(3)	-7(3)	0(3)
C(2S)	27(4)	34(4)	34(5)	-8(3)	-6(4)	4(3)
C(3S)	38(5)	43(4)	34(5)	-6(4)	-18(4)	9(4)
C(4S)	63(7)	47(5)	19(4)	10(4)	-15(4)	-14(5)
C(5S)	60(6)	39(5)	31(5)	-2(4)	16(4)	-15(4)
C(6S)	34(5)	39(4)	41(5)	1(4)	13(4)	2(4)
Cl(1)	48(2)	76(2)	62(2)	-36(1)	-16(1)	27(1)
Cl(2)	29(1)	50(1)	54(2)	3(1)	-17(1)	6(1)

I.2.5 Hydrogen Coordinates

Hydrogen coordinates (x 10^4) and isotropic displacement parameters ($Å^2$x 10^3) for $[Et_3SiN_2(CH_3)_4][Et_3Si(B_{12}Br_{12})]\cdot CD_2Cl_2$.

	x	y	z	U(eq)
H(1A)	6838	1203	1762	25
H(1B)	7521	1756	1652	25

H(2A)	7526	1144	999	44
H(2B)	6793	1624	1084	44
H(2C)	6836	601	1111	44
H(3A)	7284	-915	1581	27
H(3B)	7793	-567	1238	27
H(4A)	8776	-1216	1564	42
H(4B)	8187	-1916	1456	42
H(4C)	8260	-1571	1906	42
H(5A)	8369	-128	2404	28
H(5B)	8085	834	2451	28
H(6A)	6900	296	2478	40
H(6B)	7368	-78	2838	40
H(6C)	7203	-661	2454	40
H(7A)	793	9207	6255	70
H(7B)	375	9003	5849	70
H(7C)	1219	8945	5858	70
H(8A)	152	8205	6633	60
H(8B)	64	7233	6489	60
H(8C)	-328	7987	6252	60
H(9A)	1231	8354	6837	43
H(9B)	1735	8855	6531	43
H(9C)	2040	8071	6787	43
H(10A)	1865	6672	6602	40
H(10B)	1264	6414	6287	40
H(10C)	1049	6803	6714	40
H(11A)	454	5880	5908	48
H(11B)	-261	6424	5923	48
H(12A)	-397	6215	5223	82
H(12B)	-395	5325	5461	82

	x	y	z	U(eq)
H(12C)	297	5628	5224	82
H(13A)	1815	7720	5463	45

H(13B)	1843	6784	5658	45
H(14A)	1437	6182	5049	87
H(14B)	2149	6713	4975	87
H(14C)	1401	7117	4854	87
H(15A)	397	8467	5239	32
H(15B)	162	7610	5017	32
H(16A)	-880	7609	5443	57
H(16B)	-848	8362	5117	57
H(16C)	-657	8558	5575	57

	x	y	z	U(eq)
H(3S)	3536	8877	5314	46
H(4S)	3296	9691	5881	52
H(5S)	2266	10535	5908	52
H(6S)	1490	10536	5366	46

I.3 References

1. Bruker (2005). APEX 2 version 2.0-2. Bruker AXS Inc., Madison, Wisconsin, U.S.A.

2. Bruker (2005). SAINT version V7.21A. Bruker AXS Inc., Madison, Wisconsin, USA.

3. Bruker (2004). SADABS version 2004/1. Bruker Analytical X-Ray System, Inc., Madison, Wisconsin, USA.

4. Altomare, A., Burla, M.C., Carnalli, M. Cascarano, G. Giacovazzo, C., Guagliardi, A.; Moliterni, A.G.G.; Polidori, G. Spagan, R. SIR 97 (1999) J. Appl. Cryst. 32, 115-122.

5. Bruker (2003). SHELXTL Software Version 6.14, Dec, Bruker Analytical X-Ray System, Inc., Madison, Wisconsin, USA .